Unravelling the Physiology and Genetics of Salinity Tolerance in Chickpea (*Cicer arietinum* L.)

Judith Akinyi Atieno

A thesis submitted to the University of Adelaide in fulfilment of the requirements for the degree of Doctor of Philosophy

Faculty of sciences,
School of Agriculture, Food and Wine,
The University of Adelaide

THE UNIVERSITY of ADELAIDE

February 2017

Structure of the thesis

This thesis is presented in six chapters preceded with an Abstract which sets out the context and gives an overview of the thesis. Chapter 1 is made up of a Literature review which gives a broad background of the work presented in the subsequent chapters. Chapters 2, 3, 4 and 5 are experimental papers which have either been published, under review or unpublished work written in manuscript format shortly to be submitted for peer review. Each of the experimental papers contains an Abstract, Introduction, Materials and Methods, Results, Discussion and References. Additionally, they are prefaced by a statement of authorship that describes the contribution of each author and a link page that ties in the chapter with this thesis. General discussion and future research directions are presented in Chapter 6. This thesis is in agreement with the specification of “thesis by publication” format of the Adelaide Graduate Centre Higher Degree by Research, University of Adelaide, South Australia.

Abstract

Chickpea (*Cicer arietinum* L.) is a nutritious legume predominantly grown in semi-arid environments under rain fed conditions, but is highly sensitive to soil salinity. Until recently, there has been slow progress in the application of molecular genetics in chickpea breeding. This is primarily because the available genetic variation in international chickpea germplasm collections has not been extensively characterised due to a lack of available genomics tools and high-throughput phenotyping resources.

Molecular genetic approaches are needed to identify key loci with the potential to improve salinity tolerance in chickpea. In this project, genetic analysis was conducted on two populations: A recombinant inbred line (RIL) population of 200 individuals developed from a cross between Genesis836 and Rupali which are known to contrast in their tolerance to salinity and a diversity panel consisting of 245 chickpea accessions of diverse genetic background from ICRISAT. For phenotyping, an image-based high-throughput phenotyping platform was used. Data on growth rate, water use, plant senescence and necrosis, and agronomic traits were collected under both control and saline conditions (40 mM for diversity panel and 70 mM NaCl for RIL). In depth studies including differential metabolite accumulation and senescence detection were carried out to increase our understanding of the response of chickpea to salinity.

Genesis836 and Rupali differentially accumulated metabolites associated with the TCA cycle, carbon and amino acid metabolism. Higher senescence scores were recorded in Rupali compared to Genesis836. On average, salinity reduced plant growth rate by 20%, plant height by 15% and shoot biomass by 28%. Additionally, salinity induced pod abortion and inhibited pod filling, which consequently reduced seed number and seed yield by 16% and 32%, respectively. Path analysis was utilised to understand the intricate

relationship existing between the traits measured and aided in the identification of those most related to salinity tolerance. This analysis showed that seed number under salt was highly related to salinity tolerance in chickpea.

To identify Quantitative Trait Loci (QTL) underlying salinity tolerance in chickpea, two complimentary genetic analysis approaches were used: genome-wide association studies (GWAS) and linkage mapping. Phenotypic data was combined with genotypic data from both the diversity panel (generated through whole-genome resequencing) and RIL population (from DArTseq). Linkage mapping and GWAS identified a total of 57 QTL and 54 marker-trait associations (MTAs), respectively. The loci identified were linked to growth rate, yield, yield components and ion accumulation. A novel major QTL for relative growth rate on chromosome 4 that explained 42.6% of genetic variation, was identified by both genetic analyses. This QTL co-located with several other QTL identified, including those associated with projected shoot area, water use, 100-seed weight, the number of filled pods, harvest index, seed number and seed yield under salt. Near-isogenic lines will be developed to allow for targeted fine mapping that will help identify candidate genes for molecular analysis. Molecular markers tightly linked to this QTL will be validated as a selection tool in breeding to improve salinity tolerance in chickpea.

Declaration

I certify that this work contains no material which has been accepted for the award of any other degree or diploma in my name, in any university or other tertiary institution and, to the best of my knowledge and belief, contains no material previously published or written by another person, except where due reference has been made in the text. In addition, I certify that no part of this work will, in the future, be used in a submission in my name, for any other degree or diploma in any university or other tertiary institution without the prior approval of the University of Adelaide and where applicable, any partner institution responsible for the joint-award of this degree.

I give consent to this copy of my thesis when deposited in the University Library, being made available for loan and photocopying, subject to the provisions of the Copyright Act 1968.

I acknowledge that copyright of published works contained within this thesis resides with the copyright holder(s) of those works.

I also give permission for the digital version of my thesis to be made available on the web, via the University's digital research repository, the Library Search and also through web search engines, unless permission has been granted by the University to restrict access for a period of time.

Judith Akinyi Atieno

February, 2017

Acknowledgements

Look at a stone cutter hammering away at his rock, perhaps a hundred times without as much as a crack showing in it. Yet at the hundred-and-first blow it will split in two, and I know it was not the last blow that did it, but all that had gone before. ~Jacob A. Riis

This PhD journey has had its fair share of ups and downs just like most things in life. I managed to reach this far due to the people I interacted with in the course of this research. I would like to express my gratitude to everyone who supported me during my PhD.

First and foremost, I would like to acknowledge my supervisors Dr Tim Sutton, Prof Peter Langridge and Dr Yongle Li for their guidance, support, and invaluable constructive criticism. I feel very fortunate and privileged to have worked with you.

I am extremely grateful to Dr Tim Sutton for granting me the opportunity to undertake a PhD project within his research group. Thank you for believing in me and encouraging me to stay the course. I will always be appreciative of the time you put in my research. Many thanks for reading all the chapters in this thesis and providing constructive criticism.

Sincere thanks to Dr Yongle Li for always being available to help with various aspects of this research. Thank you for the insightful discussions, constructive criticism and guidance you provided throughout this study. I am grateful for the pieces of advice you gave me in both my professional and private life.

My heartfelt thanks to Prof Peter Langridge for the time and invaluable advice during the course of this research. You always came up with great ideas which shaped my research and led to this accomplishment. You challenged me to go an extra mile and not settle for the norm. It has been a great honour working with you.

Many thanks to Dr Julian Taylor, Dr Chris Brien, and Ms Kate Dowling for the statistical support during my PhD.

I would also like to thank Dr Julie Hayes, my independent advisor and Dr Rhiannon Schilling for the insightful discussions we had at the start of this research. I am grateful to Ms Alison Hay for technical assistance and support.

I would like to thank Dr Fredrick Maati for the assistance he accorded me during editing and formatting of this thesis. You spent many hours to help with formatting of the various chapters and for that I will always be grateful.

Gratitude to my colleagues in the lab, Amritha, Shefat, Judy, Yusuf, Hammad, John and Simon for the support and your words of encouragement.

Many thanks to my friends, Margaret, Marianne, Amelie, Yonina, Sophie, Joan, Alicia, Mouni, Nevin, Ronny, Amanda, Carol, Susan and Matt for your encouragement and motivation. I am grateful for your patience and understanding especially during the hard times.

I would like to extend my gratitude to my new family: Mrs Judith Johnson. Thank you for welcoming me into your home and making me feel at home away from home. I am grateful for the warmth and love you have always shown me.

I am forever indebted to my loving mom, Ms Patricia Odhiambo for always believing in me and encouraging me to follow my dreams. You sacrificed everything to ensure my sisters and I lead a good life. Thank you for imparting in me virtues that have made me to what I am today. May God continue to bless you. I would also like to thank my sisters, Esther, Edith and Christine for their patience, encouragement and believing in me. You are the best sisters in the whole world.

Last but not least, I would like to thank my loving husband and best friend Paul for his patience, support and encouragement. You always found ways to make me laugh even during the most stressful times. Thank you for always being there for me. You made this journey bearable. I could not accomplish this feat without you by my side.

Above all, I would like to thank God for giving me strength, determination and grace to complete this PhD program.

This research was financially supported by Australian Centre For Plant Functional Genomics and University of Adelaide.

List of publications

1. Dias D.A, Hill C.B, Jayasinghe N.S, Atieno J, Sutton T, Roessner U (2015) Quantitative profiling of polar primary metabolites of two chickpea cultivars with contrasting responses to salinity. Journal of Chromatography B 1000:1-13.doi:10.1016/j.jchromb.2015.07.002.

2. Cai J, Okamoto M, Atieno J, Sutton T, Li Y, Miklavcic SJ (2016) Quantifying the Onset and Progression of Plant Senescence by Color Image Analysis for High Throughput Applications. PLoS ONE 11(6): e0157102. doi:10.1371/journal.pone.0157102.

List of awards

1. **Best poster Award (2013)**

   Best poster presentation at Pulse Breeding Australia inaugural pulse conference held at the Sebel Playford, Adelaide.

2. **Best presentation at The School of Agriculture, Food and Wine Postgraduate Symposium (2014)**

   Best presentation in agronomy and broad-acre agriculture awarded by the Crop Science Society South Australia.

3. **The Max Tate Prize (2014)**

   Best presentation at the School of Agriculture, Food and Wine postgraduate symposium awarded by Dr Max Tate.

Table of contents

Chapter 1

Literature review

1.1 Salinity in Australia

Agricultural production is severely limited by abiotic stress. Salinity is one abiotic stress that impacts negatively on worldwide food production (Nawaz et al., 2010; Rengasamy, 2006). Most countries in the world are affected by salinity with over 800 million ha of land affected. This approximates to 6% of total global land area and is predicted to increase by 1-2% in the future (FAO, 2008).

Salinity is the biggest contributor to soil degradation in Australia and poses a major threat to the country's native species which negatively impacts on proper ecosystem functioning (ANZECC, 2001). Australia is reported to have approximately 67% of its agricultural land, equivalent to 5.7 million hectares, affected by salinity (Figure 1) (Rengasamy, 2002). Unless effective solutions are implemented, it is predicted 17 million hectares of Australian land will be salinized by 2050 (ANRA, 2001). Soil salinity can be categorised into primary salinity and secondary salinity (dry-land salinity and transient salinity, respectively) (ABS, 2002; Rengasamy, 2006). Transient salinity results from the accumulation of salts in the soil and root zones due to high rates of evaporation while dry-land salinity results from rising saline water tables caused by intensive irrigation and clearing of native vegetation (Jardine et al., 2011; Rengasamy, 2002). Approximately 70% of the Australian wheat belt is salinized due to rising water tables (NLWRA, 2001; Rengasamy, 2006).

The total estimated annual loss, in lost opportunity, in Australia as a result of salinity is AUD $1,334 million per year (Rengasamy, 2002). Therefore, developing saline tolerant plants to grow in the increasingly salinized agricultural lands will alleviate further crop losses not only in Australia but also in other parts of the world.

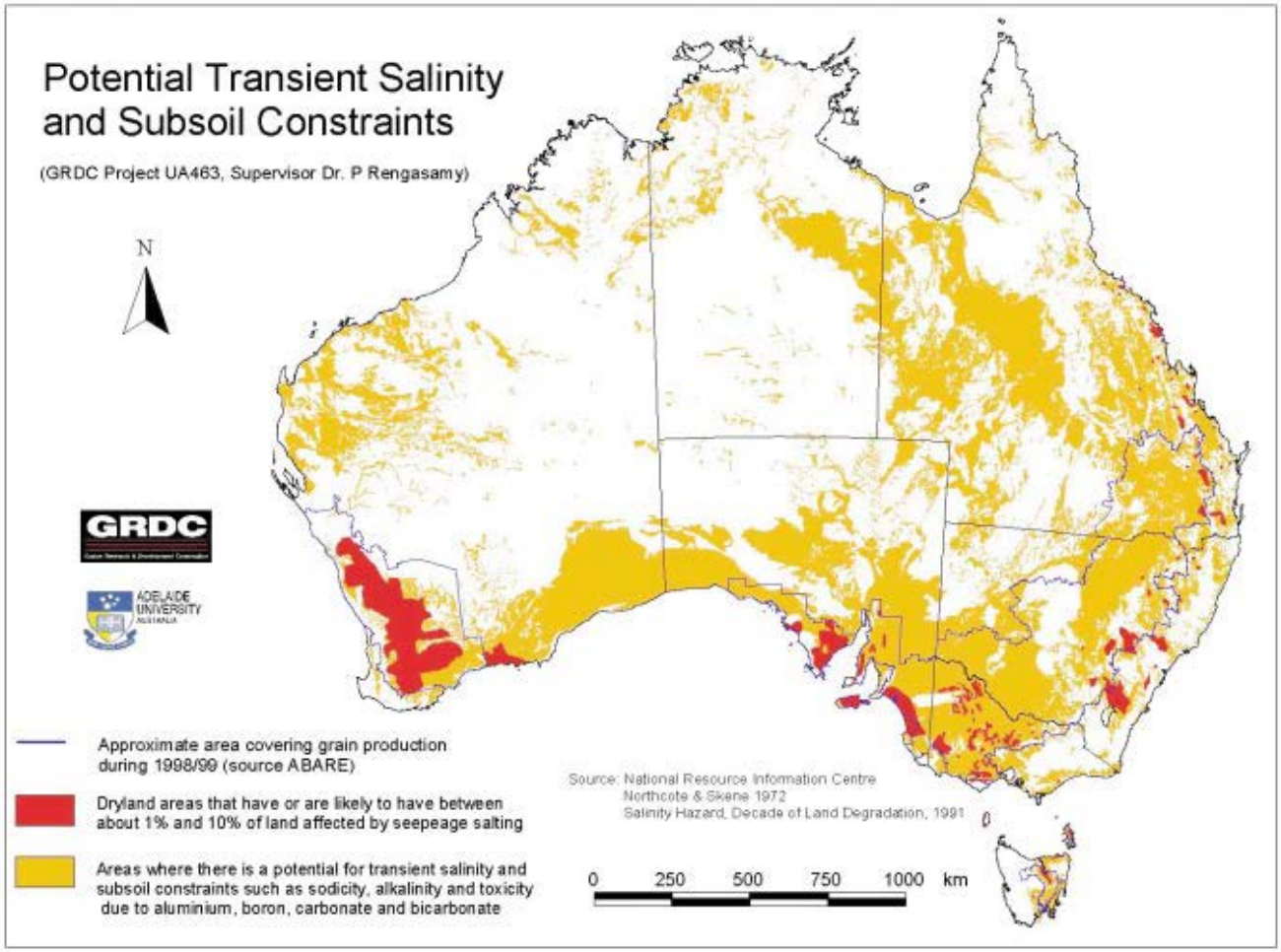

Figure 1: The extent of salinisation in Australia. Most agricultural land in Australia are affected by either dry-land salinity or transient salinity (Rengasamy, 2002).

1.2 Chickpea biology, economic importance and production

Chickpea (*Cicer arietinum* L.) is a self-pollinated diploid (2n=2x=16) plant with a relatively small genome of 740 Mb (Arumuganathan and Earl, 1991). Through next-generation sequencing, a chickpea draft genome sequence with predicted 28,000 genes has been generated (Jain et al., 2013; Parween et al., 2015; Varshney et al., 2013). This forms an important resource for chickpea improvement to improve food security in developing countries where chickpea is mostly consumed. Chickpea belongs to the family Leguminosae. Legumes comprise of soybeans, peanut, pulses, fresh peas and fresh beans (Figure 2). They are widely grown throughout the world, with chickpea ranking second in the pulse category in terms of total production (FAOSTAT, 2011; FAOSTAT, 2014; Knights and Siddique, 2002). Chickpea is classified into kabuli and desi types. The kabuli chickpea is large-seeded, cream-coloured and 'ram's head' shaped, with thin testa while desi is small-seeded, angular shaped and has a wide colour range from brown, yellow, orange, black to green with a thick testa (Flowers et al., 2010; Millan et al., 2006; Rao, 2010).

In many countries, chickpea is an important human and animal food with high nutritive value (Charles et al., 2002; Jukanti et al., 2012). Chickpea seed is composed of 20%-30% protein, 40% carbohydrates and 3%-6% oil (Gill et al., 1996). Additionally, the seeds are rich in manganese, potassium, iron, zinc, calcium, phosphorus, and beta-carotene (Ibrikci et al., 2003). Chickpea can restore and maintain soil fertility (GRDC, 2012; Saxena, 1990) and is able to fix up to 140 kg N ha^{-1} $year^{-1}$ through symbiosis with *Rhizobium* bacteria (Rupela and Rao, 1987).

The global area under chickpea production in 2014 was 14.8 million ha with 14.24 million tonnes (mt) harvested (Figure 3a) (FAOSTAT, 2014). Chickpea is grown in more than 50 countries but the main chickpea producers include India, Australia, Pakistan, Turkey, Myanmar, Ethiopia, Iran, USA, Canada, and Mexico (Figure 3a). Most of the chickpea production comes from the Asian continent (Figure 3b) (FAOSTAT, 2014). Australia is the second largest producer of chickpea after India (Figure 3a) (FAOSTAT, 2014). Chickpeas form an important component of cropping systems in Australia as a high value rotation option for wheat and barley growers (Siddique and Sykes, 1997). Australian chickpea exports comprise 25% of the total exports worldwide. Most of these exports go to the Indian subcontinent to meet the consistently high demand which exceeds domestic supply (FAOSTAT, 2014). The inability of production in India to meet local demand is partially attributed to abiotic stresses, which have a significant effect on crop productivity (Krishnamurthy et al., 2011; Upadhyaya et al., 2011). Strategies to increase chickpea yield and expand production to marginal land are urgently needed.

Figure 2: Categories of legumes. Chickpea belongs to the pulse group. Source: Pulse Canada

a)

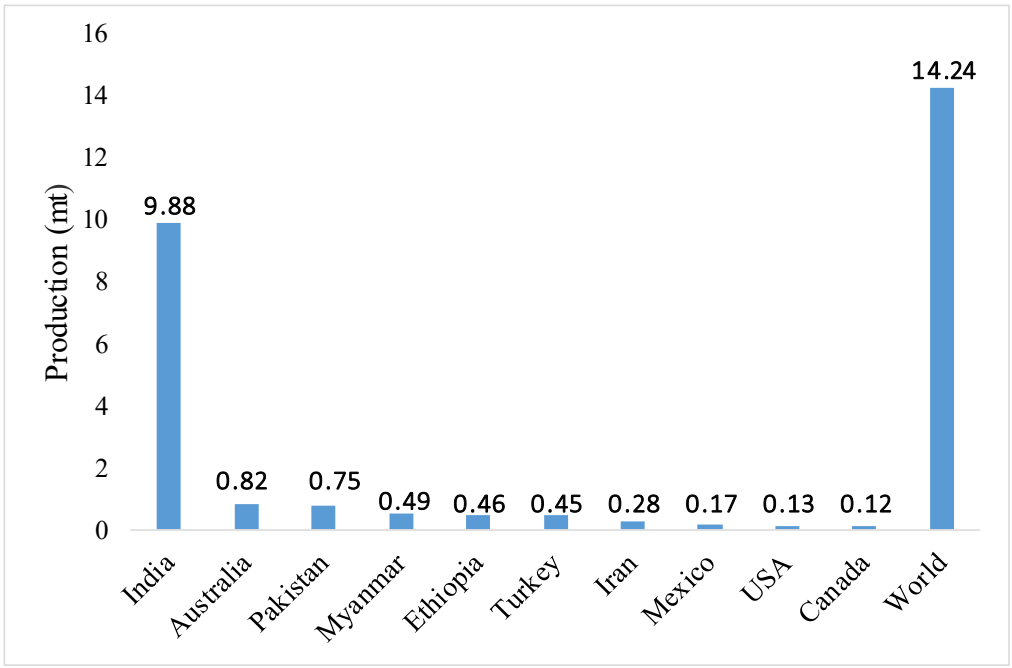

b)

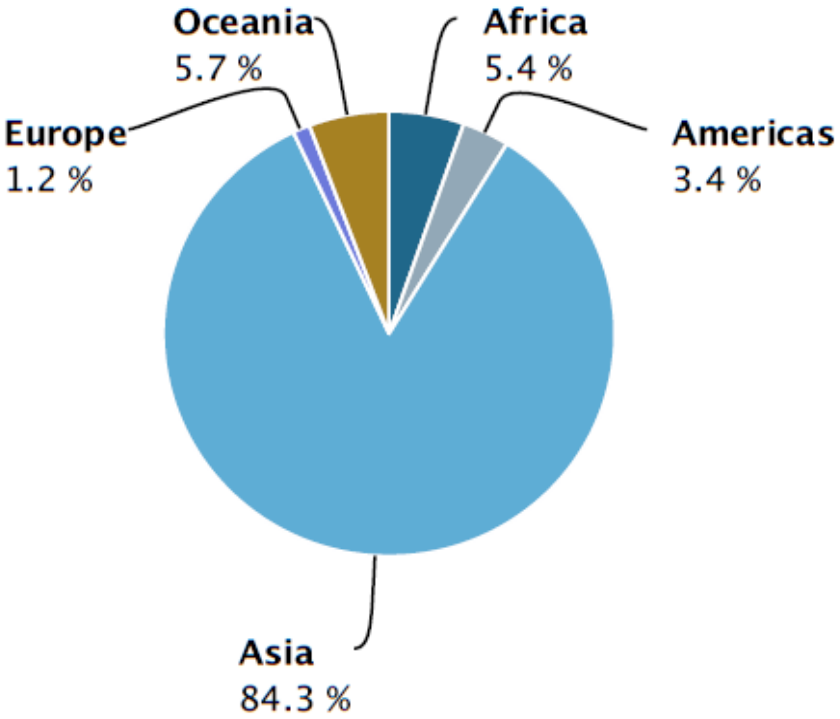

Figure 3: Chickpea production. a. World production of chickpea in 2014 (FAOSTAT, 2014) Chickpea is grown in many countries in the world with India being the main producer. b. Share of chickpea production by region in 2014. Most of chickpea production comes from Asia continent (FAOSTAT, 2014).

1.3 Sensitivity of chickpea to salinity

Global chickpea production is limited by abiotic stress, causing annual losses estimated at about 3.7 mt (Varshney & Dubey, 2009). Salinity is a major abiotic stress, which negatively affects crop production (Ali et al., 2002; Lauter and Munns, 1986). An estimated 8%-10% of the global annual chickpea yield loss is attributed to salinity (Flowers et al., 2010).

Although saline soils are said to have salinity levels (ECe) of above 4 dS/m, which is approximately 40 mM NaCl (US laboratory staff, 1954), the response of different plant species to salinity is also dependent on pH, Cation Exchange Capacity (CEC), and soil type (Vadez et al., 2007; Krishnamurthy et al., 2011).

Two phases of salinity have been described that limit plant growth and development; shoot ion independent (including osmotic component) stress and shoot ion dependent (ionic) stress (Munns and Tester, 2008; Roy et al., 2014). Shoot ion independent stress occurs immediately following salt application while shoot ion dependent stress manifests after several days or weeks once ions accumulate in plant tissues (Munns and Tester, 2008; Roy et al., 2014). Shoot ion independent stress arises from high salt concentration around plant roots which not only imposes hydraulic resistance in the plant xylem (Munns and Passioura, 1984) but also lowers soil water potential which interferes with plant water uptake (Boursiac et al., 2005; Fricke, 2004; Puniran-Hartley et al., 2014) consequently negatively affecting plant growth. The reduction in plant growth is manifested by a reduction in tillering, leaf area, and branch number (Munns and Tester, 2008). Shoot ion dependent stress is caused by the accumulation of toxic salts, mainly Na^+ and Cl^-, in leaves (Munns and Tester, 2008; Roy et al., 2014) leading to leaf necrosis and eventually leaf drop which reduces overall photosynthetic capability. Strategies to improve both shoot ion independent and shoot ion dependent tolerance of a plant will reduce yield losses caused by salt stress (Munns & Tester, 2008) (Figure 4).

Grain legumes are generally considered sensitive to salinity with chickpea among the most sensitive (Maas and Hoffman, 1977). Chickpea is more sensitive than durum wheat with exposure to 25 mM of NaCl in hydroponics system reported to kill the most sensitive chickpea genotypes (Flowers et al., 2010).

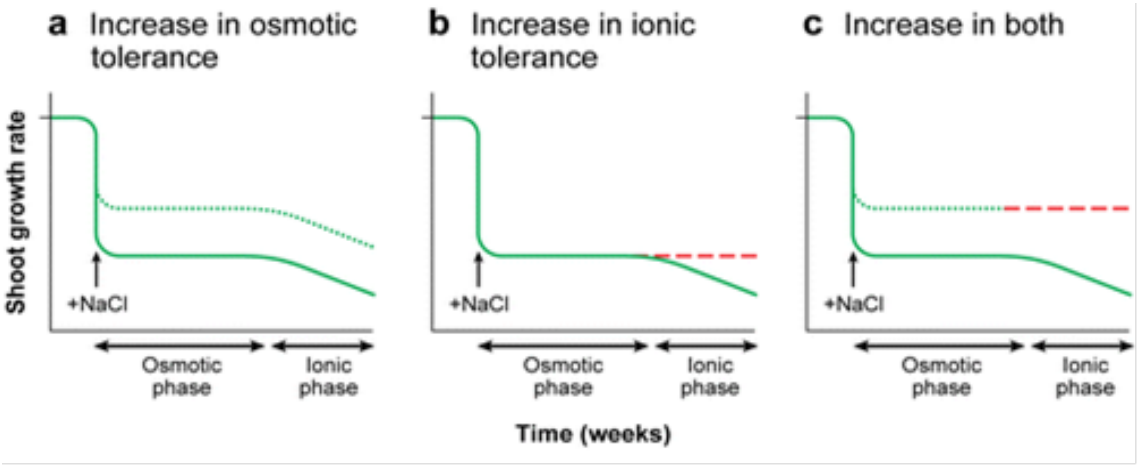

Figure 4: Osmotic stress and ionic stress in plants. Osmotic stress sets in earlier than ionic stress. Increase in osmotic stress tolerance and ionic stress tolerance improves shoot growth rate (Munns &Tester, 2008).

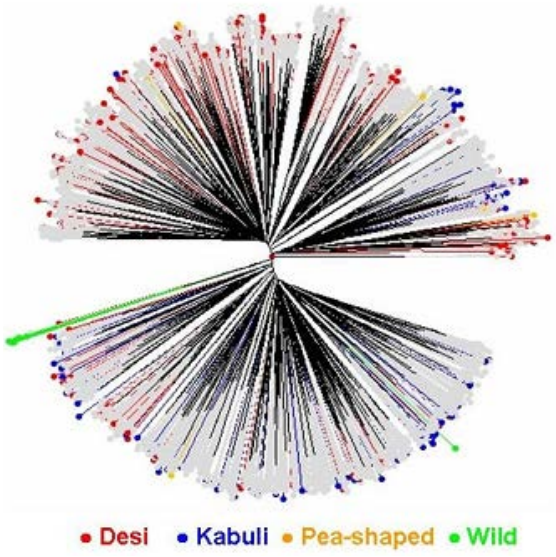

Figure 5: Neighbour-joining tree of the Reference Set. Tree diagram based on the simple matching dissimilarity matrix of 48 SSR markers showing allelic diversity across the chickpea composite collection. The Reference Set (300) accessions are represented in red (desi), blue (kabuli), yellow (pea- shaped), and green (wild *Cicer*) (Upadhyaya et al., 2008).

Salinity affects the developmental stages of chickpea in different ways. There is conflicting information regarding the effect of salinity on chickpea germination. Previous research has shown the presence of genetic variability for chickpea germination response under salinity (Esechie et al., 2002). Soltani et al. (2002) established that a positive relationship exists between seed size and seed germination under salinity. However, other studies show that salinity has a minimal effect on the germination percentage and time of germination in chickpea (Al-Mutata, 2003; Kumar, 1985; Sekeroglu et al., 1999). Furthermore, Kaya et al. (2008) reported 100% germination in Kabuli genotypes screened under salinity (16.3dsm^{-1} of NaCl). These contrasting outcomes may be due to different genotypes and screening methods employed in the different studies.

Several studies show the reproductive phase to be more sensitive to salinity than the vegetative phase in chickpea (Katerji et al., 2001; Krishnamurthy et al., 2011; Pushpavalli et al., 2015a; Samineni et al., 2011; Turner et al., 2013; Vadez et al., 2007; Vadez et al., 2012a; Vadez et al., 2012b). This has important implications when selecting for salt tolerant genotypes, as tolerance at the vegetative phase does not necessarily translate to reproductive success under salinity. Podding has been reported to be the most sensitive stage with a high rate of pod abortion reported in sensitive genotypes under saline conditions (Samineni et al., 2011). Similarly high number of filled pods and high seed number under salinity, as opposed to seed size, have been shown to be major determinants of salinity tolerance (Krishnamurthy et al., 2011; Pushpavalli et al., 2015a; Pushpavalli et al., 2015b; Samineni et al., 2011; Turner et al., 2013; Vadez et al., 2012a; Vadez et al., 2012b). However, in a breeding context, the cost of implementing phenotypic selection tools for salinity tolerance in chickpea is crucial. Therefore, it is important to identify phenotypic traits that correlate with salinity tolerance during early developmental stages in chickpea. Vadez et al. (2012a), found that a large number of tertiary branches and flowers can lead to reproductive success under salinity. However, these two traits are difficult to measure especially when a large number of genotypes are involved.

Three mechanisms of salinity tolerance have been studied in chickpea. These include; osmotic tolerance (Khan et al., 2016), ion exclusion (Pushpavalli et al., 2015a; Turner et al., 2013), and tissue tolerance (Khan et al., 2016; Kotula et al., 2015). Recently, Khan et al. (2016) used concentrated macronutrient solutions to study the response of two chickpea cultivars, Genesis836 and Rupali, to osmotic stress equivalent to osmotic potential exerted by 60 mM NaCl. This study demonstrated that chickpea is tolerant to osmotic stress, a component of shoot-ion independent stress. Previous studies have demonstrated reduction of seed yield under salinity without critical levels of toxic ions accumulating in plant tissues (Pushpavalli et al., 2015a; Turner et al., 2013; Vadez et al., 2007). Therefore, it is imperative to investigate the response of chickpea to shoot ion independent stress, which is specifically induced by NaCl. Several studies have shown chickpea is sensitive to sodium ions (Na^+) as opposed to potassium (K^+) or chloride ions (Cl^-) (Khan et al., 2016; Pushpavalli et al., 2015a; Turner et al., 2013). Turner et al.(2013) studied ion accumulation in 50 chickpea genotypes, ranging from extremely tolerant to sensitive, when subjected to 80 mM NaCl (Krishnamurthy et al., 2011). They found sensitive genotypes to accumulate significantly high levels of Na^+ and K^+ but not Cl^- in mature seeds. Additionally, they established a moderate negative relationship between salinity tolerance (seed yield under 40 mM NaCl) and Na^+ accumulation in the youngest-fully expanded leaf. Using eight genotypes, Pushpavalli et al. (2015a) demonstrated association between salinity tolerance and high K^+/Na^+ in fully expanded young leaves, low Na^+ in old green leaves, high K^+ in seeds at mid-filling stage, and high Cl^- in mature seeds. In contrast, Vadez et al. (2007) did not find association between salinity tolerance and shoot Na^+ or shoot K^+, 50 days after sowing (DAS). The discrepancy in the three studies may be due to different sampling strategies, or the tissue type and developmental stage sampled to quantify ion accumulation.

Tissue tolerance has been demonstrated in chickpea using two genotypes, Genesis836 and Rupali, which contrast for salinity tolerance (Khan et al., 2016; Kotula et al., 2015). Genesis836 accumulated a similar concentration of Na^+ as Rupali but maintained net photosynthetic activity (Khan et al., 2016) and seed yield (Kotula et al., 2015m-) under salinity.

The above studies indicate that there is a need to further explore the relative contribution of the known mechanisms of salinity tolerance in chickpea, ideally in larger germplasm collections where there is evidence that tolerance mechanisms are genotype dependant.

1.4 Breeding for improved salinity tolerance in chickpea

Plant breeders exploit genetic diversity to increase yield potential or broaden adaptation to marginal environments. The recent application of bioinformatics and genomic tools has made it possible to more readily identify novel traits and exploit naturally occurring genetic variation in breeding than previously. Previous research reported the existence of limited natural genetic variability for salinity tolerance in chickpea available for breeding (Johansen et al., 1990; Saxena, 1984; Udupa et al., 1993). This may be due to the small number of chickpea genotypes under study, limited streamlined phenotyping methodologies, and evaluation of salinity tolerance at the vegetative phase rather than reproductive phase of growth. The use of geographically diverse material (Maliro et al., 2008; Serraj et al., 2004) and the assessment of salinity tolerance based on seed yield (Krishnamurthy et al., 2011; Pushpavalli et al., 2015a; Turner et al., 2013; Vadez et al., 2007) has since provided evidence that useful genetic variation for salinity tolerance is present in chickpea. This variation can be utilised in breeding programs to improve the salinity tolerance of otherwise adapted chickpea breeding varieties and breeding lines.

1.4.1 Chickpea germplasm

Crop improvement relies heavily on the availability of rich plant genetic resources (Singh, 1987) maintained by different research institutes globally. Most of the world chickpea accessions are held by two members of the Consultative Group on International Agricultural Research (CGIAR) involved in chickpea improvement: The International Crops Research Institute for the Semi-Arid Tropics (ICRISAT) located in India, and the International Centre for Agricultural Research in Dry land Areas (ICARDA) located in Morocco. ICRISAT holds 20,267 accessions of chickpea while ICARDA has 13,462 accessions from 61 countries across five continents (Upadhyaya et al., 2011). The challenges associated with the use of diverse germplasm collections have been ameliorated by the development of core collections and a reference collection designed to represent the range of genetic variability present in the broader chickpea gene pool. It is cost effective, less labour-intensive and more practical to screen for traits of interest in smaller representative collections than in complete germplasm collections.

A number of germplasm collections have been formed to facilitate chickpea improvement. These include; the core collection, mini-core collection, composite collection, and the Reference Set. The core collection containing 1956 chickpea accessions (10% of the accessions from ICRISAT) was established to capture the diversity in the chickpea gene pool based on geographical distribution, origin of the accessions and data on 13 morphological and agronomic traits (Upadhyaya et al., 2001). Afterwards, the mini-core collection (211 accessions) which represents 10% of the core collection (1956 accessions) and 1% of the entire collection held at ICRISAT gene bank was established. The mini-core collection was formed based on data from 22 morphological and agronomic traits (Upadhyaya &Ortiz 2001). A composite collection (2915) consisting of the core collection (1956 accessions) from ICRISAT and 709

cultivated chickpea accessions from ICARDA was formed to represent the genetic diversity in the chickpea germplasm present in the two centres (Upadhyaya et al., 2006).

More recently, a further set of germplasm was established based on molecular marker diversity screening. The Reference Set (300 accessions) was selected based on 48 SSR (simple sequence repeat) markers and is reported to capture 78% of 1683 alleles present in the composite collection (2915 accessions) (Upadhyaya et al., 2008). The Reference Set includes 211 accessions from the mini-core collection. The 300 accessions of the Reference Set consist of geographically diverse material including 267 landraces, 13 advanced lines and cultivars, 7 wild *Cicer* species (*C.reticulutum* and *C. echinospermum*) and 13 accessions whose biological status is unknown. Classification based on seed type, shows the Reference Set consists of 197 desi, 86 kabuli, and 10 pea-shaped lines (Upadhyaya et al., 2008) (Figure 5). Because of the diverse nature of lines in the Reference Set, this collection is ideal for association mapping approaches to identify genomic regions controlling traits of interest. Previous studies show large genetic variation for salinity tolerance exists in the Reference Set (Krishnamurthy et al., 2011; Turner et al., 2013; Vadez et al., 2007), making this germplasm ideal for studying the genetic control of salinity tolerance in chickpea.

1.4.2 Mapping populations for genetic analysis

Different populations including filial generation two (F2), back-cross lines (BC), recombinant inbred lines (RIL), double haploid (DH) (Figure 6) and natural diverse populations can be used for genetic studies. RIL and DH populations are generally preferred for genetic studies because of their homozygous nature, enabling the multiplication and testing across different locations in different years without genetic change (Collard et al., 2005). However, RIL development is time consuming; in some cases taking between four to five years to complete. DH chickpea production has been

achieved in the Australian cultivar Sonali (desi) and Canadian cultivar CDC Xena (kabuli) by the application of different stress treatments on microspore culture (Grewal et al., 2009). Croser et al. (2011) obtained DH pro embryos from the Australian cultivar Rupali. However, there is no research reporting the development of DH pro-embryos into mature chickpea plants capable of generating seed. Using DH lines would minimise the time spent to develop a mapping populations by single seed descent (SSD) (Figure 6), but current protocols for DH chickpea production are expensive (Grewal et al., 2009) and this approach is currently unviable.

Rapid chickpea regeneration enabling the completion of three generations of chickpea in one year is only feasible in short season environments such as India (Gaur et al., 2007; Sethi, 1981). An alternative strategy involves growth under glasshouse conditions to advance beyond the F2 generation under conditions that accelerate development. Recently, researchers at the University of Western Australia have developed methods to accelerate generation time in pulses. This involves precocious germination of immature seed and customising lighting and temperature conditions in the glasshouse. This method allows chickpea generation time to be shortened to 60 days (Dr Janine Croser –personal communication).

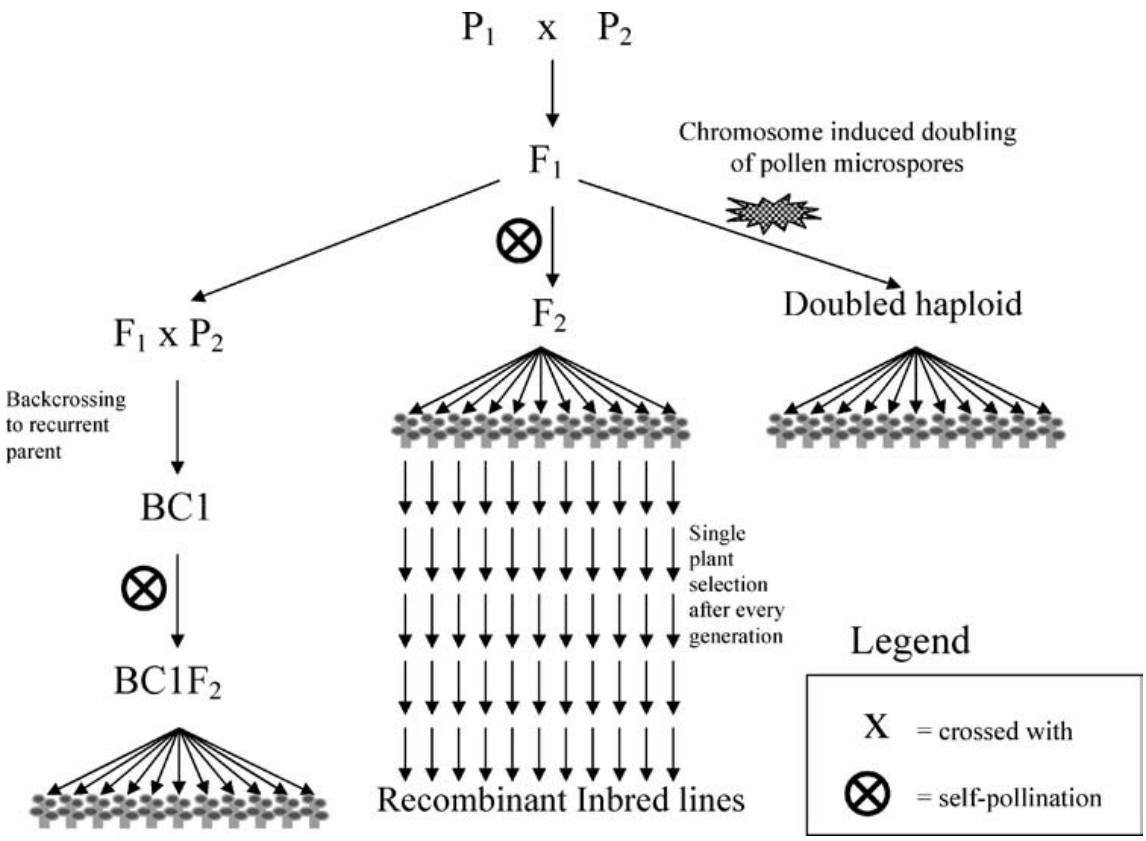

Figure 6: Types of mapping populations for self-pollinating plant species. Quantitative trait loci analysis is mostly conducted in Filial generation 2 (F2), back-cross populations (BC), recombinant inbred lines (RIL) and in double haploid lines (Collard et al., 2005)

Vegetative propagation involving the use of stem cuttings has also been proposed as a means of obtaining identical genetic plant material that could be tested in replicated experiments (Danehloueipour et al., 2006). The stem cutting technique will make it possible to propagate and evaluate chickpea material at the F2 generation, then subsequently utilise SSD to advance clones for the development of RILs. This method could also be used for seed multiplication hence accelerating RIL development (Danehloueipour et al., 2006).

Natural populations can be utilised in association mapping, which relies on historic linkage disequilibrium (LD) (the non-random association of loci) in diverse germplasm collections, to identify functional variants controlling complex traits such as salinity tolerance. Association mapping enables the identification of QTL underlying a trait of

interest in a relatively short period of time as the approach relies on the assembly of germplasm panels rather than the production of experimental populations that require many generation cycles. However, when considering an association mapping approach, it is crucial to account for population structure in the panel under study to avoid the identification of false marker-trait associations (Myles et al., 2009). To date, association mapping approaches have not been utilised to identify genomic regions controlling salinity tolerance in chickpea. This approach may be a useful tool to identify novel QTL and genes underlying salinity tolerance in chickpea.

1.4.3 Molecular markers

Marker assisted-selection (MAS) in any breeding program is facilitated by molecular markers associated with a trait of interest (Varshney and Dubey, 2009). Many DNA markers are based on restriction fragment analysis, hybridisation or amplification by PCR. Hybridisation techniques take time while restriction and amplification of DNA have the possibility of introducing errors and bias in inferring genotypic information from material under study.

DNA markers have been widely used in pulses (Choudhury et al., 2006; Dhanasekar et al., 2010; Muehlbauer et al., 1991). Some of the marker types that have been used in genetic map construction or analysis of genetic diversity in chickpea include; isozyme markers (Ahmad et al., 1992), restriction fragment length polymorphism (RFLP) (Serret et al., 1997), amplified fragment length polymorphism (AFLP) (Shan et al., 2004), random amplification of polymorphic DNA (RAPD) (Ahmad, 1999; Banerjee et al., 2001; Singh et al., 2002; Sonnante et al., 1997), simple sequence repeat (SSR) markers (Pushpavalli et al., 2015b; Sudupak, 2004; Thudi et al., 2011; Upadhyaya et al., 2008; Vadez et al., 2012b; Winter et al., 1999) and diversity array technology (DArT) markers (Thudi et al., 2011).

Due to the narrow genetic base in cultivated chickpea, most DNA marker technologies have not been effective in identifying sufficient polymorphism between chickpea genotypes. Due to their polymorphic and co-dominant nature (Gupta et al., 2010), SSR markers have been utilised in constructing genetic linkage maps to identify QTL controlling salinity tolerance (Pushpavalli et al., 2015b; Vadez et al., 2012b) as well as in characterising the diversity and allelic richness in the chickpea composite collection to form the Reference Set (Upadhyaya et al., 2008).

Single nucleotide polymorphisms (SNPs) markers are the marker of choice because of their abundant nature and transferability across platforms and breeding populations. Several studies have identified numerous SNP markers in the chickpea genome (Gujaria et al., 2011; Hiremath et al., 2011; Rajesh and Muehlbauer, 2008; Varshney and Dubey, 2009; Varshney et al., 2013). Large-scale marker discovery, high-throughput genotyping and draft genome sequences (Jain et al., 2013; Varshney et al., 2013) have made it possible to construct high-resolution genetic linkage maps in chickpea. Advances have mostly been made in inter-specific genetic maps (Gaur et al., 2015; Gaur et al., 2012; Gujaria et al., 2011; Hiremath et al., 2012; Nayak et al., 2010). Few studies have successfully developed intra-specific high-density genetic linkage maps (Kujur et al., 2015; Verma et al., 2015) but generally the populations utilised to identify these SNPs and construct genetic maps are not suitable for the mapping of salinity tolerance in chickpea because the genotypes chosen do not differ in their ability to tolerate soil salinity.

1.4.4 Genetic control of tolerance to salinity

Salinity tolerance is a polygenic trait with complex underlying genetic and physiological control (Flowers and Flowers, 2005). Breeding for salt tolerant cultivars is only possible with an increased understanding of genetic basis of salinity tolerance. QTL for salinity

tolerance have been mapped in crops such as tomato (Foolad et al., 2001), soybean (Lee et al., 2004), rice (Campbell et al., 2015; Flowers et al., 2000; Koyama et al., 2001; Wang et al., 2012), barley (Eleuch et al., 2008; Saade et al., 2016; Xu et al., 2012) and wheat (Genc et al., 2010; Shahzad et al., 2012). Similarly, loci associated with salinity tolerance have been identified in *Medicago truncatula* (Arraouadi et al., 2012) and *Medicago sativa* (Yu et al., 2016) with chromosome 1 harbouring major QTL in both studies.

To date, only three studies have focussed on identifying QTL underlying salinity tolerance in chickpea (Pushpavalli et al., 2015b; Samineni, 2010; Vadez et al., 2012b). Using recombinant inbred lines (RIL) developed between Indian adapted genotypes, Vadez et al. (2012b) found loci on chromosome 6 and chromosome 3 to control seed yield and seed yield components, respectively, under salt while Pushpavalli et al. (2015b) identified two key genomic regions on chromosome 5 and chromosome 7, which control salinity tolerance related traits in chickpea. Samineni (2010) study did not detect any major QTL. This study found 20 QTL for different traits explaining less than 10% of phenotypic variation. Besides the low resolution in genomic regions identified due to the small number of SSR markers used for map construction, these studies were limited in the number of traits under study due to phenotyping platform utilised.

Environmental factors are known to influence the expression of phenotype. It is imperative to conduct phenotyping in multiple seasons to ensure stable QTL are obtained, which can be laborious and time consuming. Hence, there is a need to combine a streamlined high-throughput phenotyping system with high density SNP information to identify genomic regions controlling salinity tolerance in different sets of germplasm.

1.5 Research Aims

The generation of high density SNP information, using the recently completed chickpea draft genome sequence, provides an excellent opportunity to identify QTL for salinity tolerance in chickpea. This research aims to address the gaps in our current understanding of the genetic basis of salinity tolerance. Currently only three studies have identified QTL for physiological and agronomic traits in chickpea, each using bi-parental populations derived from genotypes adapted to Indian environments. Additionally, there is no research reporting association mapping for traits associated with salinity tolerance in chickpea. Last but not least, robust phenotyping methodology is needed for generating quality phenotypic data for genome-wide association mapping and linkage mapping.

To address these research aims, we asked the following questions:

1. What is the level of genetic variation for salinity tolerance in chickpea germplasm using high-throughput precision phenotyping?
2. What tolerance mechanisms and key traits drive salinity tolerance in the chickpea germplasm?
3. What genomic regions and gene(s) underlie salinity tolerance in chickpea?

References

Australian Bureau of Statistics, 2002: Salinity on Australian farms. Retrieved from: http://www.abs.gov.au/ausstats/abs@.nsf/mf/4615.0. Accessed on: August 3, 2016

Ahmad, F., 1999: Random amplified polymorphic DNA (RAPD) analysis reveals genetic relationships among the annual Cicer species. Theoretical and Applied Genetics 98, 657-663.

Ahmad, F., P.M. Gaur, and A.E. Slinkard, 1992: Isozyme polymorphism and phylogenetic interpretations in the genus Cicer L. Theoretical and Applied Genetics 83, 620-627.

Al-Mutata, M., 2003: Effect of salinity on germination and seedling growth of chickpea (Cicer arietinum) genotypes. Int. J. Agric. Biol. 5, 226-229.

Ali, M.Y., L. Krishnamurthy, N.P. Saxena, O.P. Rupela, J. Kumar, and C. Johansen, 2002: Scope for genetic manipulation of mineral acquisition in chickpea. Plant and Soil 245, 123-134.

ANRA, 2001: Australian Natural Resources Atlas. Retrieved from https://data.gov.au/dataset/australian-dryland-salinity-assessment-spatial-data-12500000-nlwra-2001. Accessed on August 2,2016

ANZECC, 2001: Implications of Salinity for Biodiversity Conservation and Management. Prepared for ANZECC by a Task Force established by the Standing Committee on Conservation. Retrived from: http://www.environment.nsw.gov.au/projects/ImpactsOfSalinityOnBiodiversity.htm. Accessed on: August 3, 2016

Arraouadi, S., M. Badri, C. Abdelly, T. Huguet, and M.E. Aouani, 2012: QTL mapping of physiological traits associated with salt tolerance in Medicago truncatula Recombinant Inbred Lines. Genomics 99, 118-125.

Arumuganathan, K., and E.D. Earl, 1991: Nuclear DNA content of some important plant species. Plant Mol. Biol. Rep. 9, 208-218.

Banerjee, H., R.A. Pai, J.P. Moss, and R.P. Sharma, 2001: Use of random amplified polymorphic DNA markers for mapping the chickpea genome. Biologia Plantarum 44, 195-202.

Boursiac, Y., S. Chen, D.T. Luu, M. Sorieul, N. van den Dries, and C. Maurel, 2005: Early effects of salinity on water transport in Arabidopsis roots. Molecular and cellular features of aquaporin expression. Plant Physiol 139, 790-805.

Campbell, M.T., A.C. Knecht, B. Berger, C.J. Brien, D. Wang, and H. Walia, 2015: Integrating Image-Based Phenomics and Association Analysis to Dissect the Genetic Architecture of Temporal Salinity Responses in Rice. Plant Physiology 168, 1476-U1697.

Charles, M.T., R. Dominique, J. Kumar, and O.P. Dangi, 2002: A preliminary study of the functional properties of chickpea leaves. Annual Meeting of the Canadian Society of Food and Nutrition, May 20002.

Choudhury, P.R., B. George, L.K. Tiwari, A.K. Verma, N.P. Singh, and P.S. Kendurkar, 2006: Genetic relationship among wild and cultivated pigeonpea employing polymorphic DNA markers. Indian Journal of Agricultural Biochemistry 19, 53-57.

Collard, B.C.Y., M.Z.Z. Jahufer, J.B. Brouwer, and E.C.K. Pang, 2005: An introduction to markers, quantitative trait loci (QTL) mapping and marker-assisted selection for crop improvement: The basic concepts. Euphytica 142, 169-196.

Croser, J.S., M.M. Lulsdorf, R.K. Grewal, K.M. Usher, and K.H.M. Siddique, 2011: Isolated microspore culture of chickpea (Cicer arietinum L.): Induction of androgenesis and cytological analysis of early haploid divisions. In Vitro Cellular and Developmental Biology - Plant 47, 357-368.

Danehloueipour, N., G. Yan, H.J. Clarke, and K.H.M. Siddique, 2006: Successful stem cutting propagation of chickpea, its wild relatives and their interspecific hybrids. Australian Journal of Experimental Agriculture 46, 1349-1354.

Dhanasekar, P., K.N. Dhumal, and K.S. Reddy, 2010: Identification of RAPD markers linked to plant type gene in pigeonpea. Indian Journal of Biotechnology 9, 58-63.

Eleuch, L., A. Jilal, S. Grando, S. Ceccarelli, M. Schmising, H. Tsujimoto, A. Hajer, A. Daaloul, and M. Baum, 2008: Genetic diversity and association analysis for salinity tolerance, heading date and plant height of barley germplasm using simple sequence repeat markers. J Integr Plant Biol 50, 1004-14.

Esechie, H.A., A. Al-Saidi, and S. Al-Khanjari, 2002: Effect of Sodium Chloride Salinity on Seedling Emergence in Chickpea. Journal of Agronomy and Crop Science 188, 155-160.

FAO, 2008: Land and Plant Nutrition Management Service. Retrieved from: http://www.fao.org/ag/agl/agll/spush. Accessed on: July 14,2016

FAOSTAT, 2011: Agriculture database. Retrieved from: http:/appsfaoorg/page/collections?subset=agriculture. Accessed on: March 16, 2014

FAOSTAT, 2014: Agriculture database. Retrieved from: http://faostat3.fao.org/download/Q/QC/E 11/2/2016. Accessed on: August 3, 2016

Flowers, T.J., and S.A. Flowers, 2005: Why does salinity pose such a difficult problem for plant breeders? Agricultural Water Management 78, 15-24.

Flowers, T.J., M.L. Koyama, S.A. Flowers, C. Sudhakar, K.P. Singh, and A.R. Yeo, 2000: QTL: their place in engineering tolerance of rice to salinity. J Exp Bot 51, 99-106.

Flowers, T.J., P.M. Gaur, C.L. Gowda, L. Krishnamurthy, S. Samineni, K.H. Siddique, N.C. Turner, V. Vadez, R.K. Varshney, and T.D. Colmer, 2010: Salt sensitivity in chickpea. Plant Cell Environ 33, 490-509.

Foolad, M.R., L.P. Zhang, and G.Y. Lin, 2001: Identification and validation of QTLs for salt tolerance during vegetative growth in tomato by selective genotyping. Genome 44, 444-54.

Fricke, W., 2004: Rapid and tissue-specific accumulation of solutes in the growth zone of barley leaves in response to salinity. Planta 219, 515-25.

Gaur, P., S. Srinivasan, G. CLL, and R. BV, 2007: Rapid generation advancement in chickpea. International Crops Research Institute for the Semi-Arid Tropics (ICRISAT), Patancheru 502 324, Andhra Pradesh, India.

Gaur, R., G. Jeena, N. Shah, S. Gupta, S. Pradhan, A.K. Tyagi, M. Jain, D. Chattopadhyay, and S. Bhatia, 2015: High density linkage mapping of genomic and transcriptomic SNPs for synteny analysis and anchoring the genome sequence of chickpea. Sci Rep 5, 13387.

Gaur, R., S. Azam, G. Jeena, A.W. Khan, S. Choudhary, M. Jain, G. Yadav, A.K. Tyagi, D. Chattopadhyay, and S. Bhatia, 2012: High-throughput SNP discovery and genotyping for constructing a saturated linkage map of chickpea (Cicer arietinum L.). DNA Res 19, 357-73.

Genc, Y., K. Oldach, A.P. Verbyla, G. Lott, M. Hassan, M. Tester, H. Wallwork, and G.K. McDonald, 2010: Sodium exclusion QTL associated with improved seedling growth in bread wheat under salinity stress. Theor Appl Genet 121, 877-94.

Gill, J., S. , D. Nandal, M.T. Luna, M. A., and D. Hero., 1996: Variability of some physic-chemical characters in Desi and Kabuli chickpea types. J. Sci. Food Agric. 71, 179-184.

GRDC, 2012: An Economic Analysis of GRDC Investment in the National Chickpea Breeding Program. Accessed on August 3, 2016

Grewal, R.K., M. Lulsdorf, J. Croser, S. Ochatt, A. Vandenberg, and T.D. Warkentin, 2009: Doubled-haploid production in chickpea (Cicer arietinum L.): Role of stress treatments. Plant Cell Reports 28, 1289-1299.

Gujaria, N., A. Kumar, P. Dauthal, A. Dubey, P. Hiremath, A. Bhanu Prakash, A. Farmer, M. Bhide, T. Shah, P.M. Gaur, H.D. Upadhyaya, S. Bhatia, D.R. Cook, G.D. May, and R.K. Varshney, 2011: Development and use of genic molecular markers (GMMs) for construction of a transcript map of chickpea (Cicer arietinum L.). Theor Appl Genet 122, 1577-89.

Gupta, P.K., H.S. Balyan, and R.K. Varshney, 2010: Quantitative genetics and plant genomics: An overview. Molecular Breeding 26, 133-134.

Hiremath, P.J., A. Kumar, R.V. Penmetsa, A. Farmer, J.A. Schlueter, S.K. Chamarthi, A.M. Whaley, N. Carrasquilla-Garcia, P.M. Gaur, H.D. Upadhyaya, P.B. Kavi Kishor, T.M. Shah, D.R. Cook, and R.K. Varshney, 2012: Large-scale development of cost-effective SNP marker assays for diversity assessment and genetic mapping in chickpea and comparative mapping in legumes. Plant Biotechnol J 10, 716-32.

Hiremath, P.J., A. Farmer, S.B. Cannon, J. Woodward, H. Kudapa, R. Tuteja, A. Kumar, A. Bhanuprakash, B. Mulaosmanovic, N. Gujaria, L. Krishnamurthy, P.M. Gaur, P.B. Kavikishor, T. Shah, R. Srinivasan, M. Lohse, Y. Xiao, C.D. Town, D.R. Cook, G.D. May, and R.K. Varshney, 2011: Large-scale transcriptome analysis in chickpea (Cicer arietinum L.), an orphan legume crop of the semi-arid tropics of Asia and Africa. Plant Biotechnol J 9, 922-31.

Ibrikci, H., K. S., and G. MA., 2003: Chickpea leaves as a vegetable green for humans: evaluation of mineral composition. Journal of the Science of Food and Agriculture 83, 945-950.

Jain, M., G. Misra, R.K. Patel, P. Priya, S. Jhanwar, A.W. Khan, N. Shah, V.K. Singh, R. Garg, G. Jeena, M. Yadav, C. Kant, P. Sharma, G. Yadav, S. Bhatia, A.K. Tyagi, and D. Chattopadhyay, 2013: A draft genome sequence of the pulse crop chickpea (Cicer arietinum L.). Plant J 74, 715-29.

Jardine, A., M. Corkeron, and P. Weinstein, 2011: Dryland salinity and vector-borne disease emergence in southwestern Australia. Environ Geochem Health 33, 363-70.

Johansen, C., N.P. Saxena, Y.S. Chauhan, G.V. Subba Rao, R.P.S. Pundir, J.V.D.K. Kumar Rao, and M.K. Jana, 1990: Genotypic variation in salinity response of chickpea and pigeonpea. In: Sinha, S.K., Sane, P.V., Bhargava, S.C., Agrawal, P.K. (Eds.), Proceedings of the International Congress of Plant Physiology. Indian Society for Plant Physiology and Biochemistry, Indian Agriculture Research Institute, New Delhi. 1, 977-983.

Jukanti, A.K., P.M. Gaur, C.L. Gowda, and R.N. Chibbar, 2012: Nutritional quality and health benefits of chickpea (Cicer arietinum L.): a review. Br J Nutr 108 Suppl 1, S11-26.

Katerji, N., Van Hoorn JW, Hamdy A, Mastrorilli M, Owies T, and M. RS, 2001: Response to soil salinity of chickpea varieties differing in drought tolerance. Agr. Water Manage 50, 83-96.

Kaya, M., G. Kaya, M.D. Kaya, M. Atak, S. Saglam, K.M. Khawar, and C.Y. Ciftci, 2008: Interaction between seed size and NaCl on germination and early seedling growth of some Turkish cultivars of chickpea (Cicer arietinum L.). Journal of Zhejiang University 9, 371-377.

Khan, H.A., K.H.M. Siddique, and T.D. Colmer, 2016: Salt sensitivity in chickpea is determined by sodium toxicity. Planta, 1-15.

Knights, E., and K. Siddique, 2002: Chickpea status and production constraints in Australia. In ‘Integrated Management of Botrytis Grey Mould of Chickpea in Bangladesh and Australia: Summary Proceedings of a Project Inception Workshop (Bangladesh Agricultural Research Institute (BARI): Joydebpur, Gazipur; and

Centre for Legumes in Mediterranean Agriculture (CLIMA): Crawley, W. Aust.). (Eds MA Bakr KHM Siddique, C Johansen), 33-41.

Kotula, L., H.A. Khan, J. Quealy, N.C. Turner, V. Vadez, K.H.M. Siddique, P.L. Clode, and T.D. Colmer, 2015: Salt sensitivity in chickpea (Cicer arietinumL.): ions in reproductive tissues and yield components in contrasting genotypes. Plant Cell and Environment 38, 1565-1577.

Koyama, M.L., A. Levesley, R.M. Koebner, T.J. Flowers, and A.R. Yeo, 2001: Quantitative trait loci for component physiological traits determining salt tolerance in rice. Plant Physiol 125, 406-22.

Krishnamurthy, L., N.C. Turner, P.M. Gaur, H.D. Upadhyaya, R.K. Varshney, K.H.M. Siddique, and V. Vadez, 2011: Consistent Variation Across Soil Types in Salinity Resistance of a Diverse Range of Chickpea (Cicer arietinum L.) Genotypes. Journal of Agronomy and Crop Science 197, 214-227.

Kujur, A., H.D. Upadhyaya, T. Shree, D. Bajaj, S. Das, M.S. Saxena, S. Badoni, V. Kumar, S. Tripathi, C.L. Gowda, S. Sharma, S. Singh, A.K. Tyagi, and S.K. Parida, 2015: Ultra-high density intra-specific genetic linkage maps accelerate identification of functionally relevant molecular tags governing important agronomic traits in chickpea. Sci Rep 5, 9468.

Kumar, D., 1985: Emergence, establishment and seed yield of chickpea as affected by sodicity. Annals of Arid Zone 24, 334-340.

Lauter, D.J., and D.N. Munns, 1986: Water loss via the glandular trichomes of chickpea (Cicer arietinum L.). Journal of Experimental Botany 37, 640-649.

Lee, G.J., T.E. Carter, Jr., M.R. Villagarcia, Z. Li, X. Zhou, M.O. Gibbs, and H.R. Boerma, 2004: A major QTL conditioning salt tolerance in S-100 soybean and descendent cultivars. Theor Appl Genet 109, 1610-9.

Maas, E.V., and G.J. Hoffman, 1977: CROP SALT TOLERANCE - CURRENT ASSESSMENT. ASCE J Irrig Drain Div 103, 115-134.

Maliro, M.F.A., D. McNeil, B. Redden, J.F. Kollmorgen, and C. Pittock, 2008: Sampling strategies and screening of chickpea (Cicer arietinum L.) germplasm for salt tolerance. Genetic Resources and Crop Evolution 55, 53-63.

Millan, T., H.J. Clarke, K.H.M. Siddique, H.K. Buhariwalla, P.M. Gaur, J. Kumar, J. Gil, G. Kahl, and P. Winter, 2006: Chickpea molecular breeding: New tools and concepts. Euphytica 147, 81-103.

Muehlbauer, G.J., P.E. Staswick, J.E. Specht, G.L. Graef, R.C. Shoemaker, and P. Keim, 1991: RFLP mapping using near-isogenic lines in the soybean [Glycine max (L.) Merr.]. Theoretical and Applied Genetics 81, 189-198.

Munns, R., and J.B. Passioura, 1984: Hydraulic Resistance of Plants. III. Effects of NaCl in Barley and Lupin. Functional Plant Biology 11, 351-359.

Munns, R., and M. Tester, 2008: Mechanisms of salinity tolerance 59, 651-681.

Myles, S., J. Peiffer, P.J. Brown, E.S. Ersoz, Z. Zhang, D.E. Costich, and E.S. Buckler, 2009: Association mapping: critical considerations shift from genotyping to experimental design. The Plant cell 21.

Nawaz, K., Hussain K, Majeed A, A.S. Khan F, and A. K, 2010: Fatality of salt stress to plants:Morphological, physiological and biochemical aspects. Afr. J. Biotechnol 9, 5475-5480.

Nayak, S.N., H. Zhu, N. Varghese, S. Datta, H.K. Choi, R. Horres, R. Jungling, J. Singh, P.B. Kishor, S. Sivaramakrishnan, D.A. Hoisington, G. Kahl, P. Winter, D.R. Cook, and R.K. Varshney, 2010: Integration of novel SSR and gene-based SNP marker loci in the chickpea genetic map and establishment of new anchor points with Medicago truncatula genome. Theor Appl Genet 120, 1415-41.

NLWRA, 2001: Australian Dryland Salinity Assessment 2000: Extent, Impacts, Processes, Monitoring and Management Options, NLWRA, Canberra.

Parween, S., K. Nawaz, R. Roy, A.K. Pole, B.V. Suresh, G. Misra, M. Jain, G. Yadav, S.K. Parida, A.K. Tyagi, S. Bhatia, and D. Chattopadhyay, 2015: An advanced draft genome assembly of a desi type chickpea (Cicer arietinum L.). Scientific Reports 5.

Puniran-Hartley, N., J. Hartley, L. Shabala, and S. Shabala, 2014: Salinity-induced accumulation of organic osmolytes in barley and wheat leaves correlates with increased oxidative stress tolerance: In planta evidence for cross-tolerance. Plant Physiology and Biochemistry 83, 32-39.

Pushpavalli, R., M. Zaman-Allah, N.C. Turner, R. Baddam, M.V. Rao, and V. Vadez, 2015a: Higher flower and seed number leads to higher yield under water stress conditions imposed during reproduction in chickpea. Functional Plant Biology 42, 162-174.

Pushpavalli, R., L. Krishnamurthy, M. Thudi, P.M. Gaur, M.V. Rao, K.H.M. Siddique, T.D. Colmer, N.C. Turner, R.K. Varshney, and V. Vadez, 2015b: Two key genomic regions harbour QTLs for salinity tolerance in ICCV 2 x JG 11 derived chickpea (Cicer arietinum L.) recombinant inbred lines. Bmc Plant Biology 15.

Rajesh, P.N., and F.J. Muehlbauer, 2008: Discovery and detection of single nucleotide polymorphism (SNP) in coding and genomic sequences in chickpea (Cicer arietinum L.). Euphytica 162, 291-300.

Rao, P., Birthal PS, Bhagavatula, S and Bantilan, MCS, 2010: Chickpea and Pigeonpea Economies in Asia: Facts, Trends and Outlook Retrieved from oar.icrisat.org/191/1/98 2010 B049 CP and PP.pdf Accessed on: August 3, 2016

Rengasamy, P., 2002: Transient salinity and subsoil constraints to dryland farming in Australian sodic soils: an overview. Australian Journal of Experimental Agriculture 42, 351-361.

Rengasamy, P., 2006: World salinization with emphasis on Australia. J Exp Bot 57, 1017-23.

Roy, S.J., S. Negrão, and M. Tester, 2014: Salt resistant crop plants. Current Opinion in Biotechnology 26, 115-124.

Rupela, O.P., and J.V.D.K.K. Rao, 1987: Effects of Drought, Temperature, and Salinity on Symbiotic Nitrogen Fixation in Legumes, with Emphasis on Chickpea and Pigeonpea.

Saade, S., A. Maurer, M. Shahid, H. Oakey, S.M. Schmöckel, S. Negrão, K. Pillen, and M. Tester, 2016: Yield-related salinity tolerance traits identified in a nested association mapping (NAM) population of wild barley. Scientific Reports 6, 32586.

Samineni, S., 2010: Physiology, genetics and molecular mapping of salt tolerance in chickpea (Cicer arietinum. L). PhD thesis, The University of Western Australia.

Samineni, S., K.H.M. Siddique, P.M. Gaur, and T.D. Colmer, 2011: Salt sensitivity of the vegetative and reproductive stages in chickpea (Cicer arietinum L.): Podding is a particularly sensitive stage. Environmental and Experimental Botany 71, 260-268.

Saxena, N., 1990: Status of chickpea in the Mediterranean basin. In: Present Status and Future Prospects of Chickpea Crop Production and Improvement in the Mediterranean Countries. Options Méditerr. (CIHEAM) Ser., A 9, 17-24.

Saxena, N.P., 1984: Chickpea. In: Goldworthy, Fisher, (Eds.), The Physiology of Tropical Field Crops. John Wiley & Sons Ltd., New York, 419-452.

Sekeroglu, N., S.M. Kara, D. O., and T. Askin, 1999: Effect of salinity on germination, early seedling growth, Na and K constituents in chickpea. Turkish J. Field Crops 4, 79-84.

Serraj, R., L. Krishnamurthy, and H.D. Upadhyaya, 2004: Screening chickpea mini-core germplasm for tolerance to salinity. Int. Chickpea Pigeonpea. Newslett 11, 29-32.

Serret, M.D., S.M. Udupa, and F. Weigand, 1997: Assessment of genetic diversity of cultivated chickpea using microsatellite-derived RFLP markers: Implications for origin. Plant Breeding 116, 573-578.

Sethi, S.C., 1981: Photoperiodic response and accelerated generation turnover in chickpea. Field crops research 4, 215-225.

Shahzad, A., M. Ahmad, M. Iqbal, I. Ahmed, and G.M. Ali, 2012: Evaluation of wheat landrace genotypes for salinity tolerance at vegetative stage by using morphological and molecular markers. Genet Mol Res 11, 679-92.

Shan, F., H. Clarke, G. Yan, J.A. Plummer, and K.H.M. Siddique, 2004: Development of DNA fingerprinting keys for discrimination of Cicer echinospermum (P.H. Davis) accessions using AFLP markers. Australian Journal of Agricultural Research 55, 947-952.

Siddique, K.H.M., and J. Sykes, 1997: Grain legume production in Australia: past, present and future. In: Proceedings of the Australia Pulse Industry Workshop, August 20, 1996, Fremantle, Perth., 36-50.

Singh, K.B., 1987: Chickpea breeding. p. 127–162. In M.C. Saxena and K.B Singh, (ed.) The Chickpea. C.A.B. International, Wallingford, UK.

Singh, R., C.D. Prasad, V. Singhal, and G.J. Randhawa, 2002: Analysis of genetic diversity in Cicer arietinum L using random amplified polymorphic DNA markers. Journal of Plant Biochemistry and Biotechnology 11, 109-112.

Soltani, A., S. Galeshi, E. Zeinali, and N. Latifi, 2002: Germination, seed reserve utilization and seedling growth of chickpea as affected by salinity and seed size. Seed Science and Technology 30, 51-60.

Sonnante, G., A. Marangi, G. Venora, and D. Pignone, 1997: Using RAPD markers to investigate genetic variation in chickpea. Journal of Genetics and Breeding 51, 303-307.

Sudupak, M.A., 2004: Inter and intra-species Inter Simple Sequence Repeat (ISSR) variations in the genus Cicer. Euphytica 135, 229-238.

Thudi, M., A. Bohra, S.N. Nayak, N. Varghese, T.M. Shah, R.V. Penmetsa, N. Thirunavukkarasu, S. Gudipati, P.M. Gaur, P.L. Kulwal, H.D. Upadhyaya, P.B. KaviKishor, P. Winter, G. Kahl, C.D. Town, A. Kilian, D.R. Cook, and R.K. Varshney, 2011: Novel SSR Markers from BAC-End Sequences, DArT Arrays and a Comprehensive Genetic Map with 1,291 Marker Loci for Chickpea (Cicer arietinum L.). PLoS ONE 6.

Turner, N.C., T.D. Colmer, J. Quealy, R. Pushpavalli, L. Krishnamurthy, J. Kaur, G. Singh, K.H.M. Siddique, and V. Vadez, 2013: Salinity tolerance and ion accumulation in chickpea (Cicer arietinum L.) subjected to salt stress. Plant and Soil 365, 347-361.

Udupa, S., Sharma A, S. RP, and P. RA, 1993: Narrow genetic variability in Cicer arietinum as revealed by RFLP analysis. Journal of Plant Biochemistry and Biotechnology 2, 83-86.

Upadhyaya, H.D., P.J. Bramel, and S. Singh, 2001: Development of a Chickpea Core Subset Using Geographic Distribution and Quantitative Traits. Crop Science 41, 206-210.

Upadhyaya, H.D., M. Thudi, N. Dronavalli, N. Gujaria, S. Singh, S. Sharma, and R.K. Varshney, 2011: Genomic tools and germplasm diversity for chickpea improvement. Plant Genetic Resources: Characterisation and Utilisation 9, 45-58.

Upadhyaya, H.D., S.L. Dwivedi, M. Baum, R.K. Varshney, S.M. Udupa, C.L. Gowda, D. Hoisington, and S. Singh, 2008: Genetic structure, diversity, and allelic richness in composite collection and reference set in chickpea (Cicer arietinum L.). BMC Plant Biology 8.

Upadhyaya, H.D., B.J. Furman, S.L. Dwivedi, S.M. Udupa, C.L.L. Gowda, M. Baum, J.H. Crouch, H.K. Buhariwalla, and S. Singh, 2006: Development of a composite collection for mining germplasm possessing

allelic variation for beneficial traits in chickpea. Plant Genetic Resources: Characterisation and Utilisation 4, 13-19.

US laboratory staff, 1954: Diagnosis and improvement of saline and alkali soils. USDA Handbook 60, U.S. Government Printing Office, Washington, D. C.

Vadez, V., L. Krishnamurthy, R. Serraj, P.M. Gaur, H.D. Upadhyaya, D.A. Hoisington, R.K. Varshney, N.C. Turner, and K.H.M. Siddique, 2007: Large variation in salinity tolerance in chickpea is explained by differences in sensitivity at the reproductive stage. Field Crops Research 104, 123-129.

Vadez, V., M. Rashmi, K. Sindhu, M. Muralidharan, R. Pushpavalli, N.C. Turner, L. Krishnamurthy, P.M. Gaur, and T.D. Colmer, 2012a: Large number of flowers and tertiary branches, and higher reproductive success increase yields under salt stress in chickpea. European Journal of Agronomy 41, 42-51.

Vadez, V., L. Krishnamurthy, M. Thudi, C. Anuradha, T.D. Colmer, N.C. Turner, K.H.M. Siddique, P.M. Gaur, and R.K. Varshney, 2012b: Assessment of ICCV 2 × JG 62 chickpea progenies shows sensitivity of reproduction to salt stress and reveals QTL for seed yield and yield components. Molecular Breeding 30, 9-21.

Varshney, R.K., and A. Dubey, 2009: Novel genomic tools and modern genetic and breeding approaches for crop improvement. Journal of Plant Biochemistry and Biotechnology 18, 127-138.

Varshney, R.K., C. Song, R.K. Saxena, S. Azam, S. Yu, A.G. Sharpe, S. Cannon, J. Baek, B.D. Rosen, B. Tar'an, T. Millan, X. Zhang, L.D. Ramsay, A. Iwata, Y. Wang, W. Nelson, A.D. Farmer, P.M. Gaur, C. Soderlund, R.V. Penmetsa, C. Xu, A.K. Bharti, W. He, P. Winter, S. Zhao, J.K. Hane, N. Carrasquilla-Garcia, J.A. Condie, H.D. Upadhyaya, M.C. Luo, M. Thudi, C.L. Gowda, N.P. Singh, J. Lichtenzveig, K.K. Gali, J. Rubio, N. Nadarajan, J. Dolezel, K.C. Bansal, X. Xu, D. Edwards, G. Zhang, G. Kahl, J. Gil, K.B. Singh, S.K. Datta, S.A. Jackson, J. Wang, and D.R. Cook, 2013: Draft genome sequence of chickpea (Cicer arietinum) provides a resource for trait improvement. Nat Biotechnol 31, 240-6.

Verma, S., S. Gupta, N. Bandhiwal, T. Kumar, C. Bharadwaj, and S. Bhatia, 2015: High-density linkage map construction and mapping of seed trait QTLs in chickpea (Cicer arietinum L.) using Genotyping-by-Sequencing (GBS). Sci Rep 5, 17512.

Wang, Z., J. Cheng, Z. Chen, J. Huang, Y. Bao, J. Wang, and H. Zhang, 2012: Identification of QTLs with main, epistatic and QTL x environment interaction effects for salt tolerance in rice seedlings under different salinity conditions. Theor Appl Genet 125, 807-15.

Winter, P., T. Pfaff, S.M. Udupa, B. Hüttel, P.C. Sharma, S. Sahi, R. Arreguin-Espinoza, F. Weigand, F.J. Muehlbauer, and G. Kahl, 1999: Characterization and mapping of sequence-tagged microsatellite sites in the chickpea (Cicer arietinum L.) genome. Molecular and General Genetics 262, 90-101.

Xu, R., J. Wang, C. Li, P. Johnson, C. Lu, and M. Zhou, 2012: A single locus is responsible for salinity tolerance in a Chinese landrace barley (Hordeum vulgare L.). PLoS One 7, e43079.

Yu, L.-X., X. Liu, W. Boge, and X.-P. Liu, 2016: Genome-Wide Association Study Identifies Loci for Salt Tolerance during Germination in Autotetraploid Alfalfa (Medicago sativa L.) Using Genotyping-by-Sequencing. Frontiers in Plant Science 7, 956.

Chapter 2

Exploring genetic variation for salinity tolerance in chickpea using image-based phenotyping

Judith Atieno[1], Yongle Li[2], Peter Langridge[2], Kate Dowling[3], Chris Brien[3], Bettina Berger[3], Rajeev K Varshney[4] and Tim Sutton[5]*

[1] Australian Centre for Plant Functional Genomics, School of Agriculture, Food and Wine, University of Adelaide, Waite Campus, PMB 1, Glen Osmond, SA 5064, Australia

[2] School of Agriculture, Food and Wine, University of Adelaide, Waite Campus, PMB1, Glen Osmond, SA 5064, Australia

[3] The Plant Accelerator, School of Agriculture, Food and Wine, University of Adelaide, Waite Campus, PMB1, Glen Osmond, SA 5064, Australia

[4] Centre of Excellence in Genomics, International Crops Research Institute for the Semi-Arid Tropics (ICRISAT), Patancheru, India

[5] South Australian Research and Development Institute, GPO Box 397 Adelaide, South Australia, 5001, Australia and School of Agriculture, Food and Wine, University of Adelaide, Waite Campus, PMB1, Glen Osmond, SA 5064, Australia

*Corresponding author: tim.sutton.sa.gov.au

Statement of Authorship

Title of Paper	Exploring genetic variation for salinity tolerance in chickpea using image-based phenotyping
Publication Status	☐ Published ☐ Accepted for Publication ☑ Submitted for Publication ☐ Unpublished and Unsubmitted work written in manuscript style
Publication Details	Genetic variation for salinity tolerance in a diverse collection of chickpea was evaluated using an image-based high-throughput phenotyping platform. Shoot-ion independent stress and shoot ion dependent stress mechanisms were demonstrated to exist in chickpea. Seed number under salinity was found to be highly associated with salinity tolerance in chickpea.

Candidate contribution

Name of Candidate	Judith Akinyi Atieno
Contribution to the Paper	Contributed to the conception and design of this experiment. Developed methods for growing chickpea under controlled environment, including finding suitable growing media, watering regime, temperature and lighting conditions and pest control. Developed methods for salinity screening (optimal salt levels, salt delivery system, and symptoms scoring). Conducted salinity experiment including daily watering of plants to field capacity to maintain salt concentration in pots. Designed and conducted field trials to complement findings under controlled conditions. Performed all statistical analyses and interpreted data. Prepared all table and figures. Wrote the manuscript. This work took approximately 18 months.
Overall percentage (%)	80
Certification:	This paper reports on original research I conducted during the period of my Higher Degree by Research candidature and is not subject to any obligations or contractual agreements with a third party that would constrain its inclusion in this thesis.
Candidate signature	Date: 29/11/16
Principal supervisor signature	Date: 29/11/16

Statement of Authorship

Title of Paper: Exploring genetic variation for salinity tolerance in chickpea using image-based phenotyping

Publication Status: Submitted for Publication

Citation: Atieno J, Li Y, Langridge P, Berger B, Brien C, Dowling K, Varshney R.K, Sutton, T (under review in Scientific Reports). Exploring genetic variation for salinity tolerance in chickpea using image-based phenotyping.

Author Contributions

By signing the Statement of Authorship, each author certifies that their stated contribution to the publication is accurate and permission is granted for the publication to be included in the candidate's thesis.

Judith Atieno: Developed methods for growing chickpea under controlled environment, developed methods for salinity screening, conducted salinity experiment in the glasshouse and field, analysed and interpreted data, and wrote the manuscript.

Signature **Date** 23/11/2016

Yongle Li: Supervised the work, designed field experiment, conducted field experiment and data analysis, provided support in data interpretation provided critical comments on the manuscript and edited the manuscript.

Signature **Date** 22/11/2016

Peter Langridge: Supervised the work, evaluated the development of experiments, provided support in data interpretation, provided critical comments on the manuscript and edited the manuscript.

Signature **Date 18/11/2016**

Bettina Berger: Supervised glasshouse experiment, provided critical comments on the manuscript and edited the manuscript.

Signature **Date15/11/2016**

Kate Dowling: Performed statistical analysis on glasshouse data.

Signature **Date** 21/11/2016

Chris Brien: Designed glasshouse experiment, performed statistical analysis on glasshouse data, and edited the manuscript.

Signature **Date 15/11/16**

Rajeev K Varshney: Evaluated development of experiments, and edited the manuscript.

Signature **Date** 21/11/16

Tim Sutton: Supervised the work, evaluated the development of experiments, provided critical comments on the manuscript, edited the manuscript, and is acting as the corresponding author.

Signature **Date 15/11/2016**

Link to chapter 2

Previous studies suggest limited genetic variation for salinity tolerance exists in chickpea germplasm. This is partly due to the challenges associated with phenotyping large diverse sets of germplasm. This chapter describes image-based phenotyping in chickpea and its application in exploring genetic diversity for salinity tolerance. To complement findings from controlled environments to a breeding and agronomic context, field phenotyping was also carried out using a diverse germplasm collection assembled by ICRISAT, India. This study shows that shoot ion independent and shoot ion dependent tolerance exist in chickpea. Additionally, this chapter describes key traits that would be valuable for breeders for selecting salt tolerant genotypes. Seed number under salt was found to be highly associated with tolerance. This chapter is written in manuscript format and is currently under peer review in Scientific Reports as follows; Atieno J, Li Y, Langridge P, Berger B, Brien C, Dowling K, Varshney R.K, Sutton, T. Exploring genetic variation for salinity tolerance in chickpea using image-based phenotyping.

Abstract

Soil salinity results in reduced productivity in chickpea. However, breeding for salinity tolerance is challenging because of limited knowledge of the key traits affecting performance under elevated salt and the difficulty of high-throughput phenotyping for large and diverse germplasm collections. This study utilised an image-based phenotyping platform to study genetic variation in chickpea for salinity tolerance in 245 diverse accessions. On average salinity reduced plant growth rate (measured as leaf expansion through time) by 20%, plant height by 15% and shoot biomass by 28%. Additionally, salinity induced pod abortion and inhibited pod filling, which consequently reduced seed number and seed yield by 16% and 32%, respectively. Importantly, moderate to strong correlation was observed for different traits measured between glasshouse and two field sites indicating that the glasshouse assays are relevant to field performance. Using an image-based phenotyping platform, we were able to measure plant growth rate under salinity, and subsequently elucidate the role of shoot ion independent stress in chickpea. Broad genetic variation for salinity tolerance was observed in the diversity panel with seed number being the major determinant for salinity tolerance measured as yield. This study proposes seed number as a selection trait in breeding salt tolerant chickpea cultivars.

Introduction

Chickpea (*Cicer arietinum* L.) is an important legume crop used as human food, animal feed and is also grown in rotation with cereal crops to fix nitrogen in the soil and to act as a disease break [1]. Chickpea is generally grown in semi-arid regions which can be prone to soil salinity but it is considered to be very sensitive to salinity with an estimated global annual chickpea yield loss of between 8%-10% attributed to salinity [2]. Salinity impacts negatively on both the vegetative [3-5] and reproductive growth stages [6-9], with the reproductive stage the more salt sensitive [10]. The above studies show salinity has an adverse effect on shoot biomass, podding, and pod filling in chickpea.

Salinity limits plant growth and development through both shoot ion independent and shoot ion dependent stresses [11,12]. Shoot ion independent stress immediately follows salinity stress, whereas ionic stress manifests after several days or weeks following exposure to salt, once ions accumulate in the shoot [11,12]. Shoot ion independent stress results from hydraulic resistance imposed by NaCl in the plant xylem [13] as well as the reduction in external osmotic potential (osmotic stress) which interferes with water uptake leading to a reduction in plant growth rate [14-16]. Such a reduction in growth rate due to salinity must ultimately translate to a reduction in shoot biomass. Turner, et al. [6] and Vadez, et al. [17] found that salt tolerant chickpea genotypes (measured as seed yield under low to medium salinity) are able to maintain high shoot biomass under salinity.

Many plants species, including chickpea, can tolerate osmotic stress by producing metabolites for osmotic adjustment [11]. Recently, a study conducted by Dias, et al. [18] established differential accumulation of metabolites involved in the TCA cycle, carbon and amino acid metabolism in two chickpea genotypes (Genesis836 & Rupali) that have been shown to contrast in salinity tolerance [4]. Rupali was found to have increased levels of amino acids, sugars and organic acids from TCA cycle compared to Genesis836

following salinity treatment [18]. Production of these metabolites would be energy demanding which explains reduction in growth in Rupali when exposed to salinity. Prolonged exposure of plants to salinity causes Na^+ and Cl^- to accumulate in plant tissues to toxic levels leading to plant death manifested by leaf senescence and necrosis [11,19-21]. To protect the photosynthetic apparatus in young developing leaves from ion toxicity, plants exclude sodium from the transpiration stream by regulating as best as possible sodium net uptake and sequestering ions in the root cell vacuoles. Ions in the transpiration stream which enters the shoot can be sequestered in the lower, older leaves [11]. Screening diverse germplasm of chickpea for salinity tolerance revealed a wide spectrum of senescence displayed by different chickpea genotypes under salinity stress [22], which demonstrated that different chickpea genotypes have varying levels of ion exclusion or tissue tolerance. The contribution of ions to salt sensitivity in chickpea has recently gained interest, with Na^+ rather than Cl^- found to be toxic [6,8,23]. Vadez, et al. [7] did not find an association between salinity tolerance (seed yield per plant in saline soil) and accumulation of Na^+ in total vegetative biomass at 50 days after sowing (DAS) in a germplasm collection of chickpea, whereas, Turner, et al. [6] established a negative correlation between Na^+ accumulation in the youngest fully expanded leaf at 98 DAS with salinity tolerance (seed yield under 40 mM NaCl) in 55 chickpea genotypes. These differences could be attributed to different sampling strategies for leaf tissues (different time points and developmental stage) employed in the two studies.

Genetic variation within cultivated chickpea (*Cicer arietinum*) and related species can be exploited to improve salinity tolerance in future varieties. Previous studies on limited numbers of chickpea genotypes suggested the availability of limited genetic variation for salinity tolerance in chickpea [24,25]. However, more recent research to explore variation in chickpea germplasm collections has demonstrated a broad range of genetic variation for

salinity tolerance, such as that represented in the chickpea Reference Set [6,7,9]. Formed to enable efficient utilisation of chickpea genetic resources, the Reference Set is composed of geographically diverse material that includes; 267 landraces, 13 advanced lines and cultivars, 7 wild *Cicer* accessions and 13 accessions whose classification is unknown [26]. Characterisation of the Reference Set using 50 SSR markers revealed that it is rich in allelic diversity [26] and can be mined for genetic variation of value in breeding.

The rapid development of new, high-resolution and high-throughput phenotyping technologies in plant science has provided the opportunity to more deeply explore genetic variation for salinity tolerance in crop species and identify traits that are potentially novel and relevant to yield improvement. Vadez, et al. [27] utilised a high-throughput, 3D scanning technique to monitor leaf area development in relation to plant water use in cowpea and peanut. Several studies in cereals have used high-throughput phenotyping technology under controlled environmental conditions to gain a better understanding of the physiological processes associated with salinity stress [20,21,28-32]. In contrast, similar studies examining salinity response in legume species have not been reported. Salinity response, measured as effect of salt on growth rate at different developmental times, could explain genotypic variation for salinity tolerance in chickpea. To investigate this hypothesis, we have utilised an image-based phenotyping platform to enable quantitative, non-destructive assessment of temporal responses of chickpea to salinity and we relate these responses to seed yield under saline conditions. This has allowed investigation into the complex relationship between different traits, with the aim of identifying novel traits that can be applied as selection tools in breeding programs.

Materials and methods

Plant material

Experimental plant material consisted of 245 lines from the chickpea Reference Set [26] along with two Australian chickpea cultivars, Genesis836 and Rupali. Out of the 245 lines, 186 lines were of desi type while 59 lines were of kabuli type. 95% of the lines were landraces with the rest being advanced cultivars and breeding lines (Table S1).

Phenotyping in the glasshouse

The Reference Set, along with Genesis836 and Rupali, were phenotyped in an experiment carried out from June 2014 to November 2014 in The Plant Accelerator (http://www.plantphenomics.org.au/services/accelerator/) located at the Waite Campus of the University of Adelaide. The Plant Accelerator is a Plexiglas-clad greenhouse system which allows high penetration of natural light. Temperature and relative humidity in the glasshouse was controlled and ranged from 22±2ºC and 40% (day) and 15±2ºC and 90% (night), respectively. It was set up in two Smarthouses (separate growth rooms) utilising 24 lanes by 22 positions. Each Smarthouse was divided into six zones/blocks, each comprising 4 lanes by 22 positions. The design employed for the experiment was a split-plot design in which two consecutive carts formed a main plot (Figure S1). The split-plot design assigned genotypes to main plots, the genotypes being unequally replicated 2-3 times. Treatments (non-saline, saline) were randomized to the two subplots (carts) within each main plot. The main plot design was generated using Digger [33] and the subplot randomization was done using dae [34], packages for the R statistical computing environment [35] . The experimental layout used is shown in Figure 1.

Prior to sowing, seeds were pickled with Pickle-T fungicide and 5 seeds sown 2 cm deep in draining pots (19.5 cm height × 14.9 cm diameter) filled with 2.5 kg of 50% (v/v)

University of California (UC) mixture (1:1 peat: sand) and 50% (v/v) cocopeat amended with osmocote (pH 7.5; electrical conductivity ($EC_{1:5}$ 603 μS/cm). Rhizobium inoculum (Group N) was added to each planting hole at sowing. For the first 28 days after sowing (DAS), the volume of water in the pots was maintained approximately at 375 mL (field capacity equivalent to 15% (w/w) water content). Plants were uniformly thinned to two plants per pot. To quantify plant growth rate before salt application and to have a baseline for individual plant growth rate, plants were imaged at 28 DAS for three days (prior to 40 mM NaCl application) using a fixed 5 megapixel visible/RGB camera (Basler Pilot piA2400-12gc) with images taken from three different views (from the top and two side views, rotated at 90º). At 31 and 34 DAS, each pot received 0 or 40 mM NaCl (based on pilot study where 40 mM NaCl was sufficient to discriminate between sensitive and tolerant genotypes), equivalent to applying 100 mL of 0 or 150 mM NaCl, respectively. 40 mM NaCl was delivered in two increments through the base of the pots by standing an individual pot in its own square container containing saline solution. Saline solution moved into the soil through capillary action. Pots were watered and maintained at field capacity (15% (w/w), determined gravimetrically) to maintain salt concentration and to avoid salt leaching. Plants were imaged for a further 22 days after exposure to salt to quantify growth under saline and non-saline conditions. A total of 28,405 visible light (RGB) images obtained were processed in LemnaGrid (LemnaTec) and plant pixels used to compute projected shoot area. Cubic smoothing splines were fitted for each cart to the projected shoot areas for the observed days after sowing using the function smooth.splines in the R statistical computing environment with df set to 5. Relative growth rates (RGR) were computed from the smoothed projected shoot area for each cart for each day of imaging, as described by [36]. It was calculated as the difference in the logarithms of the smoothed projected shoot area for two consecutive days of imaging, which is then divided by the number of days between the imagings. Also

calculated was the RGR for the interval 32–56 DAS by taking the difference between the logarithms of the smoothed projected shoot area for 32 DAS and 56 DAS and then dividing by 24.

In addition to data extracted from high-resolution imaging, visual measurements of flowering time (day to first flower) and leaf chlorosis and necrosis on a scale of 1 (healthy) - 9 (dead) according to Maliro, et al. [22], were also taken. Other traits measured included leaf sodium (Na^+) and potassium (K^+) ion content, plant height, yield and yield components including shoot biomass, seed number, total pod number, empty pod number, filled pod number and 100-seed weight.

Sodium (Na^+) and potassium (K^+) ion content determination

At the podding stage, a single sample of the youngest fully expanded leaf was collected from each pot. Samples were oven dried at 60ºC for 48 hours. Leaf samples were weighed and extracted in 2 mL of 1% (w/w) nitric acid (70% [w/w] Nitric Acid; Chem-Supply NA001-500M, Gillman) at 70°C for 24 hours, then analysed for Na^+ and K^+ content using flame photometry (Model 420 Flame Photometer, Sherwood Scientific).

Phenotyping in the field

The Reference Set, along with some extra genotypes, was evaluated at two field sites, Turretfield in 2013 and Snowtown in 2014, located in the mid-North of South Australia. Soil cores up to a depth of 20 cm were used to establish pH and electrical conductivity of the soil solution (EC1:5) of the two sites. At Turretfield, a randomized complete block design with three replicates was used to assign the 255 genotypes to plots that consisted of 1 m paired rows. At Snowtown, the randomized complete block design had four replicates of 250 genotypes assigned to plots measuring 5 m by 4 m. Prior to sowing, seed was pickled with Pickle T fungicide and Rhizobium inoculum (Group N) applied to

sowing furrows. Data including, days to flower, plant height at maturity, seed number, and 100-seed weight were collected.

Data analysis

Linear mixed models employed in GenStat 17th Edition software were used to analyse a trait and to calculate Best Linear Unbiased Estimates (BLUE) for each genotype. The model for a trait from the glasshouse experiment was:

$$\mathbf{y} = \mathbf{X}\boldsymbol{\beta} + \mathbf{Z}\mathbf{u} + \mathbf{e},$$

where $\mathbf{y}$ is the response vector of values for the trait being analysed; $\boldsymbol{\beta}$ is the vector of fixed effects; $\mathbf{u}$ is the vector of random effects; and $\mathbf{e}$ is the vector of residual effects. $\mathbf{X}$, and $\mathbf{Z}$ are the design matrices corresponding to $\boldsymbol{\beta}$ and $\mathbf{u}$, respectively. The fixed effect vector, $\boldsymbol{\beta}'$, is partitioned as follows: $\left[\mu \left(\boldsymbol{\beta}^{\mathrm{G}}_{246\times1}\right)' \left(\boldsymbol{\beta}^{\mathrm{T}}_{2\times1}\right)' \left(\boldsymbol{\beta}^{\mathrm{G:T}}_{492\times1}\right)'\right]$, where μ is the overall mean and the $\boldsymbol{\beta}$s are the vectors of, Genotype main effects, Treatment main effects and Genotypes-by-Treatment interaction effects, respectively. Also, the random effects vector, $\mathbf{u}'$, is partitioned as follows: $\left[\left(\mathbf{u}^{\mathrm{S}}_{2\times1}\right)' \left(\mathbf{u}^{\mathrm{S:Z}}_{12\times1}\right)' \left(\mathbf{u}^{\mathrm{S:Z:M}}_{528\times1}\right)'\right]$, where the $\mathbf{u}$s are the vectors of, 2 Smarthouse random effects, 6 Zone random effects for each Smarthouse and 44 Main-plot random effects within each Zone within each Smarthouse, respectively. The design matrices $\mathbf{X}$ and $\mathbf{Z}$ are partitioned to conform to the partitioning of $\boldsymbol{\beta}$ and $\mathbf{u}$, respectively. It is assumed that each subvector of random effects, $\mathbf{u}^i$, is distributed $N\left(\mathbf{0}_m, \sigma_i^2\mathbf{I}_m\right)$, where $\mathbf{0}_m$ is the m-vector of zeroes, σ_i^2 is the variance of the ith set of random effects, $\mathbf{I}_m$ is the identity matrix of order m, and m is the order of $\mathbf{u}^i$. Further, residual effects $\mathbf{e}$ are assumed to be $N\left(\mathbf{0}_{1056}, \sigma^2 \otimes \mathbf{I}_{1056}\right)$, where σ^2 is the variance of individual plants after all other effects have been taken into account.

For the field studies the same general form of mixed model was used, but with the fixed-effect vector partitioned as follows: $\left[\mu \;\; \beta^{\mathrm{R}} \;\; \beta^{\mathrm{C}} \;\; \left(\boldsymbol{\beta}^{\mathrm{B}}_{b\times 1}\right)' \;\; \left(\boldsymbol{\beta}^{\mathrm{G}}_{g\times 1}\right)'\right]$ where μ is the overall mean, β^{R} and β^{C} are the linear coefficients for Rows and Columns, and the $\boldsymbol{\beta}$s are the vectors of Block (b = 4 or 3) and Genotype (g = 255 or 250) main effects, respectively. Also, the random effects vector, $\mathbf{u}'$, is partitioned as follows: $\left[\left(\mathbf{u}^{\mathrm{R}}_{r\times 1}\right)' \;\; \left(\mathbf{u}^{\mathrm{C}}_{c\times 1}\right)'\right]$, where the $\mathbf{u}$s are the vectors of Row (r = 12 or 21) and Column (c = 87 or 35) random effects, respectively. The residual effects $\mathbf{e}$ are assumed to be $N\left(\mathbf{0}_n, \sigma^2\boldsymbol{\Sigma}_{\mathrm{R}} \otimes \boldsymbol{\Sigma}_{\mathrm{C}}\right)$, where σ^2 is the variance of individual plots after all other effects have been taken into account and $\boldsymbol{\Sigma}_{\mathrm{R}}$ and $\boldsymbol{\Sigma}_{\mathrm{C}}$ are first-order autocorrelation matrices for Rows and Columns, respectively, and n =1020 or 750. Additionally, estimates of broad-sense heritability (H^2) for traits measured both in the glasshouse and field environments were calculated using the formula derived from [37].

Pearson's correlation analysis and Path analysis

Pearson's correlation analysis was conducted in the GenStat 17th edition to establish association between traits. Path analysis was conducted using SmartPLS, software for partial least squares structural equation modelling (PLS-SEM) [38], with the objective of decomposing correlation coefficients into components of direct and indirect effects to examine the strength of contribution of the different measured traits on seed yield.

Results

A diversity collection, known as the chickpea Reference Set [27] was phenotyped under salinity in The Plant Accelerator. Broad genetic variation for salinity response exists in the collection (Table 1; Figure 2; Figure 3), varying significantly between genotypes as evidenced by significant ($p \leq 0.05$) genotype-by-treatment interaction for nearly all traits (Table 1).

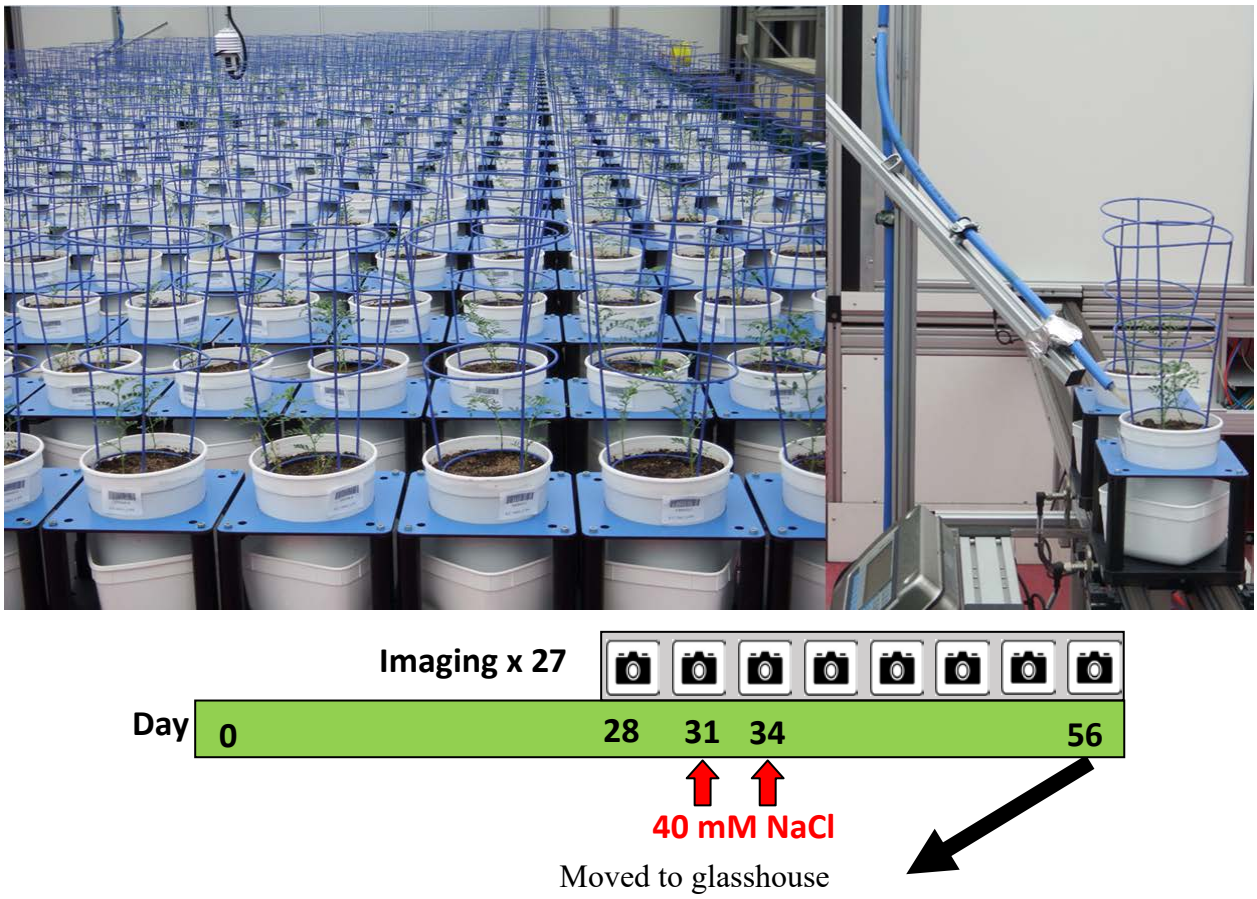

Figure 1: Salinity tolerance phenotyping in The Plant Accelerator. Plants were imaged at 28 DAS for 3 consecutive days prior to 40 mM NaCl application in two increments over 2 days. Plants were daily imaged until 56 DAS. Right pane shows 6 week old chickpea plants on conveyor belts leaving the imaging hall proceeding to an automatic weighing and watering station.

Validation of methodology

To evaluate the suitability of the methodology utilised in this experiment, two genotypes in the Reference Set previously shown to contrast for salinity tolerance were evaluated. The genotypes were ICC 95; highly tolerant to 80 mM NaCl [10] and ICC 2720; highly sensitive to 100 mM NaCl [39]. In our experiment, ICC 95 and ICC 2720 were shown to greatly differ in their response to salinity. At 53 DAS (21 days after salt application) the significant effect of salinity, manifested by stunted growth, was first seen in ICC 2720, with growth reduction as early as 35 DAS (3 days after salt application). Consequently, ICC 2720 experienced a 50% growth reduction under salinity compared to ICC 95 (Figure 2). Additionally, these two genotypes differed in their ability to maintain seed yield under salinity. There was a 25% and 80% reduction in seed yield due to salinity in ICC 95 and ICC 2720, respectively (Figure S2).

Table 1: Overall values of mean, minimum, maximum, and P-value for effects of genotypes (G), treatments (T) and genotype by treatment interaction (G×T) from the chickpea Reference Set in the glasshouse under salt and control conditions. All measurements are on a pot basis. Number of observation ranged from 201-244. P-values that are not applicable because G×T is significant are indicated by n.a.

Traits	Treatment	MEAN	MIN	MAX	G	T	G×T
Seed yield (g)	Control	4.01	1.06	9.38			
	Salt	2.74	0	7.02	n.a	n.a	0.019
Seed number	Control	22.55	1.05	51.01			
	Salt	18.88	0	48.65	n.a	n.a	0.006
Shoot biomass (g)	Control	6.36	0.69	12.08			
	Salt	4.6	0	10.07	<0.001	<0.001	0.196
Total pod number	Control	26.04	0	83.29			
	Salt	23.6	0.18	55.99	n.a	n.a	<0.001
Filled pod number	Control	18.8	0.74	40.61			
	Salt	16.17	0	42.63	n.a	n.a	0.004
Empty pod number	Control	7.24	0	64.08			
	Salt	7.43	0	32.25	n.a	n.a	0.034
100- seed weight (g)	Control	17.84	4.14	35.73			
	Salt	13.1	0	29.15	n.a	n.a	<0.001
Plant height (cm)	Control	43.54	23.11	70.18			
	Salt	37.08	12.19	56.2	<0.001	<0.001	0.9
Leaf senescence score	Control	1.45	0.27	10.05			
	Salt	4.53	0.73	10.05	n.a	n.a	<0.001
RGR 32-56	Control	0.05	0.02	0.07			
	Salt	0.04	0	0.06	<0.001	<0.001	0.326
Days to flower	Control	67.4	47.9	93.4			
	Salt	68.9	48.5	92.4	n.a	n.a	0.025
Sodium (Na) ions (µmol/gDW)	Control	32.9	0.28	92.79			
	Salt	99.62	10.03	394.36	n.a	n.a	0.006
Potassium (K) ions (µmol/gDW)	Control	969.33	296	1743			
	Salt	1210.03	347	2362	<0.001	<0.001	0.97
K:Na	Control	121.23	7.29	3532.14			
	Salt	21.32	3.42	97.13	n.a	n.a	0.034

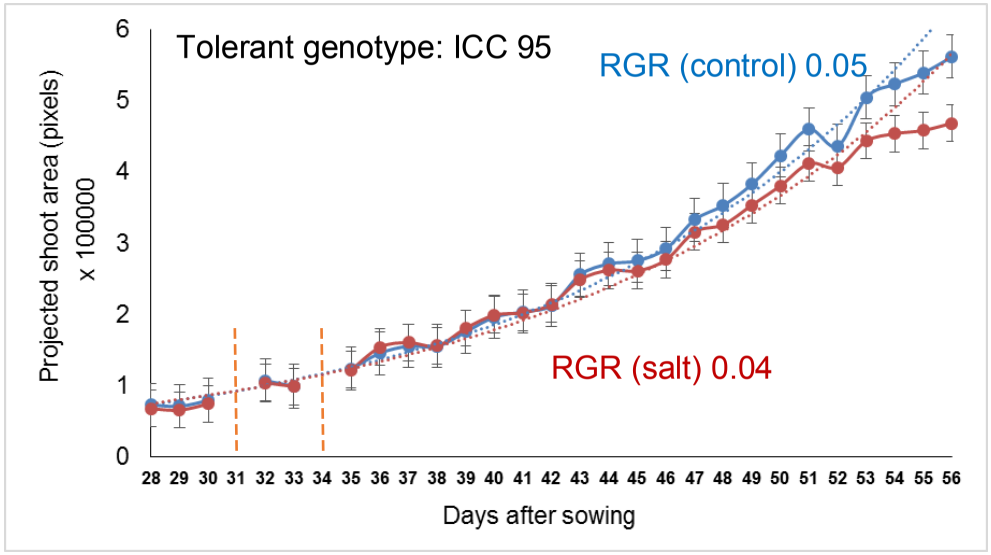

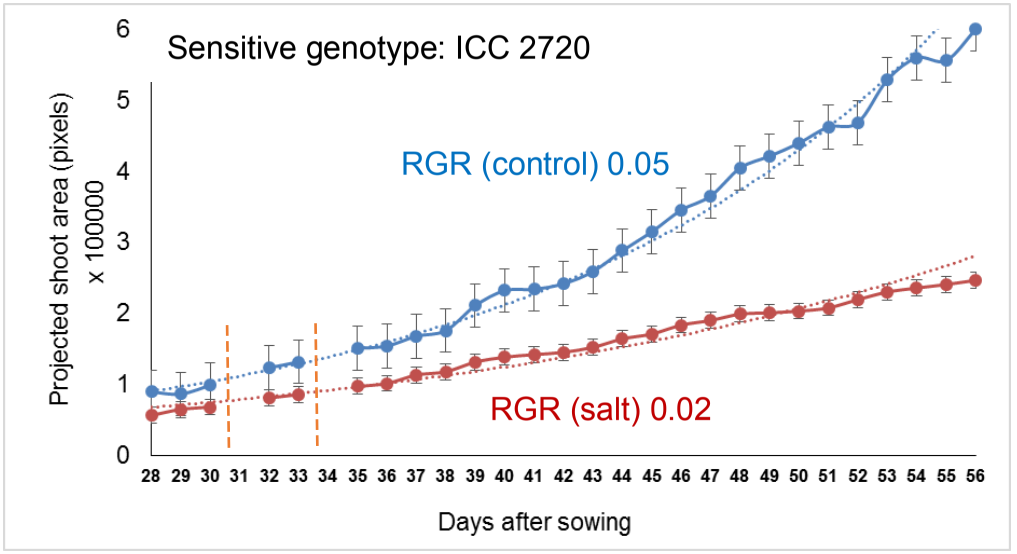

Figure 2: Non-destructive imaging of chickpea plants over time under 0 and 40 mM NaCl. Growth rates of ICC 95 (salt tolerant) and ICC 2720 (salt sensitive) under 0 mM NaCl (control) and 40 mM NaCl (salt). Plant growth is demonstrated by increments in projected shoot area (pixels) over time. Plants were imaged 3 days prior to salt application to establish a baseline for growth rate determination. Salt was applied in two equal increments, shown by orange vertical lines, at 31 DAS and 34 DAS and plants were imaged daily until 56 DAS to evaluate the effect of salt application on growth rate. Relative growth rate (RGR) is derived from the difference between the logarithms of the smoothed projected shoot area for 32 DAS and 56 DAS and then dividing by 24. Error bars are s.e.m.

To further validate the methodology used in the glasshouse experiment, measurements of days to flower, plant height, 100-seed weight, seed number and seed yield from Turretfield field site (pH 6.9 and electrical conductivity (EC1:5) 151±20 µS/cm), and Snowtown field site (pH 7.4 and EC1:5 ranging from 406 µS/cm to 173 µS/cm at the start and at the end of the trial, respectively), were established with the same measurements in the glasshouse under non-saline conditions. Over 50% of phenotypic variation for plant height, days to flower, 100-seed weight, and seed number could be attributed to genetic variation (Table 2). There was a strong positive correlation of r=0.72-r=0.74 for 100-seed weight, and moderate correlations of r=0.46, r=0.49, and r=0.24-0.34 for plant height, days to flower and seed number, respectively between the two field sites and the glasshouse. All these relationships were highly significant ($p<0.001$) (Table 2).

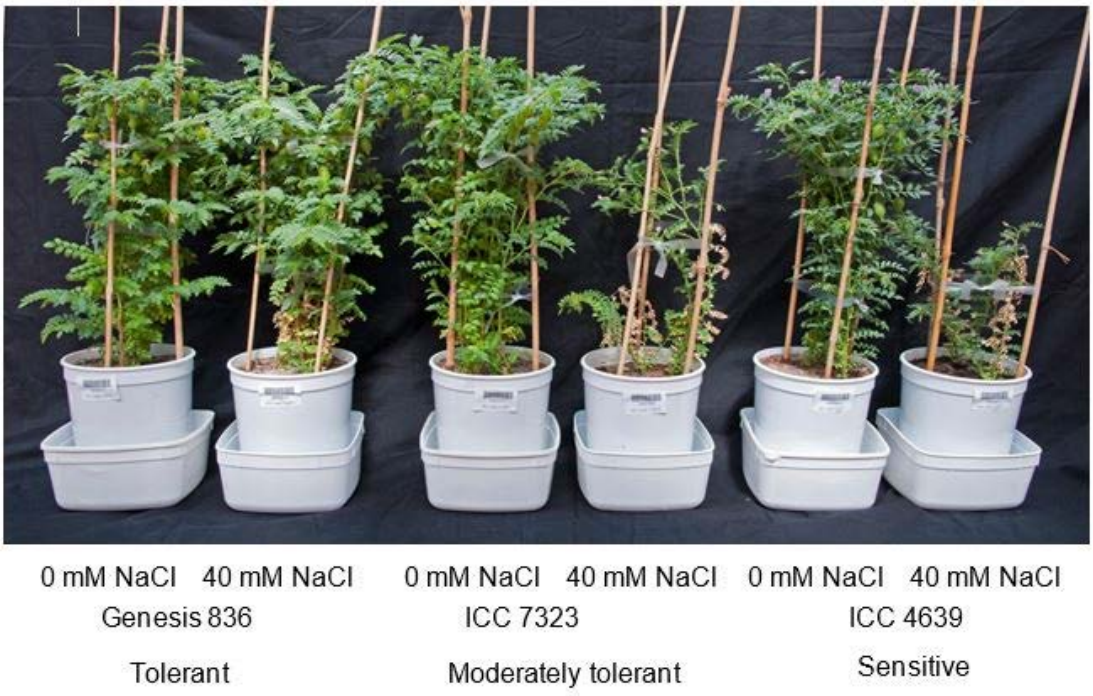

Figure 3: Genotypic variation for salinity response in the chickpea Reference Set. Varying levels of salinity tolerance exhibited by different chickpea genotypes. Exposure of sensitive genotypes to 40 mM NaCl caused severe stunted growth , leaf damage and reduced reproductive sites (number of flowers and pods) compared to moderately tolerant and tolerant genotypes

Table 2: Broad-sense heritability (H^2) and pairwise correlations between glasshouse and two field sites for seed number, 100-seed weight, days to flower and plant height. Level of significance (***=p<0.001)

Traits	Heritability (%)	Site	Glasshouse	Snowtown
Seed number	61	Snowtown	0.24***	
		Turretfield	0.34***	0.48***
100-seed weight	93	Snowtown	0.74***	
		Turretfield	0.72***	0.97***
Days to flower	65	Turretfield	0.49***	
Plant height	61	Turretfield	0.46***	

Large effect of salt on plant measurements in the glasshouse

A significant genotype-by-treatment interaction ($p \leq 0.05$) was observed for nearly all traits except for leaf potassium content, plant height, RGR and shoot biomass (Table 1). In cases where genotype-by-treatment interaction was not significant, there was significant genotype variation ($p<0.001$) and a significant treatment effect ($p<0.001$). Generally, plant growth was negatively impacted by salinity, with plants under saline conditions growing 20% slower compared to plants under non-saline conditions (Table 1; Figure S3). Salinity had a more detrimental effect on growth rate of ICC 2720 compared to ICC 95 (Figure 2), two genotypes previously reported to contrast for salinity tolerance.

On average salinity reduced shoot biomass and plant height at maturity by 28% and 15%, respectively, compared to non-saline condition (Table 1). Plants grown under saline conditions had greater leaf tissue damage, evidenced by 68% more leaf chlorosis and necrosis in these plants, compared to plants under non-saline conditions (Table 1). Salinity delayed the first appearance of flowers by two days. Plants under non-saline

conditions flowered on average at 67 DAS while plants under salinity treatment flowered on average at 69 DAS (Table 1).

The number of total pods and filled pods was negatively impacted under salinity, with plants grown under salt treatment recording a reduction of 9% and 14% in number of pods and filled pods, respectively compared to plants under non-saline conditions (Table 1). On average, the number of empty pods following salt treatment was only slightly increased by 2% (Table 1). Seed number and 100-seed weight (proxy for seed size) were significantly reduced by salt treatment by 16% and 26%, respectively (Table 1). Consequently, seed yield under saline conditions was reduced by 32% relative to non-saline conditions (Table 1).

Plants grown under saline conditions had more Na^+ in the youngest fully expanded leaf tissues compared to plants grown under non-saline conditions (Table 1). Salt treated plants accumulated 67% more Na^+ compared to plants under non-saline conditions (Table 1). The range of Na^+ accumulation in plants under saline treatment ranged from 10 μmol/g DW to 394 μmol/g DW (Table 1) with less than 10% of the genotypes accumulating more than 200 μmol/g DW. A significant genotype-by-treatment interaction ($p<0.001$) was observed for Na^+ and K:Na. Although, the genotype-by-treatment interaction ($p=0.970$) was not significant for K^+, a significant genotype variation ($p<0.001$) and a significant difference between the treatments ($p<0.001$) was observed (Table 1).

Relationship between traits in the glasshouse

Pearson's correlation analysis

Pearson's correlation analysis was performed to examine the relationship between different traits and seed yield. Seed yield under salinity had a moderate positive correlation with seed yield under non-saline conditions (R^2=0.20), a relationship that was significant (Figure 4) and confirms that yield potential explained 20% of seed yield under salinity. Hence, in this study, salinity tolerance is defined as the ratio of seed yield under salinity over seed yield under non-saline conditions (seed yield salt/seed yield control). To examine the relationship between traits, ratios of individual traits under saline and non-saline conditions were used. Salinity tolerance was strongly associated with seed number, total number of pods, number of filled pods and harvest index (Table 3; Figure S4). Seed number and number of filled pods accounted for 86% and 79%, respectively, of the variation in salinity tolerance while total number of pods accounted for 70% of the variation in salinity tolerance (Figure S4), harvest index accounted for 68% of this variation (Figure S4). RGR for the entire imaging period (r=0.33), shoot biomass (r=0.67), plant height (r=0.49) and 100-seed weight (r=0.56) had moderate correlation with salinity tolerance while RGR for the period 41-50 DAS (r=0.23) was weakly but significantly correlated with salinity tolerance (Table 3). RGR for the period 32-40 DAS (r=0.09) was not significantly correlated with seed yield (Table 3). Flowering time (r=0.08) did not play a role in seed yield determination in this study as it had a weak and non-significant relationship with salinity tolerance (Table 3).

To further explore the relationship between traits measured with seed yield, correlation analysis was conducted separately on data obtained from non-saline and saline conditions. Generally, correlations were stronger for traits measured under salinity (Table S2) compared to non-saline conditions (Table S3). Under salinity, seed number

(r=0.83) and number of filled pods (r=0.86) were strongly correlated with seed yield (Table S2). On the other hand, shoot biomass (r=0.68), total number of pods (r=0.66), 100-seed weight (r=0.50) plant height (r=0.52) and RGR for the entire imaging period (r=0.39) had a moderate correlation with seed yield (Table S2). Leaf Na^+ content had a moderate but significant negative relationship with seed yield (r=-0.3) (Table S4) while leaf K^+ had a weak relationship with seed yield (r=-0.19) (Table S4). K:Na was moderately but significantly correlated with seed yield (r=0.29) (Table S4). Na^+ had a moderately positive correlation with K^+ (r=0.52) and a negative correlation with K:Na (r=-0.64) (Table S4).

Seed number (r=0.75) and number of filled pods (r=0.80) had a high correlation with seed yield under non-saline conditions while shoot biomass (r=0.39) and total pods (r=0.53) had a moderate correlation with seed yield (Table S3). Conversely, 100-seed weight (r=0.17), plant height (r=0.21) and RGR for the whole period the plants were imaged for (r=0.21) were weakly correlated with seed yield under non-saline conditions (Table S3).

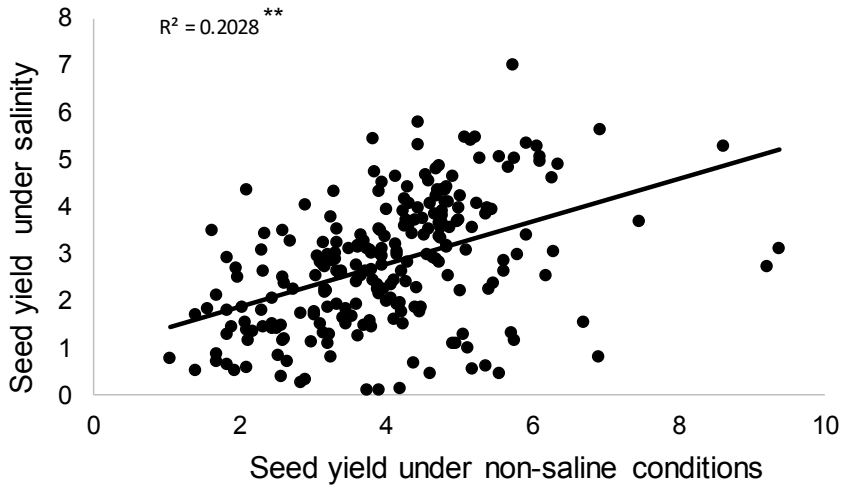

Figure 4: Relationship between seed yield under non-saline conditions and seed yield under salinity (g pot^{-1}). Level of significance ** =$p < 0.01$

Table 3: Relationship between traits, salt relative to control (salt/control), determined by correlation analysis. Highlighted, are moderate to high correlation coefficients. RGR-relative growth rate. Level of significance (***=P<0.001, **= P<0.01, *= P<0.05, ns=non-significant).

Traits	Seed yield	Seed number	Shoot biomass	Total pods	Filled pods	Empty pods	100- seed weight	Plant height	Days to flower	Senescence score	RGR 32-40	RGR 41-50	RGR 32-56
Seed yield	1												
Seed number	**0.92*** **	1											
Shoot biomass	**0.67*** **	**0.63*** **	1										
Total pods	**0.81*** **	**0.86*** **	**0.72*** **	1									
Filled pods	**0.90*** **	**0.97*** **	**0.61*** **	**0.87*** **	1								
Empty pods	0.22***	0.23***	0.27***	**0.44*** **	0.22***	1							
100- seed weight	**0.56*** **	**0.46*** **	**0.50*** **	**0.46*** **	**0.49*** **	0.15*	1						
Plant height	**0.49*** **	**0.48*** **	**0.49*** **	**0.47*** **		0.20**	**0.39*** **	1					
Days to flower	0.08 ns	0.12 ns	0.10 ns	0.13*	0.11 ns	0.14*	0.03 ns	0.07 ns	1				
Senescence score	-0.14*	-0.12*	-0.10 ns	-0.09 ns	-0.10 ns	-0.05 ns	-0.16*	-0.22**	0.06 ns	1			
RGR 32-40	0.09 ns	0.07ns	0.24***	0.22***	0.08 ns	0.07 ns	0.09 ns	0.12 ns	-0.01 ns	0.01 ns	1		
RGR 41-50	0.23***	0.29***	**0.33*** **	0.28***	**0.30*** **	0.13*	0.21***	**0.45*** **	0.17*	-0.10 ns	0.23***	1	
RGR 32-56	**0.33*** **	**0.34*** **	**0.44*** **	**0.39*** **	**0.36*** **	0.15*	0.25***	**0.45*** **	0.11 ns	-0.03 ns	0.28***	0.20***	1

Path analysis

Path analysis, a standardised partial regression coefficient, was performed to decompose correlation coefficients into components of direct and indirect effects and examine the strength of contribution of the different measured traits on seed yield. Under non-saline conditions, the number of filled pods, seed number and 100-seed weight had a moderate direct positive contribution of 0.50, 0.45 and 0.39, respectively, on seed yield while total number of pods had a moderate indirect positive effect of 0.38 and 0.31, respectively, on seed yield through number of filled pods and seed number (Table S5). Likewise, the number of filled pods had a moderate indirect positive effect of 0.43 on seed yield through seed number (Table S5).

Under salinity, the number of filled pods and seed number had a moderate positive direct effect of 0.45 and 0.41, respectively, on seed yield while 100-seed weight had a weak positive direct effect of 0.28 on seed yield (Table S6). While number of total pods had a moderate indirect positive effect of 0.37 and 0.33, respectively, on seed yield through number of filled pods and seed number, filled pods had a moderate indirect positive effect of 0.4 on seed yield through seed number (Table S6).

Salinity tolerance, defined as seed yield under salinity compared to seed yield under non-saline conditions, was directly predominantly influenced by seed number (0.90) and least influenced by senescence score (-0.006) (Table 4). The total number of pods and filled pods had a strong indirect effect of 0.77 and 0.87, respectively, through seed number, whereas RGR (0.31), plant height (0.44), shoot biomass (0.57) and 100-seed weight (0.41) had a moderate indirect effect on salinity tolerance through seed number (Table 4).

A path analysis diagram was used to examine the relationships between salinity tolerance and seed yield components. Relative growth rate (0.27) and plant height (0.37)

were found to play a bigger role on shoot biomass than leaf senescence score (-0.02) and days to flowering (0.05) (Figure 5). Total number of pods was mainly influenced by number of filled pods (0.67), which consequently had a major effect on seed number (0.86), which was the key trait influencing salinity tolerance (0.88) (Figure 5). Residual variation of only 0.12 was missing from the path diagram developed to determine traits that play direct and indirect role in salinity tolerance determination (Figure 5). The low residual demonstrates the strength of the model to explain the relationship existing between the traits measured.

Table 4: Direct and indirect effects of yield components on salinity tolerance (salt/control), determined by partial least squares algorithm. Values in the main diagonal part (path coefficients) and off-diagonal part of the table represent direct and indirect effects of yield components on salinity tolerance. Total effects, which correspond to correlation coefficients, are derived from summing up direct and indirect effects. Highlighted are direct effects (bold) moderate indirect (underlined), as well as moderate to high total effects (underlined).

Traits	RGR 32-56	Plant height	Shoot biomass	Total pods	Filled pods	Seed number	100-seed weight	Senescence score	Total effects
RGR 32-56	***-0.029***	-0.006	0.050	0.005	-0.034	0.310	0.039	0.000	0.335
Plant height	-0.013	***-0.013***	0.056	0.006	-0.045	0.435	0.060	0.001	0.488
Shoot biomass	-0.013	-0.006	***0.114***	0.009	-0.058	0.568	0.078	0.001	0.692
Total pods	-0.011	-0.006	0.082	***0.012***	-0.083	0.771	0.072	0.001	0.838
Filled pods	-0.010	-0.006	0.069	0.010	***-0.095***	0.874	0.076	0.001	0.919
Seed number	-0.010	-0.006	0.072	0.010	-0.092	***0.899***	0.071	0.001	0.944
100-seed weight	-0.007	-0.005	0.057	0.006	-0.047	0.411	***0.155***	0.001	0.570
Senescence score	0.001	0.003	-0.012	-0.001	0.010	-0.110	-0.025	***-0.006***	-0.140

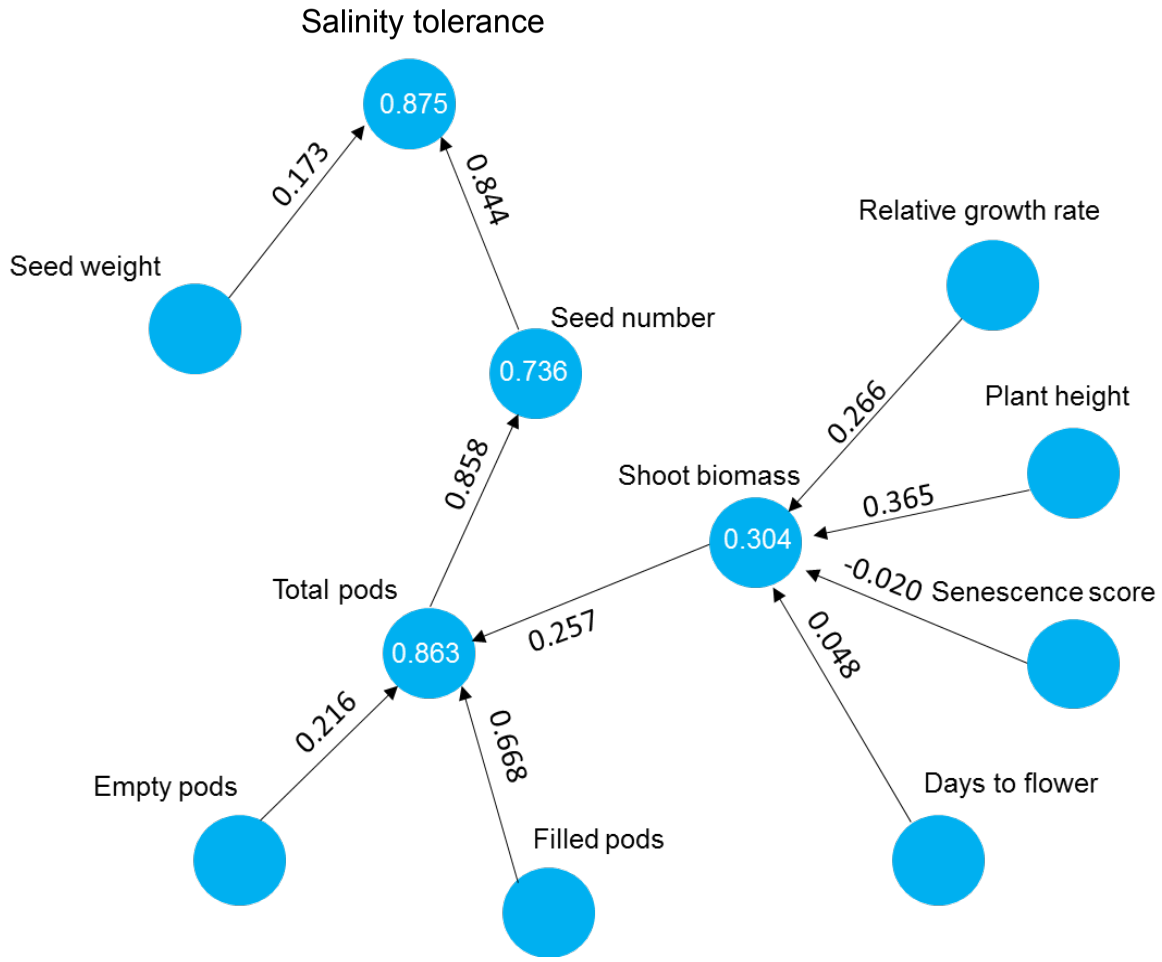

Figure 5: Path analysis diagram of seed yield and yield components. Path analysis derived from structural equation modelling using Partial Least Squares Algorithm method developed by Wold [38] to demonstrate complex relationship existing between salinity tolerance (seed yield under salt/seed yield under control) and yield related traits. Path coefficients indicated with values on the arrows show direct effect between different yield related traits. Regression coefficients are indicated by values in the circles. Values used for path analysis are relative measurements (salt/control).

Discussion

Salinity tolerance in higher plants is a complex trait comprised of many sub-traits, suggesting there may be multiple mechanisms and these are likely under the control of many genes [40]. Consequently, efforts to understand the genetic control of salinity tolerance have been challenging. Previous studies have not been able to tease apart the effect of shoot ion independent and shoot ion dependent stress on chickpea growth and yield. In a study of two genotypes contrasting for salinity tolerance (Genesis836 and Rupali), Khan, et al. [23] found that osmotic stress imposed in the form of concentrated macronutrient solution, did not have an impact on chickpea biomass. This study looked at osmotic stress, a component of shoot ion independent stress. Other salinity studies in chickpea have shown growth impairment even when toxic ion levels have not been reached in plant tissues including young and old leaves [6-8]. This suggests shoot ion independent stress plays a role in salinity response in chickpea. It is therefore crucial to look at this form of stress, which represents an early response to NaCl exposure.

Image-based phenotyping allows for non-destructive detection of early onset of salinity stress through measurement of plant growth before ions start accumulating in plant tissues. Similar studies have been conducted in barley [32], and rice [20,31]. Our study showed that 40 mM NaCl significantly reduced chickpea growth rate with a greater reduction observed in some genotypes. There was broad variation for a range in response time when growth decline was first observed. 20% of the genotypes showed a decline in growth within five days of salt application. For instance, ICC 2720 experienced a significant growth reduction within only three days of salt application, a reduction attributed to shoot ion independent stress (Figure 2).

Ion regulation plays a major role in salinity tolerance. Leaf senescence/necrosis scores together with measurements of accumulated toxic ions in the shoot can be used to make

inferences on salinity tolerance mechanisms [21]. These measures indicate the ability of plants to cope with high salt levels or to reduce salt uptake through the roots and transport to the shoots where significant tissue damage can occur. Maliro, et al. [22] scored leaf senescence in a diverse germplasm collection exposed to 60 mM NaCl and identified genotypes with low senescence. However, the genotypes were evaluated for salinity tolerance at the vegetative stage, which does not always translate to tolerance at the reproductive stage [10]. Our study scored leaf senescence at 60 days post salt application and found that some genotypes had started naturally senescing and most scores were confounded by plant age. This partly explains the weak relationship established between leaf senescence and salinity tolerance.

It is thought that Na^+ but not Cl^-, is toxic in chickpea [6,8,23]. Previous studies have established a negative relationship between Na^+ content in leaves and seed yield under salinity [6,8]. We observed a moderate negative correlation of r=-0.3 between seed yield under salinity and Na^+ content in the youngest fully expanded leaf expressed per unit dry matter (Table S4) with about 10% of the genotypes accumulating more than 200 μmol/g DW. As this study utilised a diverse collection of lines, it was expected that different genotypes may express different salinity tolerance mechanisms, which could explain the moderate correlation. The moderate negative correlation between Na^+ accumulation and seed yield demonstrates that salinity tolerance in the chickpea Reference Set is partly explained by sodium exclusion. Plants accumulating high Na^+, generally had more K^+, an observation also made by Turner et al. (2013). Further research is needed to investigate the role of K^+ and its uptake, efflux, translocation and interaction with Na^+ during salinity stress in chickpea.

The availability of genetic variation for salinity tolerance is a prerequisite to improve salinity tolerance in chickpea through selection and breeding. Until recently, a lack of

streamlined phenotyping facilities has been a bottleneck in studying large diverse collections of chickpea. Previous studies made inferences regarding availability of limited genetic variation for salinity tolerance based on examinations of a relatively small number of chickpea genotypes [24,25,41]. However, Vadez, et al. [7] demonstrated broad genetic variation for salinity tolerance (measure as seed yield per plant under soil salinity) exists in the chickpea germplasm. In this work we have utilised a high-throughput, non-destructive, efficient, and accurate phenotyping platform to study a diverse collection of chickpea, with the aim of determining traits of relevance for selection in breeding programs. Broad genetic variation for growth rate, plant height, days to flower, leaf senescence, shoot Na^+ and K^+ content, shoot biomass, pod number, seed number under salinity and salinity tolerance (measured as seed yield under salinity/seed yield under control) exists in the collection studied here (Table 1).

Salinity had a negative effect on shoot biomass as well as yield and yield components (Table 1). The reduction in seed yield under salinity was attributed to direct reduction in relative growth rate and plant biomass as well as damage to reproductive tissues leading to reductions in number of filled pods, seed number, and 100-seed weight (Table 1). Relative growth rate was only moderately related to shoot biomass at maturity and seed yield. This is because we derived these measurements at the vegetative stage, which emphasizes measurements made at this stage do not always translate to salinity tolerance determined as seed yield under salinity. The number of filled pods and seed number were major determinants of seed yield under salinity, as opposed to 100-seed weight. This is in accordance with previous studies that suggested salinity tolerance in chickpea depends on successful production of reproductive structures under salinity but not the ability to fill seeds [7,9]. Phenotyping platform development to additionally measure traits such as flower and pod number would assist in the analysis of genetic variation for salinity tolerance in

chickpea. Surprisingly, compared to performance under non-saline conditions, 24 genotypes performed better (10% more yield) under the salinity stress imposed in this experiment. This indicates that 40 mM NaCl was perceived as moderate stress by tolerant genotypes, which utilised sodium as an inexpensive osmoticum to stimulate growth and subsequently yield. This phenomenon has previously been observed by Abideen, et al. [42] in *Phragmites karka*, a potential bioenergy crop. Moderate salinity treatments have also been shown to stimulate flower production in chickpea [5] which could ultimately be advantageous to tolerant genotypes.

Correlation and path analysis create an understanding of the relationship between traits. This study showed the role of seed number as the major determinant of improved performance under salinity (Table 3; Table 4; Figure 5), in line with previous studies by Krishnamurthy, et al. [9], Vadez, et al. [7] and Vadez, et al. [10]. However, in contrast to the earlier studies, the phenotyping platform used here allowed us to decompose the correlation analysis into path coefficients to quantify the direct effect of seed number on salinity tolerance. The importance of seed number was masked when performing path analysis on data from either non-saline or salinity conditions. Hence, this points to the importance of defining salinity tolerance and removing the confounding effect of yield potential. Flowering time had no correlation with salinity tolerance (Table 3), an observation also made by other studies evaluating the chickpea Reference Set [6,9]. This observation resulted from the plants being grown under optimised conditions with adequate water and nutrients ensuring that late flowering genotypes had sufficient time to complete their growth cycles.

Field phenotyping is needed to complement findings from controlled environments to a breeding and agronomic context [43]. However, phenotyping under field conditions is challenging due to the spatial and temporal variability of salinity in the soil profile and the

restriction of trials to only one to two periods per year. The variability in stress was evident in the Snowtown field site where moderate salt levels in the soil gradually reduced with season progression possibly due to the dropping of the water table. Carefully designed pot experiments under controlled environments can help identify traits of importance [44]. A relationship was established between data obtained from the glasshouse under non-saline conditions with data from two field sites (typical field site and moderately saline- low salinity field site). Notably, a large proportion of phenotypic variation for all traits measured under both field and control conditions could be attributed to genetic variation. The two field sites had very strong correlation with each other as well as with the glasshouse for 100-seed weight. Moderate but significant correlation was observed between the glasshouse and the two field sites for plant height, days to flower and seed number. This validates the phenotyping methodology used in the glasshouse. However, there is a need to evaluate the chickpea Reference Set in a saline field environment to substantiate the results reported here.

Conclusion

Image-based phenotyping is a reliable platform for exploring genetic variation for salinity response in chickpea. The methodology used here, coupled with phenotyping platform development through implementation of algorithms to recognise and quantify pod number on plants, can be used to efficiently screen large numbers of accessions. Salt tolerant plants had the ability to maintain growth, successfully produce reproductive tissues, and maintain low levels of Na^+ in young leaves under salt stress. The study has demonstrated that chickpea is affected by shoot ion independent and to a small extent shoot ion dependent stress and hence there is a need to identify genomic regions that could contribute loci enabling chickpea to withstand the two phases of salinity stress. Seed number was found to be a major contributor to seed yield under salinity and therefore an important selection trait for breeding chickpea cultivars with improved tolerance. Phenotypic data collected from this study can now be linked with genotypic data from all genotypes to conduct genome-wide association mapping with the aim of identifying loci that underlie salinity tolerance in chickpea.

References

1. Saxena, N. Status of chickpea in the Mediterranean basin. In: Present Status and Future Prospects of Chickpea Crop Production and Improvement in the Mediterranean Countries. *Options Méditerr. (CIHEAM) Ser.,* **A 9**, 17-24 (1990).
2. Flowers, T.J. *et al.* Salt sensitivity in chickpea. *Plant Cell Environ* **33**, 490-509 (2010).
3. Katerji, N. *et al.* Response to soil salinity of chickpea varieties differing in drought tolerance. *Agr. Water Manage* **50**, 83-96 (2001).
4. Khan, H.A., Siddique, K.H.M., Munir, R. & Colmer, T.D. Salt sensitivity in chickpea: Growth, photosynthesis, seed yield components and tissue ion regulation in contrasting genotypes. *Journal of Plant Physiology* **182**, 1-12 (2015).
5. Samineni, S., Siddique, K.H.M., Gaur, P.M. & Colmer, T.D. Salt sensitivity of the vegetative and reproductive stages in chickpea (Cicer arietinum L.): Podding is a particularly sensitive stage. *Environmental and Experimental Botany* **71**, 260-268 (2011).
6. Turner, N.C. *et al.* Salinity tolerance and ion accumulation in chickpea (Cicer arietinum L.) subjected to salt stress. *Plant and Soil* **365**, 347-361 (2013).
7. Vadez, V. *et al.* Large variation in salinity tolerance in chickpea is explained by differences in sensitivity at the reproductive stage. *Field Crops Research* **104**, 123-129 (2007).
8. Pushpavalli, R. *et al.* Higher flower and seed number leads to higher yield under water stress conditions imposed during reproduction in chickpea. *Functional Plant Biology* **42**, 162-174 (2015).
9. Krishnamurthy, L. *et al.* Consistent Variation Across Soil Types in Salinity Resistance of a Diverse Range of Chickpea (Cicer arietinum L.) Genotypes. *Journal of Agronomy and Crop Science* **197**, 214-227 (2011).
10. Vadez, V. *et al.* Large number of flowers and tertiary branches, and higher reproductive success increase yields under salt stress in chickpea. *European Journal of Agronomy* **41**, 42-51 (2012).
11. Munns, R. & Tester, M. Mechanisms of salinity tolerance. **59**, 651-681 (2008).
12. Roy, S.J., Negrão, S. & Tester, M. Salt resistant crop plants. *Current Opinion in Biotechnology* **26**, 115-124 (2014).
13. Munns, R. & Passioura, J.B. Hydraulic Resistance of Plants. III. Effects of NaCl in Barley and Lupin. *Functional Plant Biology* **11**, 351-359 (1984).
14. Boursiac, Y. *et al.* Early effects of salinity on water transport in Arabidopsis roots. Molecular and cellular features of aquaporin expression. *Plant Physiol* **139**, 790-805 (2005).
15. Fricke, W. Rapid and tissue-specific accumulation of solutes in the growth zone of barley leaves in response to salinity. *Planta* **219**, 515-25 (2004).
16. Puniran-Hartley, N., Hartley, J., Shabala, L. & Shabala, S. Salinity-induced accumulation of organic osmolytes in barley and wheat leaves correlates with increased oxidative stress tolerance: In planta evidence for cross-tolerance. *Plant Physiology and Biochemistry* **83**, 32-39 (2014).
17. Vadez, V. *et al.* Assessment of ICCV 2 × JG 62 chickpea progenies shows sensitivity of reproduction to salt stress and reveals QTL for seed yield and yield components. *Molecular Breeding* **30**, 9-21 (2012).
18. Dias, D.A. *et al.* Quantitative profiling of polar primary metabolites of two chickpea cultivars with contrasting responses to salinity. *Journal of Chromatography B-Analytical Technologies in the Biomedical and Life Sciences* **1000**, 1-13 (2015).
19. Allu, A.D., Soja, A.M., Wu, A., Szymanski, J. & Balazadeh, S. Salt stress and senescence: identification of cross-talk regulatory components. *Journal of Experimental Botany* (2014).

20. Campbell, M.T. *et al.* Integrating Image-Based Phenomics and Association Analysis to Dissect the Genetic Architecture of Temporal Salinity Responses in Rice. *Plant Physiology* **168**, 1476-U1697 (2015).
21. Rajendran, K., Tester, M. & Roy, S.J. Quantifying the three main components of salinity tolerance in cereals. *Plant, Cell and Environment* **32**, 237-249 (2009).
22. Maliro, M.F.A., McNeil, D., Redden, B., Kollmorgen, J.F. & Pittock, C. Sampling strategies and screening of chickpea (Cicer arietinum L.) germplasm for salt tolerance. *Genetic Resources and Crop Evolution* **55**, 53-63 (2008).
23. Khan, H.A., Siddique, K.H.M. & Colmer, T.D. Salt sensitivity in chickpea is determined by sodium toxicity. *Planta*, 1-15 (2016).
24. Saxena, N.P. Chickpea. *In: Goldworthy, Fisher, (Eds.), The Physiology of Tropical Field Crops. John Wiley & Sons Ltd., New York*, 419-452 (1984).
25. Johansen, C. *et al.* Genotypic variation in salinity response of chickpea and pigeonpea. *In: Sinha, S.K., Sane, P.V., Bhargava, S.C., Agrawal, P.K. (Eds.), Proceedings of the International Congress of Plant Physiology. Indian Society for Plant Physiology and Biochemistry, Indian Agriculture Research Institute, New Delhi.* **1**, 977-983 (1990).
26. Upadhyaya, H.D. *et al.* Genetic structure, diversity, and allelic richness in composite collection and reference set in chickpea (Cicer arietinum L.). *BMC Plant Biology* **8**(2008).
27. Vadez, V. *et al.* LeasyScan: a novel concept combining 3D imaging and lysimetry for high-throughput phenotyping of traits controlling plant water budget. *J Exp Bot* **66**, 5581-93 (2015).
28. Takahashi, F. *et al.* Comparison of leaf sheath transcriptome profiles with physiological traits of bread wheat cultivars under salinity stress. *PLoS ONE* **10**(2015).
29. James, R.A. & Sirault, X.R. Infrared thermography in plant phenotyping for salinity tolerance. *Methods in molecular biology (Clifton, N.J.)* **913**, 173-189 (2012).
30. Pound, M.P., French, A.P., Fozard, J.A., Murchie, E.H. & Pridmore, T.P. A patch-based approach to 3D plant shoot phenotyping. *Machine Vision and Applications*, 1-13 (2016).
31. Hairmansis, A., Berger, B., Tester, M. & Roy, S.J. Image-based phenotyping for non-destructive screening of different salinity tolerance traits in rice. *Rice (N Y)* **7**, 16 (2014).
32. Schilling, R.K. *et al.* Expression of the Arabidopsis vacuolar H+-pyrophosphatase gene (AVP1) improves the shoot biomass of transgenic barley and increases grain yield in a saline field. *Plant Biotechnology Journal* **12**, 378-386 (2014).
33. Coombes, N.E. Digger:design search tool in R. (2009).
34. Brien, C.J. dae: Functions useful in the design and ANOVA experiments. in *R package version 2.7-16* (2016).
35. RCoreTeam. R: A Language and Environment for Statistical Computing. (2016).
36. Al-Tamimi, N. *et al.* Salinity tolerance loci revealed in rice using high-throughput non-invasive phenotyping. *Nature Communications* **7**, 13342 (2016).
37. Cullis, B.R., Smith, A.B. & Coombes, N.E. On the design of early generation variety trials with correlated data. *Journal of Agricultural Biological and Environmental Statistics* **11**, 381-393 (2006).
38. Wold, H. Soft Modeling: The Basic Design and Some Extensions, in Systems Under Indirect Observations. *Part II, K. G. Jöreskog and H. Wold (eds.), North-Holland: Amsterdam*, 1-54 (1982).
39. Serraj, R., Krishnamurthy, L. & Upadhyaya, H.D. Screening chickpea mini-core germplasm for tolerance to salinity. Int. Chickpea Pigeonpea. *Newslett* **11**, 29-32 (2004).
40. Yamaguchi, T. & Blumwald, E. Developing salt-tolerant crop plants: challenges and opportunities. *Trends in Plant Science* **10**, 615-620 (2005).
41. Udupa, S., Sharma A, RP, S. & RA, P. Narrow genetic variability in Cicer arietinum as revealed by RFLP analysis. *Journal of Plant Biochemistry and Biotechnology* **2**, 83-86 (1993).

42. Abideen, Z. *et al.* Moderate salinity stimulates growth and photosynthesis of Phragmites karka by water relations and tissue specific ion regulation. *Environmental and Experimental Botany* **105**, 70-76 (2014).
43. Tuberosa, R. Phenotyping for drought tolerance of crops in the genomics era. *Frontiers in Physiology* **3**(2012).
44. Passioura, J.B. Phenotyping for drought tolerance in grain crops: when is it useful to breeders? *Functional Plant Biology* **39**, 851-859 (2012).

Chapter 3

Quantitative profiling of polar primary metabolites of two chickpea cultivars with contrasting responses to salinity

Daniel Anthony Dias[a,1], Camilla Beate Hill [b,*,1], Nirupama Samanmalie Jayasinghe[a], Judith Atieno[c], Tim Sutton[c,d], Ute Roessner[a,b]

[a] Metabolomics Australia, School of BioSciences, The University of Melbourne, Parkville, Victoria 3010, Australia

[b] School of BioSciences, The University of Melbourne, Parkville, Victoria 3010, Australia

[c] Australian Centre for Plant Functional Genomics, School of Agriculture, Food and Wine, The University of Adelaide, Glen Osmond, South Australia, 5064, Australia

[d] South Australian Research and Development Institute, GPO Box 397 Adelaide, South Australia 5001, Australia

∗ Corresponding author: camilla.hill@unimelb.edu.au.

[1] Equal first authors

Statement of Authorship

Title of Paper	Quantitative profiling of polar primary metabolites of two chickpea cultivars with contrasting responses to salinity
Publication Status	☑ Published ☐ Accepted for Publication ☐ Submitted for Publication ☐ Unpublished and Unsubmitted work written in manuscript style
Publication Details	GC–*Qq*Q–MS method was developed and validated to quantify 49 primary metabolites. The method was applied to tissues of salt tolerant (Genesis836) and sensitive (Rupali) chickpea cultivars. Larger differences in sugar levels were noted in tissues of Rupali. Amino acid levels were depleted in flowers of Genesis836 but increased in flowers of Rupali after stress.

Candidate contribution

Name of candidate	Judith Akinyi Atieno
Contribution to the Paper	Contributed to the conception and design of this experiment. Developed methods for growing chickpea under controlled environment, including finding suitable growing media, watering regime, temperature and lighting conditions and pest control. Developed methods for salinity screening (optimal salt levels, salt delivery system, and symptoms scoring). Conducted salinity experiment including daily watering of plants to field capacity to maintain salt concentration in pots. Collected plant materials (leaf and pod samples) at two time points -to capture different phases of salinity stress- for metabolite profiling. Contributed to writing and proof-reading of the manuscript. This work took approximately six months.
Overall percentage (%)	25
Certification:	This paper reports on original research I conducted during the period of my Higher Degree by Research candidature and is not subject to any obligations or contractual agreements with a third party that would constrain its inclusion in this thesis.
Candidate signature	Date 29/11/16
Principal supervisor	Date 29/11/16

Statement of Authorship

Title of Paper: Quantitative profiling of polar primary metabolites of two chickpea cultivars with contrasting responses to salinity

Publication Status: Published

Citation: Dias D.A, Hill C.B, Jayasinghe N.S, Atieno J, Sutton T, Roessner U (2015) Quantitative profiling of polar primary metabolites of two chickpea cultivars with contrasting responses to salinity. Journal of Chromatography B, 1000:1-13. doi:10.1016/j.jchromb.2015.07.002

Author Contributions

By signing the Statement of Authorship, each author certifies that their stated contribution to the publication is accurate and permission is granted for the publication to be included in the candidate's thesis.

Daniel Anthony Dias: Contributed to design of the study and the experiments and wrote paper together with Dr Camilla Beate Hill (joint first authors)

Signature **Date 04/11/2016**

Camilla Beate Hill: Contributed to design of the study and the experiments, analysed and interpreted analytical data from the chickpea experiment, performed statistical analysis and prepared figures, wrote paper together with Dr Daniel Dias (joint first authors)

Signature **Date 03/11/206**

Nirupama Samanmalie Jayasinghe: Developed and validated GC-QqQ-MS MRM method, optimised sample preparation, extracted samples and acquired data on GC-QqQ-MS and performed data analysis.

Signature **Date 04/11/2016**

Judith Atieno: Developed methods for growing chickpea under controlled environment, developed methods for salinity screening, conducted salinity experiment, contributed to writing methodology section of the manuscript.

Signature **Date 23/11/2016**

Tim Sutton: Supervised development of methods for growing chickpea under controlled environment and salinity screening.

Signature **Date 04/11/2016**

Ute Roessner: Developed the experimental plan, supervised NJ, DD and CH, contributed to manuscript writing and proof-reading.

Signature **Date 04/11/2016**

Link to chapter 3

Studies on metabolic responses to environmental stresses increase our understanding of pathways involved in stress response and pin point key metabolites that can be used to discriminate between tolerant and sensitive genotypes. This chapter focuses on optimisation of methods to quantify metabolite accumulation in complex biological tissues. GC-QqQ-MS was compared to a more developed platform, LC-QqQ-MS, to compare its reproducibility, linearity and recovery. Quantification of metabolites from 4 major classes (sugars, sugar acids, sugar phosphates and organic acids) were carried out in flowers and pods of two chickpea cultivars (Genesis836 and Rupali) that contrast in salinity tolerance, prior to and after salt application. GC-QqQ-MS was seen to detect large number of polar metabolites in low concentrations and in a single analysis. Interestingly, elevated levels of amino acids, proline and sugars were noted in Rupali compared to Genesis836. In contrast to other studies carried out in different plants, this study found proline to have limited role as osmoprotectant. Additionally, this study also found metabolic differences between Genesis836 and Rupali following salt stress is associated with metabolites involved in carbon metabolism, TCA cycle as well as amino acid metabolism. This work has been published in Journal of Chromatography B as follows; Dias D.A, Hill C.B, Jayasinghe N.S, Atieno J, Sutton T, Roessner U (2015) Quantitative profiling of polar primary metabolites of two chickpea cultivars with contrasting responses to salinity. Journal of Chromatography B 1000:1-13.doi:10.1016/j.jchromb.2015.07.002.

Journal of Chromatography B, 1000 (2015) 1–13

Contents lists available at ScienceDirect

Journal of Chromatography B

journal homepage: www.elsevier.com/locate/chromb

Quantitative profiling of polar primary metabolites of two chickpea cultivars with contrasting responses to salinity

Daniel Anthony Dias[a,1], Camilla Beate Hill[b,*,1], Nirupama Samanmalie Jayasinghe[a], Judith Atieno[c], Tim Sutton[c,d], Ute Roessner[a,b]

[a] Metabolomics Australia, School of BioSciences, The University of Melbourne, Parkville, Victoria 3010, Australia
[b] School of BioSciences, The University of Melbourne, Parkville, Victoria 3010, Australia
[c] Australian Centre for Plant Functional Genomics, School of Agriculture, Food and Wine, The University of Adelaide, Glen Osmond, South Australia, 5064, Australia
[d] South Australian Research and Development Institute, GPO Box 397 Adelaide, South Australia 5001, Australia

ARTICLE INFO

Article history:
Received 11 February 2015
Received in revised form 28 June 2015
Accepted 2 July 2015
Available online 13 July 2015

Keywords:
Quantitative profiling
Primary metabolites
GC–*QqQ*–MS
LC–*QqQ*–MS
Chickpea
Salinity

ABSTRACT

This study reports a GC–*QqQ*–MS method for the quantification of forty-eight primary metabolites from four major classes (sugars, sugar acids, sugar phosphates, and organic acids) which can be applied to a number of biological systems. The method was validated in terms of linearity, reproducibility and recovery, using both calibration standards and real samples. Additionally, twenty-eight biogenic amines and amino acids were quantified using an established LC–*QqQ*–MS method. Both GC–*QqQ*–MS and LC–*QqQ*–MS quantitative methods were applied to plant extracts from flower and pod tissue of two chickpea (*Cicer arietinum* L.) cultivars differing in their ability to tolerate salinity, which were grown under control and salt-treated conditions. Statistical analysis was applied to the data sets using the absolute concentrations of metabolites to investigate the differences in metabolite profiles between the different cultivars, plant tissues, and treatments. The method is a significant improvement of present methodology for quantitative GC–MS metabolite profiling of organic acids and sugars, and provides new insights of chickpea metabolic responses to salinity stress. It is applicable to the analysis of dynamic changes in endogenous concentrations of polar primary metabolites to study metabolic responses to environmental stresses in complex biological tissues.

1. Introduction

Salinity and other environmental stresses directly affect the normal growth, development, and reproduction of a plant, and therefore the primary metabolites involved in these processes. The diversity and fluctuation in biological stresses faced by a plant has led to adaptation through biochemical defense mechanisms including both primary and secondary metabolites to directly manage environmental perturbations. With the development of specialized protocols, targeted analysis of primary metabolites can provide a substantial amount of information to investigate complex changes in metabolism caused by different genotypic and/or environmental perturbations.

Chickpea (*Cicer arietinum* L.) is one of the world's most important pulse crops and ranks third in the world for food legume production [1]. Chickpea plants suffer damage even on moderately saline soils that have little impact on bread wheat, which in turn impacts on potential yields of chickpea in rotation with wheat on areas with sub-soil salinity. The reproductive phase is known to be even more sensitive to NaCl exposure than vegetative growth and germination [2], the early development of flower meristems, the conversion of flowers to pods, and the development of seeds in the pods are particularly susceptible to salinity stress. The number of flowers, pods, and seeds is significantly decreased in salt sensitive cultivars compared to tolerant chickpea lines upon salinity treatment [3], and carbohydrate supply to reproductive structures, such as the developing embryo is believed to be a limitation.

Abbreviations: DAS, days after sowing; BSTFA, *N,O*-bis-(trimethylsilyl)trifluoroacetamide; CE, collision energy; EI, electron ionization; ESI, electrospray ionization; GC–*QqQ*–MS, gas chromatography-triple quadrupole-mass spectrometry; ISTD, internal standard; LC–*QqQ*–MS, liquid chromatography–triple quadrupole-mass spectrometry; LOQ, limit of quantification; MRM, multiple reaction monitoring; *m/z*, mass-to-charge ratio; Pro, proline; PBQC, pooled biological quality control sample; QC, quality control calibration standard mix; RI, retention time index; R^2, linear correlation coefficient; SRM, selected reaction monitoring.

* Corresponding Author.
E-mail address: camilla.hill@unimelb.edu.au (C.B. Hill).
[1] Equal first authors (D.A.D. and C.B.H.).

http://dx.doi.org/10.1016/j.jchromb.2015.07.002

Plants have developed an extraordinary genetic diversity controlling the synthesis and regulation of metabolites that has largely been unexplored in the grain legumes. Data based on transcriptomics and proteomics analyses are insufficient to provide an understanding of all aspects of biological processes in response to abiotic stress, since those are ultimately mediated by metabolites. For example, changes in transcript or protein levels do not always correlate to actual changes of cell metabolites due to post-transcriptional and post-translational modifications that modulate protein activities [4]. However, only a few studies on primary metabolism in legumes are available, and these studies cover the model legumes *Medicago truncatula* [5], both model and cultivated legume species of the *Lotus genus* [6,7] and soybean [8].

Metabolomics is now being explored as a possible solution to these problems because it can capture the "ultimate phenotype" of such gene networks and their complex interaction with the environment [9]. Primary metabolites are mostly hydrophilic molecules directly involved in all biochemical processes, including growth, development, and reproduction. Compounds present in carbohydrate metabolism can be challenging to analyze due to the high diversity of compounds with a diverse array of functionalities (including neutral carbohydrates such as saccharides and polyalcohols, polysaccharides, and sugar acids), the often very similar fragmentation of isomers, and the co-elution of two or more compounds with very similar retention times which give rise to complex chromatograms. More effective tools and methods are required for efficient identification and quantification of compound classes, i.e., sugars and organic acids.

Liquid chromatography (LC) coupled to triple quadrupole (*QqQ*)–MS systems have benefited greatly from the high sensitivity and selectivity of tandem MS in the selected reaction monitoring (SRM) mode. Although the coupling of gas-chromatography (GC) to electron impact ionization (EI) mass spectrometry (MS) is one of most well-known and established techniques in analytical chemistry and one of the most developed instrument platforms for metabolite analysis [9]. GC-based methods have suffered a notable delay in the wide acceptance of the *QqQ* analyzer in comparison to LC–MS/MS. GC–MS has been widely used in metabolomics since it has significant separating power, is reproducible, easy to establish and requires a relatively low capital investment compared to other analytical technologies. GC–MS is an ideal analytical technology for the analysis of volatile compounds however most metabolites are not volatile and therefore need to be chemically derivatized in order to make them amenable for GC–MS.

In recent years, there has been a strong emphasis within the metabolomics community that quantitative data is important for biological studies since they describe accurately the actual concentration of the metabolites of interest. New *QqQ* instrumentation allows for higher selectivity and sensitivity and minimizes chromatographic interferences and is typically operated in multiple reactions monitoring (MRM) mode in which collision energies, dwell times and resolution parameters for each individual target compound is optimized using authentic standards, thus, enhancing sensitivity and selectivity [10]. In a single chromatographic run, the application of MRM can simultaneously monitor a large number of MS–MS transitions.

Metabolomics aims to provide a comprehensive and unbiased analysis of all metabolites with a low molecular weight present in a biological sample [4,9]. Due to the structural diversity of metabolites, there is currently no single methodology that can detect the complete metabolome, which is why several extraction methods and instrument platforms are established to analyze highly complex mixtures. Here we used both GC–MS and LC–MS techniques as they are complementary to each other: to accurately quantify primary metabolites of carbon and nitrogen metabolism, GC–MS-based metabolite analysis of organic acids, sugars, sugar alcohols, and sugar acids was carried out on a GC–*QqQ*–MS (Agilent 7890 GC coupled to 7000 Triple quadrupole MS). We have demonstrated the applicability of the method specifically to the extraction of metabolites of flower and pod tissue of two chickpea cultivars, 'Genesis836 and 'Rupali', before and after salinity stress. To investigate the effects of salinity on other metabolite classes of primary metabolism, we have combined it with an established LC–MS-based metabolomics method for quantification of amine-containing metabolites carried out on a LC–*QqQ*–MS (Agilent 1290 LC coupled to 6490 triple quadrupole MS) according to the standardized protocol developed by [11].

2. Materials and methods

2.1. Chemicals and reagents

All chemicals and solvents were purchased from Sigma–Aldrich (Australia) and were either of analytical or mass spectrometric grades. Deionized water (18.2 MΩ) was produced using a Synergy UV Millipore System (Millipore) was used throughout.

2.2. Plant growth and harvest

The desi chickpea cultivars used in the experiment were Genesis836 (salt tolerant) and Rupali (salt sensitive). Genesis836 is a direct introduction from the International Centre for Research in the Semi-Arid Tropics (ICRISAT, Syria), while Rupali was bred by the Department of Agriculture, Western Australia (DAWA), and the Centre for Legumes in Mediterranean Agriculture (CLIMA), The University of Western Australia.

The experiment was conducted in a glasshouse at the University of Adelaide Plant Accelerator facility (Waite Campus, South Australia). Temperature and humidity were controlled and ranged from 24 ± 2 °C and 40% (day), and 18 ± 2 °C and 90% (night), respectively.

Five seeds of each of the cultivars were sown 2 cm deep in pots (19.46 cm height × 14.94 cm diameter) filled with 2.5 kg of 50% University of California (UC) mixture (1:1 peat:sand) and 50% cocopeat (pH 7.5; electrical conductivity ($EC_{1:5}$ 603 μs/cm)). The soil was inoculated with *Rhizobium* inoculum (Group N) prior to sowing. Prior to salt application, plants in each pot were thinned to two uniform plants. At flowering, 21 and 25 days after sowing (DAS) for Rupali and Genesis836 respectively, each pot received either 0 or 60 mM NaCl (1.3149 g NaCl pot^{-1}) equivalent to applying 100 ml of 0mM NaCl (untreated pots) or 225 mM NaCl (treated pots) delivered in two increments through the base of the pots by standing the pots in saucers containing saline solution. Each treatment was replicated four times and randomized in a randomized complete block design (RCBD). The pots were watered every two days and maintained at field capacity, 15% (w/w)-determined gravimetrically to maintain salt concentration in the pots and to also avoid salt leaching out of the pots as a result of over watering.

Flowers and pods were harvested and pooled from two plants in each pot 31 and 48 DAS (for cv. Rupali) or 35 and 52 DAS (for cv. Genesis836). The samples were immediately frozen in liquid nitrogen, and thereafter stored at −80 °C.

2.3. Plant sample extraction and preparation

A modified method for the preparation of plant extracts was used as described previously by [24]. For each chickpea cultivar, approximately 30 mg of frozen flower and pod tissues was weighed into cryomill tubes (Precellys lysing kit, Bertin Technologies). Subsequently, 400 μL of 100% methanol containing 4% internal standard (from a stock solution containing 0.5 mg mL^{-1} $^{13}C_6$-sorbitol and 0.5 mg mL $^{13}C_5$–^{15}N valine) was added to the samples,

followed by vortex-mixing for 30 s, and homogenization (3 × 45 s at 6400 rpm) and −10 °C using a Cryomill (Precellys 24, Bertin Technologies). The samples were then extracted for 15 min at 70 °C in a thermomixer at 850 rpm, and subsequently centrifuged for 5 min at 4 °C and at 13,000 rpm. The supernatants were transferred into new reaction tubes, and 400 μL of water was added into the cryo-mill tubes containing the previously ground tissue pellet. The samples were vortex-mixed for 30 s, and centrifuged at 13,000 rpm for 10 min at 4 °C. The supernatants were then transferred into the reaction tube containing the original supernatant from the previous centrifugation. After the pooled samples were vortex-mixed for 30 s, 5 and 125 μL aliquots of the supernatants were transferred into glass vial inserts and dried *in vacuo* for GC–*QqQ*–MS analysis. In addition, 10 μL aliquots were transferred into glass vial inserts and used for LC–*QqQ*–MS amino acid analysis.

2.4. Gas chromatography–mass spectrometry

2.4.1. Calibration standard sample preparation

Twenty-eight sugars, sugar phosphates, sugar acids, and sugar alcohols, as well as twenty organic acids were purchased from Sigma–Aldrich (Australia). Ten millimole stock solutions were prepared for each individual standard except for 2-ketogluconic acid for which a 2 mM stock solution was prepared. One-hundred and sixty microliters of each sugar standard was subsequently pooled to reach a final volume of 4.48 mL. A 520 μL aliquot of 50% aqueous mixture of methanol was then added to the pooled sugar standards resulting in a final volume of 5 mL with a final concentration of 320 μM. For organic acids, 160 μL of each standard was subsequently pooled to reach a final volume of 4.16 mL, and a 840 μL aliquot of 50% aqueous mixture of methanol was then added resulting in a final volume of 5 mL with a final concentration of 320 μM.

The stock solutions were serially diluted with 50% aqueous mixture of methanol resulting in the following calibration series: 320, 160, 80, 40, 20, 10, 5, 2.5, 1.25 and 0.625 μM calibration points for xylose, malonate, maleate, succinate, fumarate, pipecolate, malate, salicylate, 2-oxoglutarate, aconitate, ferulic acid, raffinose, erlose, and melezitose, respectively; 160, 80, 40, 20, 10, 5, 2.5, 1.25 and 0.625 μM calibration points for itaconate, erythritol, arabinose, ribose, xylitol, rhamnose, arabitol, fucose, citrate, isocitrate, quinate, fructose, mannose, 2-keto gluconic acid, glucose, syringic acid, mannitol, glucuronate, galactitol, gluconate, inositol, uric acid, caffeic acid, fructose-6-phosphate, sucrose, maltose, trehalose, turanose, β-gentiobiose, and melibiose, respectively; 80, 40, 20, 10, 5, 2.5, 1.25 and 0.625 μM calibration points for galactose; and 160, 80, 40, 20, and 10 μM calibration points for nicotinic acid, shikimate, and glucose-6-phosphate, respectively. Forty microliters of each calibration stock was transferred into glass vial inserts, dried *in vacuo,* and stored at −20 °C before subjecting to GC–*QqQ*–MS analysis.

2.4.2. Sugar and organic acid derivatization

All samples were re-dissolved in 20 μL of 30 mg mL^{-1} methoxyamine hydrochloride in pyridine and derivatized at 37 °C for 120 min with mixing at 500 rpm. The samples were incubated for 30 min with mixing at 500 rpm after addition of both 20 μL *N,O*-bis -(trimethylsilyl)trifluoroacetamide (BSTFA) and 1 μL retention time standard mixture [0.029% (v/v) *n*-dodecane, *n*-pentadecane, *n*-nonadecane, *n*-docosane, *n*-octacosane, *n*-dotriacontane, *n*-hexatriacontane dissolved in pyridine]. Each derivatized sample was allowed to rest for 60 min prior to injection.

2.4.3. GC–MS Instrument conditions

Samples (1 μL) were injected into a GC–*QqQ*–MS system comprising of a Gerstel 2.5.2 Autosampler, a 7890A Agilent gas chromatograph and a 7000 Agilent triple-quadrupole MS (Agilent, Santa Clara, USA) with an electron impact (EI) ion source. The GC was operated in constant pressure mode (20 psi) with helium as the carrier gas and using mannitol as a standard for retention time locking of the method. The MS was adjusted according to the manufacturer's recommendations using tris-(perfluorobutyl)-amine (CF43). A J&W Scientific VF-5MS column (30 m long with 10 m guard column, 0.25 mm inner diameter, 0.25 μm film thickness) was used. The injection temperature was set at 250 °C, the MS transfer line at 280 °C, the ion source adjusted to 250 °C and the quadrupole at 150 °C. Helium was used as the carrier gas at a flow rate of 1 mL min^{-1}. Nitrogen (UHP 5.0) was used as the collision cell gas at a flow rate of 1.5 mL min^{-1}. Helium (UHP 5.0) was used as the quenching gas at a flow rate of 2.25 mL min^{-1}. The following temperature program was used; injection at 70 °C, hold for 1 min, followed by a 7 °C min^{-1} oven temperature, ramp to 325 °C and a final 6 min heating at 325 °C.

2.4.4. Method optimization

Individual sugars, organic acids and internal standards were subsequently analyzed on the GC–*QqQ*–MS to obtain retention times and to identify a corresponding unique, precursor ion. For each precursor ion, two product ion scans were carried out using four collision energies (0, 5, 10 and 20 V) to identify product ions in which two product ions were identified. Subsequently, for the two generated products the collision energies for each major reaction monitoring (MRM) transition was optimized using a series of collision energies (CEs) between 0 and 30 V. Collision energy optimization plots for each compound are presented in Additional file 3.

Once collision energies were optimized for each MRM transition, a product ion was selected as the corresponding target ion (T) and the subsequent MRM transition was deemed as the qualifier ion (Q). In some cases, especially for organic acids, a target ion was only provided due to the lack of observable fragment ions and low molecule weight. Absolute concentrations (μM) of targeted sugar and organic acids were quantified using a MRM target ion based on the linear response of the calibration series as described previously. For PBQC samples, additional normalization steps were required to include the weight of the samples as well as the area response for $^{13}C_6$-sorbitol (extraction internal standard).

2.4.5. Method validation

Calibration standards were analyzed for each metabolite to determine retention times, retention time indices relative to the retention time standard mixture, linear correlation coefficient (R^2), recovery, and reproducibility experiments. Calibration curves created for each analyte were fitted using linear regression. Response ratios were calculated relative to the internal standards $^{13}C_1$-mannitol, and the linearity was determined by calculating the corresponding R^2 value. Method reproducibility and recovery was assessed by analysis of calibration standards and of extractions of chickpea samples analyzed in hexaplicates on separate days. The concentrations of the analytes and the standard error of the mean were calculated at each concentration within the linear range of the assay.

2.5. Liquid chromatography–mass spectrometry

2.5.1. Calibration standard sample preparation

Two stock solutions were also prepared: (i) an amino acid solution containing a standard mix of 28 amino acids and amines (4-hydroxyproline, histidine, asparagine, arginine, serine, glutamine, homoserine, glycine, aspartate, citrulline, glutamate, threonine, alanine, γ-aminobutyric acid, proline, cysteine, ornithine, octopamine, lysine, putrescine, tyrosine, methionine, valine, tyramine, isoleucine, leucine, phenylalanine, and trypto-

Table 1
Optimized GC–*QqQ*–MS parameters in multiple reaction monitoring mode (MRM) for the quantification of primary metabolites. Dwell time: 5 s. *Target (T) or qualifier (Q) transition. CE, collision energy.

Compound name	Precursor ion	Product ion	Transition*	CE (V)
Internal standards				
$^{13}C_1$-mannitol	320	130	T	5
$^{13}C_6$-sorbitol	323	132	T	8
Organic acids				
2-Ketogluconic acid	349	201	T	8
	349	186	Q	4
2-Oxoglutarate	198	167	Q	2
	198	154	T	6
Aconitate	375	211	T	4
	375	285	Q	4
Caffeic acid	219	191	T	12
Citrate	183	138.7	T	4
Ferulic acid	308	219	T	4
	308	293	Q	18
Fumarate	245	217	T	6
	245	170.9	Q	12
Isocitrate	257	200.7	T	4
Itaconate	215	132.8	T	18
	259	130.8	Q	20
Malate	233	189	T	2
Maleate	245	216.7	T	4
	245	132.7	Q	12
Malonate	233	216.8	T	2
	233	142.8	Q	8
Nicotinic acid	180	105.9	T	8
	180	135.9	Q	14
Pipecolate	156	83.9	T	6
	156	127.9	Q	6
Quinate	255	239	T	8
	345	255.1	Q	8
Salicylate	267	209	T	8
	209	91	Q	8
Shikimate	255	239	T	4
	204	189	Q	8
Succinate	172	112.9	T	4
	172	155.9	Q	0
Syringic acid	327	312	T	18
Uric acid	456	441.1	T	4
	456	382.1	Q	4
Sugars				
Arabinose	307	217	T	2
β-Gentibiose	361	243	T	6
Erlose	361	169.1	T	10
Fructose	307	217	T	2
Fucose	321	117	T	2
Galactose	319	157	T	4
Glucose	319	129	T	10
Maltose	361	169	T	10
Mannose	319	129	T	6
Melezitose	361	169	T	10
Melibiose	361	169	T	6
Raffinose	361	169	T	10
Rhamnose	364	160	T	4
Ribose	307	217	T	2
Sucrose	361	169	T	6
Trehalose	361	169	T	8
Turanose	361	169	T	6
Xylose	307	217	T	2
Sugar phosphates				
Fructose-6-phosphate	204	189	T	4
Glucose-6-phosphate	364	160	T	4
Sugar alcohols				
Arabitol	319	129	T	4
Erythritol	307	217	T	2
Galactitol	319	129	T	10
Gluconic Acid	423	333	T	4
Glucuronate	364	160	T	4
Inositol	305	217	T	8
Mannitol	319	157	T	4
Xylitol	319	157	T	2

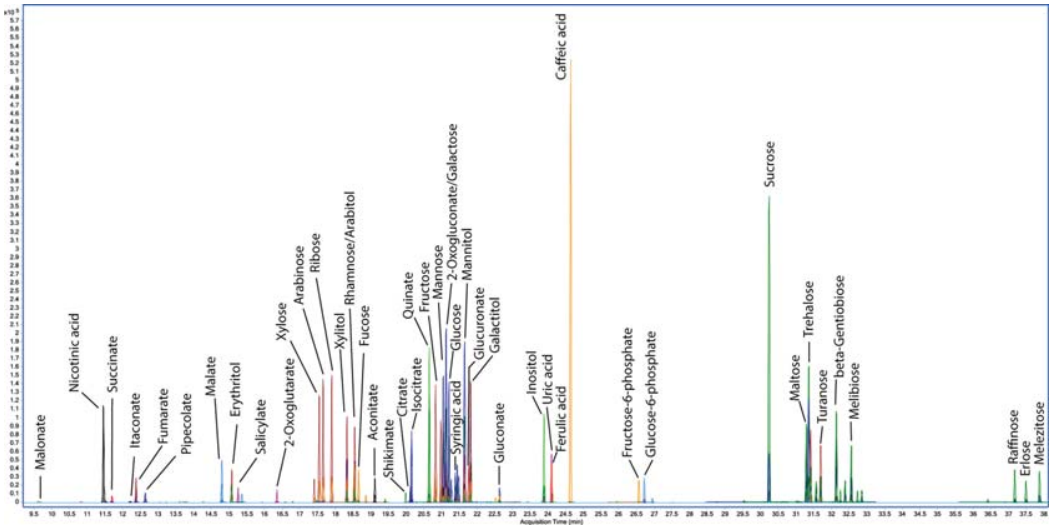

Fig. 1. GC–*QqQ*–MS chromatographic traces showing the separation of 45 primary metabolites within the standard mixes of the developed methodology. Detailed chromatograms are provided (Additional file 2).

phan) in deionized water supplemented with 0.1% formic acid, and (ii) a sulfur-containing compound solution containing glutathione (2.5 mM) and S215 adenosylhomocysteine in deionized water supplemented with 10 mM tris(2-carboxyethyl) phosphine (TCEP) and 1 mM ascorbate. The two stock solutions were mixed and diluted using volumetric glassware with water containing 10 mM TCEP, 1 mM ascorbate and 0.1% formate to produce the following calibration series of combined standards: 0.1, 0.5, 1, 5, 10, 20, 50, 100 and 150 μM.

2.5.2. Amino acid derivatization

For derivatization, an aliquot of each standard or sample (10 μL) was added to 70 μL of borate buffer (200 mM, pH 8.8 at 25 °C) containing 10 mM TCEP, 1 mM ascorbic acid and 50 μM 2-aminobutyrate. The resulting solution was vortexed before adding 20 μL of 6-aminoquinolyl-*N*-hydrosysuccinimidyl carbamate (AQC) reagent [200 mM dissolved in 100% acetonitrile (ACN)] immediately vortexing as described [11]. The 6-aminoquinolyl-*N*-hydroxysuccinimidyl carbamate (AQC) reagent was synthesized according to [25]. The samples were heated with shaking at 55 °C for 10 min then centrifuged (13,000 rpm at RT) and transferred to HPLC vials containing inserts (Agilent, springless glass inserts 250 μL) prior to injection.

2.5.3. LC–MS Instrument Conditions

An Agilent 1200 LC-system coupled to an Agilent 6410 Electrospray Ionisation-Triple Quadrupole-MS was used for quantification experiments. The injection volume used for the samples or standards was 1 μL. Ions were monitored in the positive mode using a Dynamic Multiple Reaction Monitoring (DMRM) method optimized for each analyte. The source, collision energies and fragmentor voltages were optimiszed for each analyte by infusing a derivatized standard with LC eluent. The following source conditions were used: sheath gas temperature 315 °C, gas flow 10 L min^{-1}, nebulizer pressure 45 psi and capillary voltage 3800 V. For the chromatography, an Agilent Zorbax Eclipse XDB-C18 Rapid Resolution HT 2.1 × 50 mm, 1.8 μm column was used with a flow rate of 300 μL min^{-1}, maintained at 30 °C, resulting in operating pressures below 400 bar with a 19 min run time as described in Boughton et al. [11]. A gradient LC method was used with mobile phases that comprised of (A) water 0.1% formic acid and (B) acetonitrile 0.1% formic acid (such that at 0.0 and 2.0 min, the % of B was 1 and then increased to 15 and 30% at 9.0 and 14.0 min, respectively, followed by a reduction to 1% at 14.1 and 19.0 min). These conditions provided suitable chromatographic separation of modified amino acids and although co-elution was observed for some of the species, this could be overcome by the mass-selective capabilities of the mass spectrometer using MRM.

2.6. Data processing and statistical analysis

Data were processed using the Agilent MassHunter Workstation Software, Quantitative Analysis, Version B.05.00/Build 5.0.291.0 for quantitation of all compounds. Differences between samples were validated by the Student's *t* -test. Statistical analysis was performed using Excel (Microsoft, www.microsoft.com/).

3. Results and discussion

3.1. Optimization of precursor-to-product ion transitions

The following polar primary metabolites and their internal standards were analysed using GC–*QqQ*–MS: sugars (xylose, arabinose, ribose, rhamnose, fucose, fructose, mannose, galactose, glucose, sucrose, maltose, trehalose, turanose, β-gentiobiose, melibiose, raffinose, erlose, melizitose), sugar phosphates (fructose-6-phosphate, glucose-6-phosphate), sugar alcohols (erithritol, xylitol, arabitol, mannitol, galactitol, inositol), as well as organic acids (malonate, nicotinic acid, maleate, succinate, itaconate, fumarate, pipecolate, malate, salicylate, 2-oxoglutarate, aconitate, shikimate, citrate, isocitrate, quinate, 2-oxogluconate, gluconic acid, glucuronic acid, syringic acid, ferulic acid, uric acid and caffeic acid). $^{13}C_6$-Sorbitol and $^{13}C_5$–^{15}N valine of extraction internal standards which were added into the extraction solvent to compensate for

Table 2
GC–*QqQ*–MS method validation: linearity and recovery. SE, standard error. RI, retention time index. QC, quality control sample. PBQC, pooled biological quality control sample. R^2, linear correlation coefficient.

Metabolite	RI	R^2	QC % recovery(mean + SE)	PBQC % recovery(mean + SE)
Malonate	1046.7	0.9977	105.92 ± 14.68	109.5 ± 14.34
Nicotinic acid	1296.9	0.9977	118.93 ± 12.26	92.24 ± 6.14
Maleate	1300.7	0.9928	91.2 ± 18.28	85.51 ± 5.75
Succinate	1311.7	0.9992	129.23 ± 18.81	106.13 ± 4.79
Itaconate	1339.8	0.9936	103.92 ± 15.6	107.37 ± 5.66
Fumarate	1349.2	0.9982	112.55 ± 13.15	101.87 ± 11.48
Pipecolate	1361.8	0.9982	118.97 ± 21.38	106.5 ± 10.79
Malate	1481.8	0.9972	113.87 ± 12.84	110.64 ± 18.56
Erythritol	1496.8	0.9998	91.24 ± 7.03	103.05 ± 2.09
Salicylate	1506.1	0.9709	125 ± 11.7	82 ± 5.4
2-Oxoglutarate	1577.5	0.9978	114.52 ± 9.24	77.69 ± 12.82
Xylose	1644.1	0.9992	113.9 ± 10.1	97.88 ± 3.39
Arabinose	1660	0.9984	88.93 ± 6.97	100.58 ± 6.35
Ribose	1675.2	0.9985	89.41 ± 7.31	95.86 ± 2.23
Xylitol	1702.5	0.9986	88.78 ± 6.39	114.9 ± 2.23
Rhamnose	1715.2	0.9984	88 ± 7.52	114.63 ± 3
Arabitol	1716.5	0.9985	87.58 ± 6.91	126.66 ± 2.07
Aconitate	1752.1	0.995	120.23 ± 10.4	89.91 ± 10.39
Fucose	1758.4	0.9975	96.51 ± 9.07	89.16 ± 6.53
Shikimate	1807.9	0.9952	121.42 ± 14.98	106.17 ± 4.1
Citrate	1815.6	0.9907	115.62 ± 15.67	106.79 ± 2.52
Isocitrate	1818.1	0.9926	112.57 ± 16.61	109.08 ± 5.99
Quinate	1849.2	0.9984	120.54 ± 16.84	131.25 ± 3.28
Fructose	1860.6	0.9998	86.84 ± 8.96	117.21 ± 17.72
Mannose	1870.1	0.9972	88.21 ± 9.39	106.7 ± 3.03
Galactose	1875.4	0.9986	104.92 ± 7.14	108.71 ± 2.99
2-Ketogluconic acid	1877.8	0.9948	51.31 ± 18.19	97.69 ± 2.18
Glucose	1881.3	0.9948	103 ± 6.43	110.27 ± 24.08
Syringic acid	1896.2	0.9977	85.08 ± 17.05	110.25 ± 5.36
Mannitol	1914.9	0.9957	100.02 ± 7.19	110.53 ± 3.85
Glucuronate	1922.4	0.998	90.35 ± 8.62	100.59 ± 3.21
Galactitol	1926.9	0.9961	101.66 ± 6.69	106.56 ± 1.86
Gluconate	1987.3	0.9985	99.06 ± 13.94	101.99 ± 2.35
Inositol	2080.8	0.9978	84.42 ± 9.68	105.06 ± 3.09
Ferulic acid	2097	0.9951	121.45 ± 16.02	102.71 ± 8.57
Uric acid	2097	0.9931	113.01 ± 18.16	103.3 ± 7.01
Caffeic acid	2136.6	0.9927	100.96 ± 14.22	102.57 ± 7.69
Fructose-6-P	2297.9	0.9963	99.99 ± 7.62	97.95 ± 5.51
Glucose-6-P	2311.4	0.9986	106.79 ± 14.57	104.67 ± 7.1
Sucrose	2627.5	0.9927	48.13 ± 7.5	104.9 ± 6.9
Maltose	2721.9	0.9992	94.3 ± 12.41	93.16 ± 4.05
Trehalose	2727.2	0.9921	79.86 ± 6.56	103.52 ± 4.46
Turanose	2732.6	0.9973	92.15 ± 14.15	84.97 ± 3.87
beta-Gentibiose	2797.9	0.9951	107.07 ± 17.57	99.52 ± 9.77
Melibiose	2842.9	0.9966	90.28 ± 5.8	104.56 ± 10.12
Raffinose	3346.9	0.9844	102.77 ± 6.28	98.14 ± 14.92
Erlose	3385.4	0.9809	117.63 ± 20.38	95.96 ± 24.21
Melezitose	3426.2	0.9931	113.05 ± 14.84	114.78 ± 17.74

the inefficiencies or losses in the extraction and sample preparation steps. $^{13}C_6$-Sorbitol and $^{13}C_5$-^{15}N Valine act as internal standards for GC–*QqQ*–MS analysis and LC–*QqQ*–MS analysis respectively. $^{13}C_1$-Mannitol accounts for the variations during data acquisition in GC–*QqQ*–MS including derivatization, ionization and detection of sugars, sugar acids, sugar phosphates, sugar alcohols and organic acids. Optimal MRM transitions, dwell time, and collision energies were identified using authentic standards for each metabolite (Table 1, Additional file 1).

Fig. 1 and Additional file 2 show the final chromatographic separation achieved for the 45 metabolites using GC–*QqQ*–MS. MS/MS conditions were optimized to produce maximal signal, and plots (intensity vs collision energy) showing the optimization of transitions are provided in Additional file 3.

3.2. Method validation

The validation experiments were conducted to demonstrate robustness, precision, and accuracy of this method, and to ensure that the measured concentrations are close to the unknown content of the metabolite present in real samples. For this study we evaluated the linear correlation coefficient (R^2), higher and lower limits of quantitation, recovery, and reproducibility of the analytical method for quantitation of organic acids, sugar phosphates, sugar alcohols, and sugars, in samples spiked with a known concentration of calibration standard mix as well as samples prepared from pooled biological quality control (PBQC) samples of chickpea tissues (Tables 2 and 3).

3.3. Calibration curve, limit of quantitation, and linearity

Linearity of the calibration curve for each organic acid and sugar was assessed by preparing serial dilutions of the calibration standards mixes ranging from 320 μM to 0.625 μM in triplicate for each metabolite (as detailed in Section 2). The limits of quantification (LOQ) are defined as the highest and lowest analyte concentration, which can be quantified precisely and accurately, and is identical to the lowest and highest point of the calibration curve. A linear regression was used in the calibration curve for all metabolites. For mannitol, galactitol, gluconate, caffeic acid, fructose-6-phosphate,

Table 3
GC–*QqQ*–MS method validation: reproducibility. Values obtained during the validation of the method for quantification of sugars and organic acids in spiked/unspiked QC and PBQC samples. QC, quality control sample. PBQC, pooled biological quality control sample. Mean in μM. SE, standard error, n.d.: not detected, CV: coefficient of variation; concentration of the spike: 50 μM.

Metabolite	QC spiked		QC not spiked		PBQC spiked		PBQC not spiked	
	(Mean ± SE)	CV	(Mean ± SE)	CV	(Mean ± SE)	CV	(Mean ± SE)	CV
2-Ketogluconic acid	83.46 ± 1.68	0.02	64.11 ± ±1.03	0.02	51.4 ± 0.98	0.02	2.56 ± 0.01	0.00
2-Oxoglutarate	118.06 ± 4.56	0.04	61.45 ± 3.37	0.05	72.78 ± 6.92	0.10	33.93 ± 2.09	0.06
Aconitate	127.82 ± 4.97	0.04	67.54 ± 3.03	0.04	52.38 ± 4.42	0.08	7.43 ± 0.51	0.07
Caffeic acid	116.02 ± 4.85	0.04	66.94 ± 1.57	0.02	56.77 ± 3.35	0.06	5.48 ± 0.13	0.02
Citrate	140.62 ± 3.86	0.03	86.33 ± 1.97	0.02	78.39 ± 2.43	0.03	25 ± 1.68	0.07
Ferulic acid	135.33 ± 6.76	0.05	74.16 ± 1.37	0.02	54.84 ± 3.85	0.07	3.49 ± 0.02	0.01
Fumarate	137.24 ± 7.18	0.05	79.35 ± 2	0.03	72.64 ± 4.75	0.07	21.71 ± 1.23	0.06
Isocitrate	133.99 ± 5.08	0.04	80.32 ± 2.22	0.03	60.29 ± 2.64	0.04	5.75 ± 0.2	0.03
Itaconate	134.55 ± 7.71	0.06	81.23 ± 1.62	0.02	56.36 ± 2.6	0.05	2.68 ± 0.31	0.11
Malate	140.7 ± 6.35	0.05	83 ± 1.44	0.02	226.29 ± 3.49	0.02	170.97 ± 10.29	0.06
Maleate	109.58 ± 4.75	0.04	69.65 ± ±3.08	0.04	44.52 ± 2.32	0.05	1.76 ± 0.5	0.28
Malonate	120.78 ± 9.25	0.08	62.98 ± 4.42	0.07	63.56 ± 6.86	0.11	8.81 ± 0.55	0.06
Nicotinic acid	135.55 ± 8.18	0.06	71.66 ± 1.11	0.02	78.35 ± 7.75	0.10	22.3 ± 2.34	0.10
Pipecolate	133.23 ± 9.2	0.07	78.7 ± 2.69	0.03	61.22 ± 4.65	0.08	7.97 ± 0.25	0.03
Quinate	149.72 ± 5.41	0.04	91.79 ± 0.92	0.01	70.12 ± 1.5	0.02	4.49 ± 0.04	0.01
Salicylate	124.31 ± 6.19	0.05	59.27 ± 3.8	0.06	81.63 ± 3.6	0.04	13.5 ± 0.05	0.00
Shikimate	137.77 ± 8.66	0.06	73.26 ± 0.47	0.01	66.45 ± 2.09	0.03	13.36 ± 0.42	0.03
Succinate	139.51 ± 7.39	0.05	76.52 ± 1.38	0.02	138.67 ± 8.65	0.06	86.34±4.57	0.05
Syringic acid	112.93 ± 3.73	0.03	74.45 ± 0.99	0.01	56.18 ± 2.39	0.04	1.06 ± 0.02	0.02
Uric acid	131.75 ± 6.07	0.05	77.26 ± 1.26	0.02	56.34 ± 3.14	0.06	4.69 ± 0.04	0.01
Erlose	114.67 ± 12.15	0.11	47.32 ± 2.68	0.06	49.68 ± 10.84	0.22	1.67 ± 0.04	0.02
Arabinose	124.27 ± 5.37	0.04	75.5 ± 1.21	0.02	56.79 ± 2.7	0.05	6.57 ± 0.21	0.03
Arabitol	137.93 ± 4.85	0.04	90.65 ± 1.14	0.01	64.37 ± 0.91	0.01	1.02 ± 0.04	0.04
β-Gentibiose	116.86 ± 7.48	0.06	60.24 ± 1.41	0.02	58.24 ± 4.72	0.08	8.47 ± 0.41	0.05
Erythritol	125.25 ± 5.81	0.05	74.83 ± 1.27	0.02	52.79 ± 0.93	0.02	1.27 ± 0.01	0.00
Fructose	122.87 ± 5.77	0.05	74.99 ± 0.71	0.01	174.73 ± 6.35	0.04	116.38 ± 1.67	0.01
Fructose-6-P	115.93 ± 4.21	0.04	63.14 ± 1.76	0.03	53.61 ± 2.47	0.05	4.64 ± 0	0.00
Fucose MX1	117.88 ± 6.34	0.05	64.64 ± 0.95	0.01	54.26 ± 3.13	0.06	9.74 ± 0.52	0.05
Galactitol	129.71 ± 4.26	0.03	75.76 ± 0.73	0.01	54.02 ± 0.84	0.02	0.72 ± 0.04	0.04
Galactose	111.02 ± 2.57	0.02	59.18 ± 4.45	0.08	54.46 ± 1.34	0.02	0.1 ± 0	0.00
Gluconate	108.57 ± 7.55	0.07	54.22 ± 1.2	0.02	51 ± 1.05	0.02	n.d.	-
Glucose	126.79 ± 4.29	0.03	72.33 ± 0.96	0.01	227.41 ± 7.93	0.03	172.25 ± 2.94	0.02
Glucose-6-P	113.79 ± 6.95	0.06	56.74 ± 1.22	0.02	54.95 ± 3.82	0.07	6.53 ± 0.01	0.00
Glucuronate	120.37 ± 5.13	0.04	71.66 ± 1.09	0.02	51 ± 1.44	0.03	0.71 ± 0.01	0.00
Inositol	122.87 ± 5.26	0.04	77.2 ± 1.42	0.02	69.62 ± 1.7	0.02	16.67 ± 1.12	0.07
Maltose	112.59 ± 5.18	0.05	63.54 ± 1.81	0.03	49.39 ± 1.81	0.04	2.82 ± 0.01	0.00
Mannitol	125.36 ± 4.52	0.04	71.94 ± 0.82	0.01	55.74 ± 1.72	0.03	0.48 ± 0.02	0.03
Mannose	121.61 ± 4.99	0.04	74.16 ± 0.8	0.01	53.35 ± 1.36	0.03	n.d.	-
Melezitose	121.59 ± 13.14	0.11	52.02 ± 2.25	0.04	63.29 ± 7.99	0.13	5.94 ± 0.08	0.01
Melibiose	117.96 ± 7.17	0.06	62.33 ± 1.56	0.02	57.25 ± 4.57	0.08	4.98 ± 0.07	0.01
Raffinose	133.74 ± 16.41	0.12	60.25 ± 1.04	0.02	69.66 ± 6.75	0.10	20.59 ± 0.07	0.00
Rhamnose	126.78 ± 5.51	0.04	78.46 ± 1.01	0.01	57.52 ± 1.26	0.02	0.52 ± 0	0.00
Ribose	124.76 ± 5.48	0.04	75.76 ± 1.22	0.02	48.54 ± 1.34	0.03	0.61 ± 0.01	0.00
Sucrose	91.39 ± 3.03	0.03	66.06 ± 1.27	0.02	86.25 ± 2.53	0.03	33.73 ± 0.69	0.02
Trehalose	117.41 ± 3.11	0.03	78.39 ± 1.97	0.03	51.76 ± 2	0.04	n.d.	-
Turanose	110.73 ± 6.43	0.06	61.66 ± 1.5	0.02	43.85 ± 1.9	0.04	1.14 ± 0.36	0.32
Xylitol	126.13 ± 4.96	0.04	77.76 ± 0.95	0.01	57.69 ± 1	0.02	0.24 ± 0.01	0.01
Xylose	139.1 ± 7.57	0.05	75.91 ± 0.96	0.01	52.55 ± 1.52	0.03	3.62 ± 0.01	0.00

and β-gentiobiose, a weighting of $(1/x)$ would then be applied to calculate the concentration(s) for metabolites detected at the lower range of the calibration curves. For all other analytes no weighting factor was applied. Thus, these factors and regression were applied in every analytical curve during the whole validation study. Response ratios were calculated relative to the internal standard $^{13}C_1$-mannitol. R^2 values ranged from 0.9809 (for erlose) to 0.9998 (for both erythritol and fructose) (Table 2).

3.4. Recovery

The recovery of an analyte from a biological matrix is based upon the efficiency of the solvent(s) of choice in the extraction process as well as the instrument response which can affect the determination of final concentrations [12–14]. Recovery was calculated by comparing the amount of each metabolite present in (i) a calibration standard mix (QC) with a concentration of 80 μM spiked with additional 50 μM of the same calibration standard mix, as well as in (ii) PBQC sample (100 μM and 5 μM) spiked with the calibration standard mix (80 μM). All recovery tests were prepared in hexaplicates, and the values of recovery for the QC and PBQC samples are provided in Table 2.

The recovery values for the spiked QC samples were high (90–110%) for 28 out of the analyzed 48 metabolites, including fucose (100%), pipecolate (99%), and erythritol (99%). However, for 2-keto gluconic acid and sucrose the overall recoveries were 34% and 49%, respectively. Several sugars, including erlose (135%), raffinose (147%), and melezitose (133%), show a slightly higher recoveries as previously reported [15–18].

The recovery values for the spiked PBQC samples were high (90–110%) for 37 out of the analysed 48 metabolites, including nicotinic acid (101%), arabinose (99%), and glucuronate (100%). Only arabitol (127%) and quinate (126%) showed slightly higher recoveries as previously reported [15–18]. For most metabolites recovery

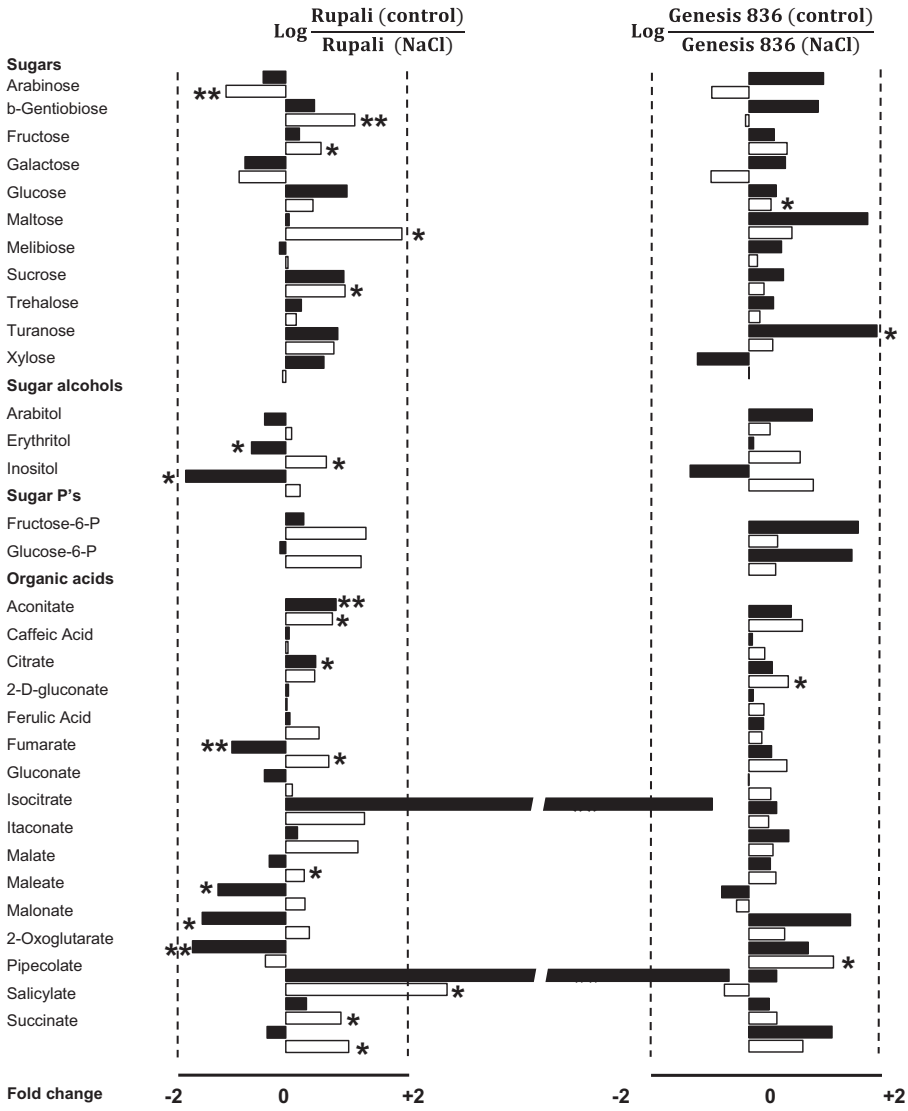

Fig. 2. Logarithmic ratios of sugar and organic acid contents in flowers (black bars) and pods (white bars) of chickpea cvs Rupali (left column), and Genesis836 (right column). Comparisons are made before (control) and after treatment with 60 mM NaCl for four weeks. Relative response ratios were calculated using the metabolite peak area divided by both the peak area of the internal standard and the sample dry weight (g). Fold changes were calculated by dividing the response ratios of control by the response ratios of salt treated per line. Values that are significantly higher at the $^{*}P < 0.05$ and $^{**}P < 0.01$ level are indicated with asterisks. The threshold of a ±2-fold change is indicated as a dashed line. P: phosphate

values for the spiked versus unspiked PBQC samples were in the range of 72–110% which is in close agreement with previous reports for polar metabolite determination via GC–MS [18].

3.5. Reproducibility

The validation of reproducibility (standard error) assesses the variability observed within an instrument over a short period to assess the method's accuracy and precision. Reproducibility was evaluated by spiking (i) a calibration standard mix (QC) with a concentration of 80 μM with additional 50 μM of the same calibration standard mix, as well as spiking (ii) 100 μM of PBQC sample with the calibration standard mix (80 μM). For malonate, malate, shikimate, citrate, fructose, glucose and sucrose only 5 μL of PBQC standard mix was used. All reproducibility tests were prepared in hexaplicates. The determined variability values (standard errors)

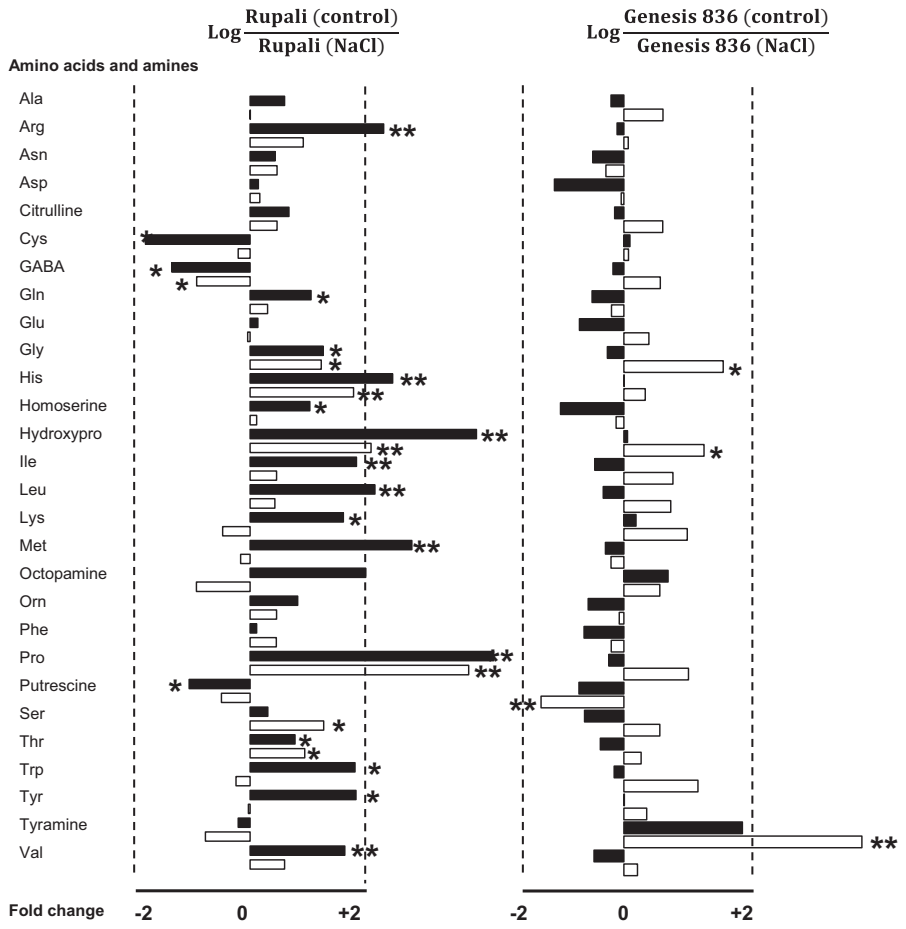

Fig. 3. Logarithmic ratios of amino acid and amine contents in flowers (black bars) and pods (white bars) of cvs Rupali (left column), and Genesis836 (right column). Comparisons are made before (control) and after treatment with 60 mM NaCl. Other details are the same as in the legend to Fig. 2.

are listed in Table 3. The standard error for practically all metabolites were below 10% for both the spiked calibration standards and PBQC samples, indicating that this method is precise and accurate for quantification of organic acids and sugars. These levels of variability are broadly in agreement with previously reported values for metabolite profiling of different compound classes using GC or LC-MS/MS systems [15–19].

3.6. Comparison of primary metabolite concentrations of tissues from two chickpea cultivars upon salinity stress

Following the validation of the GC–*QqQ*–MS method, it was applied to study metabolic responses in flower and pod tissue of the desi-type chickpea cultivars 'Genesis836 and 'Rupali' which differ in their tolerance to salinity [20]. Cv. Rupali is salt sensitive, whereas cv. Genesis836 is more tolerant to salt, and plants of both cultivars were grown in the greenhouse under control and salinity stress (60 mM NaCl for four weeks). To account for differences in maturity, salt treatment was performed 21 days after sowing (DAS) for cv. Rupali, and 25 DAS for cv. Genesis836 Flow-ers and seeds were harvested after 31 and 48 DAS (for cv. Rupali) or 35 and 52 DAS (for cv. Genesis836), and immediately frozen in liquid nitrogen (N_2). Frozen tissue (~30 mg) was extracted in 50 % methanol-water solution including the internal standards $^{13}C_6$ -sorbitol and $^{13}C_5$–^{15}N valine, and organic acid and sugar concentrations were analyzed using GC–*QqQ*–MS using three replicates per cultivar and treatment.

The objective of this part of the study was to understand how salt imposition affects the primary metabolite profile of flowers and pods of the different chickpea cultivars. Therefore, pairwise comparisons between the concentrations of sugars and organic acids of flowers and pods before and after salinity stress for Rupali (Fig. 2, left column) and Genesis836 (Fig. 2, right column) was performed (Additional file 4). Unless otherwise stated, only metabolite changes which are considered as statistically significant (Student's *t*-test *p*-value < 0.05) will be discussed.

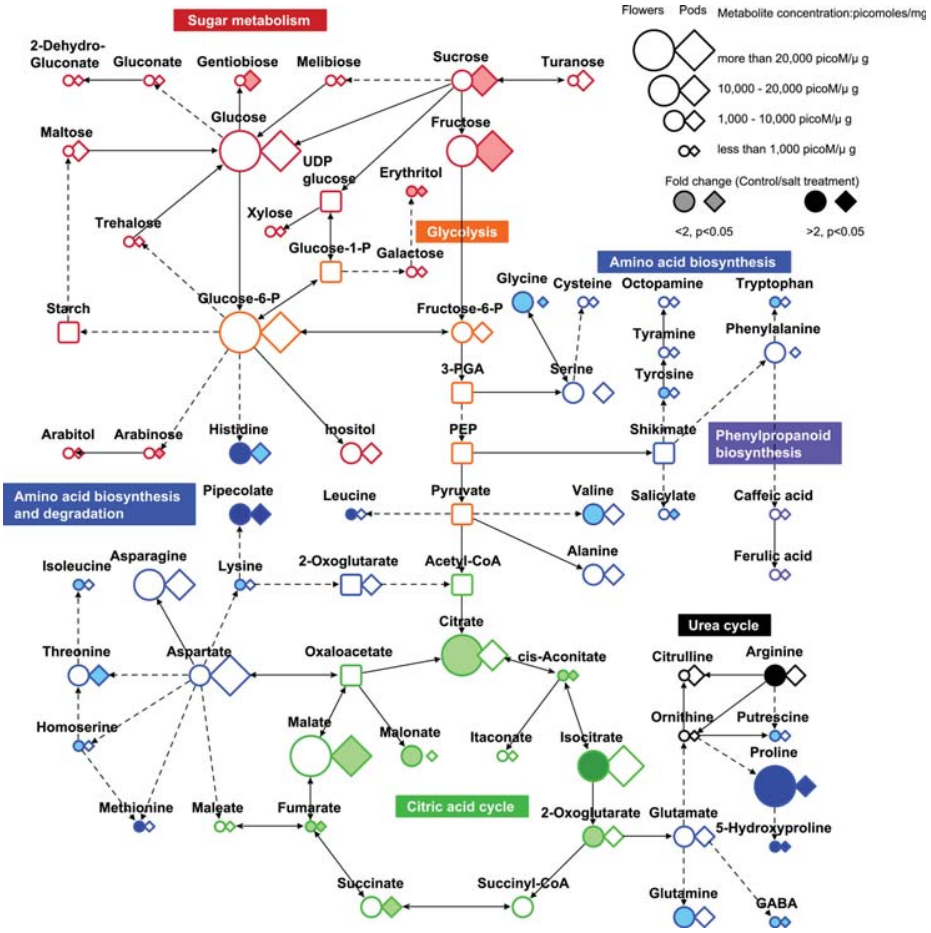

Fig. 4. Metabolic pathway altered by salinity treatment in flowers and pods of chickpea cv Rupali. Changes in concentration are indicated by the size of either the circles (for flowers) or rhombi (for pods). Metabolites that were not measured in this study are depicted by squares. Metabolites that show significant changes ($P > 0.05$) after salinity stress of less than two-fold are highlighted with light colors, whereas significant changes of more than two-fold are highlighted with dark colors. More details are provided in the legend.

In total, eleven sugars, three sugar alcohols, two sugar phosphates, and sixteen organic acids could be detected and quantified in both tissues of the cultivars. Profiles of the metabolites in Rupali show small reductions in the concentration of arabinose (−1.4-fold), but also small increases in the concentrations of β-gentiobiose, fructose and sucrose in pods of between 1.2 and 1.4-fold after salinity stress. Furthermore, erythritol and inositol levels were depleted in flowers, but increased (erythritol) or unchanged (inositol) in pods after salinity stress.

Noticeably, the magnitude of changes was generally larger for organic acids, with particularly pipecolate showing a large increase (flowers and pods, 12.6 and 2.5-fold, respectively) after salinity stress. The tricarboxylic acid (TCA) cycle metabolites isocitrate (flowers, 11.5-fold), cis-aconitate (flowers and pods, 1.33-fold and 1.31-fold, respectively), citrate (flowers and pods, both 1.18-fold), fumarate (pods, 1.28-fold), and malate (pods, 1.11-fold) also showed large salinity stress-induced increases.

Fewer differences in sugar levels were noted in flowers and pods of the salinity tolerant cultivar Genesis836 compared to Rupali, with only turanose showing a small but significant increase of 1.8 fold after salinity stress. No significant changes were detected for sugar phosphates or sugar acids, and only two small but significant increases in the levels of the organic acids citrate and 2-oxoglutarate in pods were measured after salinity stress.

3.7. Alteration of amino acid and amine contents after salinity stress in two chickpea cultivars

To accurately quantify additional metabolites of the carbon and nitrogen metabolism, LC–MS-based metabolite quantification of amino acids and amines was carried out on a LC–*QqQ*–MS accord-

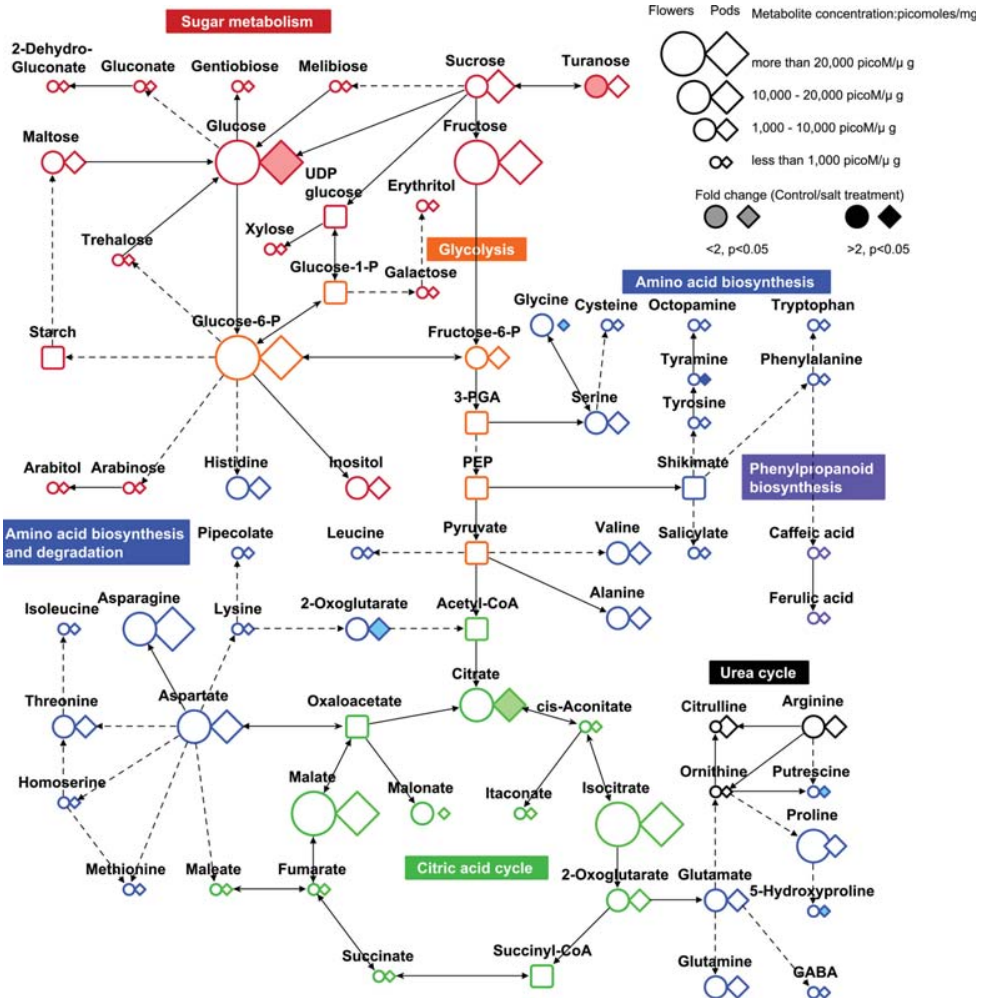

Fig. 5. Metabolic pathway altered by salinity treatment in flowers and pods of chickpea cv Genesis836 Other details are the same as in the legend to Fig. 4.

ing to the standardized protocol developed by Boughton et al. [11] (Fig. 3, Additional file 4).

Striking differences were seen in the amino acid concentrations in flowers following salt treatment of the salt sensitive cv. Rupali compared to the salt tolerant cv. Genesis836 In cv. Rupali, 14 out of the 28 measured amines and amino acids (Arg, Glu, Gly, His, homoserine, hydroxyproline, Ile, Leu, Lys, Met, Pro, Thr, Trp, Val) had significantly higher concentrations of between 1.4 and 4.7-fold, and three (Cys, GABA, putrescine) had significantly lower concentrations of between 1.5 and −1.9-fold after salinity treatment compared to control conditions. With the exception of Trp, the concentrations of these amino acids and amines were also much higher in salt affected flowers than pods. On the other hand, cv. Genesis836 only showed very few significant changes in amino acid concentrations: Gly, hydroxyproline, and tyramine concentrations increased between 1.5 and 3.5-fold, and putrescine decreased −1.5-fold in pods after salinity treatment. Interestingly, the vast majority of amino acids and amines measured in this study were depleted (although not significantly) in flowers of Genesis836 after salinity stress, whereas the opposite trend is seen in Rupali, where the vast majority of amino acids and amines increased in flowers after salinity stress.

To compile information on connections between all primary metabolites quantified in this study upon salinity exposure and to determine possible sites of metabolic regulation, we created an author-generated metabolite pathway map of primary metabolism of cv Rupali (Fig. 4) and cv Genesis836 (Fig. 5). Both maps show metabolite concentrations in flowers and pods, the fold change and the significance of changes after salinity stress. Although the overall concentrations of the metabolites are nearly identical after salinity

stress for both cultivars, the primary metabolite pathway map of the salt-sensitive cv Rupali shows significantly higher concentrations for amino acids derived from glucose-6-phosphate, aspartate, and pyruvate upon exposure to salt than in the salt-tolerant cv Genesis836 The elevated amino acid levels can be a reaction to salt stress and related to tissue damage in the salt-sensitive culti-var rather than a plant response associated with tolerance, which is supported by many other recent studies studying the effect of salinity on the metabolite levels in *Arabidopsis thaliana*, *Lotus japon-icus*, *Oryza sativa*, *Hordeum vulgare*, and *Triticum aestivum* [7,21,22]. Although many studies suggest a link between increased levels of osmolytes such as proline and sugars, as well as an induction of metabolic pathways including glycolysis and sugar metabolism, and salinity tolerance, the results in this study do not support this: Both Pro and its hydroxylation product 5-hydroxyproline as well as sucrose and fructose were significantly increased in the salt-sensitive cultivar Rupali but not in salt-tolerant Genesis836 after salinity stress, supporting recent findings that the contribution of Pro to osmotic pressure being relatively small [23] and not always correlated with enhanced salinity tolerance [21]. However, many organic acids from the TCA cycle including isocitrate and aconitate were also increased in cv Rupali upon stress but not in cv Genesis836 consistent with recent findings showing that salt-sensitive plant lines use these metabolites increasingly as pre-cursors for *de novo* amino acid biosynthesis after exposure to salt. As these changes in the pool of metabolites from the TCA cycle coin-cided with a decrease of several sugars (particularly in pods), this points towards an increased rate of glycolysis to provide carbohy-drates for use in the TCA cycle, which in turn provides precursors for other reactions such as amino acid synthesis and organic acid as well as chemical energy in the form of adenosine triphosphate (ATP) and reduced nicotinamide adenine dinucleotide (NADH) at an increased rate to support plant survival under salinity stress.

4. Conclusions

Despite improvements in analytical techniques for GC–*QqQ*–MS, the comprehensive analysis and quantitation of metabolites in complex samples remains a challenge, particularly when they are present at varying concentration levels. The ability to detect a large number of polar metabolites in low concentrations in a single analysis offers important benefits compared to other analytical methods. We developed a profiling method which was validated for the quantification of more than 40 metabolites from four major classes of polar compounds, including sugars, sugar alcohols, sugar phosphates, and organic acids. This method was applied to flower and pod samples from two chickpea cultivars differing in their ability to tolerate salt. In this study we were unable to find any evidence that Pro, the most highly studied osmoprotectant, was affected by salinity when comparing metabolite concentrations in the control and the salt-treated samples of the tolerant and the intolerant chickpea line. Instead, we conclude that metabolic differences between cvs Rupali and Genesis836 following salt stress involve metabo-lites involved in carbon metabolism and in the TCA cycle, as well as amino acid metabolism. The integration of the developed metabolite profiling method provided unambiguous metabolite identities and absolute quantitative data. Although the method was applied to the analysis of chickpea samples, it is equally applicable for metabolic profiling of other biological samples as the majority of the metabolites play key roles in central biosynthetic pathways.

Competing interests

The authors declare that they have no competing interests.

Acknowledgements

The authors thank Chia Feen Ng (Metabolomics Australia, School of BioSciences, The University of Melbourne) for performing the amino acid analysis. The authors are grateful to the Victorian Node of Metabolomics Australia, which is funded through Bioplatforms Australia Pty. Ltd., a National Collaborative Research Infrastructure Strategy (NCRIS), 5.1 Biomolecular platforms and informatics investment, and co-investment from the Victorian State Government and The University of Melbourne. This research was funded by grants through the Australian Research Council (ARC), The Grains Research and Development Corporation (GRDC), The South Australian Government, The University of Adelaide, The University of Queensland and The University of Melbourne, and the Australia–India Strategic Research Fund, Australian Government Department of Industry.

Appendix A. Supplementary data

Supplementary data associated with this article can be found, in the online version, at http://dx.doi.org/10.1016/j.jchromb.2015.07.002

References

[1] FAOSTAT, 2012. http://faostat.fao.org (accessed 09.12.14.).
[2] V. Vadez, L. Krishnamurthy, R. Serraj, P.M. Gaur, H.D. Upadhyaya, D.A. Hoisington, R.K. Varshney, N.C. Turner, K.H.M. Siddique, Large variation in salinity tolerance in chickpea is explained by differences in sensitivity at the reproductive stage, Field Crops Res. 104 (2007) 123–129.
[3] V. Vadez, M. Rashmi, K. Sindhu, M. Muralidharan, R. Pushpavalli, N.C. Turner, L. Krishnamurthy, P.M. Gaur, T.D. Colmer, Large number of flowers and tertiary branches, and higher reproductive success increase yields under salt stress in chickpea, Eur. J. Agron. 41 (2012) 42–51.
[4] L.W. Sumner, P. Mendes, R.A. Dixon, Plant metabolomics: large-scale phytochemistry in the functional genomics era, Phytochemistry 62 (2003) 817–836.
[5] M.A. Farag, D.V. Huhman, R.A. Dixon, L.W. Sumner, Metabolomics reveals novel pathways and differential mechanistic and elicitor-specific responses in phenylpropanoid and isoflavonoid biosynthesis in *Medicago truncatula* cell cultures, Plant Physiol. 146 (2008) 387–402.
[6] H. Suzuki, R. Sasaki, Y. Ogata, Y. Nakamura, N. Sakurai, M. Kitajima, H. Takayama, S. Kanaya, K. Aoki, D. Shibata, K. Saito, Metabolic profiling of flavonoids in *Lotus japonicus* using liquid chromatography Fourier transform ion cyclotron resonance mass spectrometry, Phytochemistry 69 (2008) 99–111.
[7] D.H. Sanchez, M.R. Siahpoosh, U. Roessner, M. Udvardi, J. Kopka, Plant metabolomics reveals conserved and divergent metabolic responses to salinity, Physiol. Plant 132 (2008) 209–219.
[8] S. Komatsu, A. Yamamoto, T. Nakamura, M.Z. Nouri, Y. Nanjo, K. Nishizawa, K. Furukawa, Comprehensive analysis of mitochondria in roots and hypocotyls of soybean under flooding stress using proteomics and metabolomics techniques, J. Prot. Res. 10 (2011) 3993–4004.
[9] C.B. Hill, U. Roessner, Metabolic Profiling of Plants by GC-MS, in: W. Weckwerth, G. Kahl (Eds.), The Handbook of Plant Metabolomics: Metabolite Profiling and Networking, first ed., Wiley-VCH Verlag GmbH & Co., Weinheim, 2013, pp. 3–23.
[10] L.W. Sumner, Z. Lei, B.J. Nikolau, K. Saito, Modern plant metabolomics: advanced natural product gene discoveries, improved technologies, and future prospects, Nat. Prod. Rep. 32 (2014) 212–229.
[11] B.A. Boughton, D.L. Callahan, C. Silva, J. Bowne, A. Nahid, T. Rupasinghe, D.L. Tull, M.J. McConville, A. Bacic, U. Roessner, Comprehensive profiling and quantitation of amine group containing metabolites, Anal. Chem. 83 (2011) 7523–7530.
[12] Eurachem/CITAC guide: Quantifying Uncertainty in Analytical Measurement S.L.R. Ellison , A. Williams , third ed. 2012; 1-132 http://www.eurachem.org (accessed 09.01.15.).
[13] U. Roessner, D.A. Dias, Plant tissue extraction for metabolomics, in: U. Roessner, D.A. Dias (Eds.), Methods in Molecular Biology, Metabolomics Tools for Natural Product Discoveries, Humana Press, New York, 2013, pp. 21–28.
[14] U. Roessner, A. Nahid, B. Chapman, A. Hunter, M. Bellgard, Metabolomics – the combination of analytical biochemistry, biology, and informatics, in: M. Moo-Young (Ed.), Comprehensive Biotechnology, second ed., Elsevier, 2011, pp. 447–459.
[15] A. Lytovchenko, R. Beleggia, N. Schauer, T. Isaacson, J.E. Leuendorf, H. Hellmann, J.K.C. Rose, A.R. Fernie, Application of GC–MS for the detection of lipophilic compounds in diverse plant tissues, Plant Methods 5 (2009) 1–11.

[16] T. Shepherd, G. Dobson, S.R. Verrall, S. Conner, D.W. Griffiths, J.W. McNicol, H.W. Davies, D. Stewart, Potato metabolomics by GC–MS: what are the limiting factors? Metabolomics 3 (2007) 475–488.
[17] T. Frenzel, A. Miller, K.H. Engel, Metabolite profiling – a fractionation method for analysis of major and minor compounds in rice grains, Cereal Chem. 79 (2002) 215–221.
[18] U. Roessner, C. Wagner, J. Kopka, R.N. Trethewey, L. Willmitzer, Simultaneous analysis of metabolites in potato tuber by gas chromatography–mass spectrometry, Plant J. 23 (2000) 131–142.
[19] M.A. Trapp, G.D. De Souza, E. Rodrigues-Filho, W. Boland, A. Mithöfer, Validated method for phytohormone quantification in plants, Front. Plant Sci. 5 (2014), 417.
[20] N.C. Turner, T.D. Colmer, J. Quealy, R. Pushpavalli, L. Krishnamurthy, J. Kaur, G. Singh, K.H.M. Siddique, V. Vadez, Salinity tolerance and ion accumulation in chickpea (*Cicer arietinum* L.) subjected to salt stress, Plant Soil 365 (2013) 347–361.
[21] J.H. Widodo, E. Patterson, M. Newbigin, A. Tester, Bacic, U, Roessner, Metabolic responses to salt stress of barley (*Hordeum vulgare* L.) cultivars, Sahara and Clipper, which differ in salinity tolerance, J. Exp. Bot. 60 (2009) 4089–4103.
[22] C.B. Hill, D. Jha, A. Bacic, M. Tester, U. Roessner, Characterization of ion contents and metabolic responses to salt stress of different *Arabidopsis AtHKT1;1* genotypes and their parental strains, Mol. Plant 6 (2013) 350–368.
[23] D. Gagneul, A. Aïnouche, C. Duhaze, R. Lugan, F.R. Larher, A. Bouchereau, A reassessment of the function of the so-called compatible solutes in the halophytic Plumbaginaceae *Limonium latifolium*, Plant Physiol. 144 (2007) 1598–1611.
[24] C.B. Hill, J.D. Taylor, J. Edwards, D. Mather, A. Bacic, P. Langridge, U. Roessner, Whole genome mapping of agronomic and metabolic traits to identify novel quantitative trait loci in bread wheat (*Triticum aestivum* L.) grown in a water-limited environment, Plant Physiol. 162 (2013) 1266–1281.
[25] H. Liu, M.C. Sanuda-Pena, J.D. Harvey-White, S. Kalra, S.A.J. Cohen, Determination of submicromolar concentrations of neurotransmitter amino acids by fluorescence detection using a modification of the 6-aminoquinolyl-*N*-hydroxysuccinimidyl carbamate method for amino acid analysis, J. Chromatogr. A 828 (1998) 383–395.

Chapter 4

Quantifying the onset and progression of plant senescence by color image analysis for high throughput applications

Jinhai Cai[1], Mamoru Okamoto[2], Judith Atieno[2], Tim Sutton[3], Yongle Li[2], Stanley J. Miklavcic[1]*

[1] Phenomics and Bioinformatics Research Centre, University of South Australia, Mawson Lakes, SA 5095, Australia

[2] Australian Centre for Plant Functional Genomics, University of Adelaide, Hartley Grove, Urrbrae SA 5064, Australia

[3] South Australian Research and Development Institute, 2b Hartley Grove, Urrbrae SA 5064, Australia

*Corresponding author: Stan.Miklavcic@unisa.edu.au

Statement of Authorship

Title of Paper	Quantifying the Onset and Progression of Plant Senescence by Color Image Analysis for High Throughput Applications
Publication Status	☑ Published ☐ Accepted for Publication ☐ Submitted for Publication ☐ Unpublished and Unsubmitted work written in manuscript style
Publication Details	Plant senescence by color image analysis for use in a high-throughput plant phenotyping pipeline was evaluated. An algorithm that features a color distortion correction and image restoration step prior to a senescence analysis was used to quantify the onset and progression of senescence in stressed chickpea and wheat plants. This method was demonstrated to provide correct estimation of senescence.

Candidate contribution

Name of Candidate	Judith Akinyi Atieno
Contribution to the Paper	Contributed to the conception of this experiment. Developed methods for growing chickpea under controlled environment, including finding suitable growing media, watering regime, temperature and lighting conditions and pest control. Developed methods for salinity screening (optimal salt levels, salt delivery system, and symptoms scoring). Conducted salinity experiment including daily watering of plants to field capacity to maintain salt concentration in pots. Visually scored for salinity symptoms at different time points to show progression of salt stress. Provided data on senescence scores from high-throughput imaged-based phenotyping. Contributed to writing and reviewing of the manuscript. This work took approximately six months.
Overall percentage (%)	25
Certification:	This paper reports on original research I conducted during the period of my Higher Degree by Research candidature and is not subject to any obligations or contractual agreements with a third party that would constrain its inclusion in this thesis.
Candidate signature	Date: 29/11/16
Principal supervisor signature	Date: 29/11/16

Statement of Authorship

Title of Paper: Quantifying the Onset and Progression of Plant Senescence by Color Image Analysis for High Throughput Applications

Publication Status: Published

Citation: Cai J, Okamoto M, Atieno J, Sutton T, Li Y, Miklavcic SJ (2016) Quantifying the Onset and Progression of Plant Senescence by Color Image Analysis for High Throughput Applications. PLoS ONE 11(6): e0157102. doi:10.1371/journal.pone.0157102

Author Contributions

By signing the Statement of Authorship, each author certifies that their stated contribution to the publication is accurate and permission is granted for the publication to be included in the candidate's thesis.

Jinhai Cai: Conceived and designed the experiments, conducted the experiments, analysed the data, wrote the paper, designed the analysis algorithm, developed the software used in analysis, reviewed the manuscript.

Signature **Date**

Mamoru Okamoto: Conceived and designed the experiments, conducted the experiments, contributed reagents/materials/analysis tools, reviewed the manuscript.

Signature **Date** 01/11/2016

Judith Akinyi Atieno: Conducted salinity experiment, manually scored for senescence in chickpea plants, contributed to writing methodology section of the manuscript, contributed reagents/materials/analysis tools .

Signature **Date**

Yongle Li: Contributed reagents/materials/analysis tools

Signature **Date** 1/11/16

Tim Sutton: Contributed reagents/materials/analysis tools

Signature **Date** 1/11/16

Stanley J. Miklavcic: Conceived and designed the experiments, analysed the data, wrote the paper, designed the analysis algorithm, reviewed the manuscript.

Signature **Date**

01/11/16

Link to chapter 4

Leaf senescence is a trait that has an application in assessing plant's response to salinity stress. Leaf senescence can be scored manually, but this is time consuming, inaccurate and subjective. High-throughput platforms like the LemnaTec imaging system provide a sound alternative to screen a large number of plants within a short time. However, these images could be blurred and as a result senescence quantification and progression would be error prone. This chapter focuses on quantifying the onset and progression of plant senescence by colour image analysis for high-throughput applications, using a new algorithm which has the capability to correct for colour distortion and restore image quality. Australian spring wheat cultivars, Gladius and Kukri, and chickpea cultivars, Genesis836 and Rupali, were exposed to different levels of nitrogen and salt, respectively. Plant senescence was quantified using manual inspection and colour image analysis using the new algorithm. A strong relationship was obtained between the two methods, validating the use of this algorithm in quantifying the onset and progression of senescence in monocots and dicots. This work has been published in PLoS ONE as follows; Cai J, Okamoto M, Atieno J, Sutton T, Li Y, Miklavcic SJ (2016) Quantifying the Onset and Progression of Plant Senescence by Color Image Analysis for High Throughput Applications. PLoS ONE 11(6): e0157102. doi:10.1371/journal.pone.0157102.

PLOS ONE

RESEARCH ARTICLE

Quantifying the Onset and Progression of Plant Senescence by Color Image Analysis for High Throughput Applications

Jinhai Cai[1], Mamoru Okamoto[2], Judith Atieno[2], Tim Sutton[3], Yongle Li[2], Stanley J. Miklavcic[1]*

1 Phenomics and Bioinformatics Research Centre, University of South Australia, Mawson Lakes, SA 5095, Australia, **2** Australian Centre for Plant Functional Genomics, University of Adelaide, Hartley Grove, Urrbrae SA 5064, Australia, **3** South Australian Research and Development Institute, 2b Hartley Grove, Urrbrae SA 5064, Australia

* Stan.Miklavcic@unisa.edu.au

Citation: Cai J, Okamoto M, Atieno J, Sutton T, Li Y, Miklavcic SJ (2016) Quantifying the Onset and Progression of Plant Senescence by Color Image Analysis for High Throughput Applications. PLoS ONE 11(6): e0157102. doi:10.1371/journal.pone.0157102

Editor: Panagiotis Kalaitzis, Mediterranean Agronomic Institute at Chania, GREECE

Received: November 30, 2015

Accepted: May 24, 2016

Published: June 27, 2016

Data Availability Statement: Instructions for users, software and sample image data will be available online at: https://sourceforge.net/projects/plant-senescence-analysis/.

Funding: The authors express their gratitude for partial funding provided by the Australian Research Council, the Australian Grains Research and Development Corporation, the South Australian Government, and the South Australian Government Department of Further Education, Employment, Science and Technology (http://www.sa.gov.au/) for partial support of JC, MO, YL and JA; and the

Abstract

Leaf senescence, an indicator of plant age and ill health, is an important phenotypic trait for the assessment of a plant's response to stress. Manual inspection of senescence, however, is time consuming, inaccurate and subjective. In this paper we propose an objective evaluation of plant senescence by color image analysis for use in a high throughput plant phenotyping pipeline. As high throughput phenotyping platforms are designed to capture whole-of-plant features, camera lenses and camera settings are inappropriate for the capture of fine detail. Specifically, plant colors in images may not represent true plant colors, leading to errors in senescence estimation. Our algorithm features a color distortion correction and image restoration step prior to a senescence analysis. We apply our algorithm to two time series of images of wheat and chickpea plants to quantify the onset and progression of senescence. We compare our results with senescence scores resulting from manual inspection. We demonstrate that our procedure is able to process images in an automated way for an accurate estimation of plant senescence even from color distorted and blurred images obtained under high throughput conditions.

Introduction

Even though image processing and computer vision methods have been applied in a range of plant biology contexts and over a span of years [1–6], the use of these techniques in a fully automated and high-throughput setting is still being established. This applies particularly to the topic addressed in this paper: the automated phenotypic analysis of leaf senescence, one of the trademark indicators of plant age and ill health.

Leaf senescence is the integral response of leaf cells to the regular ageing process but also to unfavorable environmental conditions [7]. Many physiological, biochemical, and molecular studies of leaf senescence [7–11] have shown that during senescence, leaf cells undergo highly

Australia-India Strategic Research Fund, Department of Industry and Science, Australian Federal Government. Australian Research Council Linkage Grant # LP140100347 was received by SM and JC (http://www.arc.gov.au/). The funders had no role in study design, data collection and analysis, decision to publish, or preparation of the manuscript.

Competing Interests: The authors have declared that no competing interests exist.

coordinated changes in cell structure, metabolism and gene expression. The earliest and most significant change is the breakdown of chloroplasts; leaf senescence leads to the degradation of photosynthetic pigments such as chlorophyll, with the degradation manifested in observable leaf colour changes from the usual deep green to pale green, to yellow and finally to brown. Given our ability to observe these visual cues, it would be natural to consider the use of image processing techniques for a high-throughput plant leaf senescence analysis.

In this respect it would seem reasonable to consider employing the Normalized Difference Vegetation Index (NDVI), which indeed has been widely used for vegetative studies to estimate crop yield, pasture performance as well as plant senescence [12, 13]. However, this measure is sensitive to many factors including soil condition and water content [14]. This sensitivity limits the reliable and practical use of NDVI to the detection of vegetation coverage. With the introduction of hyperspectral imaging, a richer variety of quantitative measures (vegetation indices) is possible and indeed has already been introduced [15, 16] to quantify leaf traits (such as chlorophyll content, detection of leaf disease symptoms or indeed senescence determination). The simplex volume maximization concept [15] appears particularly promising for drought stress detection. A particularly recent technological development is HyperART [16], a hyperspectral imaging system which utilizes both reflectance and transmittance information to determine an absorption spectrum, used to estimate leaf chlorophyll content. One key innovation with HyperART lies in its ability to non-destructively scan an entire leaf still attached to a plant. This represents an advance on previous methodologies which were limited to point measurements (scan area of a few cm^2) and being of lower resolution. Despite advances such as HyperART, the state of the art technology (compounded by the practical problem of cost effectiveness) is not yet geared for high throughput phenotyping applications on the whole plant scale (or whole canopy scale). With NDVI unsuitable for senescence analysis and with visual inspection [13], even by trained inspectors, being slow, weakly quantitative and prone to human subjectivity, and until high throughput hyperspectral phenotyping becomes viable, a need exists in the interim for the application of non-destructive and fully automated RGB image-based techniques for the objective estimation of plant senescence.

Ideally, using high definition, high resolution RGB images at the leaf level, one could attribute leaf image color into a few categories of classification and use the ensuing full color distribution to estimate the senescence level of an entire plant. However, for the high-throughput practices we envisage, it is not feasible to take high definition images of all individual plant leaves. Instead, one resorts to taking a single image, or at most a few images from different perspectives, of a whole plant, which are then analyzed to determine the degree of senescence at the whole plant level. Under these pragmatic conditions, even if the global image resolution is high, the local resolution, at the leaf level, may not be. For example, Fig 1 shows an image of a young plant that in reality exhibits no actual senescence, but based on the image itself (a target for an automated procedure) would be assessed as already exhibiting senescence. Consequently, it can be problematic to apply a color classification scheme as such images may suffer from significant image blurring and therefore significant image color distortion, *at the level of an individual leaf*. It is an inescapable fact that the color of a pixel in a blurred image is affected by the colors of neighboring pixels [17]; the color of a pixel in a blurred image would then not represent the true color of an object feature at that specific location. For the analysis of plant senescence, this has unfavorable implications: the application of an image-based, color classification scheme could result in significant error. Consequently, a deblurring or restoration stage is required to reduce the extent of color distortion in such blurred images.

In this paper, we propose a new approach for color distortion correction in blurred images for the specific purpose of analyzing plant senescence. While this is important for the accurate quantification of senescence over the lifetime of the plant, it is absolutely essential for the

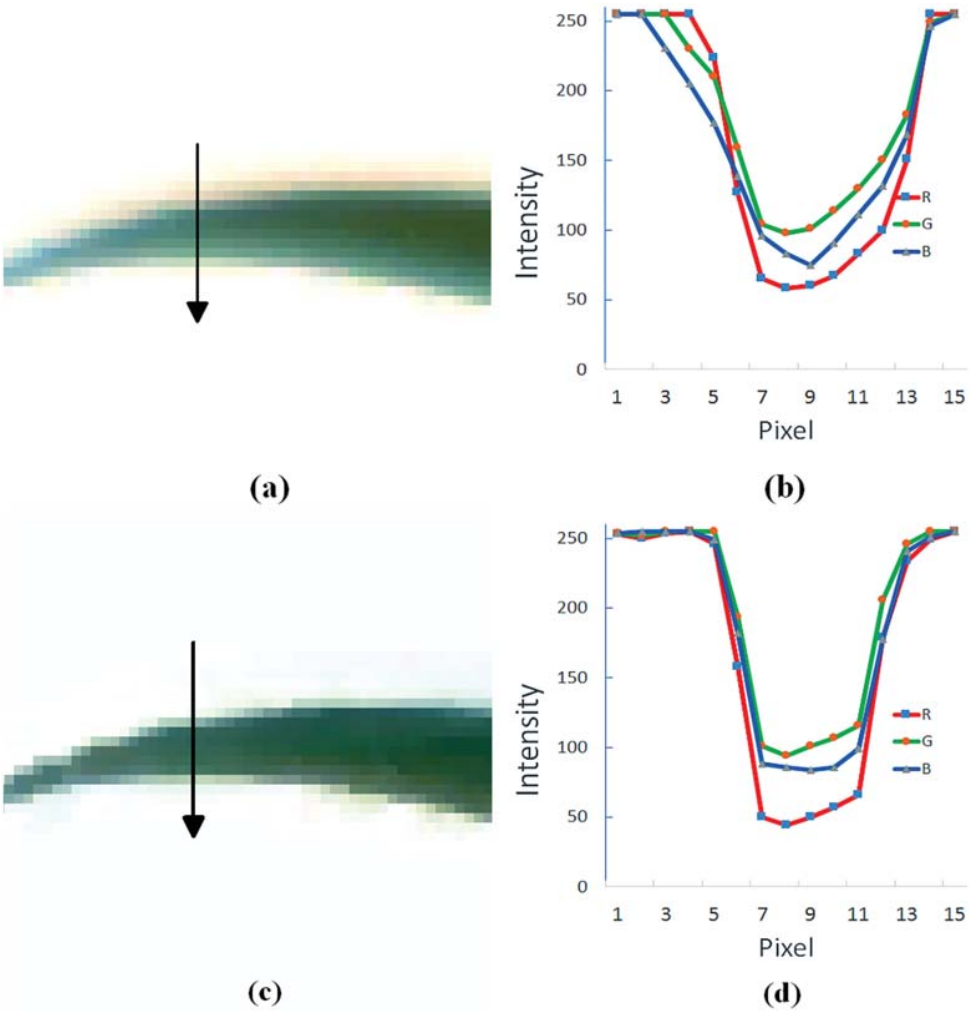

Fig 1. The color distortion effect and its correction using the method presented in this paper. (a) original image of a young and green leaf; (b) the corresponding color profile at the cross-section indicated by the arrow in (a); (c) image of the same leaf after color distortion correction; (d) corresponding color profile at the exact same cross-section.

doi:10.1371/journal.pone.0157102.g001

purpose of pinpointing the time at which senescence in a plant first appears. Both aspects are important phenotypic traits. The approach we adopt, described in the next section, does not assume any of the currently adopted circumstances (color channel independence and point spread function (PSF)-based model de-blurring). However, we do make the reasonable and practical assumption that during the course of an experiment, or for a given image data set to

be analyzed, the camera settings remain fixed. That is, we assume that the effects of blurring and color distortion remain consistent across all images acquired in a complete experiment. With this reasonable assumption of constant camera settings, we can take advantage of a priori knowledge of the conditions of the experiment to develop an algorithm for the correction of color distortion. In the results section we demonstrate and discuss the performance of our correction and analysis approach through applications to two time series of images for two different plant types, wheat and chickpea plants. We make concluding comments in the final section, where we point out that the proposal has the potential for a broader range of applications to quantify other phenotypic traits based on color discrimination.

Materials and Methods

Plant material and growth condition

Wheat: Australian spring wheat (*Triticum aestivum*) cultivars Gladius and Kukri were grown in pots in glasshouse conditions between January and June, and between August and December, 2013. Preselected similar sized seeds were sown in pots filled with 2.5kg of soil mix (coco-peat based potting media containing different amounts of nitrogen (N)). Nitrogen as urea was applied at sowing at 10mg (N1), 25mg (N2), 75mg (N3), 150mg (N4), and 450mg (N5) N/kg of soil. Plants were grown and watered in a glasshouse with average temperatures ranging between 22°C during the day and 15°C at night. At four weeks, the plants were transferred into a special growth room at the Australian Plant Phenomics Facility, University of Adelaide, Australia (The Plant Accelerator) for regular automated imaging using a LemnaTec imaging system (LemnaTec GbmH, Aachen, Germany). RGB images were automatically captured daily for 21 days.

Chickpea pilot experiment: Plant material consisted of two *Cicer arietinum* genotypes (Genesis836 and Rupali). Experiments were again conducted in The Plant Accelerator. Temperature and humidity were controlled in the glasshouse and ranged from 24±2°C, 40% (day) and 16±2°C, and 90% (night), respectively. Three seeds were sown 2 cm deep in pots containing Goldilocks mix (50% clay loam, 25% University of California (UC) mixture, and 25% cocopeat). Rhizobium inoculum was added to each planting hole at sowing. Prior to salt application, plants were uniformly thinned to 1 plant per pot. At 25 days after sowing (DAS), each pot received either 0, 30, 40 or 60 mM NaCl. Each treatment was replicated 4 times in a Randomized Complete Block Design (RCBD). Pots were watered and maintained at field capacity to maintain the salt concentration and to avoid salt leaching.

Imaging and manual senescence scoring

To allow for quantification of onset and to track the progression of plant senescence (chlorosis and necrosis), plants were imaged from 18 DAS up to 39 DAS. For each plant, RGB images were taken automatically from three different views (one top and two side views, the latter with a relative rotation of 90°).

To establish a correlation between visual scoring and digital image estimation of plant senescence, visual scores of the plants were taken based on a 1–10 scale [18] at 41 and 42 DAS.

Scoring scale:

1 = A green and healthy plant with no symptoms of illhealth (e.g., salinity stress);

2 = Bottom leaves beginning to yellow or become necrotic;

3 = Necrosis on a quarter of bottom leaves (25%) and yellowing on the rest of the bottom half of the plant;

4 = Necrosis on bottom half (50%) of plant;

5 = Necrosis on bottom half and yellowing appearing in the top half of the plant;

6 = Necrosis in the range 50%–75% of the plant;

7 = Necrosis on 75% of the plant;

8 = Necrosis on the whole plant with apical leaves still green/yellowing;

9 = Only stems and shoot tips remain green;

10 = Plant death.

Modeling color distortion

Deblurring has been a subject of intensive study for decades [19]. Most deblurring algorithms developed thus far focus on estimating so-called shift-invariant point spread functions (PSFs) [20], under the assumption that blurring is caused either by the relative motion of the camera-object system, camera defocussing or by lens aberrations [21]. Recent research has also included the study of images blurred as a result of large depth differences (caused mainly by the limited focal depth of cameras). In this case, the focus is placed on estimating the PSFs [19, 21, 22] to produce better quality images, similar to those produced by an ideal pin-hole camera, except possibly for "ringing artifacts" [17, 20], a problem yet to be solved.

One assumption commonly adopted in previous works on deblurring is that the different spectral bands of visible light have the same properties, which implies that these spectral bands have identical PSFs. A second assumption is that of no interference between spectral band signals detected by different image sensors. Unfortunately, as Fig 1 indicates, these assumptions are not valid in the present context. Fig 1(a) is (actually) an image of a healthy green leaf of a young wheat plant. The image itself, however, clearly possesses significant yellowness around the leaf edges, this color distortion effect is quantified in Fig 1(b). The latter figure demonstrates that the three spectral bands are affected to different degrees and thus have different PSFs. Moreover, the curves appear asymmetric suggesting that they are not amenable to modelling by PSFs at all. In summary, existing deblurring algorithms are not applicable and indeed do not produce restored images of suitable quality. To improve the quality of restored images for an accurate estimation of plant senescence requires a less restrictive approach.

The task of deblurring an image is commonly called image deconvolution. If the blur kernel is not known, the problem is referred to as blind image deconvolution. Many methods have been proposed for deblurring from a single image [23, 24]. Existing blind deconvolution methods assume that the blur kernel has a simple parametric form, such as a Gaussian or a composition of low-frequency Fourier components [25].

In our procedure, we define the blurring degradation process by the expression

$$\mathbf{X} = \mathbf{GD} + \mathbf{N}, \tag{1}$$

where $\mathbf{X}$ is the observed or degraded image, $\mathbf{D}$ is the degradation matrix or PSF, $\mathbf{G}$ is the image without degradation or blurring, and $\mathbf{N}$ denotes noise in the observed image. Note that we do not assume that any two spectral bands have the same PSF ($\mathbf{D}$), nor do we assume that the PSF of a particular spectral band is independent of other spectral bands. In contrast to established methods where knowledge of the PSF is essential, in the formulation represented by Eq 1, the PSF is not invertible as it is inhomogeneous and multi-channelled. In the approach proposed here, we attempt to estimate directly the color distortion correction matrix ($\mathbf{C}$) defined in the

deblurring process, expressed mathematically as,

$$\mathbf{G} = (\mathbf{X} - \mathbf{N})\mathbf{C},$$
$$\text{or} \tag{2}$$
$$\mathbf{E} = \mathbf{G} - \mathbf{X}\mathbf{C}.$$

The matrix **C** denotes the matrix for the color distortion correction and **E** is the estimation error for the given level of noise. By minimising the mean square error, we can estimate the correction matrix using knowledge of both the undistorted and the observed images

$$\mathbf{C} = (\mathbf{X}^t\mathbf{X})^{-1}\mathbf{X}^t\mathbf{G}, \tag{3}$$

where $\mathbf{X}^t$ denotes the transpose of the matrix **X** and $\mathbf{X}^{-1}$ denotes the inverse of **X**. In Eq (3), we assume that at least one *undistorted image* **G** is available for the estimation of **C**.

Estimation of ground-truth color

In a pragmatic sense, the problem of estimating the color distortion correction matrix in Eq (1) reduces to the problem of obtaining at least one undistorted image for the subsequent application of Eq (3) to all distorted images assuming the same camera settings. The solution of the reduced problem could form part of an initialization step, being camera calibration; a standard color chart can be used to reconstruct an undistorted image given that the colors of the individual pixels of the color chart image are known. However, in the possibly more common event that camera calibration has not been attempted, with the notional consequence that an undistorted image cannot be reconstructed, it is still possible to estimate the undistorted image from the distorted image.

In the current application (which can be modified to suit other applications) we rely on the premise that plant leaves are green at the early stage of plant growth and development, particularly under advantageous conditions (*i.e.*, under no stress) to infer that any yellowness appearing in images of leaf edges is due solely to color distortion. As with conventional blind deblurring approaches, we exploit the information from the edges of two objects. We observe that the red channel signal in Fig 1(a) is sharpest at the edges of leaves. With this feature, the red channel of an image of a young plant can be used in an initial segmentation attempt in order to estimate the undistorted image of the young plant, for which leaf and stem color is unvarying across the whole plant. In this specific application we can estimate the real color at a leaf edge by the color of the interior section of that leaf image. We also manually select simple background regions of one image of the training set to estimate the true background color at boundaries between the plant and the background (and in this instance also between the blue plant support frame and the background). As there is color distortion in the original image, the initial segmentation attempt based on the red channel signal alone is not perfect. To improve the result, a manual correction is performed on this initial segmented image.

The results at the end of each step in the sequence of ground-truth color estimation are illustrated in Fig 2. A tell-tale sign that the initial attempt at color estimation is imperfect, is the bluish appearance of the leaf tips and of leaves of only a few pixels width.

Color distortion correction

Now that an undistorted image has been obtained, we can use Eq (3) to estimate the correction matrix **C**. However, any two-dimensional image with multiple color channels cannot be directly represented by a single two-dimensional matrix. If, on the other hand, we assume that each channel is independent of others, Eq (3) can be directly used to deduce the correction matrix for each channel. Unfortunately, different color sensor cells corresponding to a given

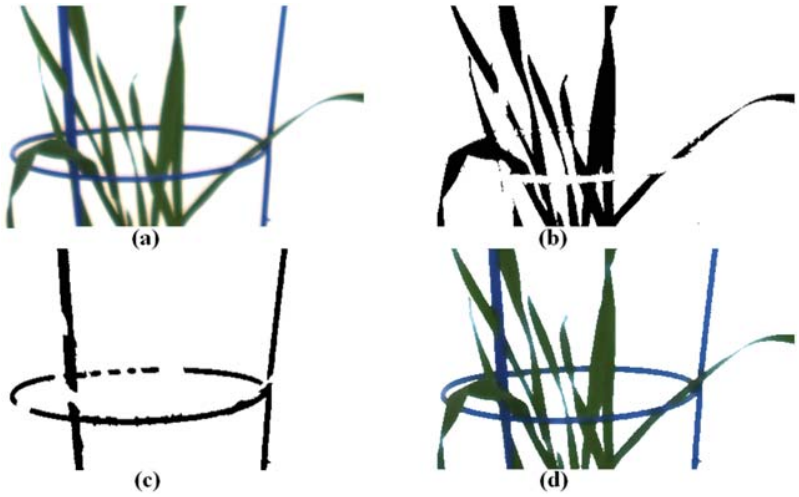

Fig 2. Example results at the end of each step in the process of ground-truth color estimation. In sequence: (a) the original image of a young plant; (b) the automatically segmented plant leaves with manual correction; (c) the automatically segmented frame with manual correction; and (d) the estimated image of the young plant after color distortion correction.

doi:10.1371/journal.pone.0157102.g002

pixel are physically close to each other in the sensor panel. Therefore, it is possible that blurring effects are not channel independent. To treat the general case, we consider the correction matrix as a $M \times N_c$ matrix, where $M = L^2 \times N_c$, L is the kernel size of the correction matrix, and N_c is the number of color channels, usually with $N_c = 3$. Furthermore, we arrange the estimated undistorted image into a $S_i \times N_c$ matrix, where S_i is the image size, *i.e.*, the total number of image pixels. We arrange the original, distorted image into a $S_i \times M$ matrix, which means that all pixels within the kernel are included for a given position. With this formulation, we make no explicit assumption about the correction matrix. The only disadvantage with this formulation is that the resulting size of matrix **X** is considerable making the calculation of **C** slow. Fortunately, the calculation of **C** is only required once for an entire experiment.

The final color distortion corrected matrix, **R** (the restored image), is obtained by a simple matrix multiplication: $\mathbf{R} = \mathbf{XC}$.

Results and Discussion

Analysis of the color distortion correction

Given the absence of actual ground-truth information and given that a correction matrix is constructed from distorted data, it is prudent to first assess the performance of our approach based on an image of a young plant that we have used for training. Comparing Fig 3(a) with Fig 3(b) and Fig 3(c) with Fig 3(d), the restored images are sharper than the original images and the problem of yellowish tinge between green leaves has been significantly reduced. Confirmation of the effectiveness of the scheme can be derived from Fig 1(c) and 1(d), which highlight the improvement in color representation of the single leaf in Fig 1(a) and the effect on the color intensity profiles over the lateral cross-section indicated. The key feature of Fig 1(d) to note is the increased sharpness in the intensity changes across the boundaries of the leaf, now

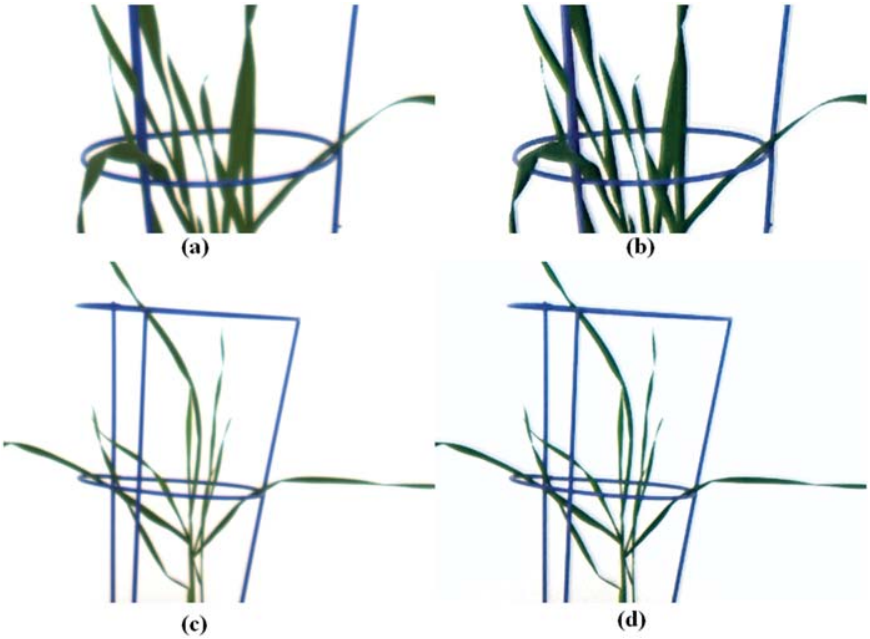

Fig 3. Result of a color distortion correction as applied to a young (non-senescent) plant. (a) the original image used for training;(b) the restored image after color distortion correction from (a); (c) the original image and (d) the restored image after color distortion correction from (c).

doi:10.1371/journal.pone.0157102.g003

consistent across all three color channels. Admittedly, the process has introduced ringing artifacts [17, 20] in the restored images. As in the case of ringing resulting from deblurring algorithms, this problem has yet to be solved. Fortunately, the color possessed by the artifacts is bluish, which is thus distinct from the color of either green or senescent leaves. Therefore, such artifacts do not affect our senescence analysis.

With regard to images of plants with both green and yellow leaves, the restored image in Fig 4(b) has sharper edges than the original image (Fig 4(a)). Comparing Fig 4(c) with Fig 4(d), a significant amount of the blurred background area with characteristic yellow has been removed; such areas would lead to an overestimation of leaf senescence. Indeed it can be concluded from Fig 4(e) and 4(f) that our procedure does not affect the coloration of senescent leaves. In fact, the opposite appears to be the case, the color contrast between the green and the senescence regions of leaves is enhanced, which only benefits a color classification assessment. Although our procedure corrects for color distortion and enhances resolution and color contrast, the procedure is not perfect, as evidenced by the traces of yellow tinge found at leaf tips and corners of leaf image overlap.

Senescence analysis

To analyze leaf senescence in plants, we first separate plant objects from background and then divide the segmented plant image into three vertical regions (zones) equidistant in height, as

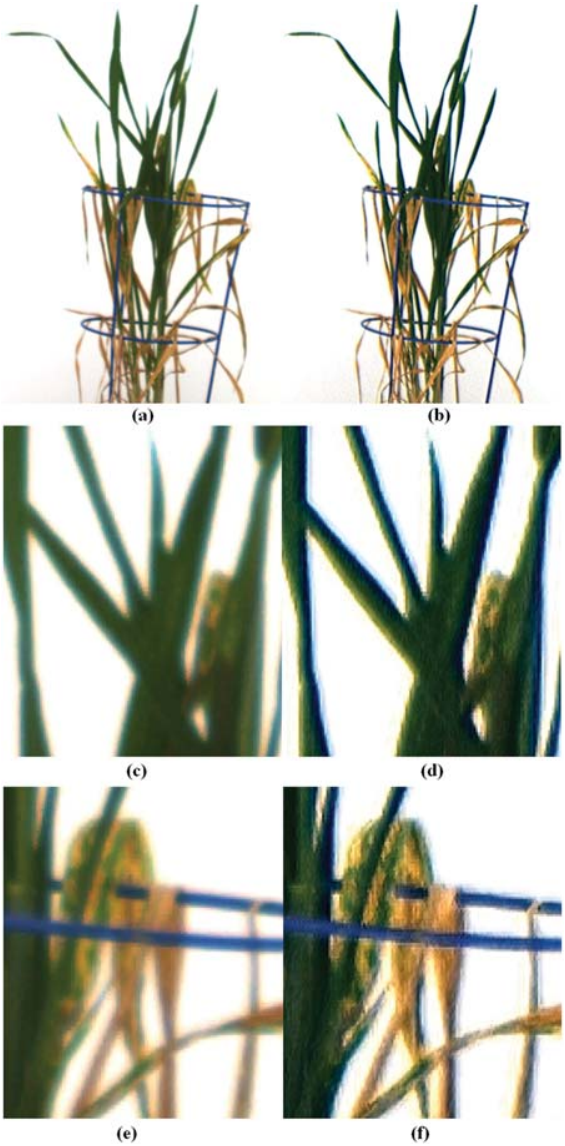

Fig 4. Results of application of the color correction process on plants exhibiting senescence. (a) shows the original image, while (b) shows the post processed, restored image. Panels (c) and (e) are enlarged regions of the original image in (a), while (d) and (f) are corresponding enlarged regions of the restored image (b).

doi:10.1371/journal.pone.0157102.g004

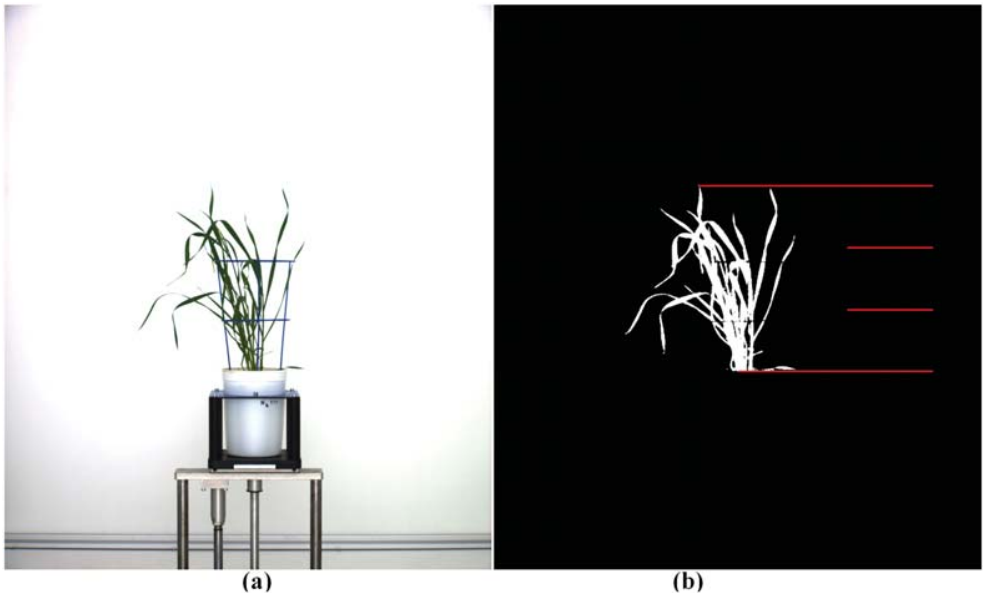

Fig 5. Demonstration of the image segmentation process and zonal partitioning of plant foreground. (a) is the original image, while (b) shows just the segmented plant image with overlayed horizontal lines partitioning the image foreground into three zones.

doi:10.1371/journal.pone.0157102.g005

illustrated in Fig 5 (see also S1 Appendix). In each zone, the colors are classified into four categories: dark green, light green, light yellow and brown. Any part of a leaf with yellow or brown color is classified as undergoing or having succumbed to senescence. Note that any leaves that have dropped below the bottom line are assigned to the bottom zone.

Wheat experiment. Our procedure (as well as a color classification analysis) was applied to images of wheat plants to assess the affect of nitrogen availability on the development of leaf senescence. A full biological analysis of this experiment will appear elsewhere. For the purposes of this paper, we show in Fig 6 examples of the color analysis on images of three plants, each exposed to a different level of nitrogen (low, medium and high, respectively). The top row of figures shows restored images of the plants as they appeared on the same day. The bottom row shows the corresponding four-category, color classification assessment as a function of zone as well as measured overall.

It should come as no surprise that all images exhibit some degree of blurring and color distortion. These effects can be substantial if the camera setting is far from optimal and if the plants being imaged are small; color distortion effects, extending across several pixels orthogonal as well as along leaf boundaries, can be significant. With the view to applying our method in high throughput facilities. It makes sense to compare the outcome of our analysis with the options currently available in such systems. Accordingly, we consider results using a typical system's in-built, color analysis software (in the present case, The Plant Accelerator's LemnaTec imaging system software). A direct application on the original images gives an estimated senescence level, measured as a percentage of whole plant area, of greater than 10%, even for initial images in the sequence known not to exhibit any senescence. A quantitative comparison

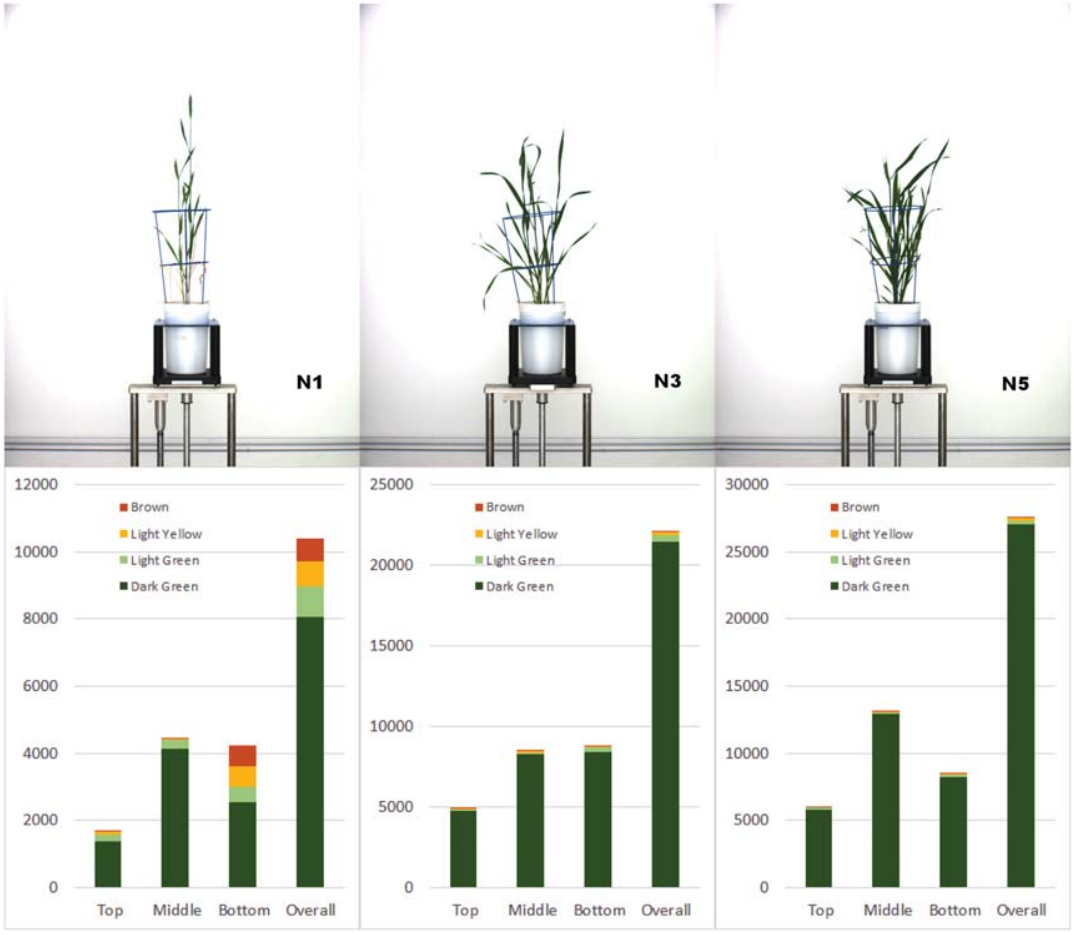

Fig 6. Zonal assessment of green versus senescence leaf areas in pixels. Top figures show original images of three Gladius plants each grown under a different level of nitrogen (N1, N3 and N5). The bottom figures show the results of color classification in pixel area as a function of zone, according to our four-category color scheme: dark green, light green, yellow and brown.

doi:10.1371/journal.pone.0157102.g006

of results using our method with those of a direct color scheme analysis applied to a specific plant image series is shown in Fig 7. In the case of our method, the results include an "Overall" measure (whole plant) and two separated measures, "Mid" and "Bottom", to indicate that onset appears primarily (though not always) in the bottom zone. Results of the LemnaTec system is not separated so only the "Overall" measure is given.

It is clear from Fig 7 that a direct application of color analysis results in a significant error. Two facts emerge from that analysis: first, when the plant is young and therefore small, blurring and color distortion significantly distorts the senescence estimation; second, when actual

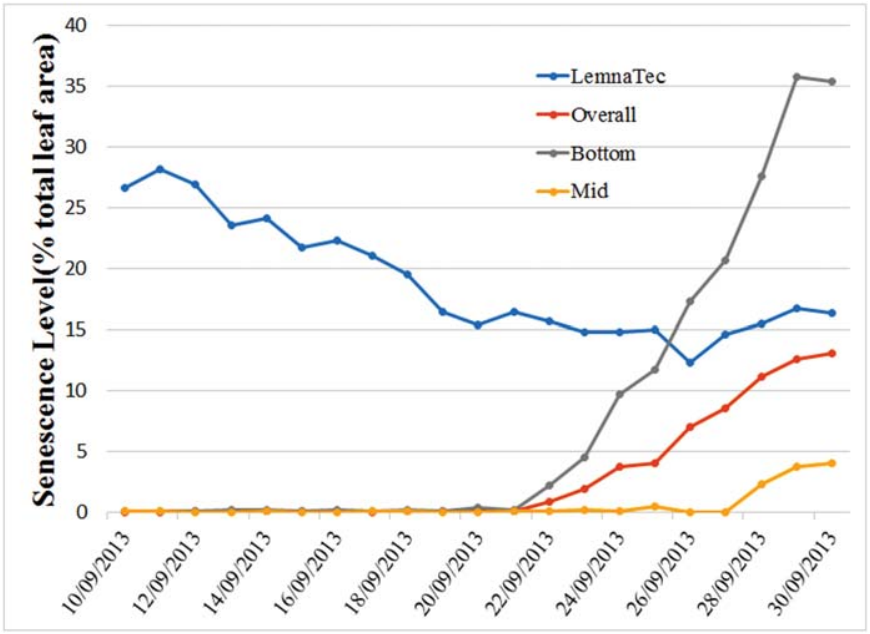

Fig 7. Comparison of senescence estimations using the method proposed here (curves denoted Overall, Mid and Bottom) and a direct application of the color analysis software provided by The Plant Accelerator's LemnaTec imaging system. For the Lemnatec results, only a whole-of-plant measure is available with which we compare a corresponding measure, which in turn is broken down into the senescence levels determined in the bottom and middle zones.

doi:10.1371/journal.pone.0157102.g007

senescence is present and significant, the estimated level may qualitatively mimic the true development, but (a) is quantitatively overestimated and (b) cannot be used to establish the point of onset.

A recent LemnaTec software upgrade offers the user the option of using machine learning methods to learn color differences between typical plant greens, recurring background colors and colors associated with senescent leaves as well as the colors (usually light yellow) caused by burring and color distortion. This refinement dramatically improves the accuracy of the in-built tool. An updated comparison for the same image sequence is given in Fig 8; the difference between the two analyses is significantly reduced (the bias is now between 2.0% and 5.0%). To be more precise, when the plants are young, possessing small green leaves, the machine learning result slightly overestimates the senescence level (see figure inset), which is enough to eliminate any possibility of using this method to detect the onset of senescence. The disparity between the estimated senescence levels becomes greater when there is a significant level of senescence present. The disparity is due to the machine learning procedure itself: the color subspaces associated with the yellow due to blurring and color distortion and the yellow of plant senescence overlap. It is therefore inevitable that some parts of senescent leaves will be classified as background, resulting in an underestimation of the level of senescence actually present.

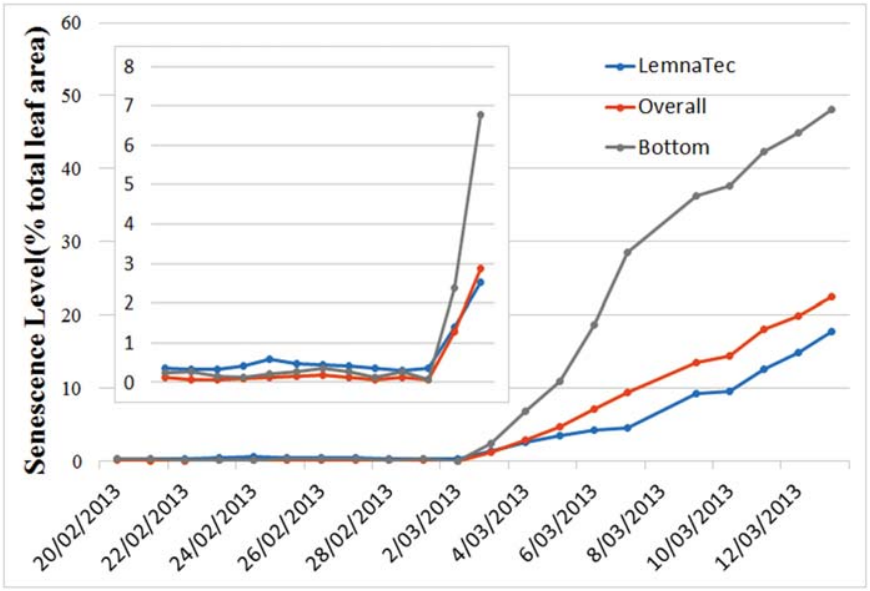

Fig 8. Comparison of senescence estimations using the method proposed here (curves denoted Overall and Bottom) and the application of a machine-learned, color analysis provided by The Plant Accelerator's LemnaTec imaging system (curve labelled "LemnaTec".

doi:10.1371/journal.pone.0157102.g008

It is important also to point out that although there is a clear improvement in the LemnaTec system's senescence estimation, it comes at a price and with limitations. The price is that some manual labelling of images is required for training of the machine learning algorithm. This detracts from the use of this solution for high throughput applications. As with all machine learning techniques, another limitation is that the learning step, which is valid for one experiment, may not be valid for another experiment, even for the same plant species, if the camera settings differ.

In Fig 9 we summarize the overall measures for two individual plants over the 15 days that images were taken. Two time series are shown. Fig 9(a) features the time series of total visible plant area for the two plants, while Fig 9(b) highlights the percentage of senescence (yellow and brown color categories) present relative to total plant area as a function of time.

The regular imaging of plants (particularly imaging from several perspectives at once) over a significant period of time offers the potential for the time-course capture of a significant amount of information on a number of important phenotypic traits. Realizing that potential cannot be achieved using either subjective means or inadequate processing tools. Fig 9 highlights the possibility of realizing the potential with the application of our color correction and classification procedure to quantify traits such as plant growth over time. What is particularly clear from Fig 9(b) is that the development of plant senescence and its dependence on applied stress can now be quantified rigorously. Indeed, two specific features of the senescence process can be quantified, namely, the day on which senescence first appears (onset) on an individual plant (and where) and the rate at which senescence progresses, either absolutely or as a relative

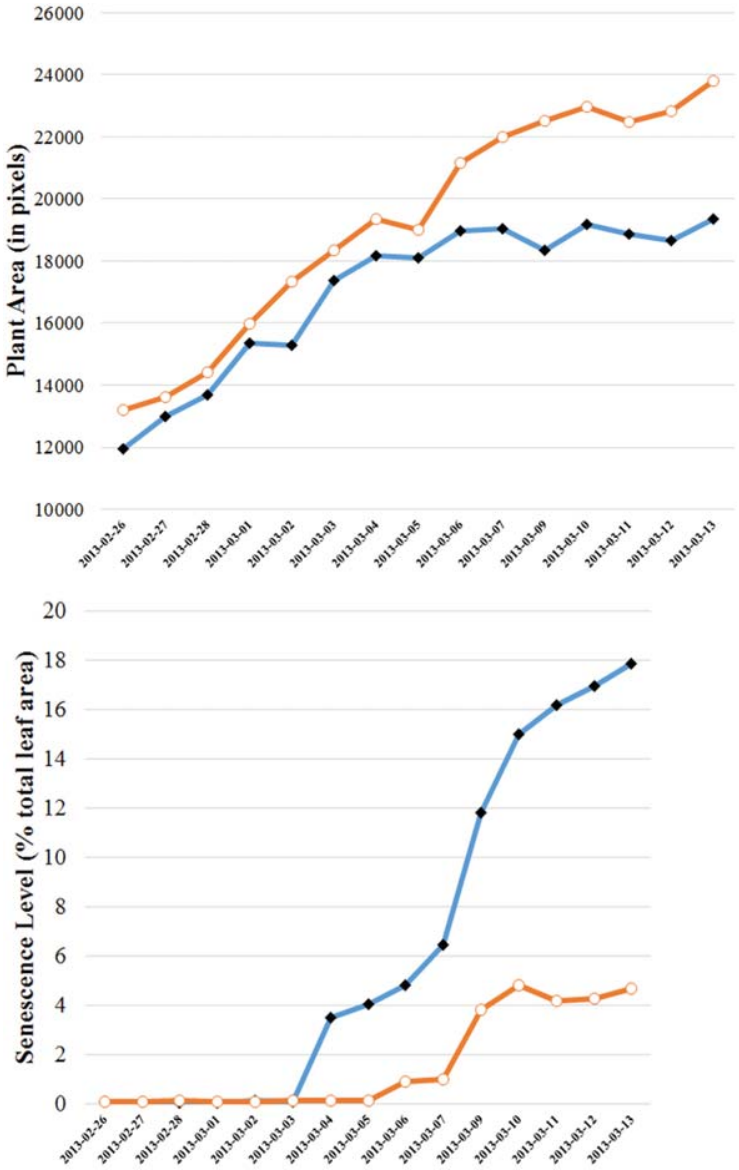

Fig 9. Whole-of-plant assessment of growth (plant area) and senescence as a function of time for two individual plants under N2, chosen arbitrarily. Top figure features the time developments of total projected plant area (all leaves and stems) for the two plants, depicting similar growth behavior. Bottom figure shows the percentage of senescence present in the leaves of these plants relative to their total plant area. The two individual plants exhibit different rates of senescence development as well as different onset dates.

doi:10.1371/journal.pone.0157102.g009

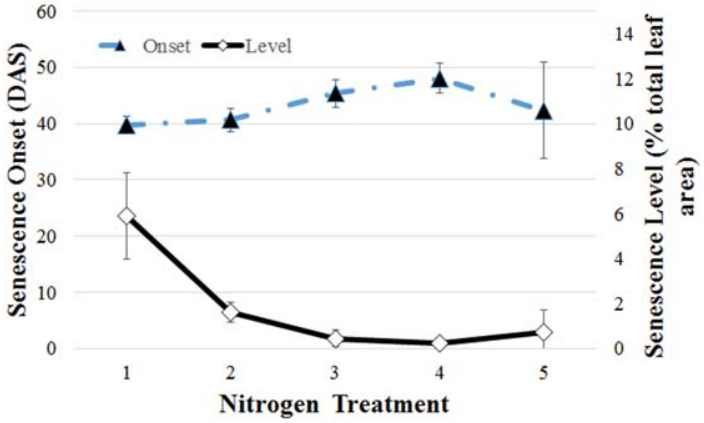

Fig 10. Summary of senescence dependence on nitrogen treatment (*N*1 – *N*5, horizontal axis) for the Gladius wheat plant variety. Shown are mean values of onset determination (days after sowing, DAS, dashed curve and solid triangles, left vertical axis) and final degree of senescence (percentage of total project leaf area, solid curve and open diamonds, right vertical axis). Error bars show the variation across three repeats.

doi:10.1371/journal.pone.0157102.g010

percentage of leaf area. Moreover, the latter information can be refined into zones for a detailed study of senescence.

These two specific features are exemplified in Fig 10, which summarizes the effects of nitrogen treatment on both the time of onset and on the final degree of senescence, the latter relative to the total projected leaf area. Only one wheat variety (the genotype Gladius) is represented, with results averaged over a number of repeats. The error bars therefore refer to variation over the repeats and are not indicative of errors in senescence estimation. A more extensive study comparing plant responses to nitrogen across a range of genotypes is the subject of a separate publication. Although the Gladius variety appears less sensitive to nitrogen level than do other varieties, it is nevertheless evident that the method is able to detect even minor variations with added nitrogen for this genotype. The delay of onset seen here with application of medium levels of nitrogen agree with previous observations. The results in Fig 10 also demonstrate that our method can quantify the final proportion of senescent leaves relative to the total leaf area, reflecting the stasis in senescence relative to total leaf mass that manifests with the addition of nitrogen.

Chickpea pilot experiment. The experiment on chickpea plants represents a pilot study of the effects of salt stress as well the influence of soil condition. This experiment exemplifies a common case where only post-processing of an image sequence is possible, and where the resolution of plant images is satisfactory to quantify some features but is not sufficiently high to assess plant senescence. In these images, the color distortion between two pixels along leaf boundaries is significant. Application of the in-built color analysis software on the original images estimated a senescence level, measured in terms of percentage of senescence to whole plant area, of greater than 10% even for the first images in the sequence, of young plants exhibiting no senescence. An application of our color correction procedure followed by a color analysis on the recovered images found an estimated senescence level of less than 1.0%, while the in-built, machine-learned color analysis tool estimated a senescence level of around 2.0% for these first images.

Table 1. Evaluation of the performance of our senescence analysis algorithm as applied to chickpea images.

Treatment	Our method (Percentage of senescent leaves)		Manual (after 2 days) (Senescence score)		Manual (after 3 days) (Senescence score)	
(mM NaCl)	Genesis836	Rupali	Genesis836	Rupali	Genesis836	Rupali
0	0.73	1.64	1	4	3	4
	0.53	8.03	1	5	2	6
	3.30	1.08	2	2	4	5
	0.53	2.27	1	4	3	3
30	1.14	3.69	2	5	5	5
	0.34	5.65	1	4	4	5
	0.91	11.81	2	7	3	10
	0.84	1.71	2	4	3	7
40	0.71	3.13	2	4	5	5
	1.05	9.80	2	7	5	8
	0.91	11.81	2	4	3	6
	0.78	10.15	2	8	3	10
60	0.99	1.40	4	5	5	5
	0.50	2.77	1	5	4	5
	0.81	2.70	1	5	4	10
	1.81	25.75	2	8	3	10

In this table our estimated level or percentage of leaf senescence is based on the last image in the sequence of 8 chickpea plant images.

doi:10.1371/journal.pone.0157102.t001

To further evaluate the performance of our color correction procedure, our results were compared with those of manual inspection based on the 1–10 scale [18] described in the Materials and Methods section. Note that the manual inspection was undertaken 2 and 3 days after the last imaging day. The results of both the subjective and the objective means of quantifying senescence level are presented for comparison in Table 1.

Despite the two diametrically contrasting measures of senescence, there remains a definite correlation between the outcomes, even though the manual inspections were conducted 2 and 3 days after the final images were taken. This is demonstrated quite convincingly in Fig 11, which exhibits a highly correlated functional (logarithmic) relationship between the two measures; the R-squared values are 0.7503 (0.754 in the case of the LemnaTec estimate) and 0.536, respectively, for the manual inspection 2 and 3 days after the last image was taken. A decreasing R-squared value is expected with increasing time difference between the day of imaging and the day of manual inspection. What is not yet clear from the results obtained so far (Fig 11), is whether a more refined manual inspection score and more frequent inspections, to compare with a simultaneous objective senescence measure, will add meaning to the fitted functional relationship. Unfortunately, manual inspection is time consuming, costly and highly subjective, which only highlights the effectiveness of the automated and objective process proposed here.

As with the wheat experiment, by utilizing the regularly taken sequence of chickpea plant images we are able to track both the growth behavior as well as the senescence process over time. In Fig 12 we demonstrate this functionality based on the time series of images for two individual plants. Although the growth behavior, in terms of projected plant area (all types), is similar to wheat in the sense of increasing with time, in contrast to the wheat experiment, the analysis reveals a decreasing trend in senescence of one plant and a semi-steady, but fluctuating behavior for the other plant. The differences can be attributed to the genotypic responses of the two plants under salt stress: for one plant (blue curve), the senescence pattern did not spread

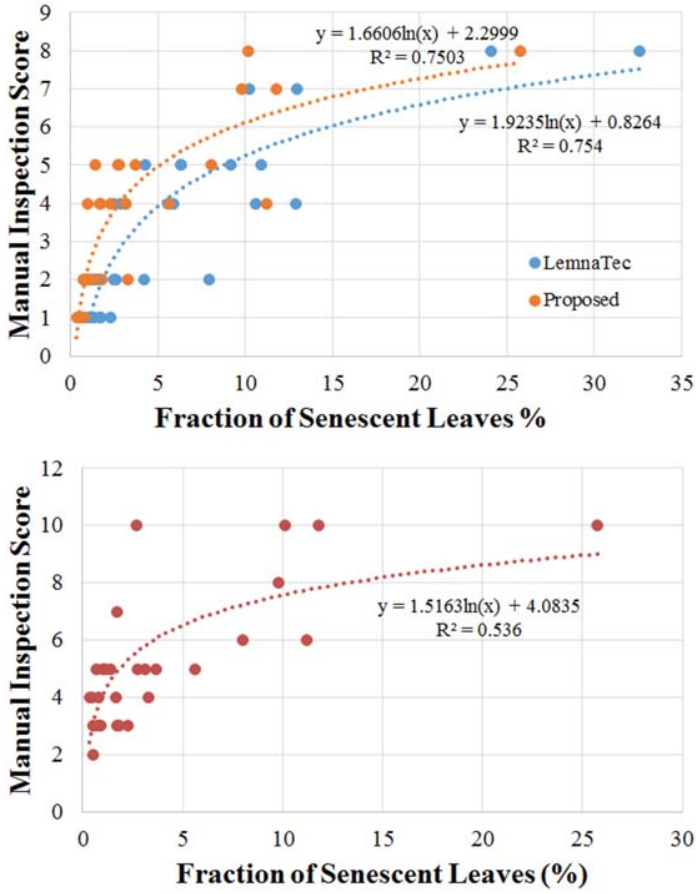

Fig 11. Scatter plots of manual inspection scores versus the objectively estimated senescence measure proposed in this paper and that of the machine learning method adapted by the LemnaTec system for a set of chickpea plants. Manual scoring was performed on two occasions: 2 days after the last imaging day (top panel) and 3 days after the last imaging day (bottom panel).

doi:10.1371/journal.pone.0157102.g011

over the plant during the plant's continual growth, leading to a decreasing fraction of leaf senescence. This can be verified by appeal to the image comparison in Fig 13(a) and 13(b). In contrast, for the other plant (red curve) senescence increased with time, but leaf fall resulted in a significant fluctuation in the percentage of leaves exhibiting senescence. This is exemplified in Fig 13(c) and 13(d).

Conclusions and Future Work

In plant phenomics it is not only those characteristics associated with the plant growth phase that are important factors to capture to assess a plant's performance against growth conditions,

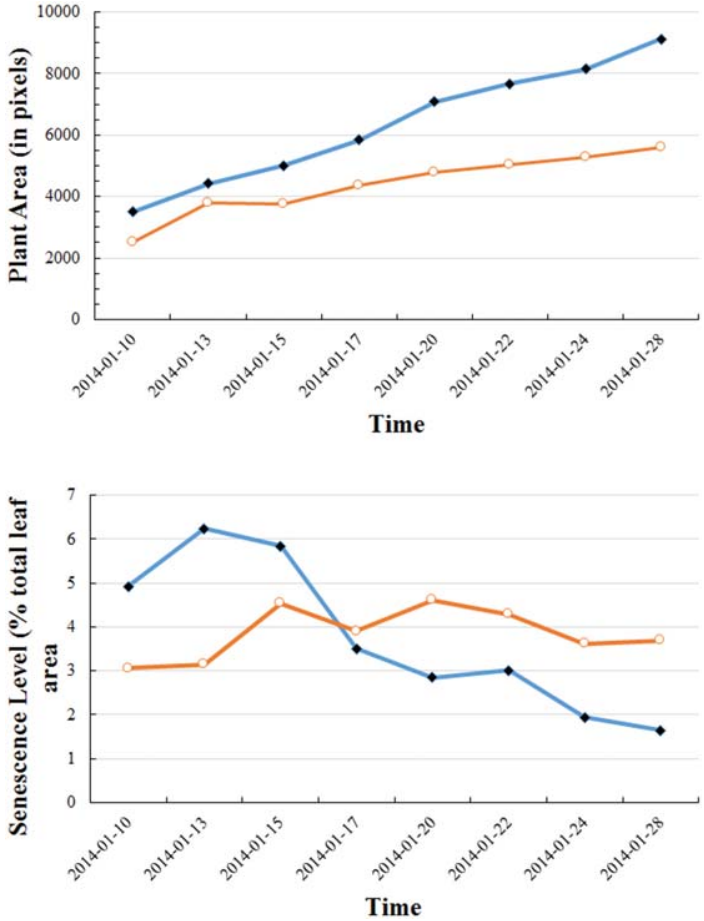

Fig 12. Whole-of-plant assessment of growth (plant area) and senescence as a function of time for two individual chickpea plants. Top figure shows the time developments of total projected plant area (all leaves and stems) for the two plants, depicting qualitatively similar but quantitatively different growth behavior. Bottom figure shows the percentage of senescence present in the leaves of these plants relative to their total plant area. The two individual plants exhibit different rates of senescence development.

doi:10.1371/journal.pone.0157102.g012

i.e., a plant's stress response. It is equally important to quantify traits indicative of a plant's age and ill health, such as senescence. In this paper we have proposed a fully automated algorithmic tool for senescence estimation, encompassing the restoration of color, plant foreground segmentation and a color classification for senescence analysis. One less obvious outcome of our efforts is the demonstration that manual inspection is inadequate as a means of assessing the senescence state of a plant. Image analysis based on color differentiation is a sound alternative. However, under high throughput conditions where the entire plant is imaged, the resolution

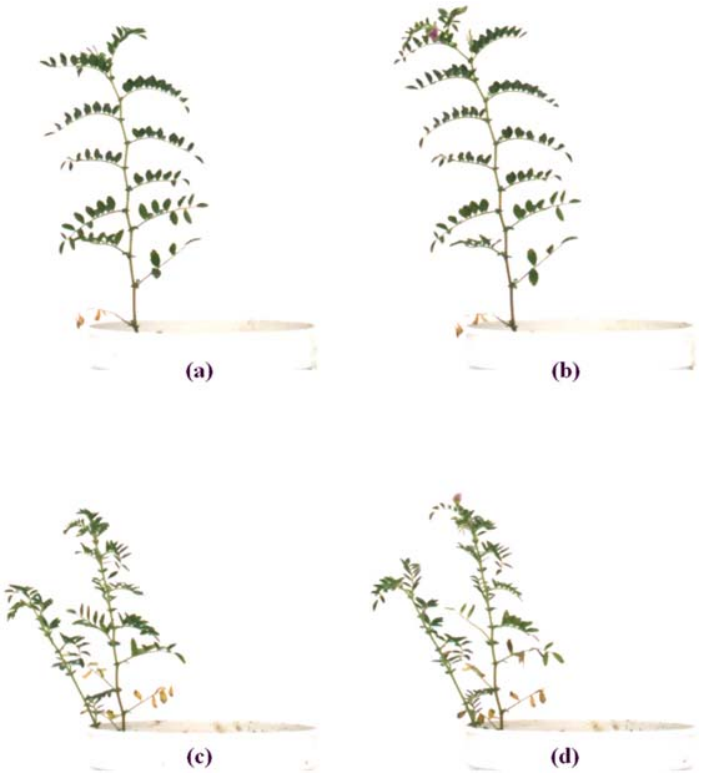

Fig 13. Two examples of senescence patterns. (a) and (b) depict similar sized leaf areas of the same plant on different days; in (b) the plant has grown a little larger. Figs (c) and (d) show the same plant (different from (a) and (b)) on different days but at a much later stage of development when more leaves have become senescent and after some senescent leaves have fallen off.

doi:10.1371/journal.pone.0157102.g013

may be insufficient to accurately capture senescence onset and development. Another related major problem is the absence of adequate camera color calibration. The approach we advocated here addresses, in a practical way, these major problems. As a result, we not only can reduce image color distortion but also improve image quality sufficiently to quantify senescence accurately. To verify the procedure's effectiveness, we compared our results with senescence scores attained by manual inspection and the senescence levels estimated by the in-built tool. We found that there is a correlation between the these measures, which no doubt has its origins in the fact that these measures are based on plant appearance.

It is worth reiterating that the process of labelling or annotating of images for the training of a machine learning approach is time consuming, with the final result intrinsically dependent on the quality of annotation. As mentioned already, machine learning approaches have their limitations, which can prevent them from being used in high throughput applications. In contrast, the philosophy of the approach proposed here is inherently high throughput, and whose

full automation can be reinforced by using, as benchmark, the image of a standard color chart at the beginning of an experiment, instead of estimating an undistorted image of a young plant.

One direction for further study is to undertake a more extensive comparison between the manual and the automated approaches to identify (if possible) a reason for the observed functional form for this correlation. A second direction for further study was identified in the chickpea study, where both the decreasing senescence trend and the fluctuating behavior of the two curves in Fig 12(b) indicate that a detailed and aggregated monitoring of leaf senescence, including the (time) tracking of leaf fall, is required for a complete assessment of senescence for this phenotypic trait to properly characterize a plant's stress response.

Supporting Information

S1 Appendix. Detailed description of the segmentation process.
(PDF)

Acknowledgments

The authors would like to thank Drs Hamid Laga and Jason Connor from the University of South Australia, Associate Professor Qiongyan Li from Bejing Forest University and Dr. Bettina Berger from The Plant Accelerator at Adelaide University for many insightful discussions. Finally, we express our gratitude for partial funding provided by the Australian Research Council, the Australian Grains Research and Development Corporation, the South Australian Government, and the Australia-India Strategic Research Fund, Department of Industry and Science, Australian Federal Government.

Author Contributions

Conceived and designed the experiments: JC MO SM. Performed the experiments: JC MO JA YL. Analyzed the data: JC SM. Contributed reagents/materials/analysis tools: MO JA YL TS. Wrote the paper: JC SM. Designed the analysis algorithm: JC SM. Developed the software used in analysis: JC.

References

1. Harris BN, Sadras VO, Tester M. A water-centred framework to assess the effects of salinity on the growth and yield of wheat and barley. Plant Soil. 2010; 336:377–389. doi: 10.1007/s11104-010-0489-9
2. Gerlai R. Phenomics: fiction or the future? Trends in Neurosciences. 2002; 25:506–509. doi: 10.1016/S0166-2236(02)02250-6 PMID: 12220878
3. Furbank RT. Plant phenomics: from gene to form and function. Functional Plant Biology. 2009; 36:5–6.
4. Niklas KJ, Enquist BJ. On the vegetative biomass partitioning of seed plant leaves, stems, and roots. American Naturlist. 2002; 159:482–497. doi: 10.1086/339459
5. Kumar P, Huang C, Cai J, Miklavcic SJ. Root phenotyping by root tip detection and classification through statistical learning. Plant Soil. 2014; 380:193–209. doi: 10.1007/s11104-014-2071-3
6. Cai J, Zeng Z, Connor JN, Huang CY, Melino V, Kumar P, et al. RootGraph: a graphic optimization tool for automated image analysis of plant roots. Journal of Experimental Botany. 2015; 66:6551–6562. doi: 10.1093/jxb/erv359 PMID: 26224880
7. Lim PO, Kim HJ, Gil Nam H. Leaf Senescence. Annual Review of Plant Biology. 2007; 58(1):115–136. doi: 10.1146/annurev.arplant.57.032905.105316 PMID: 17177638
8. Can S, Amasino RM. Making Sense of Senescence: Molecular Genetic Regulation and Manipulation of Leaf Senescence. Plant Physiology. 1997; 113(2):313–319.
9. Distelfeld A, Avni R, Fischer AM. Senescence, nutrient remobilization, and yield in wheat and barley. Journal of Experimental Botany. 2014; 65(14):3783–3798. doi: 10.1093/jxb/ert477 PMID: 24470467

10. Gaju O, Allard V, Martre P, Gouis JL, Moreau D, Bogard M, et al. Nitrogen partitioning and remobilization in relation to leaf senescence, grain yield and grain nitrogen concentration in wheat cultivars. Field Crops Research. 2014; 155:213–223. doi: 10.1016/j.fcr.2013.09.003

11. Gregersen P, Foyer C, Krupinska K. Photosynthesis and Leaf Senescence as Determinants of Plant Productivity. In: Kumlehn J, Stein N, editors. Biotechnological Approaches to Barley Improvement. vol. 69 of Biotechnology in Agriculture and Forestry. Springer Berlin Heidelberg; 2014. p. 113–138.

12. Dibella CM, Paruelo JM, Becerra JE, Bacour C, Baret F. Effect of senescent leaves on NDVI-based estimates of fAPAR: experimental and modelling evidences. International Journal of Remote Sensing. 2004; 25(23):5415–5427. doi: 10.1080/01431160412331269724

13. Kant S, Burch D, Badenhorst P, Palanisamy R, Mason J, Spangenberg G. Regulated Expression of a Cytokinin Biosynthesis Gene *IPT* Delays Leaf Senescence and Improves Yield under Rainfed and Irrigated Conditions in Canola (*Brassica napus* L.). PLoS ONE. 2015 01; 10(1):e0116349. doi: 10.1371/journal.pone.0116349 PMID: 25602960

14. Nicholson SE, Farrar TJ. The influence of soil type on the relationships between NDVI, rainfall, and soil moisture in semiarid Botswana. I. {NDVI} response to rainfall. Remote Sensing of Environment. 1994; 50(2):107–120. doi: 10.1016/0034-4257(94)90038-8

15. Römer C, Wahabzada M, Ballvora A, Pinto F, Rossini M, Panigada C, et al. Early drought stress detection in cereals: simplex volume maximisation for hyperspectral image analysis. Functional Plant Biology. 2012; 39(11):878–890. doi: 10.1071/FP12060

16. Bergsträsser S, Fanourakis D, Schmittgen S, Cendrero-Mateo MP, Jansen M, Scharr H, et al. HyperART: non-invasive quantification of leaf traits using hyperspectral absorption-reflectance-transmittance imaging. Plant Methods. 2015; 11(1). doi: 10.1186/s13007-015-0043-0 PMID: 25649124

17. Whyte O, Sivic J, Zisserman A, Ponce J. Non-uniform Deblurring for Shaken Images. International Journal of Computer Vision. 2012; 98(2):168–186. doi: 10.1007/s11263-011-0502-7

18. Maliro MFA, McNeil D, Redden B, Kollmorgen JF, Pittock C. Sampling strategies and screening of chickpea (Cicer arietinum L.) germplasm for salt tolerance. Genetic Resources and Crop Evolution. 2008; 55(1):53–63. doi: 10.1007/s10722-007-9214-9

19. Zhu X, Cohen S, Schiller S, Milanfar P. Estimating spatially varying defocus blur from a single image. IEEE Transactions on Image Processing. 2013; 22(12):4879–4891. doi: 10.1109/TIP.2013.2279316 PMID: 23974627

20. Shan Q, Jia J, Agarwala A. High-quality motion deblurring from a single image. ACM Transactions on Graphics. 2008; 27(3):Article No 73. doi: 10.1145/1360612.1360672

21. Tai YW, Brown MS. Single image defocus map estimation using local contrast prior. In: the International Conference on Image Processing; 2009. p. 1797–1800.

22. Zhang L, Nayar S. Projection defocus analysis for scene capture and image display. ACM Transactions on Graphics. 2006; 25(3):907–915. doi: 10.1145/1141911.1141974

23. Campisi P, Egiazarian K. Blind Image Deconvolution: Theory and Applications. Taylor & Francis; 2007.

24. Nishiyama M, Hadid A, Takeshima H, Shotton J, Kozakaya T, Yamaguchi O. Facial Deblur Inference Using Subspace Analysis for Recognition of Blurred Faces. IEEE Transactions on Pattern Analysis and Machine Intelligence. 2011 April; 33(4):838–845. doi: 10.1109/TPAMI.2010.203 PMID: 21079280

25. Fergus R, Singh B, Hertzmann A, Roweis ST, Freeman WT. Removing Camera Shake from a Single Photograph. ACM Transactions on Graphics. 2006 July; 25(3):787–794. doi: 10.1145/1141911.1141956

Chapter 5

Major loci underlying salinity tolerance in chickpea identified by genome-wide association study and linkage mapping

Judith Atieno[1], Yongle Li[2], Peter Langridge[2], Julian Taylor[2], Kate Dowling[3], Chris Brien[3], Federico Ribalta[4], Janine Croser[4], Manish Roorkiwal [5], Rajeev K. Varshney[5], Tim Sutton[6]

Authors' affiliations

[1] Australian Centre for Plant Functional Genomics, School of Agriculture, Food and Wine, University of Adelaide, Waite Campus, PMB 1, Glen Osmond, SA 5064, Australia

[2] School of Agriculture, Food and Wine, University of Adelaide, Waite Campus, PMB1, Glen Osmond, SA 5064, Australia

[3] The Plant Accelerator, School of Agriculture, Food and Wine, University of Adelaide, Waite Campus, PMB1, Glen Osmond, SA 5064, Australia

[4]Centre for Plant Genetics and Breeding, The University of Western Australia, 35 Stirling Highway, Crawley WA 6009, Australia

[5]Centre of Excellence in Genomics, International Crops Research Institute for the Semi-Arid Tropics (ICRISAT), Patancheru, India

[6] Corresponding author: South Australian Research and Development Institute, GPO Box 397 Adelaide, South Australia, 5001, Australia and School of Agriculture, Food and Wine, University of Adelaide, Waite Campus, PMB1, Glen Osmond, SA 5064, Australia

*Corresponding author: tim.sutton.sa.gov.au

Statement of Authorship

Title of Paper	Major loci underlying salinity tolerance in chickpea identified by both genome-wide association study and linkage mapping
Publication Status	☐ Published ☐ Accepted for Publication ☐ Submitted for Publication ☑ Unpublished and Unsubmitted work written in manuscript style
Publication Details	Genome-wide association study (GWAS) and linkage mapping were utilised to understand the genetic control of salinity tolerance traits in chickpea. Several loci underlying salinity tolerance traits were identified by both mapping approaches. Loci on chromosome 4 and chromosome 7, were found to control many yield and yield related traits under salt and control conditions.

Candidate contribution

Name of Candidate	Judith Akinyi Atieno
Contribution to the Paper	Contributed to the conception and design of this experiment. Developed methods for growing chickpea under controlled environment, including finding suitable growing media, watering regime, temperature and lighting conditions and pest control. Developed methods for salinity screening (optimal salt levels, salt delivery system, and symptoms scoring). Conducted salinity experiment including daily watering of plants to field capacity to maintain salt concentration in pots. Performed crosses between two chickpea cultivars, developed F_2 population and coordinated accelerated single seed descent for RIL population development. Coordinated genotyping and analysed SNP marker data and constructed a linkage map. Determined population structure in a diverse collection of chickpea, performed genome-wide association study, performed all statistical analyses and interpreted data. Prepared all table and figures. Wrote the manuscript. This work took approximately 18 months.
Overall percentage (%)	80
Certification:	This paper reports on original research I conducted during the period of my Higher Degree by Research candidature and is not subject to any obligations or contractual agreements with a third party that would constrain its inclusion in this thesis.
Candidate signature	Date 29/11/16
Principal supervisor signature	Date 29/11/16

Statement of Authorship

Title of Paper: Major loci underlying salinity tolerance in chickpea identified by both genome-wide association study and linkage mapping

Publication Status: Unpublished and Unsubmitted work written in manuscript style

Citation: Atieno J, Li Y, Langridge P, Taylor J, Ribalta F, Croser J, Dowling K, Brien C, Roorkiwal M, Varshney R.K, Sutton, T (unpublished). Major loci underlying salinity tolerance in chickpea identified by both genome-wide association study and linkage mapping

Author Contributions

By signing the Statement of Authorship, each author certifies that their stated contribution to the publication is accurate and permission is granted for the publication to be included in the candidate's thesis.

Judith Atieno: Developed F_2 population, developed methods for growing chickpea under controlled environment, developed methods for salinity screening, conducted salinity experiment, constructed a linkage map, performed genome-wide association study, analysed and interpreted data, and wrote the manuscript.

Signature **Date** 23/11/2016

Yongle Li: Supervised the work, provided support in data analysis and interpretation, provided critical comments on the manuscript and edited the manuscript.

Signature **Date** 22/11/2016

Peter Langridge: Supervised the work, evaluated the development of experiments, provided support in data interpretation, provided critical comments on the manuscript and edited the manuscript.

Signature **Date** 18/11/2016

Julian Taylor: Provided scripts for map construction and QTL analysis, provided critical comments on the manuscript and edited the manuscript.

Signature **Date** 18/11/2016

Federico Ribalta: Developed protocols for assisted single seed descent and used the method to progress F_2 population to F_5 population.

Signature **Date** 17/11/2016

Janine Croser: Supervised protocol development for assisted single seed descent.

Signature **Date** 15/11/2016

Kate Dowling: Performed statistical analysis on glasshouse data.

Signature **Date** 21/11/2016

Chris Brien: Designed glasshouse experiment, performed statistical analysis on glasshouse data, and edited the manuscript.

Signature **Date** 15/11/2016

Manish Roorkiwal: Contributed to generate and analyse whole genome resequencing of 300 chickpea lines.

Signature **Date** Nov. 18, 2016

Rajeev K Varshney: Supervised generation and analysis of whole genome resequencing of 300 chickpea lines and provided SNP data.

Signature **Date** 18.11.2016

Tim Sutton: Supervised the work, evaluated the development of experiments, provided critical comments on the manuscript, edited the manuscript, and will be acting as the corresponding author.

Signature **Date** 15/11/2016

Link to chapter 5

Limited genetic studies in chickpea have been done to understand the genetic control of important salinity tolerance related traits. Linkage mapping and a high-resolution genome-wide association study (GWAS) were utilised to identify QTL underlying salinity tolerance, with the ultimate objective of introgressing salinity tolerance traits into sensitive varieties. The confounding influence of population structure and flowering time were taken into account. Several loci controlling plant growth, water use and yield and yield related traits under salinity were identified. Loci on chromosome 4 and chromosome 7 controlling growth, yield and yield related traits were identified by both mapping approaches. Molecular markers tightly linked to these QTL will be validated as a selection tool in breeding to improve salinity tolerance in chickpea. This work is written in manuscript format and will shortly be submitted for peer review.

Abstract

Salinity tolerance is a complex trait under the control of several quantitative trait loci (QTL) and genes. This study combined approaches involving linkage mapping and a high-resolution genome-wide association study (GWAS) to identify QTL underlying salinity tolerance in chickpea, with the ultimate objective of introgressing salinity tolerance traits into new varieties. The influence of flowering time and population structure were taken into account to ensure QTL found were not related with maturity and population stratification. Linkage mapping conducted on a bi-parental population at F_6 generation identified 57 QTL while GWAS utilising a diversity panel known as the chickpea Reference Set, identified 54 marker-trait associations (MTAs) linked to growth rate, yield and yield components and ion accumulation under salt stress. Both GWAS and linkage mapping identified two loci regulating several yield and yield related traits including seed number under both salt and control conditions. Firstly, a locus on chromosome 4 regulating relative growth rate with LOD score of 3.6 explaining 42.6% of genetic variation was detected by both approaches. This QTL was found to co-locate with QTL for projected shoot area, water use, 100-seed weight, number of filled pods and seed number under salt. The second locus on chromosome 7 controlled seed number under both salt and control conditions with LOD score of 4.4 and explaining 12.6 % of genetic variation. This QTL co-located with other QTL for number of pods, number of filled pods and harvest index. Molecular markers linked to these loci will be validated in different sets of germplasm under different environments and developed for marker-assisted breeding to improve salinity tolerance in sensitive cultivars.

Introduction

Salinity is an abiotic stress, which severely impacts on crops' productivity (Nawaz et al., 2010; Rengasamy, 2006). Grain legumes are generally sensitive to salinity, with faba bean, field pea and chickpea being the most sensitive (Maas and Hoffman, 1977). Chickpea is the second most cultivated legume globally (FAOSTAT, 2014) and sensitive genotypes can be killed by as little as 25 mM NaCl in hydroponics (Flowers et al., 2010). Several studies have shown that chickpea is most sensitive at the reproductive stage (Krishnamurthy et al., 2011; Samineni et al., 2011; Vadez et al., 2007; Vadez et al., 2012b).

Salinity has been reported to delay the time to flower and maturity in chickpea (Krishnamurthy et al., 2011; Pushpavalli et al., 2015a; Vadez et al., 2012a). Vadez et al. (2007) described a relationship between days to flower and seed yield with very early and late maturing genotypes having increased sensitivity to salt due to the confounding effect of putative heat stress towards the end of the season. This phenomenon was not observed in studies conducted by Turner et al. (2013) and Krishnamurthy et al. (2011). Therefore, it is crucial to address flowering time during analyses to remove the confounding effect of flowering and allow for accurate quantification of salinity tolerance. Vadez et al. (2012a) conducted separate analyses within early and late flowering groups in a population developed between JG 62 (tolerant) and ICCV 2 (sensitive) chickpea genotypes segregating for flowering time to reduce the confounding effect of maturity. This analysis, however, results in small sample size, which considerably lowers the power and reliability of QTL detection. This study describes an effective strategy to control the effects of flowering time by incorporating flowering loci as cofactors during the genetic analysis in a mapping population developed between Genesis836 (salt tolerant) and Rupali (salt sensitive). Utilising bi-parental populations to map QTL, can result in the identification of chromosomal regions controlling different traits (Mackay et al., 2009).

Linkage mapping has been used to identify chromosome segments underlying salinity tolerance related traits in the model plant Arabidopsis (DeRose-Wilson and Gaut, 2011; Kobayashi et al., 2016) as well as in crops, such as wheat (Genc et al., 2014; Genc et al., 2013), barley (Fan et al., 2015; Ma et al., 2015; Nguyen et al., 2013), rice (Tiwari et al., 2016; Zheng et al., 2015), and soybean (Qi et al., 2014; Zhang et al., 2014). To date, there are only three studies that have employed linkage mapping to identify loci controlling salinity tolerance in chickpea (Pushpavalli et al., 2015b; Samineni, 2010; Vadez et al., 2012a). Using linkage maps with low marker density, these studies identified QTL within big intervals associated with seed yield and yield related traits under salinity. All three of these studies utilised Indian adapted cultivars and the QTL detected may not be useful in other production environments such as Australia. Our study has utilised a linkage map with high marker density to map salt-tolerance related traits in a population developed between two Australian adapted cultivars.

GWAS takes advantage of natural genetic variation and historic recombination in diverse germplasm to generally provide higher resolution mapping compared to biparental linkage mapping (Cardon and Bell, 2001; Sonah et al., 2015). GWAS has been used to identify regions controlling salinity tolerance in several crops, such as Arabidopsis (DeRose-Wilson and Gaut, 2011), rice (Campbell et al., 2015; Kumar et al., 2015), barley (Nguyen et al., 2013), and soybean (Kan et al., 2015). In chickpea, GWAS has been successfully utilised to identify genomic regions associated with phenology (Upadhyaya et al., 2015), agronomic traits including pod number, seed number and 100-seed weight (Kujur et al., 2015), drought and heat stress, (Thudi et al., 2014), seed quality, (Bajaj et al., 2015; Upadhyaya et al., 2016), and plant architecture (Bajaj et al., 2016). However, this approach has not yet been used to analyse salinity tolerance in chickpea.

The aim of this study is to understand the physiological and genetic mechanisms

underlying salinity tolerance in chickpea. This study integrates image-based phenotyping described in Atieno et al. (2016), linkage mapping and GWAS while controlling for phenology to identify tolerance QTL.

Material and methods

Plant material

Recombinant Inbred Line (RIL) population

A RIL population consisting of 200 lines was developed from a cross between two desi Australian adapted chickpea cultivars, Genesis836 and Rupali, previously shown to contrast for salinity tolerance (Khan et al., 2015; Turner et al., 2013). Genesis836 is a direct introduction from the International Centre for Research in the Semi-Arid Tropics (ICRISAT, India) while Rupali was bred by the Department of Agriculture and Food Western Australia (DAFWA) and the Centre for Legumes in Mediterranean Agriculture (CLIMA), based at the University of Western Australia. Genesis836 and Rupali generally flower at 52 days after sowing (DAS) and 48 DAS, respectively, under glasshouse conditions. F_1 plants derived from Genesis836 & Rupali cross were vegetatively propagated according to the protocol of Danehloueipour et al. (2006). F_2 plants were advanced to F_5 generation by assisted single seed descent using a protocol developed by Dr Janine croser and team based at the University of Western Australia. In this protocol, mature embryos from developing pods were collected and put through precocious germination treatment. Plants were grown in growth rooms with optimised light and temperature for rapid generation turnover, achieving 6-7 generations per year.

Chickpea Reference Set

A subset of the chickpea Reference Set (Upadhyaya et al., 2008) composed of 245 diverse genotypes was utilised in this study. Details of this set are shown in Table S1.

Phenotyping in the glasshouse

Phenotyping of the Reference Set was conducted in The Plant Accelerator (http://www.plantphenomics.org.au/services/accelerator/), located at the Waite Campus of the University of Adelaide as described in Atieno et al. (2016). Phenotyping of the RIL population followed the same protocol as that used for the Reference Set with minor modifications. The experiment was conducted between June 2015 and November 2015. The glasshouse temperature and humidity were controlled and ranged from 24±2ºC and 40% (day) and 16±2ºC and 90% (night), respectively. The experiment was set up in two smarthouses (growth rooms) utilising 20 lanes and 22 positions. Each RIL was replicated twice while the parents were replicated 10 times in a design described in Atieno et al. (2016). Four hrs of supplemental lighting was provided in growth rooms to extend daylight to 12 hrs. Plants were first imaged at 30 days after sowing (DAS) for three days prior to salt application to quantify plant growth rate before salt application. At 33 DAS, each pot received either 0 or 70 mM NaCl, equivalent to applying 100 ml of 0 or 250 mM NaCl respectively. To maintain salt concentration in the pots, all pots were watered and maintained at field capacity (17% (w/w), determined gravimetrically). Plants were imaged for a further 13 days to quantify growth under salt. A total of 14,080 visible light (RGB) images were obtained and processed in LemnaGrid (LemnaTec, Germany) to compute projected shoot area (PSA). Relative growth rates (RGR) were computed from smoothed cubic splines fitted for each cart to the observed PSA for each day of imaging. The difference in the logarithms of the smoothed projected shoot area for two consecutive days of imaging was divided by the number of days between imagings to constitute RGR. In addition to measurements extracted from high-resolution imaging, other measurements taken included; days to first flower, leaf sodium (Na^+) ion and potassium (K^+) ion content, plant height, yield and yield components including shoot biomass at maturity, seed number, total pod number, empty pod number, filled pod number and 100 -seed weight.

To check for the effect of photoperiod on flowering, Genesis836 and Rupali were grown under 3 different light regimes (8 hrs, 12 hrs 16 hrs). Similarly, genotypes from the RIL population with relatively early and late flowering times under 12 hrs of light were also grown under 16 hrs of light.

Genotyping

DNA was extracted from 200 RILs and parents (Genesis836 and Rupali) using DNeasy plant mini kit (QIAGEN). The quantity and quality of DNA was checked using a Nano drop (ND-100 spectrophotometer, Biolab). Genotyping was performed using DArTseq, a next generation sequencing (NGS) based platform that uses genome complexity reduction to capture informative segments in the genome (http://www.diversityarrays.com/dart-application-dartseq).

SNP data, in HapMap format, resulting from whole genome resequencing of the Reference Set with 5× -13× coverage was obtained from Dr Rajeev K. Varshney at the International Crops Research Institute for the Semi-Arid Tropics (ICRISAT). SNPs with minor allele frequency lower than 5% and SNPs that were not biallelic were eliminated from the genotypic data with the remaining 562,000 SNPs used for population structure determination and GWAS.

Linkage map construction

The linkage map of the Genesis836 x Rupali RIL population was constructed using a synergistic combination of qtl (Broman and Sen, 2009; Broman and Wu, 2016) and ASMap (Taylor and Butler, 2016) R packages available in the R Statistical Computing Environment (RCoreTeam, 2016). Preceding linkage map construction, the genetic marker set was diagnostically analysed. This included a dissimilarity analysis of the progeny to determine their relatedness. Individuals sharing more than 90% of their alleles

across the markers set were deemed to be genetic clones and used to form consensus genotypes. Marker quality was refined through the removal of markers with less than 80% observed allelic information. Additionally, markers were removed if they exhibited significant segregation distortion greater than a Bonferroni corrected p-value for a familywise alpha level equal to 0.05. The remaining set of markers was then initially clustered into nine linkage groups and the markers were optimally ordered within each linkage group using the MSTMap algorithm (Wu et al., 2008) functionality available in the ASMap package. A graphical diagnosis of the recombinations and double recombinations of the genotypes for the initial constructed map revealed several genotypes to be removed from further linkage map construction. After this removal, the markers within each linkage group were reordered and a simultaneous graphical examination of the marker and interval profiles was conducted. This indicated several markers with excessive double recombinations and these were removed. The markers within linkage groups were optimally ordered a final time and the identification and orientation of the linkage groups occurred through marker sequence comparison using the BLAST portal https://blast.ncbi.nlm.nih.gov/Blast.cgi. From this information, two linkage groups were merged to form the final linkage map.

The linkage map was prepared for analysis, by condensing each co-locating set of markers to form a representative consensus marker with a unique map position. Alleles were numerically encoded (AA = 1, BB = -1) and the remaining missing allele calls were numerically imputed using the flanking marker rules of Martinez and Curnow (1992). This complete marker information was then used to calculate pseudo mid-point markers using the formulae derived in Verbyla et al. (2007).

Phenotypic linear mixed model analysis

All phenotypic traits of the RIL population and Reference Set were analysed using a linear mixed model that appropriately partitioned and accounted for genetic and non-genetic sources of variation (Gilmour et al., 1997). Where necessary, traits were transformed to satisfy modelling assumptions. For each of the traits, the linear mixed model consisted of fixed effects containing a term to differentiate smarthouses in the Plant Accelerator as well as model linear spatial trend across rows within each smarthouse. The fixed model also contained an indicator term to ensure estimation of an overall mean effect for the RIL lines, and the population parents independently for the salt and control treatments. To ensure the genetic component of the traits was adjusted for flowering time, two previously identified flowering loci were also included in the fixed model as numerical covariates and modelled independently for both treatments. Extraneous non-genetic variation arising from the experiment including variation from zones in the smarthouse and non-linear trend across the ranges within smarthouses was captured using random effects. The residuals of the linear mixed model; were partitioned to ensure the control and salt treatments had their own residual variance. The random component of the model also contained a genetic term consisting of a factor with a level for each member of the RIL population and this was also partitioned to ensure separate genetic variances were estimated for the control and salt treatments. From this model best linear unbiased predictors (BLUPs) of the individual RILs for each treatment trait were extracted and used to calculate heritability using the formula derived in Cullis et al. (2006) and to perform correlation analysis. All linear mixed model analysis of the RIL population was conducted in GenStat 17th Edition software.

Whole genome QTL analysis

The whole genome average interval mapping (WGAIM) approach of Verbyla et al. (2007) and Verbyla et al. (2012) was used for detection and summary of QTL for the traits of the RIL population. The WGAIM approach uses an extension of linear mixed models by incorporating the complete set of linkage map intervals into the random component of the linear mixed model as a single term containing a contiguous block of covariates. The inclusion of this term is then tested and if found to be significant at an alpha level equal to 0.05, an outlier detection method is used to select a putative interval QTL to move to the fixed part of the linear mixed model. This forward selection process is repeated until the term containing the remaining set of linkage map intervals is non-significant. The selected set of additive QTL intervals are then summarised with their flanking markers, interval distance, size of the putative QTL effect, contribution to genetic variance and LOD score. All QTL analyses and summaries were performed using the wgaim R package (Taylor and Verbyla, 2011) available in the R Statistical Computing Environment. To derive confidence intervals for selected QTL, LOD drop-off of 1.5 units on each side of QTL was applied according to Lander and Botstein (1989) in GenStat 17th Edition software. MapChart 2.3 software (Voorrips, 2002) was used to graphically represent QTL with confidence intervals on linkage map.

Population structure

To determine the population structure of the Reference Set, the ADMIXTURE 1.23 program (Alexander et al., 2009) was used to identify patterns of ancestry, admixture and the number of underlying population sub-groups (K). To select the number of population sub-groups, a range of K = 1, …,10 was chosen and a maximum likelihood estimation (MLE) approach of ancestry (Alexander et al., 2009) was conducted for each K based on 562,000 SNP markers (Figure S1).The estimated number of subgroups of the population

was then chosen using the cross validation method of Alexander and Lange (2011). Additionally, a neighbor-joining clustering method utilising the 562,000 SNP markers was run in Trait Analysis by aSSociation, Evolution, and Linkage (TASSEL) 5.2.19 program (Bradbury et al., 2007) and a phylogenetic tree was produced showing clustering of genotypes in the Reference Set.

Genome-wide association mapping (GWAS)

For each of the traits measured from the Reference Set, Best Linear Unbiased Estimates (BLUE) were extracted from the associated linear mixed model and used as a phenotype in GWAS. The GWAS approach used a linear mixed model that partitioned and accounted for several components of genetic variation. To ensure the global genetic population structure of the Reference Set was captured, the ancestry fractions returned from using ADMIXTURE 1.23 with 562,000 SNP markers and K = 9 population subgroups was added as a set of fixed covariates. Additionally, family relatedness was also included in the model through a kinship matrix calculated using the method of Van Raden (2008). Marker-trait associations were then determined by including individual markers as fixed covariates in the model and scanning across the complete set of 562 000 SNP markers. Marker effects were found to be significant if they exceeded a Bonferroni corrected p-value threshold of 9×10^{-8}. All computations were carried out using the Genome Association and Prediction Integrated Tool (GAPIT) software available as standalone functions (Lipka et al., 2012) in the R Statistical Computing Environment. Using Legume Information System gbrowse http://legumeinfo.org/genomes/gbrowse/cicar. CDCFrontier.v1.0, genes within 190 kb of significant SNPs were identified as candidates for salinity tolerance. This was based on the estimation from analysis of the Reference Collection that LD decayed in landraces at an average distance of 190 kb (Dr Rajeev K. Varshney, personal communication, March 2015).

Results

Phenotyping

Phenotypic data from the Reference Set has been described in detail in (Atieno et al., 2016). This section will describe phenotypic data from Genesis836 and Rupali bi-parental population. Means of most traits measured for the RILs were within range of Genesis836 and Rupali means with the exception of plant height and days to flower, where the RILs displayed transgressive phenotypes compared to the parents (Table 1). Significant genotype by treatment interaction (G×T) was observed for most traits but not for 100-seed weight, plant height, projected shoot area, relative growth rate, days to flower, potassium ions, water use and water use efficiency (Table 1). In instances where G×T was not significant, genotype and treatment effects were significant (< .001) (Table 1). As seed yield under salinity was independent of yield potential (Figure S2), salinity stress response was defined in terms of seed yield under salt (70 mM NaCl). Salinity treatment led to a significant reduction on seed yield and yield components. Seed yield reduction of 34%, 50% and 16% was observed in parents (Genesis836, Rupali), and RILs under salinity, respectively (Table 1). Genesis836 was observed to yield 43% more under salt compared to Rupali (Table 1). Even though the parents clearly contrasted for reductions in seed number, (19% and 35% for Genesis836 and Rupali, respectively) and number of filled pods, (19% and 32% for Genesis836 and Rupali, respectively) as a result of salinity treatment, an average small reduction of 4% and 7% in RILs was observed for seed number and number of filled pods, respectively with some RILs affected more than others (Table 1). A reduction of 23% in 100-seed weight was recorded in RILs, although G×T for 100-seed weight was not significant (Table 1). Similarly, relative growth rate and shoot biomass were reduced by 25% and 36%, respectively, in RILs (Table 1). Rupali accumulated 74% more sodium ions (Na^+) compared to Genesis836 under salt with RILs

accumulating an average of 78.13 µmol/gDW of Na^+ in leaves (Table 1). Days to flower was not affected by salinity, both parents and RILs recorded similar days to flower under both salt and control conditions. Additionally, G×T for days to flower was not significant (Table 1). Heritability indices of the traits under salinity ranged from 27% for water use efficiency to 96% for days to flower (Table 1).

Relationship between yield and yield related traits

Strong positive correlations of r=0.78, r=0.70, r=0.78 under salt and r=0.8, r=0.74, r=0.82 under control was observed between seed yield and seed number, total pod number, and number of filled pods, respectively (Table 2). This demonstrates the important role these traits play in yield determination under both salt and control conditions. Strong correlations of r=0.71, r=0.65, r=0.41 under salt was established between seed yield and shoot biomass, plant height and days to flower, respectively (Table 2). However, negative albeit weak correlations of r=-0.33, r=-0.27, r=-0.35 under control, was observed between seed yield and shoot biomass, plant height and days to flower, respectively (Table 2). Even though harvest index was highly and positively correlated with seed yield under control conditions (r=0.70), it was only weakly correlated with seed yield under salt (r=0.28) (Table 2). Under salt treatment, a moderate relationship of r=0.64 and r=0.40 was observed between seed yield and 100-seed weight and relative growth rate (RGR), respectively (Table 2). Conversely, seed yield did not have a significant relationship with these traits under control conditions (Table 2). Seed yield under salt treatment had moderate negative correlations of r=-0.49, r=-0.48, with sodium (Na^+) and potassium (K^+), respectively (Table 2). Water use efficiency and number of empty pods did not have a significant relationship with seed yield under both salt and control (Table 2). However, water use had strong correlations of r=0.73 and r=0.84 with projected shoot area under salt and control conditions, respectively (Table 2).

Table 1: Summary of measurements taken in the glasshouse under salt and control conditions. Overall trait means, and P-value for effects of genotypes (G), treatments (T) and genotype by treatment interaction (G×T) for Genesis836 and Rupali and RIL population consisting of 200 genotypes. n.a is indicated for non-informative p-values where G×T is significant. Broad-sense heritability is indicated by H^2.

Traits	Treatment	Genesis836	Rupali	Mean	Min	Max	G	T	G×T	H2
Seed yield (g)	Control	6.7	5.05	4.79	1.03	7.99				51
	Salt	4.4	2.5	4.03	0.7	7.43	n.a	n.a	< .001	69
Seed number	Control	32	37	26.9	8.11	48.72				61
	Salt	26	24	25.8	4.34	48.17	n.a	n.a	< .001	54
100-seed weight (g)	Control	21.3	13.91	19.27	10.62	27.91				74
	Salt	17.12	10.04	14.92	5.11	25.1	< .001	< .001	0.67	79
Total pod number	Control	30	32	24.47	5	42.39				59
	Salt	24	25	23.75	7.89	45.39	n.a	n.a	< .001	57
Filled pod number	Control	27	28	20.9	6.54	40.96				85
	Salt	22	19	19.44	3.08	35.43	n.a	n.a	< .001	56
Empty pod number	Control	4	4	5.04	-0.24	15.44				88
	Salt	2	6	2.87	-0.44	13.02	n.a	n.a	0.024	52
Harvest index	Control	0.44	0.32	0.31	0.06	0.51				82
	Salt	0.45	0.3	0.36	0.18	0.5	n.a	n.a	< .001	51
Relative growth rate	Control	0.07	0.07	0.08	0.05	0.1				52
	Salt	0.06	0.05	0.06	0.04	0.09	< .001	< .001	0.29	49
Plant height (cm)	Control	53.8	52.8	61.72	34.96	86.44				89
	Salt	41.6	41.2	51.54	27.96	72.41	< .001	< .001	0.645	88

Traits	Treatment	Genesis836	Rupali	Mean	Min	Max	G	T	G×T	H^2
Shoot biomass (g)	Control	8.5	10.6	11.29	2.19	21.43				84
	Salt	5.2	5.6	7.18	2.23	13.18	n.a	n.a	< .001	78
Projected shoot area (pixels)	Control	3.12×10^5	3.38×10^5	3.22×10^5	1.29×10^5	5.17×10^5				79
	Salt	2.72×10^5	2.90×10^5	2.78×10^5	1.24×10^5	4.87×10^5	< .001	< .001	0.159	81
Water use (ml)	Control	43.2	42.6	43.87	18.57	65				50
	Salt	26.88	29.27	28.48	12.76	46.32	< .001	< .001	0.242	41
Apparent water use efficiency (pixels/ml)	Control	7.67×10^3	7.20×10^3	7.49×10^3	2.87×10^3	1.13×10^4				37
	Salt	1.04×10^4	1.02×10^4	1.05×10^4	5.49×10^3	1.68×10^4	< .001	< .001	0.263	27
Potassium (µmol/gDW)	Control	982	969	905.87	519	1554				43
	Salt	1361	1374	1329.71	795	2549	< .001	< .001	0.283	52
Sodium (µmol/gDW)	Control	5.2	9.57	8.43	5.61	80.32				53
	Salt	49.9	193.43	78.13	2.47	452.28	n.a	n.a	< .001	61
Potassium: Sodium	Control	189.94	101.25	107.04	1.64	980.85				47
	Salt	27.27	7.1	17.18	3.63	148.57	n.a	n.a	< .001	63
Days to flower	Control	48	46	59.5	35	90				97
	Salt	48	46	60.3	36	95	< .001	< .001	0.26	96

Table 2: Relationship between traits, under control (left panel) and salt (right panel) determined by Pearson's correla tion analysis. Highlighted, are moderate to high correlation coefficients. Level of significance (***=P<0.001, **= P<0.01, *= P<0.05, ns=non-significant).

Traits	Seed yield	Seed number	100-seed weight	Total pods	Filled pods	Empty pods	Days to flower	Shoot biomass
Seed yield	1	**0.80*****	0.09 ns	**0.74*****	**0.82*****	0.04 ns	**-0.35*****	-0.33***
Seed number	**0.78*****	1	**-0.48*****	**0.81*****	**0.95*****	-0.05 ns	**-0.48*****	**-0.54*****
100-seed weight	**0.64*****	0.04 ns	1	-0.24***	**-0.37*****	0.16*	**0.35*****	**0.49*****
Total pods	**0.70*****	**0.84*****	0.10 ns	1	**0.87*****	**0.49*****	-0.26***	-0.26***
Filled pods	**0.78*****	**0.92*****	0.15*	**0.94*****	1	0.00 ns	**-0.43*****	**-0.46*****
Empty pods	-0.02 ns	0.02 ns	-0.09 ns	**0.44*****	0.10 ns	1	0.23**	0.28***
Days to flower	**0.41*****	0.23***	**0.38*****	0.36***	0.31***	0.21**	1	**0.74*****
Shoot biomass	**0.71*****	**0.46*****	**0.59*****	**0.62*****	**0.58*****	0.27***	**0.72*****	1
Harvest index	0.28***	0.32***	0.07 ns	-0.01 ns	0.17*	**-0.45*****	**-0.46*****	**-0.43*****
Sodium (Na^+)	**-0.49*****	-0.32***	-0.37***	**-0.38*****	**-0.40*****	-0.07 ns	**-0.52*****	**-0.56*****
Potassium (K^+)	**-0.48*****	-0.27***	**-0.42*****	-0.34***	-0.33***	-0.12 ns	**-0.61*****	**-0.60*****
K:Na ratio	**0.37*****	0.18**	0.34***	0.24***	0.23**	0.10 ns	0.27***	0.32***
Plant height	**0.65*****	**0.39*****	**0.58*****	**0.55*****	**0.49*****	0.28***	**0.75*****	**0.90*****
Relative growth rate	**0.40*****	**0.48*****	0.02 ns	**0.50*****	**0.49*****	0.14*	0.19**	0.32***
Water use	0.30***	0.27***	0.15*	0.21**	0.24***	0.00 ns	-0.29***	0.14 ns
Projected shoot area	0.27***	0.04 ns	**0.38*****	0.00 ns	0.06	-0.14	-0.34***	0.10 ns
Water use efficiency	-0.10 ns	-0.24***	0.12 ns	-0.22**	-0.19**	-0.16*	0.02 ns	-0.04 ns

Harvest index	Sodium (Na+)	Potassium (K+)	K:Na ratio	Plant height	Relative growth rate	Water use	Projected shoot area	Water use efficiency
0.70***	-0.12 ns	0.11 ns	-0.01 ns	-0.27***	0.01 ns	0.14*	0.16*	0.07 ns
0.77***	0.06 ns	**0.37***	0.04 ns	**-0.52***	-0.08 ns	0.00 ns	-0.04 ns	0.01 ns
-0.32***	**-0.35***	**-0.49***	-0.10 ns	**0.52***	0.17*	0.28***	0.33***	0.06 ns
0.50***	-0.18*	0.15*	0.08 ns	-0.22**	0.16*	0.02 ns	-0.04 ns	-0.02 ns
0.70***	-0.03 ns	0.32***	0.06 ns	**-0.43***	-0.01 ns	0.02 ns	0 ns	0.05 ns
-0.23***	-0.29***	-0.25***	0.05 ns	0.31**	0.34**	0.01 ns	-0.09 ns	-0.13 ns
-0.73***	**-0.39***	**-0.49***	-0.02 ns	**0.75***	**0.41***	-0.17**	-0.26***	-0.18**
-0.89***	**-0.47***	**-0.57***	-0.04 ns	**0.90***	**0.40***	0.16*	0.07 ns	-0.12 ns
1	0.33***	**0.50***	0.01 ns	**-0.81***	-0.32***	-0.04 ns	0.03 ns	0.10 ns
0.18**	1	**0.48***	-0.03 ns	**-0.48***	**-0.35***	-0.18*	-0.12 ns	-0.02 ns
0.23***	**0.70***	1	-0.01 ns	**-0.64***	-0.23**	-0.17*	-0.18*	-0.06 ns
-0.02 ns	**-0.54***	**-0.42***	1	-0.01	0.00 ns	-0.12 ns	-0.11 ns	0.00 ns
-0.39***	**-0.63***	**-0.67***	**0.42***	1	0.41***	0.12 ns	0.06 ns	-0.10 ns
-0.01 ns	**-0.35***	-0.20**	0.27***	0.35*	1	0.00 ns	-0.19**	-0.31***
0.20**	0.11 ns	0.13 ns	-0.01 ns	0.05	0.28***	1	**0.84***	0.00 ns
0.23**	0.10 ns	0.11 ns	0.02 ns	0.02	-0.08 ns	**0.73***	1	**0.38***
-0.06 ns	-0.01 ns	-0.02 ns	-0.03 ns	-0.04	-0.28***	-0.28***	0.17**	1

Genetic analysis

Rupali/Genesis836 Genetic linkage map

An intra-specific genetic map for Rupali/Genesis836 spanned 1043.3 cM and consisted of 614 polymorphic markers (391 DArT and 223 SNP) mapped on 8 linkage groups (Table 3; Figure S3). A heat map was used to confirm the quality of the constructed map and correct order of markers along the linkage groups (Figure S4). This is the first high-resolution genetic linkage map developed to map QTL for salinity tolerance in chickpea. The number of markers and length of linkage groups varied, with linkage group (LG) 3, corresponding to chromosome 7 having the most number of mapped markers (139) and LG 2, corresponding to chromosome 5 having the least number of mapped markers (47) (Table 3). Overall, chromosome 7 was densely populated with markers with an average spacing and maximum spacing between markers of 0.8 cM and 10.8 cM, respectively (Table 3). Chromosome 1 was least populated with markers; it consisted of 49 markers with an average spacing and maximum spacing between markers of 3.3 cM and 70.4 cM, respectively (Table 3)

Table 3: Rupali/Genesis836 genetic linkage map. Each linkage group has a corresponding chromosome number derived from anchoring the genetic map to the chickpea physical map. Length of each linkage group, average and maximum spacing between markers are indicated using centimorgan (cM) units.

Linkage group	Chromosome number	Number of markers	Length cM)	Average spacing (cM)	Maximum spacing (cM)
L.1	2	110	143.5	1.3	16.3
L.2	5	47	142.9	3.1	14.3
L.3	7	139	111.3	0.8	10.8
L.4	4	112	150.5	1.4	26.8
L.5	6	59	138.4	2.4	28
L.6	8	49	75.7	1.6	12.4
L.7	3	49	121.5	2.5	20.1
L.8	1	49	159.4	3.3	70.4
OVERALL		614	1043.3	1.7	70.4

QTL mapped in Rupali/Genesis836 population

Flowering time can have confounding effects on salinity. Therefore, we first investigated genetic control of flowering time in the Rupali/Genesis836 RIL population. Days to flower followed a bimodal distribution, with most genotypes flowering at 45 days after sowing (DAS) and 70 DAS. The distribution was largely skewed to the right showing most genotypes belonged to the late flowering group (Figure 1a). While the RIL population flowered from 35-90 DAS, Rupali and Genesis836 flowered at 45 DAS and 48 DAS, respectively (Figure 1a). This demonstrates the presence of transgressive segregation, with most RILs flowering much later compared to the parents. Mapping for QTL controlling flowering in this population revealed two loci on chromosome 5 and chromosome 3 (Figure 1b) with 49.7 % and 4.3 % of genotypic variation explaned (GVE), respectively. Extended photoperiod from 12 hrs to 16 hrs drastically shortened days to flower especially in the late flowering RILs (Figure 2a). Genesis836 and Rupali time to flowering was equally progressively shortened by increasing daylength from 8 hrs to 16 hrs (Figure 2b).

a).

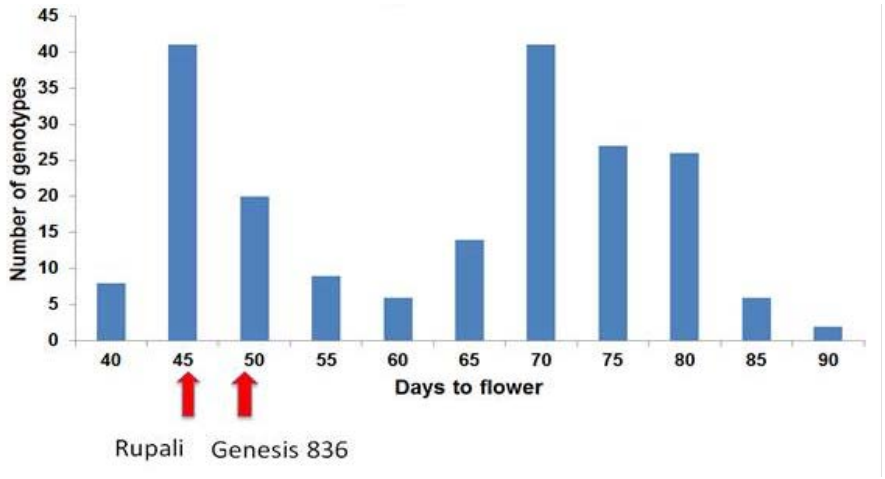

b).

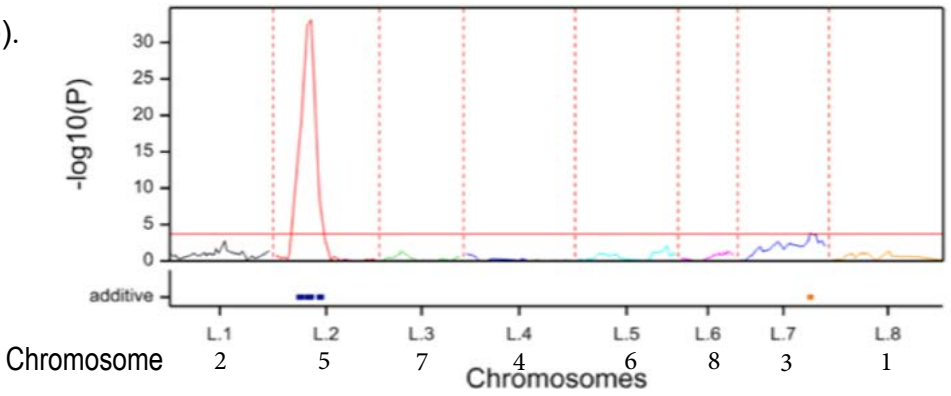

Figure 1: Flowering in Rupali/Genesis836 RIL mapping population. a). Bimodal distribution showing transgressive segregation for flowering time in the RIL population. Red arrows indicate flowering times for Rupali and Genesis836. b). LOD curve derived from QTL analysis of days to flower, showing flowering time in Rupali/Genesis836 population is controlled by two loci on chomosomes three and five.

a

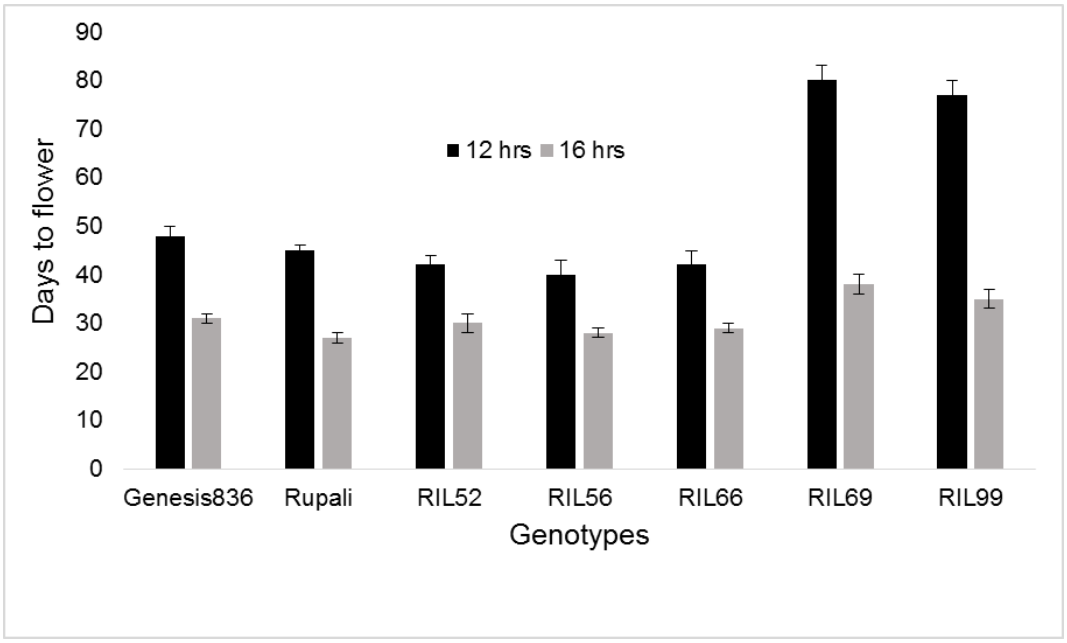

b

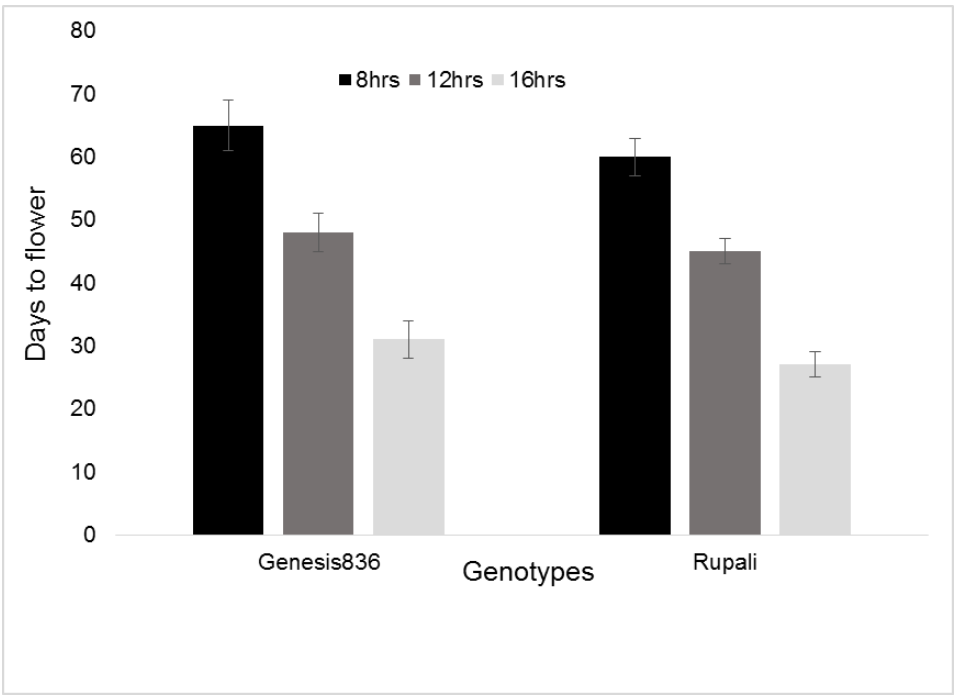

Figure 2: Effect of photoperiod on flowering. a). Bar graph showing flowering times of Genesis836, Rupali, and 5 recombinant inbred lines under 12 hrs and 16 hrs of lighting. b). Bar graph showing flowering times of Genesis836 and Rupali under 8 hrs, 12 hrs and 16 hrs of lighting. In all cases, temperature was maintained at 24±2ºC and 16±2ºC (night). Error bars indicate standard error.

Conducting QTL analysis on Rupali/Genesis836 population prior to adjusting for flowering, found all QTL to locate on the same position as flowering loci on either chromosome 5 or chromosome 3. After adjusting for flowering, 57 QTL, 32 QTL under control (Figure 3a; Table S2;) and 25 QTL under salt (Figure 3b; Table S2) spread across all chromosomes for 19 traits. Major QTL found under salt comprised of QTL for water use (10.7% GVE), water use efficiency (WUE) (18.5%-23.9% GVE), projected shoot area (15.2% GVE), relative growth rate (37%-42.6% GVE), number of filled pods (18.2% GVE), 100-seed weight (14.1% GVE), and harvest index (14.9% GVE) (Table S2). Additionally, major QTL detected under control conditions included QTL for water use (21.9% GVE projected shoot area (10.6% GVE, relative growth rate (17.9% GVE), number of filled pods (12.5% GVE), seed number (12.6% GVE), 100-seed weight (18.7% GVE), and harvest index (19.4% GVE) (Table S2). There were QTL found to control the same traits under both control and salt treatments. For instance, a locus on chromosome 4 flanked by SNP201 and SNP1069 controlled water use, plant growth rate, seed number, and 100-seed weight under both control and saline conditions (Table S2). Some of the loci detected were seen to regulate many traits. For example, a locus on chromosome 7 flanked by DArT1046 and DArT1128 was seen to control plant height, total pod number, number of filled pods, seed number and harvest index under control conditions (Table S2). Similarly, total pod number, number of filled pods, seed number, 100-seed weight, WUE, projected shoot area, and relative growth rate under salt were under the control of a locus on chromosome 4 flanked by SNP201 and SNP1069 (Table S2).

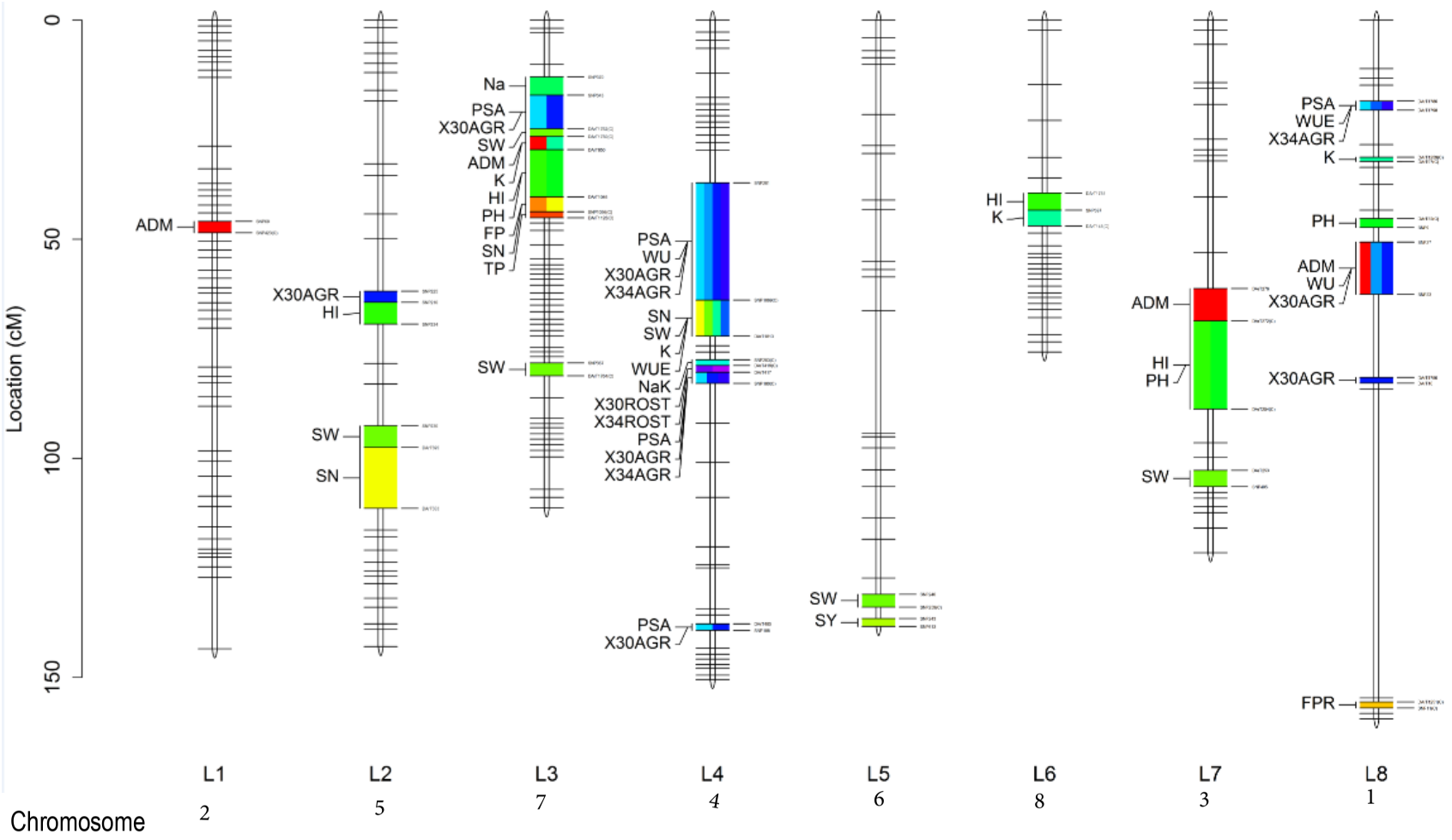

Figure 3a: QTL position on Rupali/Genesis genetic linkage map from control condition. Linkage groups and corresponding chromosome numbers are indicated on x-axis while genetic distances in cM are indicated on y-axis. The different colour bars indicate QTL for different traits. Different colour bars on one region show co-located QTL. On each of the linkage groups, QTL names are indicated on the left in black while flanking markers are indicated on the right. Abbreviations of the traits are given in supplementary Table S2.

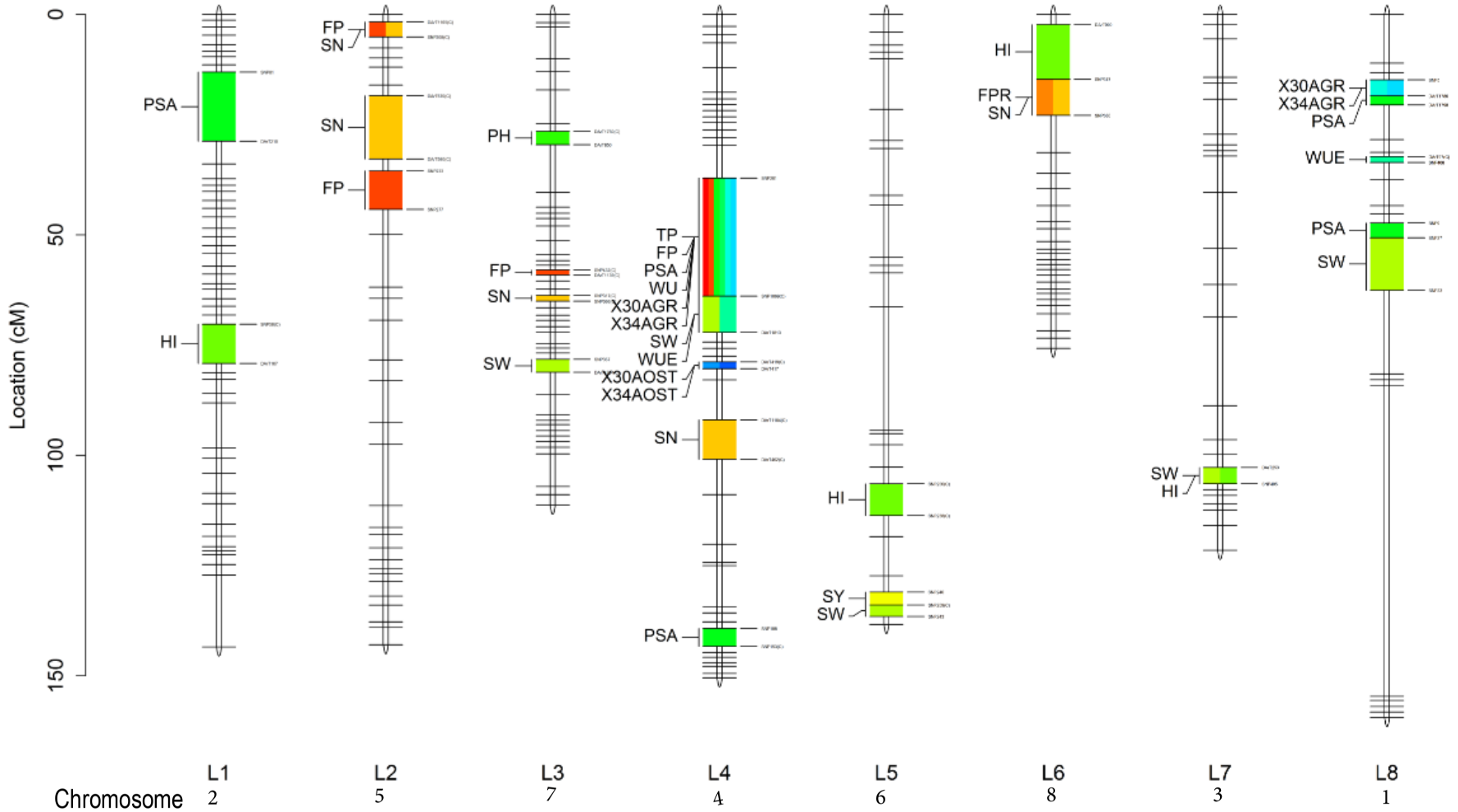

Figure 3b: QTL position on Rupali/Genesis genetic linkage map from salinity treatment. Linkage groups are indicated on x-axis while genetic distances in cM are indicated on y-axis. The different colour bars indicate QTL for different traits. Different colour bars on one region show co-located QTL. On each of the linkage groups, QTL names are indicated on the left in black while flanking markers are indicated on the right. Abbreviations of the traits are given in supplementary Table S2.

Population structure

The ADMIXTURE software, employing maximum likelihood estimation of ancestry with membership coefficient threshold of 0.7, identified 9 groups in the chickpea Reference Set (Figure 4). Phylogenetic analysis based on the neighbour-joining clustering method grouped the genotypes in the same manner as the ADMIXTURE software. All nine clusters were interspersed with landraces, advanced cultivars and breeding lines. Desi and Kabuli types were generally seen to cluster in different groups, with groups 5 and 7 dominated with kabuli in proportions of 89% and 77%, respectively. The rest of the groups were 85%-100% predominantly comprised of desi. A cluster comprised of groups 1-4, consisting of genotypes from India, separated out from the rest of the groups (Figure 4). Groups 5, 6 and 9 were predominantly made up of genotypes from the Middle East including Afghanistan, Iran, and Turkey. Even though groups 7 and 8 were comprised of genotypes from different geographic origin all genotypes from Ethiopia were found in group 8 (Figure 4).

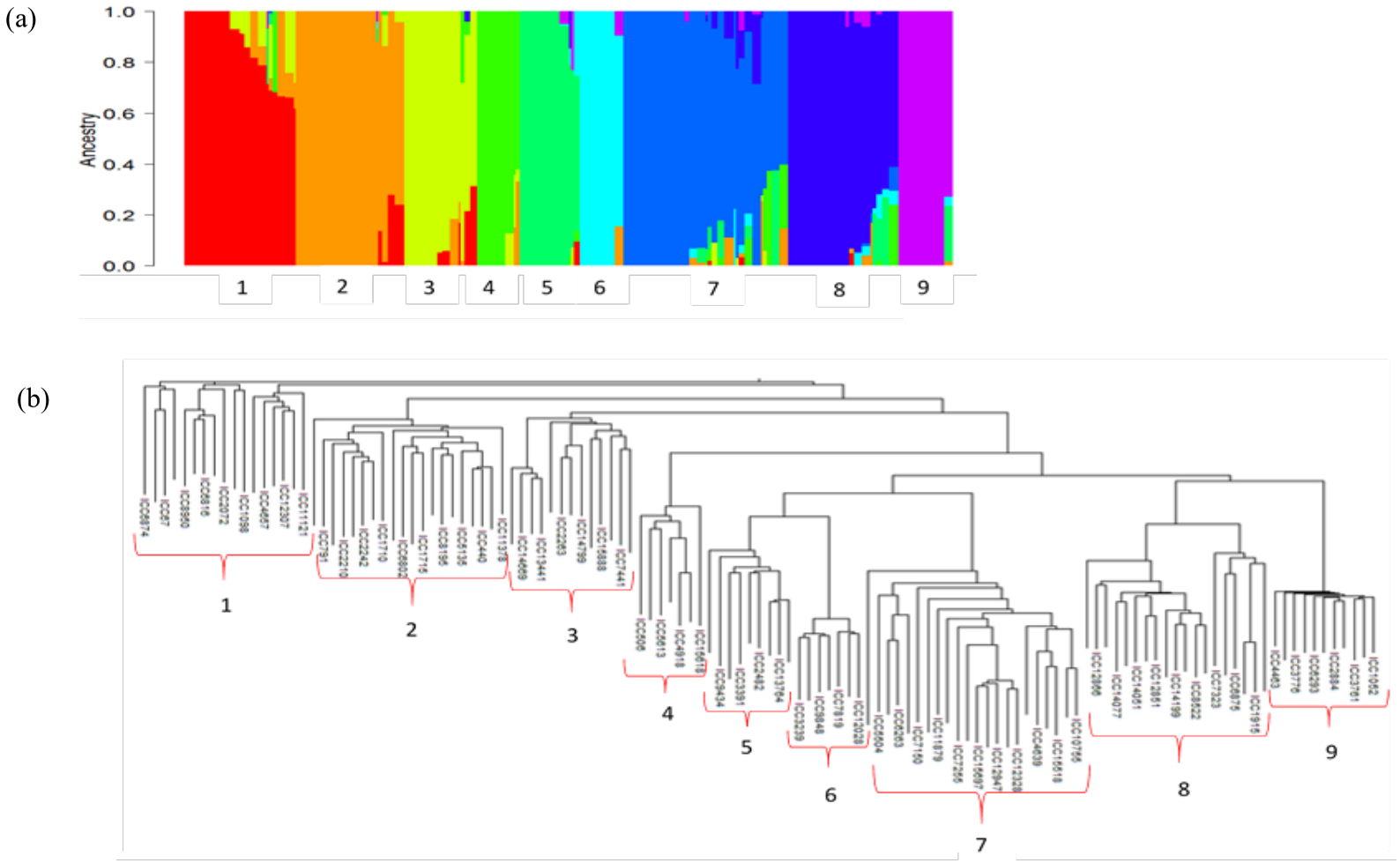

Figure 4: Population structure of genotypes in the chickpea Reference Set derived using the ADMIXTURE software. K=9 with lowest cross validation error represents the number of groups in the Reference Set (a) Structure plot showing grouping of genotypes in the Reference Set. Groups are denoted by different colours and each genotype is represented by a single vertical line (b) Phylogenetic tree constructed using neighbour-joining clustering method.

Genome-wide association mapping (GWAS)

Phenotypic data (Atieno et al., 2016) together with SNP marker data from Dr Rajeev K. Varshney were used to perform GWAS. A total of 54 marker-trait associations (MTAs) were identified for 10 salinity tolerance traits (Table 4; Figure S5). 21 MTAs for plant relative growth rate (for period 32-56 and 41-50) with phenotypic variation explained (PVE) ranging 12.5%-23.8% (Table 4) were identified. SNP locus 33012193 on chromosome 7 in linkage disequilibrium (LD) with a cation/calcium exchanger 4 gene had the highest PVE of 23.8% (Table 4). Projected shoot area had 14 MTAs, with SNP 36364948 on LG1 having a PVE of 17.9%. This SNP was in LD with Ubiquitin-associated/translation elongation factor EF1B gene (Table 4). Twelve MTAs were found for harvest index with 20.4% PVE observed for SNP 42203447 on chromosome 4, a SNP in LD with transcription factor TGA6 (Table 4). Additionally, 5 MTAs were observed for Na^+ and K^+ homeostasis with 16.1% PVE observed for SNP 47763801 on chromosome 4. This SNP was found to be in LD with MYB family transcription factor and a Sugar/inositol transporter gene (Table 4). Additionally, 2 MTAs were found for filled pod number with PVE of 14.5% found for SNP 42203447 on chromosome 4, a SNP in LD with various genes previously reported to be associated with salinity tolerance including Serine/threonine-protein phosphatase 7 long form homolog and Potassium channel AKT1-like genes (Table 4). Some MTAs were found to control more than one trait. For example, SNP 42633538 on chromosome 4 was shown to control both filled pod ratio and harvest index and was in LD with Serine/threonine-protein phosphatase 7 long form homolog and Trihelix transcription factor ASIL1 (Table 4). Several traits including relative growth rate, harvest index, seed number and seed yield under salt were under the control of two genomic regions located on chromosomes 4 and 7 (Figure 5).

Table 4: Significant marker-trait association (MTAs) for salinity tolerance related traits using mixed linear model (MLM) analysis. Significant MTAs determined by alpha threshold of 9.0×10-8, equivalent to Bonferroni-adjusted alpha threshold of 0.05. PVE (%): Phenotypic variation explained. Salinity tolerance candidate genes were identified within 190 kb of a significant MTA. RGR: relative growth rate; PSA: projected shoot area; SC: ratio of salt over control; S: under salt; Chr: Chromosome; BP: Position

Trait	Chr	BP	P.value	PVE(%)	Candidate genes
32-56 OST	7	15724015	4.207E-09	15.872045	Ubiquitin-Associated/translation elongation factor EF1B; Glutathione s-transferase;Transducin/WD40 repeat protein
32-56 OST	5	6458423	2.473E-08	14.177996	Transmembrane protein putative; Zinc finger C3HC4 type (Ring finger) protein
32-56 OST	7	15682837	2.667E-08	14.106431	Ubiquitin-Associated/translation elongation factor EF1B; glutathione S-transferase zeta class-like;Transducin/WD40 repeat protein
32-56 RGRS	7	15724015	2.092E-10	17.825905	Ubiquitin-Associated/translation elongation factor EF1B; glutathione S-transferase zeta class-like;Transducin/WD40 repeat protein;
32-56RGRS	7	15682837	1.912E-09	15.765538	Ubiquitin-Associated/translation elongation factor EF1B; glutathione S-transferase zeta class-like;Transducin/WD40 repeat protein
32-56 RGRS	4	29622025	2.409E-09	15.552803	Zinc finger protein 7-like; E3 Ubiquitin-protein ligase SINAT-2 like
32-56RGRS	5	6458423	5.307E-09	14.829714	Transmembrane protein putative; Zinc finger C3HC4 type (Ring finger) protein
32-56 RGRS	4	25984043	1.197E-08	14.091269	Zinc finger C3HC4 type (Ring finger) protein;probable voltage-gated potassium channel
32-56RGRS	7	16149182	2.072E-08	13.596205	Sugar/Inositol transporter/Monosaccharide sensing protein 2-like;serine/threonine-protein phosphatase 7
32-56 RGRS	7	15704848	2.613E-08	13.38787	Ubiquitin-Associated/translation elongation factor EF1B; glutathione S-transferase zeta class-like;Transducin/WD40 repeat protein;
32-56RGRS	7	32569714	3.906E-08	13.02775	Vacuolar protein sorting-associated protein 2 homolog 1-like; RING-H2 finger protein ATL52-like;Calcium- binding EF-Hand 1
32-56 RGRS	7	32673647	4.068E-08	12.991554	ubiquitin-like protein ATG12; AP2-like ethylene-responsive transcription factor ;Vacuolar protein sorting-associated protein 2 homolog 1-like; RING-H2 finger protein ATL52-like;Calcium- binding EF-Hand 1

32-56RGRS	7	15704842	5.203E-08	12.771953	Ubiquitin-Associated/translation elongation factor EF1B; glutathione S-transferase zeta class-like;Transducin/WD40 repeat protein
32-56 RGRS	4	34282038	6.381E-08	12.590339	Sucrose-phosphatase 1-like
41-50 OST	7	33012193	7.248E-13	23.883076	Cation/calcium exchanger 4
41-50 OST	7	48065892	3.342E-08	13.488204	Serine-threonine/tyrosine-protein kinase
41-50 OST	4	35233486	3.773E-08	13.377039	Type I inositol 1,4,5-trisphosphate 5-phosphatase CVP2-like, Peroxidase 5-like
41-50 OST	4	31127132	5.874E-08	12.972415	C2 calcium-dependent membrane targeting; ras-related protein RABA4d; Transcription factor bHLH130
41-50 OST	4	30245455	5.962E-08	12.958871	Heat shock protein DnaJ; Probable protein phosphatase 2C 25; 11 kDa late embryogenesis abundant protein-like
41-50 OST	4	30576733	7.946E-08	12.697323	Myb-like transcription factor; G patch domain-containing protein 11; C2 calcium-dependent membrane targeting
41-50 OST	4	35368828	8.095E-08	12.680444	Type I inositol 1,4,5-trisphosphate 5-phosphatase CVP2-like; Peroxidase 5-like; Sugar transport protein 10-like
PSA56 SC	1	36364948	3.733E-10	17.90417	Ubiquitin-associated/translation elongation factor EF1B;
PSA56 SC	8	8287297	1.763E-09	16.411177	Vacuolar protein sorting-associated protein 25; Probable transcription factor KAN2; Transcription factor HBP-1a
PSA56 SC	4	508770	2.765E-09	15.98237	Zinc finger HIT domain-containing protein 3; Transcription factor PIF1-like
PSA56 SC	2	28631550	4.174E-09	15.591867	Serine/threonine-protein phosphatase 7 long form homolog; Calcium-binding protein CML24
PSA56 SC	7	26746935	8.306E-09	14.942942	Serine/threonine-protein kinase HT1-like; Probable polyol transporter 6; Proline-rich receptor-like protein kinase PERK4; Sugar transporter ERD6-like 6
PSA56 SC	2	13779408	1.902E-08	14.167401	Serine/threonine-protein phosphatase 7 long form homolog; Probable WRKY transcription factor 57; Probable WRKY transcription factor 26
PSA56 SC	2	36186009	1.989E-08	14.125846	Probable serine/threonine-protein kinase WNK11; SNF1-related protein kinase regulatory subunit beta-2-like

PSA56 SC	5	20791466	2.263E-08	14.005454	Threonine--tRNA ligase, cytoplasmic-like
PSA56 SC	2	19770625	2.321E-08	13.982057	Agamous-like MADS-box protein AGL5
PSA56 SC	1	40809430	3E-08	13.74364	C2 domain-containing protein At1g53590-like
PSA56 SC	4	17837766	3.748E-08	13.537165	Calumenin; Probable glutathione S-transferase; RING-H2 finger protein ATL18-like; ras-related protein RABE1c-like; aquaporin TIP1-3-like; Glutathione S-transferase DHAR2-like
PSA56 SC	4	35114839	5.247E-08	13.226414	Phytochrome-associated serine/threonine-protein phosphatase; Type I inositol 1,4,5-trisphosphate 5-phosphatase CVP2-like; 65-kDa microtubule-associated protein 6
PSA56 SC	3	28198290	5.934E-08	13.112992	WAT1-related protein At5g07050-like; ubiquitin carboxyl-terminal hydrolase 5; protein NRT1/ PTR FAMILY 3.1-like; bZIP transcription factor 17-like; two-component response regulator ARR22-like; calmodulin-interacting protein 111
PSA56 SC	4	40933826	6.132E-08	13.082684	Dehydration-responsive protein RD22; transcriptional activator Myb-like; glycosyltransferase family protein 64 C3
Harvest index S	4	42203447	7.205E-11	19.792389	Transcription factor TGA6
Harvest index S	7	37531520	2.307E-09	16.384389	Inositol polyphosphate multikinase beta
Harvest index S	2	31451065	3.297E-09	16.040144	Transcription factor ICE ; Cation/H+ exchanger; E3 Ubiquitin protein ligase BREA-1 like
Harvest index S	4	42633538	7.352E-09	15.270849	Serine/threonine-protein phosphatase 7 long form homolog; Trihelix transcription factor ASIL1
Harvest index S	4	25167467	5.735E-08	13.32889	GDSL esterase/lipase At1g29670-like; Probable indole-3-pyruvate monooxygenase
Harvest index SC	4	42203447	9.129E-11	20.404478	Transcription factor TGA6
Harvest index SC	2	31451065	3.889E-09	16.570213	Transcription factor ICE1 ; Cation/H+ exchanger; E3 Ubiquitin protein ligase BREA-1 like
Harvest index SC	4	42633538	1.03E-08	15.597869	Serine/threonine-protein phosphatase 7 long form homolog; Trihelix transcription factor ASIL1

Harvest index SC	7	29241909	1.613E-08	15.153192	putative ABC transporter C family member 15; NADH dehydrogenase [ubiquinone] 1 alpha subcomplex assembly factor 3; EF- HAND 2; NAC transcription factor 29-like
Harvest index SC	7	29329744	4.592E-08	14.124235	Calcium-binding EF hand protein; probable polygalacturonase At3g15720; ubiquitin-like-conjugating enzyme ATG10
Harvest index SC	3	23515029	5.464E-08	13.954372	E3 ubiquitin-protein ligase At3g02290-like ; Probable receptor-like protein kinase At5g24010; desiccation protectant protein Lea14 homolog; WRKY transcription factor 22; Wall-associated kinase receptor-like 1
Harvest index SC	4	25167467	5.899E-08	13.879678	GDSL esterase/lipase At1g29670-like; Probable indole-3-pyruvate monooxygenase
Sodium ionsSC	4	35441496	4.899E-08	13.719363	Peroxidase 5-like; Sugar transport protein 10-like
Sodium ionsSC	4	1059487	9.581E-08	13.081274	Vacuolar protein sorting-associated protein 2 homolog 3-like; Serine/threonine-protein kinase 19; Ethylene-responsive transcription factor ERF098-like; CHROMATIN REMODELING 8
Potassium ions SC	7	33247108	1.355E-08	14.953624	Cation/calcium exchanger 4; sm-like protein LSM1B
Na:K SC	4	47763801	3.2E-09	16.149237	MYB family transcription factor; Sugar/inositol transporter
Na:K SC	3	8730808	3.267E-08	13.924232	Vacuolar-processing enzyme-like; Wall-associated receptor kinase-like 20
Filled pod ratioSC	4	42203447	3.718E-08	14.545036	Potassium channel AKT1-like; Serine/threonine-protein phosphatase 7 long form homolog; Basic-leucine zipper (bZIP) transcription factor TGA6;
Filled pod ratioSC	4	42633538	9.908E-08	13.574799	E3 ubiquitin-protein ligase KEG; Serine/threonine-protein phosphatase 7 long form homolog

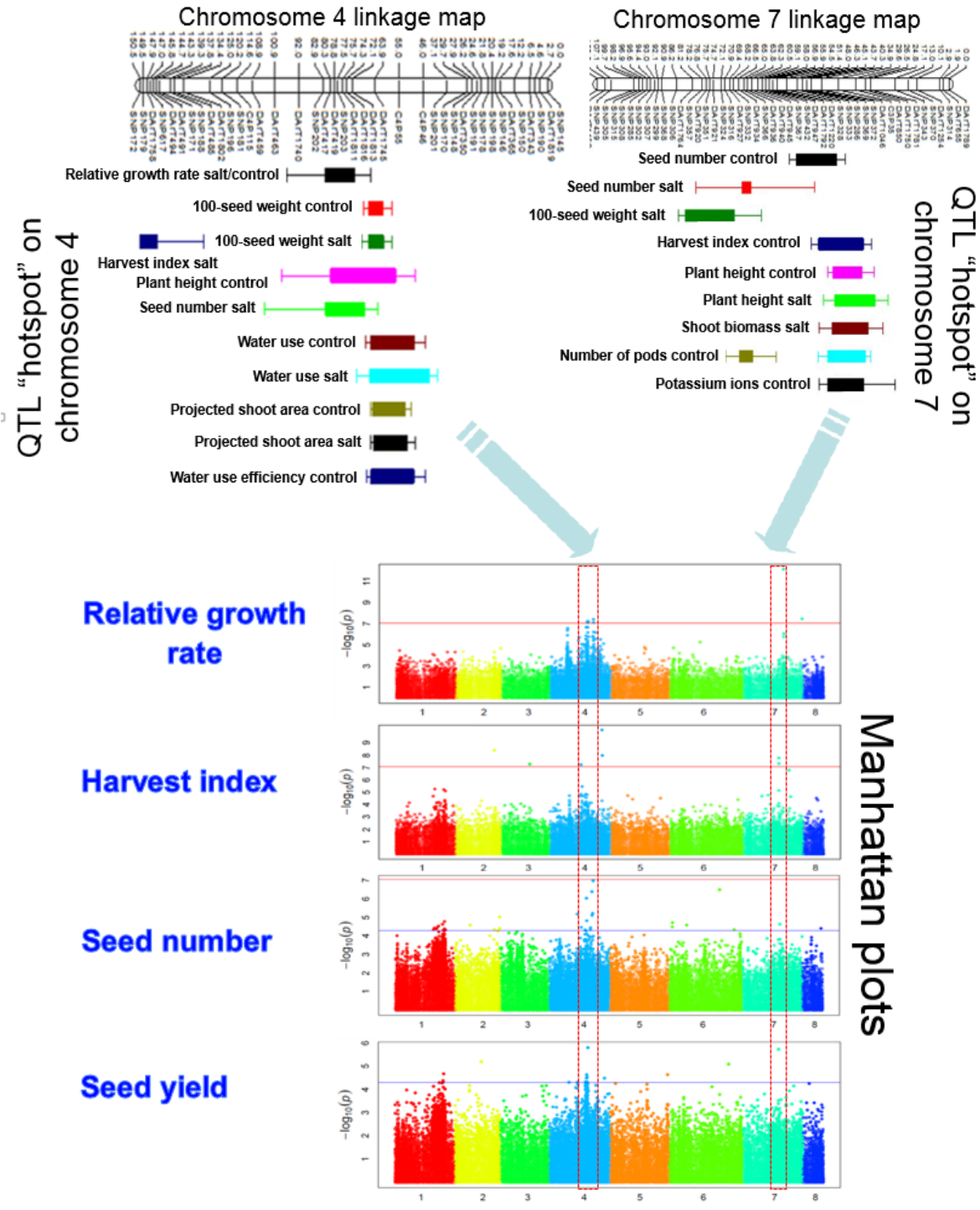

Figure 5: Genetic loci controlling salinity tolerance in chickpea. Graphical representation of two genomic regions on chromosome 4 and 7 on genetic linkage map and Manhattan plots identified by linkage mapping and GWAS respectively, showing several co-locating QTL controlling salinity tolerance in chickpea. SNPs above a set threshold are considered to be significantly associated with the trait under analysis. Blue line and red line indicate a significant threshold of 1.4×10^{-5} and 9.0×10^{-8}, respectively.

Discussion

Genetic analysis integrates phenotypic data and molecular markers to identify regions in the genome underlying traits of interest. Recently, large numbers of SNP markers became available for chickpea due to advances in DNA sequencing technologies (Shendure and Ji, 2008) and cost-effective genotyping platforms (Elshire et al., 2011). This has improved the progress for the identification and introgression of useful quantitative trail loci (QTL) and genes for crop improvement.

Linkage mapping and GWAS are complementary approaches that have been used in the identification of loci underlying agronomically important traits in plants (Li et al., 2016; Mahuku et al., 2016; Mammadov et al., 2015; Sonah et al., 2015). In chickpea, an integrated approach combining linkage mapping and GWAS has been used to identify loci regulating flowering (Upadhyaya et al., 2015), seed protein content (Upadhyaya et al., 2016) and seed coat color (Bajaj et al., 2015). These approaches rely on reliable and accurate phenotyping methodology to achieve meaningful outcomes. We reported on high-throughput phenotyping methodology (Atieno et al., 2016) which is now coupled with linkage mapping and GWAS to identify genomic regions that regulate salinity tolerance in chickpea.

Salinity tolerance is a complex polygenic trait and achieving improvements in tolerance levels in breeding germplasm has been challenging. “Sub-traits” that contribute to salinity tolerance depend on the plant species and mapping population under study. This study found that seed number and number of filled pods play major roles in salinity tolerance in the Rupali/Genesis836 mapping population, a finding in line with previous studies (Krishnamurthy et al., 2011; Vadez et al., 2007; Vadez et al., 2012a). Similarly, shoot biomass was found to strongly associate with salinity tolerance in this population. This finding is consistent with Vadez et al. (2012a), where shoot biomass showed a strong

relationship with seed yield under salinity in early flowering genotypes. Performance under salt was independent of yield potential as demonstrated by different mechanisms underlying the different traits measured under control and salt conditions. For example, plants with large biomass were generally high yielding under salt. This was not true under control conditions where plants partitioned more resources to reproductive structures compared to vegetative structures. This explains the high correlation observed between harvest index and seed yield under control and not salt conditions (Table 2). Growth of plants in both treatments was dependent on plant water uptake. Projected shoot area, a surrogate for shoot fresh weight, was higher in plants with greater water use. However, this relationship weakened at plant maturity as water use was only quantified at the pre-flowering stage. Plant growth dynamics would have changed between pre-flowering and maturity altering this relationship.

To precisely understand the genetic control of salinity tolerance related traits, confounding factors such as flowering, population structure and familial relatedness of the population under study must be taken into account. Flowering plays a major role in influencing crop duration. Thus, early flowering, usually associated with early maturity in most genotypes, has an influence in crop adaptation. It is therefore critical to eliminate the confounding effect of flowering time by choosing genotypes with minimal differences in flowering time as parents for mapping population development (Pinto et al., 2010). Rupali and Genesis836 were chosen as parents because besides contrasting for salinity tolerance, they have restricted range in flowering time (Genesis836 and Rupali flower in 52 DAS and 48 DAS, respectively under glasshouse conditions). However, transgressive segregation, likely due to complementary gene action, was observed for flowering time in the RIL population with the majority of lines flowering later than the parents. In this study, it was established that 16 hr days reduced the observed flowering variation in the RILs. However, phenotyping plants under long day conditions would have an impact on

plant development and may not be optimal for studying yield related traits. During QTL analysis, all detected QTL were shown to co-locate with two major flowering loci, on chromosome 3 and chromosome 5, segregating in this population (Figure 1). Fitting flowering allele scores to each genotype during QTL analysis enabled the detection of true QTL underlying salinity tolerance.

The complexity of salinity tolerance poses a challenge when it comes to understanding and unravelling mechanisms and genes underlying this trait. Previous studies have used traditional linkage mapping approaches to study the genetic basis of salinity tolerance in chickpea (Pushpavalli et al., 2015b; Samineni, 2010; Vadez et al., 2012a). However, these studies utilised sparsely populated genetic linkage maps, which have limited resolution. Our study used a high-density genetic linkage map, coupled with GWAS employing a large amount of SNP information from whole-genome resequencing to discover QTL that control salinity tolerance in chickpea. These two approaches are complimentary and can be used to validate each other.

Linkage mapping and GWAS identified 57 and 54 genomic regions, respectively, associated with the different traits measured. There were unique and similar genomic regions identified by the two approaches, which is not unexpected as there are likely to be mechanisms for the genetic control of salinity tolerance unique between the two populations studied. For instance, a locus on chromosome 5, (33.6 Mb-47.7 Mb) was seen to control number of filled pods under salt by linkage mapping (Table S2) but not GWAS. This region was also found to harbour 6 QTL for salinity tolerance related traits in the Pushpavalli et al. (2015b) study. Additionally, a study by Samineni (2010) found a minor QTL for yield in the same region. As number of filled pods was demonstrated to strongly correlate with seed yield under salt, this region may be important for salt tolerance improvement in chickpea.

Both linkage mapping and GWAS identified two major genomic regions on chromosomes 4 and 7 regulating yield and yield related traits under both salt and control treatments (Figure 5). The genomic region on chromosome 7 (13.6 Mb- 37.5 Mb) was found to control total pod number, number of filled pods, seed number, and harvest index under control conditions using linkage mapping (Table S2). A similar region (33.1 Mb-44.8 Mb) was previously identified by Pushpavalli et al. (2015b), and was found to be associated with above ground dry matter, total pod number, seed number and yield under salinity. Based on GWAS, the same region was seen to control relative measures (salt/control) of relative growth rate, harvest index and potassium ions and significant SNPs were in LD with genes previously reported to be associated with salinity tolerance, including Cation/calcium exchanger 4, Serine-threonine/tyrosine-protein kinase and Calcium- binding EF-Hand 1 (Table 4). Additionally, both linkage mapping and GWAS in our study detected an interesting genomic region on chromosome 4 (12.5 Mb-39.4 Mb) which controlled many different physiological and agronomic traits under both salt and control conditions (Figure 5), hence this is an important region of the genome associated with higher plant vigour. Linkage mapping found this region to harbour clusters of QTL including those associated with relative growth rate, 100-seed weight, plant height, seed number, water use, and projected shoot area (Table S2). Similarly, GWAS identified this region to control relative measures (salt/control) of relative growth rate, harvest index, seed number and seed yield. Some of the genes in LD with significant SNPs in this region include; Serine-threonine protein kinase (SOS2) which interacts with CBLs (SOS3) upon calcium spikes as a result of salinity exposure to maintain sodium potassium homeostasis (Ma et al., 2014), E3- Ubiquitin-protein ligase which plays a role in ABA mediated high salinity response (Kim and Kim, 2013), and Late-embryogenesis abundant protein and Dehydration responsive protein RD22 which play roles in alleviating adverse effects of water deficit and high salinity (Xu et al., 1996). The genes identified in this region are

potential candidates for marker-assisted breeding. Previous studies by Kale et al. (2015) and Varshney et al. (2014) identified the same region as a "QTL-hotspot" for drought tolerance in chickpea. Both drought and salt stress have osmotic stress components, which would share common tolerance mechanisms.

Conclusion

This study has used image-based phenotyping coupled with linkage mapping and GWAS to dissect mechanisms and genetic basis of salinity tolerance in chickpea. The analysis has not only identified traits related to salinity tolerance but also revealed a novel genomic region on chromosome 4 associated with salinity tolerance and high vigour in chickpea. GWAS has the potential to offer high resolution mapping compared to traditional linkage mapping which allowed us to narrow down to a few salinity tolerance candidate genes. Near isogenic lines (NILs) will be developed to fine map the QTL detected on chromosome 4 and molecular markers applied in marker assisted breeding to improve salinity tolerance in existing chickpea cultivars.

Reference

Alexander, D.H., and K. Lange, 2011: Enhancements to the ADMIXTURE algorithm for individual ancestry estimation. BMC Bioinformatics **12**, 246.

Alexander, D.H., J. Novembre, and K. Lange, 2009: Fast model-based estimation of ancestry in unrelated individuals. Genome Research **19**, 1655-1664.

Atieno, J., Y. Li, P. Langridge, B. Berger, C.J. Brien, K. Dowling, V. R.K., and T. Sutton, 2016: Exploring genetic variation for salinity tolerance in chickpea using image-based phenotyping . Manuscript submitted for publication.

Bajaj, D., S. Das, H.D. Upadhyaya, R. Ranjan, S. Badoni, V. Kumar, S. Tripathi, C.L.L. Gowda, S. Sharma, S. Singh, A.K. Tyagi, and S.K. Parida, 2015: A Genome-wide Combinatorial Strategy Dissects Complex Genetic Architecture of Seed Coat Color in Chickpea. Frontiers in Plant Science **6**, 979.

Bradbury, P.J., Z. Zhang, D.E. Kroon, T.M. Casstevens, Y. Ramdoss, and E.S. Buckler, 2007: TASSEL: software for association mapping of complex traits in diverse samples. Bioinformatics **23**, 2633-2635.

Broman, K.W., and S. Sen, 2009: A Guide to QTL Mapping with R/qtl Springer-Verlag.

Broman, K.W., and H. Wu, 2016: Rqtl: Tools for Analyzing QTL Experiments. R package version 1-39-5.

Campbell, M.T., A.C. Knecht, B. Berger, C.J. Brien, D. Wang, and H. Walia, 2015: Integrating Image-Based Phenomics and Association Analysis to Dissect the Genetic Architecture of Temporal Salinity Responses in Rice. Plant Physiology **168**, 1476-U1697.

Cardon, L.R., and J.I. Bell, 2001: Association study designs for complex diseases. Nat Rev Genet **2**, 91-99.

Cullis, B.R., A.B. Smith, and N.E. Coombes, 2006: On the design of early generation variety trials with correlated data. Journal of Agricultural Biological and Environmental Statistics **11**, 381-393.

Danehloueipour, N., G. Yan, H.J. Clarke, and K.H.M. Siddique, 2006: Successful stem cutting propagation of chickpea, its wild relatives and their interspecific hybrids. Australian Journal of Experimental Agriculture **46**, 1349-1354.

DeRose-Wilson, L., and B.S. Gaut, 2011: Mapping salinity tolerance during Arabidopsis thaliana germination and seedling growth. PLoS ONE **6**.

Elshire, R.J., J.C. Glaubitz, Q. Sun, J.A. Poland, K. Kawamoto, E.S. Buckler, and S.E. Mitchell, 2011: A Robust, Simple Genotyping-by-Sequencing (GBS) Approach for High Diversity Species. Plos One **6**.

Fan, Y., S. Shabala, Y. Ma, R. Xu, and M. Zhou, 2015: Using QTL mapping to investigate the relationships between abiotic stress tolerance (drought and salinity) and agronomic and physiological traits. BMC Genomics **16**.

FAOSTAT, 2014: Agriculture database Retrieved from http://faostat3.fao.org/download/Q/QC/E 11/2/2016 Accessed on: August 3, 2016

Flowers, T.J., P.M. Gaur, C.L. Gowda, L. Krishnamurthy, S. Samineni, K.H. Siddique, N.C. Turner, V. Vadez, R.K. Varshney, and T.D. Colmer, 2010: Salt sensitivity in chickpea. Plant Cell Environ **33**, 490-509.

Genc, Y., J. Taylor, J. Rongala, and K. Oldach, 2014: A major locus for chloride accumulation on chromosome 5A in bread wheat. PLoS ONE **9**.

Genc, Y., K. Oldach, B. Gogel, H. Wallwork, G.K. McDonald, and A.B. Smith, 2013: Quantitative trait loci for agronomic and physiological traits for a bread wheat population grown in environments with a range of salinity levels. Molecular Breeding **32**, 39-59.

Gilmour, A.R., B.R. Cullis, A. Verbyla, x16b, and P. nas, 1997: Accounting for Natural and Extraneous Variation in the Analysis of Field Experiments. Journal of Agricultural, Biological, and Environmental Statistics **2**, 269-293.

Kale, S.M., D. Jaganathan, P. Ruperao, C. Chen, R. Punna, H. Kudapa, M. Thudi, M. Roorkiwal, M.A. Katta, D. Doddamani, V. Garg, P.B.K. Kishor, P.M. Gaur, H.T. Nguyen, J. Batley, D. Edwards, T. Sutton, and R.K. Varshney, 2015: Prioritization of candidate genes in "QTL-hotspot" region for drought tolerance in chickpea (Cicer arietinum L.). Scientific Reports **5**, 15296.

Kan, G., W. Zhang, W. Yang, D. Ma, D. Zhang, D. Hao, Z. Hu, and D. Yu, 2015: Association mapping of soybean seed germination under salt stress. Molecular Genetics and Genomics **290**, 2147-2162.

Khan, H.A., K.H.M. Siddique, R. Munir, and T.D. Colmer, 2015: Salt sensitivity in chickpea: Growth, photosynthesis, seed yield components and tissue ion regulation in contrasting genotypes. Journal of Plant Physiology **182**, 1-12.

Kim, J.H., and W.T. Kim, 2013: The Arabidopsis RING E3 Ubiquitin Ligase AtAIRP3/LOG2 Participates in Positive Regulation of High-Salt and Drought Stress Responses. Plant Physiology **162**, 1733-1749.

Kobayashi, Y., A. Sadhukhan, T. Tazib, Y. Nakano, K. Kusunoki, M. Kamara, R. Chaffai, S. Iuchi, L. Sahoo, M. Kobayashi, O.A. Hoekenga, and H. Koyama, 2016: Joint genetic and network analyses identify loci associated with root growth under NaCl stress in Arabidopsis thaliana. Plant, Cell and Environment **39**, 918-934.

Krishnamurthy, L., N.C. Turner, P.M. Gaur, H.D. Upadhyaya, R.K. Varshney, K.H.M. Siddique, and V. Vadez, 2011: Consistent Variation Across Soil Types in Salinity Resistance of a Diverse Range of Chickpea (Cicer arietinum L.) Genotypes. Journal of Agronomy and Crop Science **197**, 214-227.

Kumar, V., A. Singh, S.V.A. Mithra, S.L. Krishnamurthy, S.K. Parida, S. Jain, K.K. Tiwari, P. Kumar, A.R. Rao, S.K. Sharma, J.P. Khurana, N.K. Singh, and T. Mohapatra, 2015: Genome-wide association mapping of salinity tolerance in rice (Oryza sativa). DNA Research **22**, 133-145.

Lander, E.S., and D. Botstein, 1989: Mapping Mendelian Factors Underlying Quantitative Traits Using RFLP Linkage Maps. Genetics **121**, 185-199.

Li, X., Z. Zhou, J. Ding, Y. Wu, B. Zhou, R. Wang, J. Ma, S. Wang, X. Zhang, Z. Xia, J. Chen, and J. Wu, 2016: Combined Linkage and Association Mapping Reveals QTL and Candidate Genes for Plant and Ear Height in Maize. Frontiers in Plant Science **7**, 833.

Lipka, A.E., F. Tian, Q. Wang, J. Peiffer, M. Li, P.J. Bradbury, M.A. Gore, E.S. Buckler, and Z. Zhang, 2012: GAPIT: genome association and prediction integrated tool. Bioinformatics **28**, 2397-2399.

Ma, D.-M., W.-R. Xu, H.-W. Li, F.-X. Jin, L.-N. Guo, J. Wang, H.-J. Dai, and X. Xu, 2014: Co-expression of the Arabidopsis SOS genes enhances salt tolerance in transgenic tall fescue (Festuca arundinacea Schreb.). Protoplasma **251**, 219-231.

Ma, Y., S. Shabala, C. Li, C. Liu, W. Zhang, and M. Zhou, 2015: Quantitative trait loci for salinity tolerance identified under drained and waterlogged conditions and their association with flowering time in barley (Hordeum vulgare. L). PLoS ONE **10**.

Maas, E.V., and G.J. Hoffman, 1977: CROP SALT TOLERANCE - CURRENT ASSESSMENT. ASCE J Irrig Drain Div **103**, 115-134.

Mackay, T.F.C., E.A. Stone, and J.F. Ayroles, 2009: The genetics of quantitative traits: challenges and prospects. Nat Rev Genet **10**, 565-577.

Mahuku, G., J. Chen, R. Shrestha, L.A. Narro, K.V.O. Guerrero, A.L. Arcos, and Y. Xu, 2016: Combined linkage and association mapping identifies a major QTL (qRtsc8-1), conferring tar spot complex resistance in maize. Theoretical and Applied Genetics **129**, 1217-1229.

Mammadov, J., X. Sun, Y. Gao, C. Ochsenfeld, E. Bakker, R. Ren, J. Flora, X. Wang, S. Kumpatla, D. Meyer, and S. Thompson, 2015: Combining powers of linkage and association mapping for precise dissection of QTL controlling resistance to gray leaf spot disease in maize (Zea mays L.). BMC Genomics **16**, 1-16.

Martinez, O., and R.N. Curnow, 1992: Estimating the Locations and the Sizes of the Effects of Quantitative Trait Loci Using Flanking Markers. Theoretical and Applied Genetics **85**, 480-488.

Nawaz, K., Hussain K, Majeed A, A.S. Khan F, and A. K, 2010: Fatality of salt stress to plants:Morphological, physiological and biochemical aspects. Afr. J. Biotechnol **9**, 5475-5480.

Nguyen, V.L., S.A. Ribot, O. Dolstra, R.E. Niks, R.G.F. Visser, and C.G. van der Linden, 2013: Identification of quantitative trait loci for ion homeostasis and salt tolerance in barley (Hordeum vulgare L.). Molecular Breeding **31**, 137-152.

Pinto, R.S., M.P. Reynolds, K.L. Mathews, C.L. McIntyre, J.-J. Olivares-Villegas, and S.C. Chapman, 2010: Heat and drought adaptive QTL in a wheat population designed to minimize confounding agronomic effects. TAG. Theoretical and Applied Genetics. Theoretische Und Angewandte Genetik **121**, 1001-1021.

Pushpavalli, R., M. Zaman-Allah, N.C. Turner, R. Baddam, M.V. Rao, and V. Vadez, 2015a: Higher flower and seed number leads to higher yield under water stress conditions imposed during reproduction in chickpea. Functional Plant Biology **42**, 162-174.

Pushpavalli, R., L. Krishnamurthy, M. Thudi, P.M. Gaur, M.V. Rao, K.H.M. Siddique, T.D. Colmer, N.C. Turner, R.K. Varshney, and V. Vadez, 2015b: Two key genomic regions harbour QTLs for salinity tolerance in ICCV 2 x JG 11 derived chickpea (Cicer arietinum L.) recombinant inbred lines. Bmc Plant Biology **15**.

Qi, X., M.W. Li, M. Xie, X. Liu, M. Ni, G. Shao, C. Song, A. Kay-Yuen Yim, Y. Tao, F.L. Wong, S. Isobe, C.F. Wong, K.S. Wong, C. Xu, C. Li, Y. Wang, R. Guan, F. Sun, G. Fan, Z. Xiao, F. Zhou, T.H. Phang, X. Liu, S.W. Tong, T.F. Chan, S.M. Yiu, S. Tabata, J. Wang, X. Xu, and H.M. Lam, 2014: Identification of a novel salt tolerance gene in wild soybean by whole-genome sequencing. Nature Communications **5**.

RCoreTeam, 2016: R: A Language and Environment for Statistical Computing. Retrieved from: . http://www.r-project.org. Accessed on: July 12, 2016

Rengasamy, P., 2006: World salinization with emphasis on Australia. J Exp Bot **57**, 1017-23.

Samineni, S., 2010: Physiology, genetics and molecular mapping of salt tolerance in chickpea (Cicer arietinum. L). PhD thesis, The University of Western Australia.

Samineni, S., K.H.M. Siddique, P.M. Gaur, and T.D. Colmer, 2011: Salt sensitivity of the vegetative and reproductive stages in chickpea (Cicer arietinum L.): Podding is a particularly sensitive stage. Environmental and Experimental Botany **71**, 260-268.

Shendure, J., and H.L. Ji, 2008: Next-generation DNA sequencing. Nature Biotechnology **26**, 1135-1145.

Sonah, H., L. O'Donoughue, E. Cober, I. Rajcan, and F. Belzile, 2015: Identification of loci governing eight agronomic traits using a GBS-GWAS approach and validation by QTL mapping in soya bean. Plant Biotechnol J **13**, 211-21.

Taylor, J., and A. Verbyla, 2011: R Package wgaim: QTL Analysis in Bi-Parental Populations Using Linear Mixed Models. Journal of Statistical Software **40**, 1-18.

Taylor, J., and D. Butler, 2016: R Package ASMap: Efficient Genetic Linkage Map Construction and Diagnosis. Journal of Statistical Software, Conditionally Accepted.

Tiwari, S., K. Sl, V. Kumar, B. Singh, A.R. Rao, A.M. Sv, V. Rai, A.K. Singh, and N.K. Singh, 2016: Mapping QTLs for Salt Tolerance in Rice (Oryza sativa L.) by Bulked Segregant Analysis of Recombinant Inbred Lines Using 50K SNP Chip. PLoS ONE **11**.

Turner, N.C., T.D. Colmer, J. Quealy, R. Pushpavalli, L. Krishnamurthy, J. Kaur, G. Singh, K.H.M. Siddique, and V. Vadez, 2013: Salinity tolerance and ion accumulation in chickpea (Cicer arietinum L.) subjected to salt stress. Plant and Soil **365**, 347-361.

Upadhyaya, H.D., S.L. Dwivedi, M. Baum, R.K. Varshney, S.M. Udupa, C.L. Gowda, D. Hoisington, and S. Singh, 2008: Genetic structure, diversity, and allelic richness in composite collection and reference set in chickpea (Cicer arietinum L.). BMC Plant Biology **8**.

Upadhyaya, H.D., D. Bajaj, L. Narnoliya, S. Das, V. Kumar, C.L. Gowda, S. Sharma, A.K. Tyagi, and S.K. Parida, 2016: Genome-Wide Scans for Delineation of Candidate Genes Regulating Seed-Protein Content in Chickpea. Front Plant Sci **7**, 302.

Upadhyaya, H.D., D. Bajaj, S. Das, M.S. Saxena, S. Badoni, V. Kumar, S. Tripathi, C.L. Gowda, S. Sharma, A.K. Tyagi, and S.K. Parida, 2015: A genome-scale integrated approach aids in genetic dissection of complex flowering time trait in chickpea. Plant Mol Biol **89**, 403-20.

Vadez, V., L. Krishnamurthy, R. Serraj, P.M. Gaur, H.D. Upadhyaya, D.A. Hoisington, R.K. Varshney, N.C. Turner, and K.H.M. Siddique, 2007: Large variation in salinity tolerance in chickpea is explained by differences in sensitivity at the reproductive stage. Field Crops Research **104**, 123-129.

Vadez, V., L. Krishnamurthy, M. Thudi, C. Anuradha, T.D. Colmer, N.C. Turner, K.H.M. Siddique, P.M. Gaur, and R.K. Varshney, 2012a: Assessment of ICCV 2 × JG 62 chickpea progenies shows sensitivity of reproduction to salt stress and reveals QTL for seed yield and yield components. Molecular Breeding **30**, 9-21.

Vadez, V., M. Rashmi, K. Sindhu, M. Muralidharan, R. Pushpavalli, N.C. Turner, L. Krishnamurthy, P.M. Gaur, and T.D. Colmer, 2012b: Large number of flowers and tertiary branches, and higher reproductive success increase yields under salt stress in chickpea. European Journal of Agronomy **41**, 42-51.

Varshney, R.K., M. Thudi, S.N. Nayak, P.M. Gaur, J. Kashiwagi, L. Krishnamurthy, D. Jaganathan, J. Koppolu, A. Bohra, S. Tripathi, A. Rathore, A.K. Jukanti, V. Jayalakshmi, A. Vemula, S.J. Singh, M. Yasin, M.S. Sheshshayee, and K.P. Viswanatha, 2014: Genetic dissection of drought tolerance in chickpea (Cicer arietinum L.). Theoretical and Applied Genetics **127**, 445-462.

Verbyla, A.P., B.R. Cullis, and R. Thompson, 2007: The analysis of QTL by simultaneous use of the full linkage map. Theoretical and Applied Genetics **116**, 95-111.

Verbyla, A.P., J.D. Taylor, and K.L. Verbyla, 2012: RWGAIM: an efficient high-dimensional random whole genome average (QTL) interval mapping approach. Genetics Research **94**, 291-306.

Voorrips, R.E., 2002: MapChart: Software for the Graphical Presentation of Linkage Maps and QTLs. Journal of Heredity **93**, 77-78.

Wu, Y., P.R. Bhat, T.J. Close, and S. Lonardi, 2008: Efficient and Accurate Construction of Genetic Linkage Maps from the Minimum Spanning Tree of a Graph. PLoS Genet **4**, e1000212.

Xu, D., X. Duan, B. Wang, B. Hong, T.H.D. Ho, and R. Wu, 1996: Expression of a Late Embryogenesis Abundant Protein Gene, HVA1, from Barley Confers Tolerance to Water Deficit and Salt Stress in Transgenic Rice. Plant Physiology **110**, 249-257.

Zhang, W.J., Y. Niu, S.H. Bu, M. Li, J.Y. Feng, J. Zhang, S.X. Yang, M.M. Odinga, S.P. Wei, X.F. Liu, and Y.M. Zhang, 2014: Epistatic association mapping for alkaline and salinity tolerance traits in the soybean germination stage. PLoS ONE **9**.

Zheng, H., H. Zhao, H. Liu, J. Wang, and D. Zou, 2015: QTL analysis of Na+ and K+ concentrations in shoots and roots under NaCl stress based on linkage and association analysis in japonica rice. Euphytica **201**, 109-121.

Chapter 6

General discussion

Soil salinity affects plant growth which results in reduced crop productivity. Chickpea is sensitive to sub-soil constraints including boron toxicity, sodicity and salinity. In Australia, chickpea is mainly grown in the northern grain production region as a winter pulse. In 2012, there were reports from northern New South Wales and southern Queensland of chickpea crop lost to salinity. This was attributed to rising water tables followed by high evaporation which concentrated salts in the upper soil layers (Moore et al., 2013). To improve salinity tolerance in chickpea, there is a need to broaden our understanding of the physiology and genetic control of salinity tolerance traits and develop tools that can be applied to improve the efficiency of breeding.

When this research began, the genetic resources needed to map salinity tolerance traits in Australian chickpea germplasm had not been established. The objective of this study was to exploit diversity in the chickpea germplasm to understand the genetic basis of salinity tolerance in chickpea. The chickpea Reference Set was the appropriate germplasm for this work as it is thought to represent 78% of allelic diversity present in a much larger collection of chickpea referred to as the core collection (Upadhyaya et al., 2008). Additionally, the Reference Set was shown to have broad genetic variation for salinity tolerance (Krishnamurthy et al., 2011). This set consists of 300 chickpea accessions, of which 95% are landraces, collected from 28 different countries (Upadhyaya et al., 2008) and is maintained by the International Centre of Agriculture in the Semi-Arid Tropics (ICRISAT), India.

Despite the availability of extensive germplasm collections for chickpea, a major challenge faced by genebanks is germplasm flow. Countries that host important plant genetic resources may place restrictions on the movement of material to other countries for political reasons. Another contentious issue is biopiracy of a country's genetic resources. Countries may be sceptical about sharing germplasm, as there is the possibility

that their local landraces may be utilised commercially with no compensation. In this case the research was done in collaboration with ICRISAT, India, making it possible to have access to the Reference Set.

Improved characterisation and cataloguing of germplasm is of utmost importance in genebanks. During the course of this research, this study uncovered some discrepancies that could have resulted from inaccurate cataloguing and characterisation of material in the Reference Set. For instance, phylogenetic analysis of the Reference Set showed material from the same geographic origin to generally cluster together but with some inconsistencies. These anomalies could be due to two reasons: firstly, some of the material may not have been well characterised or there could have been problems associated with cataloguing of the material so that inaccurate inferences of countries of origin were made for some of the accessions. Secondly, there may have been direct introduction of material without proper documentation making it difficult to track the flow of germplasm between countries. Additionally, this research found Indian germplasm to have less genetic diversity compared to material from other countries. The loss of diversity in the material could be due to ongoing selection made by local farmers. Alternatively, this material could have been inaccurately classified and may have been sourced from breeding programs where diversity had been lost through breeding. Another instance where characterisation of the Reference Set could be improved is keeping records of exact coordinates where the material was collected. This research was met with challenges in trying to understand flowering time in relation to latitude. Material from countries at low latitude, like Ethiopia and Tanzania, generally had early flowering times compared to material from countries at high latitude, like Turkey and Iran. However, this relationship was not maintained in the whole collection. This could be attributed to other factors like rainfall and photoperiod sensitivity, which has an influence on crop duration. Nevertheless, since some countries span a wide range of latitudes, more information on exact position where the material was collected could have significantly improved our

understanding of the influence of latitude on flowering time in the Reference set.

To mitigate problems associated with germplasm characterisation and to identify a bigger pool of rare alleles for chickpea improvement, large numbers of wild relatives of cultivated chickpea, *Cicer reticulutum* and *Cicer echinospermum*, are currently being collected in a systematic manner in Southeastern Turkey with the help of GPS technology. This material will be evaluated for traits of economic importance and novel genes underlying these traits introgressed into modern chickpea cultivars (Prof. Doug Cook, University of California's Davis Campus, personal communication).

To complement genetic diversity in the Reference Set and for the purposes of investigating traits and genetic loci that would be applicable to the Australian environment, a bi-parental RIL population was developed from a cross between Genesis836 and Rupali, two Australian adapted chickpea cultivars. To rapidly advance the generation time of the population, we collaborated with Dr Janine Croser's group based at the University of Western Australia to utilise the latest developments in single seed descent technology. Doubled haploid technology utilised in cereals has not been very successful in pulses due to technical difficulties. Hence, assisted single seed descent has been used as an alternative, reducing generation time and making it possible to achieve 6-7 generations of pulses per year. Pre-breeders and breeders can utilise this technology for fast and efficient trait discovery and to lock in improved varietal traits.

Evaluation of germplasm for traits of economic importance requires a streamlined phenotyping platform. At the start of this research, there was limited knowledge regarding the physiological characteristics of salinity tolerance in chickpea. Conventional phenotyping for complex traits like salinity tolerance can be very laborious and time-consuming, often limiting screening to a few measurements of a small number of lines,

resulting in a phenotyping bottleneck. For efficient utilisation of the broad genetic variation present in chickpea germplasm collections, and to circumvent the disadvantages of conventional phenotyping, high-throughput phenotyping tools are needed to examine subtle and complex plant characteristics of a large number of lines within a short period of time.

High-throughput, non-destructive, image-based phenotyping of salinity response has only been reported in cereals (Campbell et al., 2015; Hairmansis et al., 2014; Schilling et al., 2014). In this study, a protocol incorporating image-based phenotyping was established to investigate novel traits linked to salinity tolerance in chickpea under a controlled environment. This study found relative growth rate to be moderately associated with salinity tolerance, hence there is a need to develop and implement algorithms that can recognise traits such as pod number, which was found to be highly associated with salinity tolerance. Conducting research in a breeding and sound agronomic context requires field phenotyping. However, field sites often present with other confounding sub-soil constraints such as sodicity and boron toxicity. Additionally, spatial and temporal variability of salinity is often observed in the field. To achieve uniform salinity levels in a field trial, Saade et al. (2016) used saline water for irrigation. There is also a move towards artificially salinizing field trial sites (Dr. Timothy Colmer, personal communication; Prof. Rana Munns, personal communication). Further research is needed to utilise such fields with ground based and aerial phenotyping platforms (reviewed by Araus and Cairns, 2014). The Phenospex FieldScan high-throughput, high precision phenotyping platform and the Field Scanalyzer at Rothamsted Research could be used to complement high-throughput phenotyping performed under controlled environments.

Linking phenotypic to genotypic data relies on both high throughput phenotyping but also cheap, high-density DNA marker analysis. Due to the availability of whole-genome

resequencing data from the chickpea Reference Set (provided by Dr Rajeev K. Varshney, ICRISAT), a large number of SNP markers became available for genetic analysis. Conducting genetic analysis in the Reference Set met with some challenges. Firstly, population structure was detected in this panel, with accessions from the same geographic origin generally clustering together. However, using different molecular markers to study the population structure in the panel also resulted in different outcomes, which posed a challenge in selecting the appropriate Q matrix that would effectively account for structure in this panel. Secondly, linkage disequilibrium (LD) on a region on chromosome 4, found to associate with several salinity tolerance traits, extended over several megabases. This made it impossible to narrow down the identified genomic region to a few candidate genes. Similarly, the same region spanning several megabases was identified in the RIL population. Positional cloning approaches involving population development to saturate critical regions with recombination events, followed by targeted phenotyping of key recombinant families could significantly narrow the region to a genomic interval containing a few candidate genes, which could be functionally characterised to determine possible roles in salinity tolerance in chickpea. Moreover, further research could utilise mapping populations which are intermediate between bi-parental populations and natural diverse collections, such as MAGIC and NAM populations to take advantage of high-resolution QTL detection, and allelic diversity without the confounding effects of population structure. Presently, a MAGIC population consisting of 1200 chickpea lines is being screened for different agronomic traits at ICRISAT (Dr. Pooran Gaur, personal communication). Additionally, the CGIAR consortium, including ICARDA and ICRISAT, is developing a NAM population (Nagaraji, 2015).

An interesting outcome from this study is that loci on chromosome 4 and 7, which were independent of flowering time, were identified as being associated with several salinity

tolerance traits in the Reference Set and the RIL population. This implies a strong positive natural/artificial selection for these two regions and their applicability in improving salinity tolerance in a wide range of genetic background. Furthermore, this research found these loci were associated with traits under both salt and control conditions implying a role in the regulation of plant vigour as opposed to salinity tolerance *per se*. The locus on chromosome 4 has been reported as being associated with drought tolerance (Kale et al., 2015). Clearly, these loci are important in maintaining yield stability under unfavourable environments. To ensure global food security in the face of climate change, a shift to identify loci underlying multiple stress adaptation mechanisms would be of utmost importance.

In conclusion, this study has contributed towards the development of tools that can be applied to improve the efficiency of breeding in chickpea. Application of molecular markers has a consequence of changing a breeding program considerably. Currently, the priority of the Australian chickpea breeding program is maintaining disease resistance including resistance to Phytophthora root rot and Botrytis grey mould, earliness and chilling tolerance whereas salinity tolerance is classed as a desirable trait. Salinity is a big problem in the southern drier regions of Australia like Balaklava and Southern Mallee. Developing cultivars which could maintain yield in these areas would improve production significantly (Dr. Kristy Hobson, Australian chickpea breeder, personal communication).

The Australian breeding program uses pot-based assays under controlled conditions to screen plants at seedling stage for salinity tolerance (Dr. Kristy Hobson, Australian chickpea breeder, personal communication). Molecular markers would save on time and speed up selection and breeding process. The two loci, on chromosome 4 and chromosome 7, identified in this research are not only associated with salinity tolerance but plant vigour which is important for a wide range of traits. Molecular markers closely

linked to these loci will be evaluated in the breeding program for their suitability in efficiently selecting for lines that can maintain yield across multiple environments under salinity and other stress conditions. Once deemed suitable, these markers will be implemented in the breeding program for marker-assisted and genomic selection.

References

Araus, J.L., and J.E. Cairns, 2014: Field high-throughput phenotyping: the new crop breeding frontier. Trends in Plant Science **19**, 52-61.

Bajaj, D., S. Das, S. Badoni, V. Kumar, M. Singh, K.C. Bansal, A.K. Tyagi, and S.K. Parida, 2015: Genome-wide high-throughput SNP discovery and genotyping for understanding natural (functional) allelic diversity and domestication patterns in wild chickpea. Scientific Reports **5**, 12468.

Campbell, M.T., A.C. Knecht, B. Berger, C.J. Brien, D. Wang, and H. Walia, 2015: Integrating Image-Based Phenomics and Association Analysis to Dissect the Genetic Architecture of Temporal Salinity Responses in Rice. Plant Physiology **168**, 1476-U1697.

Deokar, A.A., L. Ramsay, A.G. Sharpe, M. Diapari, A. Sindhu, K. Bett, T.D. Warkentin, and B. Tar'an, 2014: Genome wide SNP identification in chickpea for use in development of a high density genetic map and improvement of chickpea reference genome assembly. BMC Genomics **15**, 708.

Gaur, R., S. Azam, G. Jeena, A.W. Khan, S. Choudhary, M. Jain, G. Yadav, A.K. Tyagi, D. Chattopadhyay, and S. Bhatia, 2012: High-throughput SNP discovery and genotyping for constructing a saturated linkage map of chickpea (Cicer arietinum L.). DNA Res **19**, 357-73.

Hairmansis, A., B. Berger, M. Tester, and S.J. Roy, 2014: Image-based phenotyping for non-destructive screening of different salinity tolerance traits in rice. Rice (N Y) **7**, 16.

Kale, S.M., D. Jaganathan, P. Ruperao, C. Chen, R. Punna, H. Kudapa, M. Thudi, M. Roorkiwal, M.A. Katta, D. Doddamani, V. Garg, P.B.K. Kishor, P.M. Gaur, H.T. Nguyen, J. Batley, D. Edwards, T. Sutton, and R.K. Varshney, 2015: Prioritization of candidate genes in "QTL-hotspot" region for drought tolerance in chickpea (Cicer arietinum L.). Scientific Reports **5**, 15296.

Krishnamurthy, L., N.C. Turner, P.M. Gaur, H.D. Upadhyaya, R.K. Varshney, K.H.M. Siddique, and V. Vadez, 2011: Consistent Variation Across Soil Types in Salinity Resistance of a Diverse Range of Chickpea (Cicer arietinum L.) Genotypes. Journal of Agronomy and Crop Science **197**, 214-227.

Kujur, A., D. Bajaj, H.D. Upadhyaya, S. Das, R. Ranjan, T. Shree, M.S. Saxena, S. Badoni, V. Kumar, S. Tripathi, C.L.L. Gowda, S. Sharma, S. Singh, A.K. Tyagi, and S.K. Parida, 2015: Employing genome-wide SNP discovery and genotyping strategy to extrapolate the natural allelic diversity and domestication patterns in chickpea. Frontiers in Plant Science **6**.

Moore, K., M. Ryley, M. Sharman, J.v. Leur, L. Jenkins, and R. Brill, 2013: Developing a plan for chickpea 2013, In: GRDC, (ed.).

Nagaraji, S., 2015: Identifying the genetic architecture of complex traits in chickpea, In: CGIAR, (ed.), Research Program on Grain Legumes.

Saad, M.S., and V.R. Rao, eds. 2001: Establishment and Management of Field Genebank, a Training Manual. IPGRI-APO, Serdang.

Saade, S., A. Maurer, M. Shahid, H. Oakey, S.M. Schmöckel, S. Negrão, K. Pillen, and M. Tester, 2016: Yield-related salinity tolerance traits identified in a nested association mapping (NAM) population of wild barley. Scientific Reports **6**, 32586.

Schilling, R.K., P. Marschner, Y. Shavrukov, B. Berger, M. Tester, S.J. Roy, and D.C. Plett, 2014: Expression of the Arabidopsis vacuolar H+-pyrophosphatase gene (AVP1) improves the shoot biomass of transgenic barley and increases grain yield in a saline field. Plant Biotechnology Journal **12**, 378-386.

Upadhyaya, H.D., S.L. Dwivedi, M. Baum, R.K. Varshney, S.M. Udupa, C.L. Gowda, D. Hoisington, and S. Singh, 2008: Genetic structure, diversity, and allelic richness in composite collection and reference set in chickpea (Cicer arietinum L.). BMC Plant Biology **8**.

Varshney, R.K., C. Song, R.K. Saxena, S. Azam, S. Yu, A.G. Sharpe, S. Cannon, J. Baek, B.D. Rosen, B. Tar'an, T. Millan, X. Zhang, L.D. Ramsay, A. Iwata, Y. Wang, W. Nelson, A.D. Farmer, P.M. Gaur, C. Soderlund, R.V. Penmetsa, C. Xu, A.K. Bharti, W. He, P. Winter, S. Zhao, J.K. Hane, N. Carrasquilla-Garcia, J.A. Condie, H.D. Upadhyaya, M.C. Luo, M. Thudi, C.L. Gowda, N.P. Singh, J. Lichtenzveig, K.K. Gali, J. Rubio, N. Nadarajan, J. Dolezel, K.C. Bansal, X. Xu, D. Edwards, G. Zhang, G. Kahl, J. Gil, K.B. Singh, S.K. Datta, S.A. Jackson, J. Wang, and D.R. Cook, 2013: Draft genome sequence of chickpea (Cicer arietinum) provides a resource for trait improvement. Nat Biotechnol **31**, 240-6.

Addendum

Supplementary information

Line numbers: grey - lines replicated twice (1 - 213); green = lines replicated thrice (214 -245); blue = check lines (246 - 247)

SW Positions

Lanes	23	22	21	20	19	18	17	16	15	14	13	12	11	10	9	8	7	6	5	4	3	2
1	3	3	238	238	213	213	237	237	7	7	2	2	229	229	223	223	20	20	214	214	92	92
2	5	5	210	210	206	206	228	228	18	18	48	48	147	147	165	165	65	65	54	54	76	76
3	140	140	8	8	104	104	234	234	129	129	116	116	161	161	63	63	12	12	159	159	162	162
4	233	233	156	156	199	199	218	218	84	84	176	176	197	197	154	154	24	24	196	196	10	10
5	13	13	45	45	85	85	115	115	215	215	218	218	49	49	193	193	32	32	111	111	64	64
6	29	29	225	225	119	119	79	79	195	195	138	138	66	66	59	59	224	224	51	51	245	245
7	133	133	123	123	139	139	75	75	112	112	53	53	232	232	182	182	44	44	40	40	137	137
8	243	243	226	226	120	120	19	19	21	21	110	110	164	164	55	55	167	167	61	61	174	174
9	108	108	56	56	130	130	189	189	67	67	181	181	239	239	179	179	235	235	102	102	94	94
10	86	86	60	60	217	217	128	128	72	72	225	225	124	124	16	16	42	42	227	227	77	77
11	101	101	201	201	121	121	71	71	117	117	28	28	219	219	114	114	113	113	163	163	9	9
12	151	151	186	186	14	14	214	214	241	241	208	208	160	160	200	200	6	6	173	173	209	209
13	41	41	142	142	222	222	80	80	93	93	43	43	240	240	126	126	217	217	143	143	68	68
14	37	37	33	33	152	152	187	187	246	246	36	36	148	148	204	204	226	226	88	88	103	103
15	223	223	17	17	190	190	183	183	31	31	4	4	146	146	144	144	78	78	231	231	150	150
16	87	87	221	221	134	134	25	25	212	212	131	131	216	216	205	205	50	50	96	96	52	52
17	69	69	82	82	185	185	118	118	236	236	244	244	207	207	180	180	30	30	73	73	22	22
18	198	198	35	35	122	122	39	39	194	194	170	170	27	27	203	203	178	178	175	175	171	171
19	211	211	242	242	246	246	224	224	127	127	141	141	219	219	81	81	125	125	107	107	228	228
20	177	177	157	157	47	47	74	74	220	220	26	26	38	38	191	191	23	23	222	222	91	91
21	1	1	153	153	57	57	34	34	70	70	166	166	149	149	188	188	97	97	98	98	90	90
22	99	99	100	100	106	106	95	95	202	202	220	220	184	184	105	105	158	158	109	109	132	132
23	227	227	89	89	135	135	216	216	230	230	15	15	145	145	247	247	215	215	11	11	58	58
24	46	46	229	229	155	155	168	168	83	83	169	169	172	172	136	136	62	62	221	221	192	192

SE Positions

Lanes	2	3	4	5	6	7	8	9	10	11	12	13	14	15	16	17	18	19	20	21	22	23
1	1	1	234	234	247	247	229	229	48	48	237	237	138	138	160	160	228	228	32	32	9	9
2	37	37	120	120	106	106	239	239	16	16	244	244	176	176	179	179	113	113	40	40	22	22
3	41	41	156	156	142	142	115	115	141	141	110	110	166	166	182	182	20	20	30	30	132	132
4	230	230	47	47	14	14	183	183	216	216	93	93	27	27	167	167	42	42	73	73	150	150
5	13	13	46	46	118	118	212	212	80	80	43	43	242	242	235	235	191	191	88	88	162	162
6	56	56	57	57	95	95	152	152	244	244	84	84	161	161	148	148	196	196	111	111	209	209
7	225	225	153	153	75	75	243	243	185	185	81	81	236	236	105	105	214	214	126	126	137	137
8	5	5	86	86	29	29	202	202	21	21	70	70	197	197	11	11	241	241	92	92	68	68
9	89	89	60	60	139	139	31	31	240	240	146	146	204	204	63	63	59	59	239	239	90	90
10	100	100	3	3	122	122	190	190	72	72	154	154	222	222	200	200	178	178	109	109	64	64
11	241	241	112	112	8	8	220	220	233	233	116	116	53	53	55	55	165	165	77	77	91	91
12	242	242	213	213	177	177	28	28	134	134	232	232	49	49	169	169	107	107	6	6	58	58
13	133	133	45	45	155	155	128	128	135	135	170	170	234	234	203	203	193	193	52	52	143	143
14	99	99	211	211	33	33	18	18	195	195	224	224	235	235	145	145	240	240	62	62	54	54
15	151	151	168	168	71	71	218	218	238	238	149	149	144	144	231	231	24	24	102	102	94	94
16	35	35	108	108	223	223	79	79	7	7	4	4	219	219	180	180	51	51	175	175	158	158
17	157	157	101	101	243	243	181	181	187	187	231	231	38	38	205	205	245	245	12	12	10	10
18	85	85	130	130	186	186	82	82	36	36	83	83	34	34	97	97	65	65	50	50	103	103
19	198	198	201	201	199	199	74	74	129	129	15	15	184	184	232	232	215	215	61	61	247	247
20	210	210	104	104	119	119	189	189	194	194	217	217	208	208	125	125	78	78	171	171	159	159
21	140	140	123	123	206	206	237	237	236	236	127	127	66	66	245	245	188	188	230	230	192	192
22	69	69	233	233	39	39	19	19	67	67	221	221	114	114	44	44	131	131	163	163	174	174
23	87	87	17	17	25	25	227	227	2	2	172	172	117	117	124	124	23	23	98	98	76	76
24	246	246	121	121	238	238	226	226	207	207	147	147	26	26	164	164	96	96	136	136	173	173

Condition numbers: 2-control 1-salt

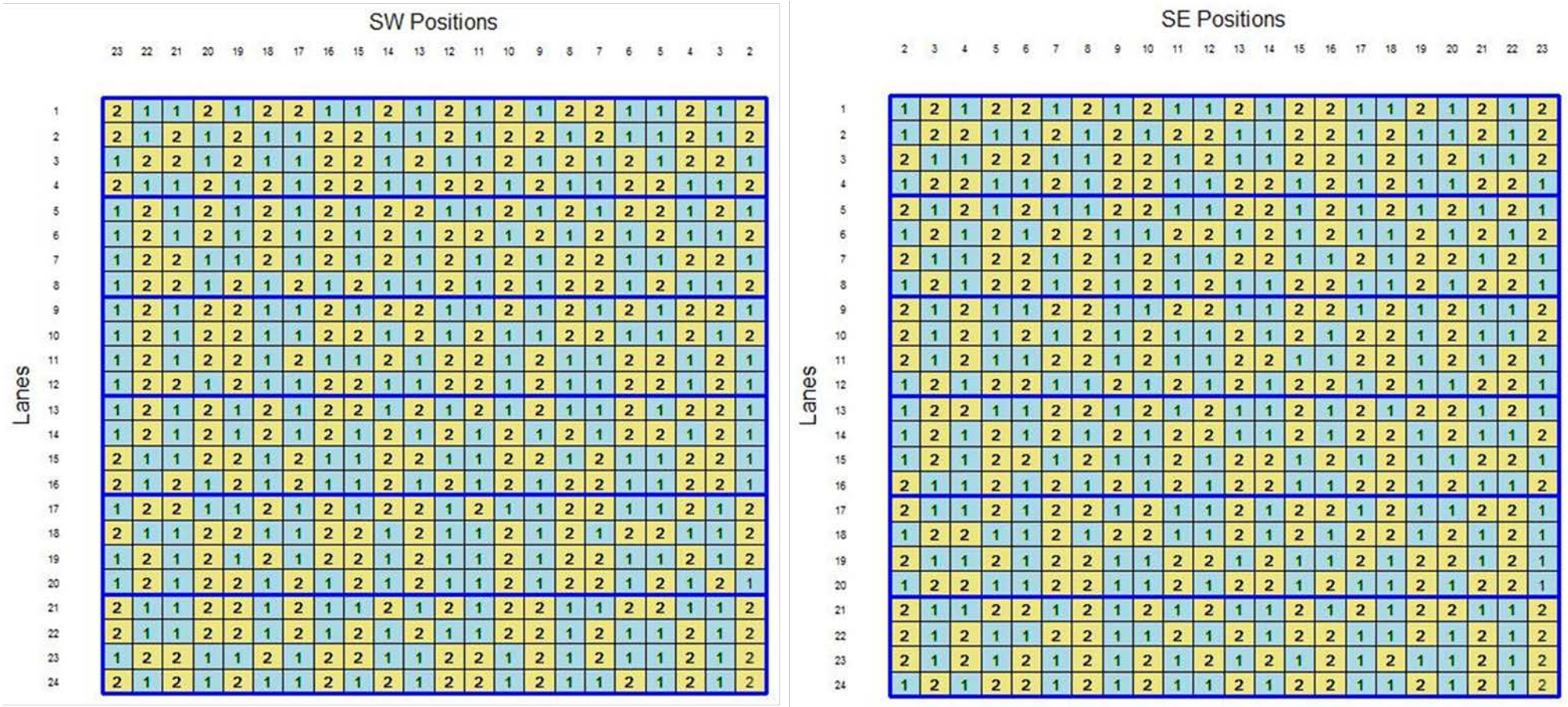

Figure S1: A split-plot design with unequally-replicated, nearly-trend-free main-plot design

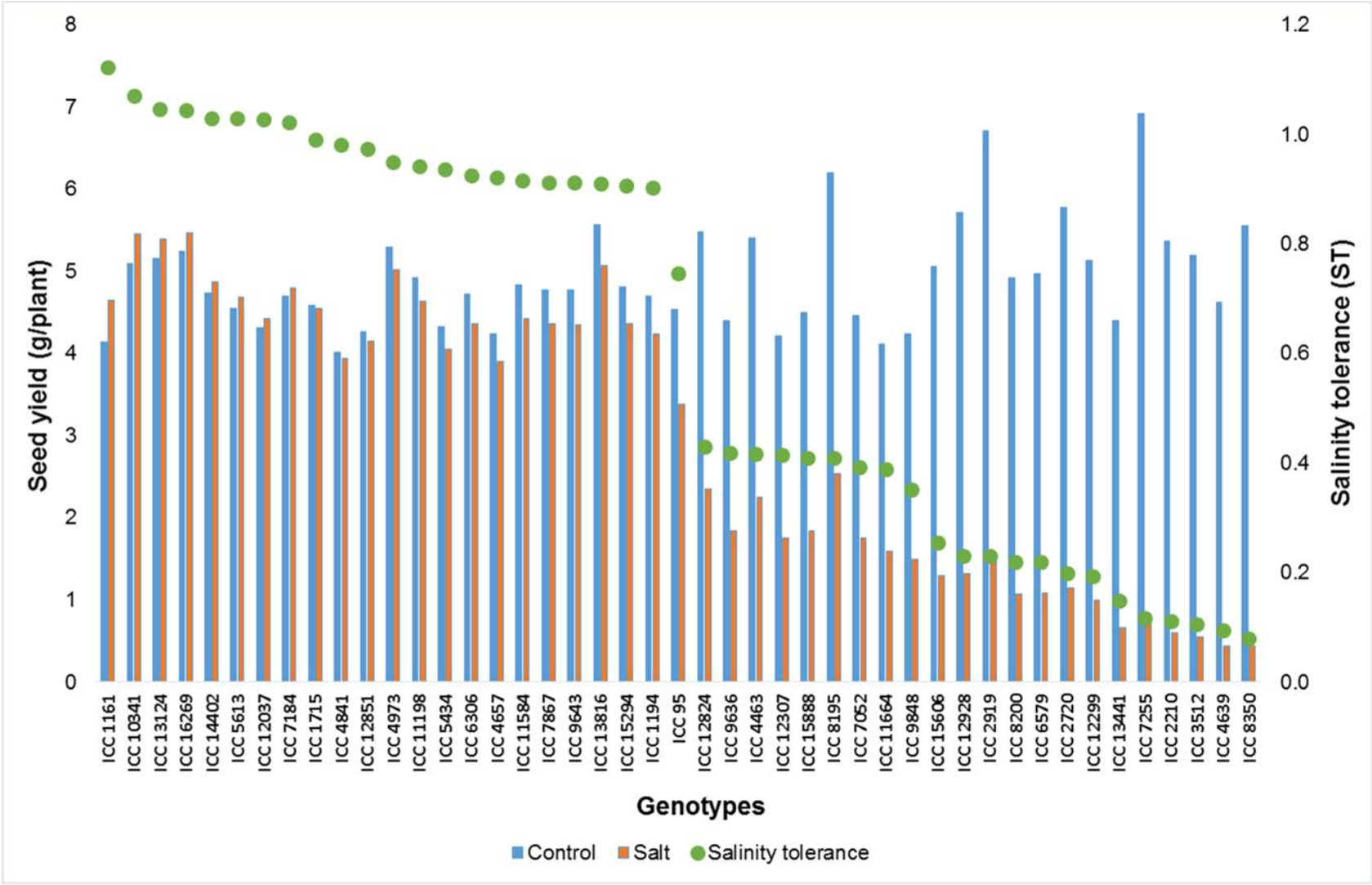

Figure S2: Genotypic variation for salinity tolerance in the chickpea reference set. Genotypes ranking from the most salt tolerant to salt sensitive based on salinity tolerance (seed yield under salinity/seed yield under non-saline conditions).

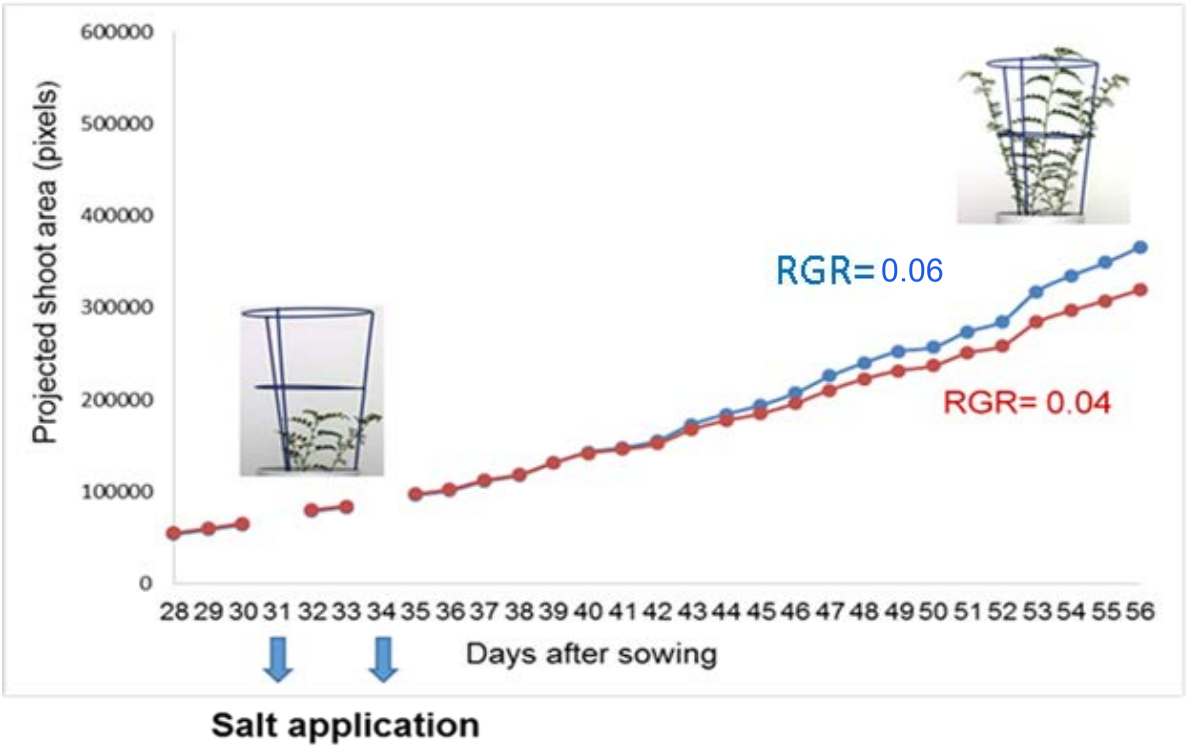

Figure S3: Non-destructive imaging of chickpea plants to determine average growth rate of all genotypes over time under 0 (blue line) and 40 mM NaCl (red line). Plant growth is demonstrated by increments in projected shoot area (pixels) over time. Salt application was done in two equal increments at 31 DAS and 34 DAS and the plants were imaged daily up to 56 DAS to evaluate the effect of salt application on growth of the plants. RGR (relative growth rate) was obtained by taking the difference between the logarithms of the smoothed projected shoot area for 32 DAS and 56 DAS and then dividing by 24. Inset pictures show RGB image of a chickpea plant at 31 DAS and 56 DAS.

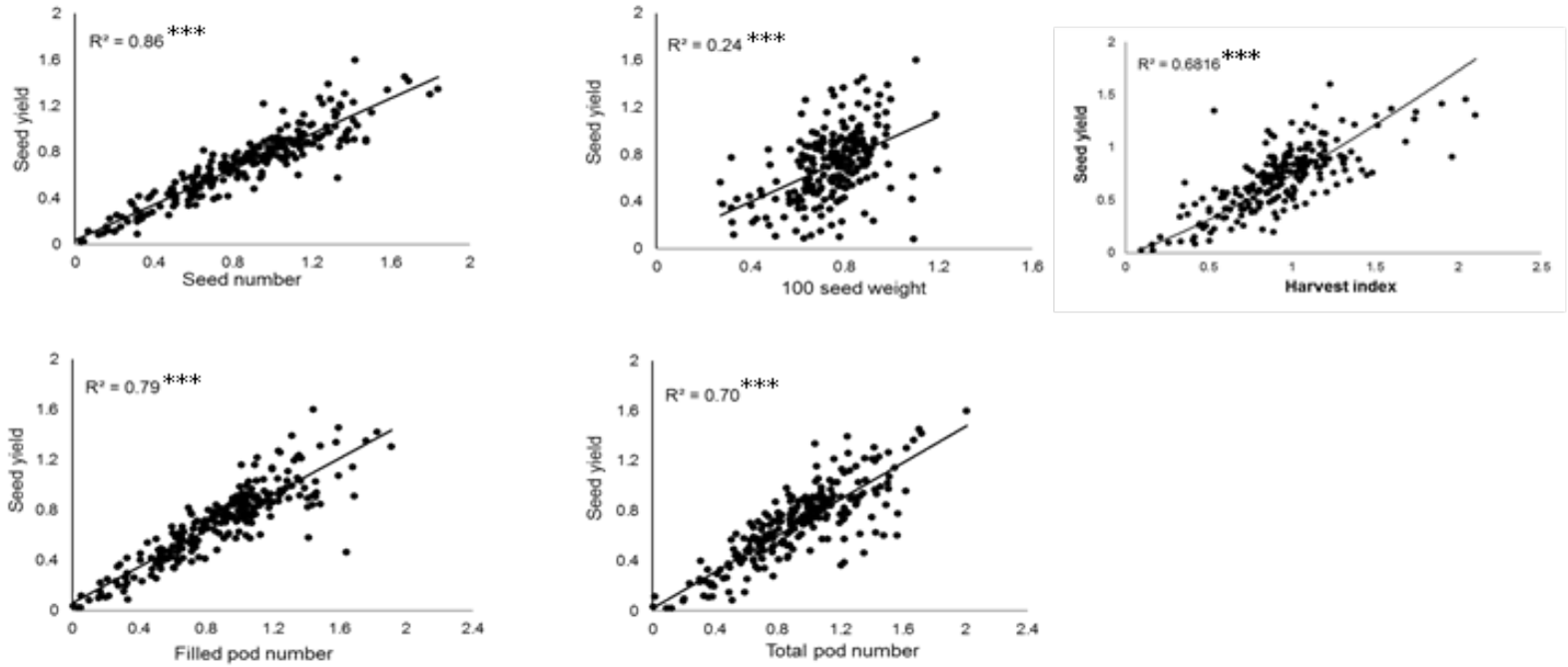

Figure S4: Relationship between seed yield and seed number, 100-seed weight, harvest index, filled pod number and total pod number. These are relative measurements (salt/control) per plant. Level of significance; ***= $p < 0.001$ ** =$p < 0.01$ *= $p < 0.05$

Table S1: Composition of the chickpea reference set

Genotype	Origin	Biological status	Market type
ICC 10018	India	Landrace	Desi
ICC 10341	Turkey	Landrace	Pea-shaped
ICC 10393	India	Landrace	Desi
ICC 10399	India	Landrace	Desi
ICC 1052	Pakistan	Landrace	Desi
ICC 10673	Turkey	Landrace	Desi
ICC 10685	Turkey	Landrace	Desi
ICC 10755	Turkey	Landrace	Kabuli
ICC 1083	Iran	Landrace	Desi
ICC 10885	Ethiopia	Landrace	Kabuli
ICC 10945	India	Landrace	Desi
ICC 1098	Iran	Landrace	Desi
ICC 11121	India	Landrace	Desi
ICC 11198	India	Landrace	Desi
ICC 11279	Pakistan	Landrace	Desi
ICC 11284	USSR	Landrace	Desi
ICC 11303	Chile	Landrace	Kabuli
ICC 11498	India	Breeding material	Desi
ICC 11584	India	Landrace	Desi
ICC 1161	Pakistan	Landrace	Desi
ICC 11627	India	Landrace	Desi
ICC 1164	Nigeria	Landrace	Desi
ICC 11664	India	Landrace	Desi
ICC 11764	Chile	Landrace	Kabuli
ICC 1180	India	Landrace	Desi
ICC 11879	Turkey	Landrace	Kabuli
ICC 11903	Germany	Landrace	Desi
ICC 1194	India	Landrace	Desi
ICC 11944	Nepal	Landrace	Desi
ICC 12028	Mexico	Landrace	Desi
ICC 12037	Mexico	Breeding material	Kabuli
ICC 1205	India	Landrace	Desi
ICC 12155	Bangladesh	Landrace	Desi
ICC 12299	Nepal	Landrace	Desi
ICC 1230	India	Landrace	Desi
ICC 12307	Myanmar	Landrace	Desi
ICC 12328	Cyprus	Landrace	Kabuli
ICC 12379	Iran	Landrace	Desi
ICC 12492	India	Landrace	Kabuli
ICC 12537	Ethiopia	Landrace	Desi
ICC 12654	Ethiopia	Landrace	Desi
ICC 12726	Ethiopia	Landrace	Desi
ICC 12824	Ethiopia	Landrace	Desi
ICC 12851	Ethiopia	Landrace	Desi
ICC 12866	Ethiopia	Landrace	Desi
ICC 12916	India	Landrace	Desi
ICC 12928	India	Landrace	Desi
ICC 12947	India	Landrace	Desi

ICC 13077	India	Landrace	Kabuli
ICC 13124	India	Landrace	Desi
ICC 13187	Iran	Breeding material	Kabuli
ICC 13219	Iran	Landrace	Desi
ICC 13283	Iran	Landrace	Kabuli
ICC 13357	Iran	Landrace	Kabuli
ICC 13441	Iran	Landrace	Kabuli
ICC 13461	Iran	Landrace	Kabuli
ICC 13523	Iran	Landrace	Kabuli
ICC 13524	Iran	Landrace	Desi
ICC 1356	India	Landrace	Desi
ICC 13599	Iran	Landrace	Desi
ICC 13628	Iran	Landrace	Kabuli
ICC 13764	Iran	Landrace	Kabuli
ICC 13816	USSR	Landrace	Kabuli
ICC 13863	Ethiopia	Landrace	Desi
ICC 1392	India	Landrace	Desi
ICC 1397	India	Landrace	Desi
ICC 1398	India	Landrace	Desi
ICC 14051	Ethiopia	Landrace	Desi
ICC 14077	Ethiopia	Landrace	Desi
ICC 14098	Ethiopia	Landrace	Desi
ICC 14199	Mexico	Breeding material	Kabuli
ICC 1431	India	Landrace	Desi
ICC 14402	India	Breeding material	Desi
ICC 14595	India	Landrace	Desi
ICC 14669	India	Landrace	Desi
ICC 14778	India	Landrace	Desi
ICC 14799	India	Landrace	Desi
ICC 14815	India	Landrace	Desi
ICC 14831	India	Landrace	Desi
ICC 1510	India	Landrace	Desi
ICC 15248	Iran	Landrace	Desi
ICC 15294	Iran	Landrace	Desi
ICC 15406	Morocco	Landrace	Kabuli
ICC 15435	Morocco	Landrace	Kabuli
ICC 15510	Morocco	Landrace	Desi
ICC 15518	Morocco	Landrace	Kabuli
ICC 15567	India	Breeding material	Desi
ICC 15606	India	Landrace	Desi
ICC 15610	India	Landrace	Desi
ICC 15612	Tanzania	Landrace	Desi
ICC 15614	Tanzania	Landrace	Desi
ICC 15618	India	Landrace	Desi
ICC 15697	Syria	Landrace	Kabuli
ICC 15762	Syria	Landrace	Desi
ICC 15785	Syria	Landrace	Desi
ICC 15802	Syria	Landrace	Kabuli
ICC 15868	India	Landrace	Desi
ICC 15888	India	Landrace	Pea-shaped
ICC 16207	Myanmar	Landrace	Desi

ICC 16261	Malawi	Landrace	Desi
ICC 16269	Malawi	Landrace	Desi
ICC 16374	Malawi	Breeding material	Desi
ICC 16524	Pakistan	Landrace	Desi
ICC 16654	China	Landrace	Kabuli
ICC 16796	Portugal	Landrace	Kabuli
ICC 16903	India	Landrace	Desi
ICC 16915	India	Landrace	Desi
ICC 1710	India	Landrace	Desi
ICC 1715	India	Landrace	Desi
ICC 1882	India	Landrace	Desi
ICC 1915	India	Landrace	Desi
ICC 1923	India	Landrace	Desi
ICC 2065	India	Landrace	Desi
ICC 2072	India	Landrace	Desi
ICC 2210	Algeria	Landrace	Desi
ICC 2242	India	Landrace	Desi
ICC 2263	Iran	Landrace	Desi
ICC 2277	Iran	Landrace	Kabuli
ICC 2482	Iran	Landrace	Kabuli
ICC 2507	Iran	Landrace	Desi
ICC 2580	Iran	Landrace	Desi
ICC 2593	Iran	Landrace	Kabuli
ICC 2629	Iran	Landrace	Desi
ICC 2720	Iran	Landrace	Desi
ICC 2737	Iran	Landrace	Desi
ICC 283	India	Landrace	Desi
ICC 2884	Iran	Landrace	Desi
ICC 2919	Iran	Landrace	Desi
ICC 2969	Iran	Landrace	Desi
ICC 2990	Iran	Landrace	Desi
ICC 3218	Iran	Landrace	Desi
ICC 3230	Iran	Landrace	Desi
ICC 3239	Iran	Landrace	Desi
ICC 3325	Cyprus	Landrace	Desi
ICC 3362	Iran	Landrace	Desi
ICC 3391	Iran	Landrace	Desi
ICC 3410	Iran	Landrace	Kabuli
ICC 3421	Israel	Landrace	Kabuli
ICC 3512	Iran	Landrace	Desi
ICC 3582	Iran	Landrace	Desi
ICC 3631	Iran	Landrace	Desi
ICC 3761	Iran	Landrace	Desi
ICC 3776	Iran	Landrace	Desi
ICC 3946	Iran	Landrace	Desi
ICC 4093	Iran	Landrace	Desi
ICC 4182	Iran	Landrace	Desi
ICC 4363	Iran	Landrace	Desi
ICC 440	India	Landrace	Desi
ICC 4418	Iran	Landrace	Desi
ICC 4463	Iran	Landrace	Desi

ICC 4495	Turkey	Landrace	Desi
ICC 4533	India	Landrace	Desi
ICC 456	India	Landrace	Desi
ICC 4567	India	Landrace	Desi
ICC 4593	India	Landrace	Desi
ICC 4639	India	Landrace	Desi
ICC 4657	India	Landrace	Desi
ICC 4814	Iran	Landrace	Desi
ICC 4841	Morocco	Landrace	Kabuli
ICC 4872	India	Landrace	Pea-shaped
ICC 4918	India	Advanced cultivar	Desi
ICC 4991	India	Advanced cultivar	Desi
ICC 506	India	Landrace	Desi
ICC 5135	India	Breeding material	Desi
ICC 5221	India	Breeding material	Desi
ICC 5337	India	Landrace	Kabuli
ICC 5383	India	Landrace	Desi
ICC 5434	India	Landrace	Desi
ICC 5504	Mexico	Landrace	Desi
ICC 5613	India	Landrace	Desi
ICC 5639	India	Landrace	Desi
ICC 5845	India	Landrace	Desi
ICC 5878	India	Landrace	Desi
ICC 6263	Union of Soviet Socialist Republics	Landrace	Kabuli
ICC 6279	India	Landrace	Desi
ICC 6293	Italy	Landrace	Desi
ICC 6294	Iran	Advanced cultivar	Desi
ICC 6306	Union of Soviet Socialist Republics	Advanced cultivar	Desi
ICC 637	India	Landrace	Desi
ICC 6537	Iran	Breeding material	Desi
ICC 6571	Iran	Landrace	Desi
ICC 6579	Iran	Landrace	Desi
ICC 67	India	Landrace	Desi
ICC 6802	Iran	Landrace	Desi
ICC 6811	Iran	Landrace	Desi
ICC 6816	Iran	Landrace	Desi
ICC 6874	Iran	Landrace	Desi
ICC 6875	Iran	Landrace	Desi
ICC 6877	Iran	Landrace	Desi
ICC 7052	Iran	Landrace	Desi
ICC 708	India	Landrace	Desi
ICC 7150	Turkey	Landrace	Desi
ICC 7184	Turkey	Landrace	Desi
ICC 7255	India	Landrace	Kabuli
ICC 7272	Algeria	Landrace	Kabuli
ICC 7305	Afghanistan	Landrace	Desi
ICC 7308	Peru	Landrace	Kabuli
ICC 7315	Iran	Landrace	Kabuli
ICC 7323	USSR	Landrace	Pea-shaped
ICC 7413	India	Landrace	Pea-shaped
ICC 7441	India	Landrace	Desi

ICC 7554	Iran	Landrace	Desi
ICC 7571	Israel	Landrace	Kabuli
ICC 762	India	Landrace	Desi
ICC 7668	USSR	Landrace	Kabuli
ICC 7819	Iran	Landrace	Desi
ICC 7867	Iran	Landrace	Desi
ICC 791	India	Landrace	Desi
ICC 8151	USA	Landrace	Kabuli
ICC 8195	Pakistan	Landrace	Desi
ICC 8200	Iran	Landrace	Desi
ICC 8261	Turkey	Landrace	Kabuli
ICC 8318	India	Landrace	Desi
ICC 8350	India	Landrace	Pea-shaped
ICC 8384	India	Landrace	Desi
ICC 8515	Greece	Landrace	Desi
ICC 8522	Italy	Landrace	Desi
ICC 8621	Ethiopia	Landrace	Desi
ICC 867	India	Landrace	Desi
ICC 8718	Afghanistan	Landrace	Desi
ICC 8740	Afghanistan	Landrace	Kabuli
ICC 8752	Afghanistan	Landrace	Kabuli
ICC 8855	Afghanistan	Landrace	Kabuli
ICC 8950	India	Landrace	Desi
ICC 9002	Iran	Landrace	Desi
ICC 9137	Iran	Landrace	Kabuli
ICC 9402	Iran	Landrace	Kabuli
ICC 9434	Iran	Landrace	Kabuli
ICC 95	India	Landrace	Desi
ICC 9586	India	Landrace	Desi
ICC 9590	Egypt	Landrace	Desi
ICC 9636	Afghanistan	Landrace	Desi
ICC 9643	Afghanistan	Landrace	Desi
ICC 9712	Afghanistan	Landrace	Desi
ICC 9755	Afghanistan	Landrace	Desi
ICC 9848	Afghanistan	Landrace	Pea-shaped
ICC 9862	Afghanistan	Landrace	Pea-shaped
ICC 9872	Afghanistan	Landrace	Kabuli
ICC 9895	Afghanistan	Landrace	Pea-shaped
ICC 9942	India	Landrace	Desi

Table S2: **Relationship between traits measured under salinity determined by correlation analysis**. Highlighted, are moderate to high correlation coefficients. Level of significance (***=P<0.001, **=P<0.01, *=P<0.05, ns=non-significant)

Traits	Seed yield	Seed number	Shoot biomass	Total pods	Filled pods	Empty pods	100-seed weight	Plant height	Senescence score	RGR 32-56
Seed yield	1									
Seed number	**0.829*** **	1								
Shoot biomass	**0.679*** **	**0.48*** **	1							
Total pods	**0.657*** **	**0.796*** **	**0.538*** **	1						
Filled pods	**0.86*** **	**0.967*** **	**0.525*** **	**0.817*** **	1					
Empty pods	0.014 ns	0.115*	0.245**	**0.661*** **	0.108 ns	1				
100-seed weight	**0.499*** **	0.11*	**0.642*** **	0.099 ns	0.197*	-0.083 ns	1			
Plant height	**0.517*** **	**0.358*** **	**0.604*** **	**0.459*** **	**0.417*** **	0.247***	**0.463*** **	1		
Senescence score	-0.292**	-0.192*	-0.259**	-0.178*	-0.196*	-0.052 ns	**0.336*** **	**-0.349*** **	1	
RGR 32-56	**0.378*** **	**0.439*** **	**0.323*** **	**0.405*** **	**0.428*** **	0.142*	0.138*	0.258**	-0.179*	1

Table S3: **Relationship between traits measured under non-saline conditions determined by correlation analysis.** Highlighted, are moderate to high correlation coefficients. Level of significance (***=P<0.001, **=P<0.01, *=P<0.05, ns=non-significant).

Traits	Seed yield	Seed number	Shoot biomass	Total pods	Filled pods	Empty pods	100-seed weight	Plant height	Senescence score	RGR 32-56
Seed yield	1									
Seed number	**0.75*** **	1								
Shoot biomass	**0.392*** **	0.119*	1							
Total pods	**0.527*** **	**0.682*** **	0.215**	1						
Filled pods	**0.795*** **	**0.946*** **	0.187*	**0.751*** **	1					
Empty pods	-0.075 ns	-0.011 ns	0.124*	**0.684*** **	0.033 ns	1				
100-seed weight	0.169*	**-0.322*** **	**0.533*** **	-0.223**	-0.213**	-0.103*	1			
Plant height	0.211**	0.054 ns	**0.516*** **	0.199**	0.124*	0.163*	**0.337*** **	1		
Senescence score	0.065 ns	0.002 ns	-0.1*	0.036 ns	0.044 ns	0.001 ns	-0.067 ns	-0.202**	1	
RGR 32-56	0.208**	**0.32*** **	0.14*	0.274**	**0.312*** **	0.067 ns	-0.095 ns	0.051 ns	-0.089 ns	1

Table S4: Relationship between seed yield and sodium and potassium ions determined by correlation analysis. Highlighted, are moderate to high correlation coefficients. Level of significance (***=P<0.001, **=P<0.01, ns=non-significant).

	Na	K	K:Na	Seed yield
Na	1			
K	**0.52*** **	1		
K:Na	**-0.64*** **	-0.16 ns	1	
Seed yield	**-0.3** **	-0.19 ns	0.29**	1

Table S5: Direct and indirect effects of yield components on seed yield under non-saline conditions determined by partial least squares algorithm. Values in the main diagonal part (path coefficients) and off-diagonal part of the table represent direct and indirect effects of yield components on seed yield. Total effects which corresponds to correlation coefficients is derived from summing up direct and indirect effects. Highlighted are direct effects (bold), moderate indirect effects (underlined) as well as moderate to high total effects (underlined).

Traits	RGR 32-56	Plant height	Shoot biomass	Total pods	Filled pods	Seed number	100-seed weight	Senescence score	Total effects
RGR 32-56	***-0.041***	0	0.013	-0.024	0.157	0.145	-0.034	-0.006	0.208
Plant height	-0.002	***-0.009***	0.047	-0.018	0.062	0.024	0.121	-0.015	0.211
Shoot biomass	-0.006	-0.005	***0.091***	-0.019	0.094	0.054	0.191	-0.007	0.393
Total pods	-0.011	-0.002	0.02	***-0.089***	0.377	0.309	-0.08	0.003	0.526
Filled pods	-0.013	-0.001	0.017	-0.067	***0.502***	0.429	-0.076	0.003	0.794
Seed number	-0.013	0	0.011	-0.061	0.475	***0.453***	-0.115	0	0.749
100-seed weight	0.004	-0.003	0.049	0.02	-0.107	-0.146	***0.358***	-0.005	0.17
Senescence score	0.004	0.002	-0.009	-0.003	0.022	0.001	-0.024	***0.072***	0.064

Table S6: Direct and indirect effects of yield components on seed yield under salinity determined by partial least squares algorithm. Values in the main diagonal part (path coefficients) and off-diagonal part of the table represent direct and indirect effects of yield components on seed yield. Total effects which corresponds to correlation coefficients is derived from summing up direct and indirect effects. Highlighted are direct effects (bold), moderate indirect effects (underlined) as well as moderate to high total effects (underlined).

Traits	RGR 32-56	Plant height	Shoot biomass	Total pods	Filled pods	Seed number	100-seed weight	Senescence score
RGR 32-56	***-0.03***	0.013	0.038	-0.059	0.193	0.182	0.039	0.003
Plant height	-0.01	***0.049***	0.071	-0.067	0.188	0.148	0.129	0.005
Shoot biomass	-0.01	0.03	***0.118***	-0.079	0.237	0.199	0.179	0.004
Total pods	-0.01	0.022	0.063	***-0.146***	0.368	0.33	0.028	0.002
Filled pods	-0.01	0.02	0.062	-0.119	***0.451***	0.4	0.055	0.003
Seed number	-0.01	0.018	0.057	-0.116	0.436	***0.414***	0.031	0.003
100-seed weight	0	0.023	0.076	-0.014	0.089	0.046	***0.279***	0.005
Senescence score	0.005	-0.017	-0.031	0.026	-0.088	-0.079	-0.094	***-0.014***

Chapter 3: Supplementary

Supplementary data associated with this article can be found, in the online version, at http://dx.doi.org/10.1016/j.jchromb.2015.07.002

Chapter 4: Supplementary

PLOS

Quantifying the onset and progression of plant senescence by color image analysis for high throughput applications

Jinhai Cai, Mamoru Okamoto, Judith Atieno, Tim Sutton, Yongle Li, Stanley J. Miklavcic

S1 Appendix

Automated Plant Segmentation

The segmentation between plants and the background is a difficult task for many reasons, particularly the background is consisting of several objects in the greenhouse such as the pot and the supporting frame. The change of plant colors is the only constant thing during the whole life cycle of plants. It is expected that the color of senescent leaves will be similar to the color of pot rim, where the dirt on the pot rim is yellow as illustrated in S1 Fig(a). Clearly the color space of pot rims and that of plants are overlapped, thus significant segmentation error is inevitable if the segmentation algorithm is based on color analysis. However, this problem can be solved if we known the background.

The estimation of background

There are many algorithms developed for the estimation of background [1]. Most of them assume that the background is still and the foreground is moving. However, in this case, plants cannot move to other locations instead they are growing. These background estimation algorithms are not suitable for our experiments. The LemnaTec commercial software uses a pot with no plant in for background estimation. This approach is useful in reducing the segmentation error. However, pots are different from each other due to different labels and rim colors.

In all our experiments conducted in the greenhouse, plants are very young and green on the first imaging day. This allow us to estimate the background by removing green areas and replacing with surrounding background in the images from the first imaging days. In some experiments, a blue frame is used to support the plant in a pot from falling. The position of a blue frame in a pot can be changed by the plant during its life cycle, so it is not treated as a part of the background. We use the same way to remove the frame by replacing blue areas with surrounding background. S1 Fig(b) shows an example of the background estimation.

S1 Fig. The estimation of the background. (a) is the original image; and (b) is the estimated background.

The segmentation

With the estimated background, it is common to segment the foreground by subtracting the background and then thresholding. In the greenhouse, the convey system sends the pot to almost the same location for imaging. However, there is a small disparity, which result in a small shift of the pot in the image. In order to handle the small shift, we calculate the modified difference between the image and the estimated background and then apply the thresholding. The modified difference is defined as

$$d_m(x,y) = min_{i=-t,j=-t}^{i=t,j=t} |I(x,y) - B(x+i,y+j)|, \tag{S1}$$

where $I(x, y)$ is the pixel of the image at (x, y), $B(x, y)$ is the pixel of the estimated background at (x, y) and t is a value for the small shift in images. S2 Fig shows an example of the segmentation results. The segmentation results are pretty good but not perfect as very small areas of the blue frame are segmented as plants.

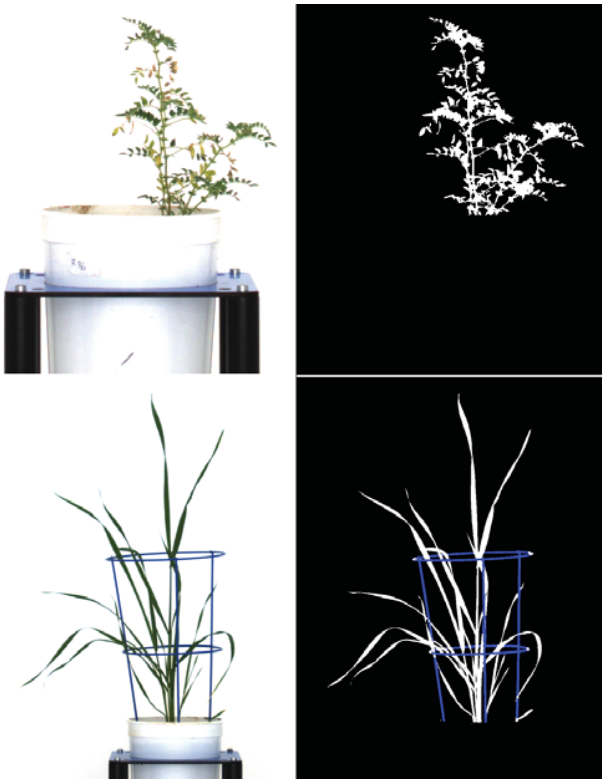

S2 Fig. The image segmentation. Left images are the original images and right images are the segmented images, where the parts in blue color are the blue frames.

Color Classification

The color classification is relatively straightforward. We selected two segmented images of plants, one at a relatively early growth stage so that most leaves are with dark green and light green color and another plant with significant senescence so that some leaves

are with light yellow color and some leaves (dead leaves) are with brown color. We labelled these two images with four color categories. The color classification can be conducted by the k-Nearest Neighbours (kNN) algorithm [2]. In order to reduce the computational cost, we apply the k-means clustering algorithm [3] to form clusters and we use the cluster centres instead of directly using pixels in the labelled images as color feature points in the kNN algorithm. In our experiments, the number of color clusters for plants is set to 18 as there is no visible difference from using the two labelled images directly. At the same time, the computational cost is significantly reduced.

References

1. Sobral A, Vacavant A. A comprehensive review of background subtraction algorithms evaluated with synthetic and real videos. Computer Vision and Image Understanding. 2014;122:4 – 21.

2. Altman NS. An introduction to kernel and nearest-neighbor nonparametric regression. The American Statistician. 1992;46(3):175–185.

3. Kanungo T, Mount DM, Netanyahu NS, Piatko CD, Silverman R, Wu AY. An efficient k-means clustering algorithm: Analysis and implementation. IEEE Transactions on Pattern Analysis and Machine Intelligence. 2002;24:881–892.

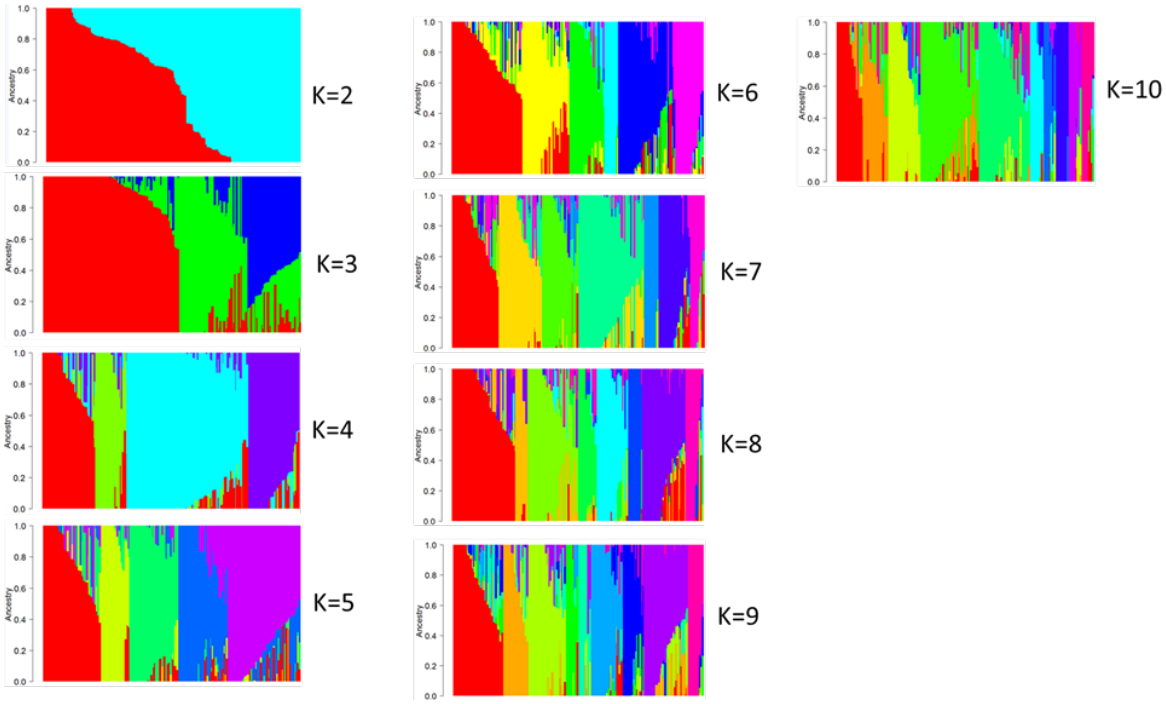

Figure S1: Population structure among genotypes in the chickpea Reference Set using SNP markers. Structure of sub-populations at K values ranging from 2-10.

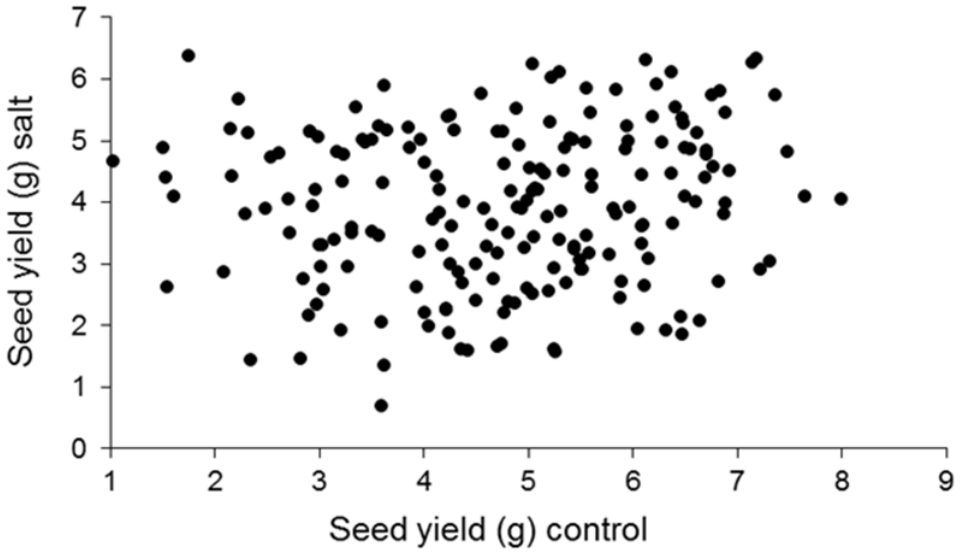

Figure S2: Relationship between seed yield under salt (70 mM NaCl) and seed yield under control conditions. Seed yield measurement is on pot basis.

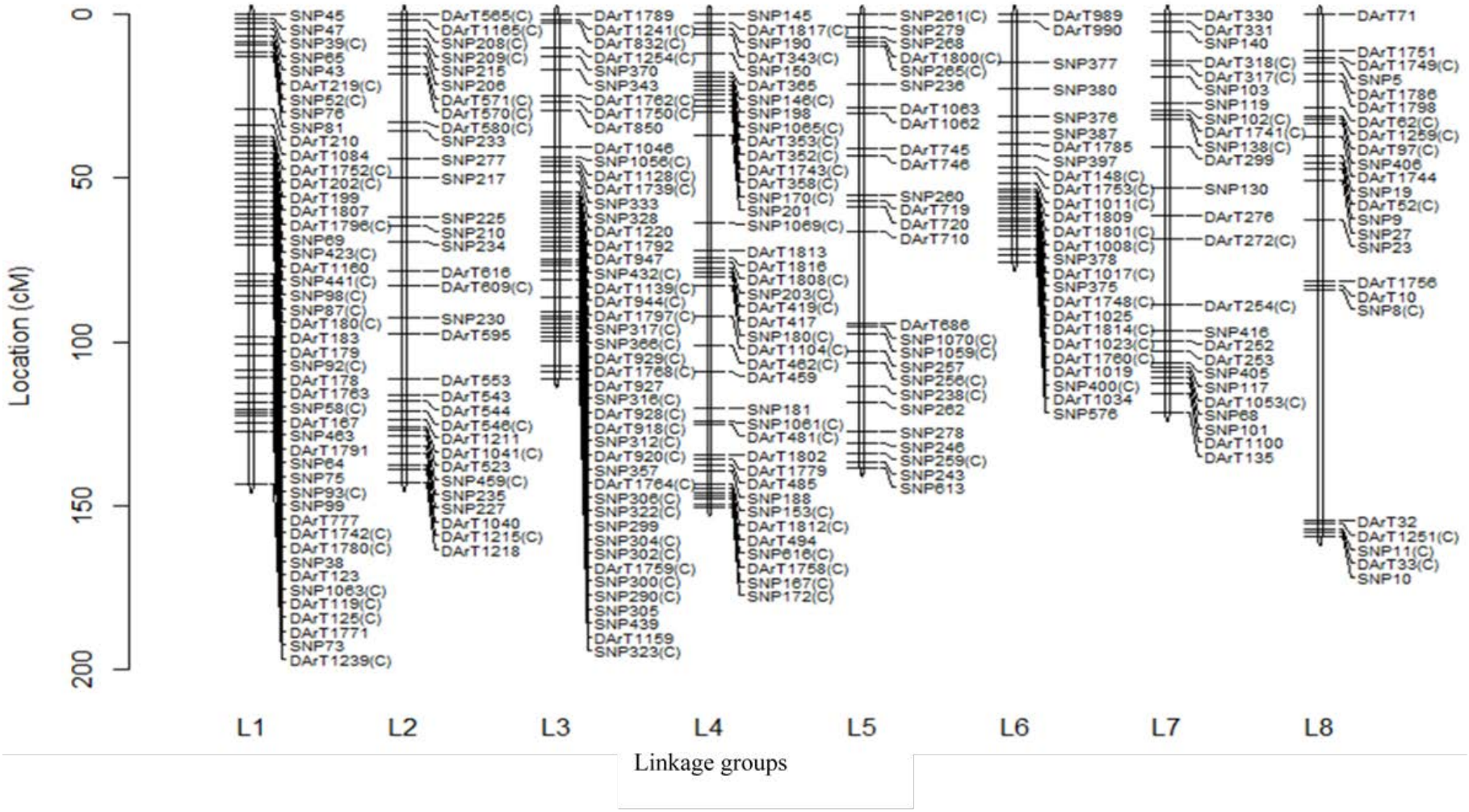

Figure S3: Rupali/Genesis836 genetic linkage map. 614 SNP and DArT polymorphic markers were used to construct the map based on recombination frequencies. Genetic distances are indicated as centimorgan (cM) on the y-axis while linkage groups are indicated on the x-axis of the genetic map.

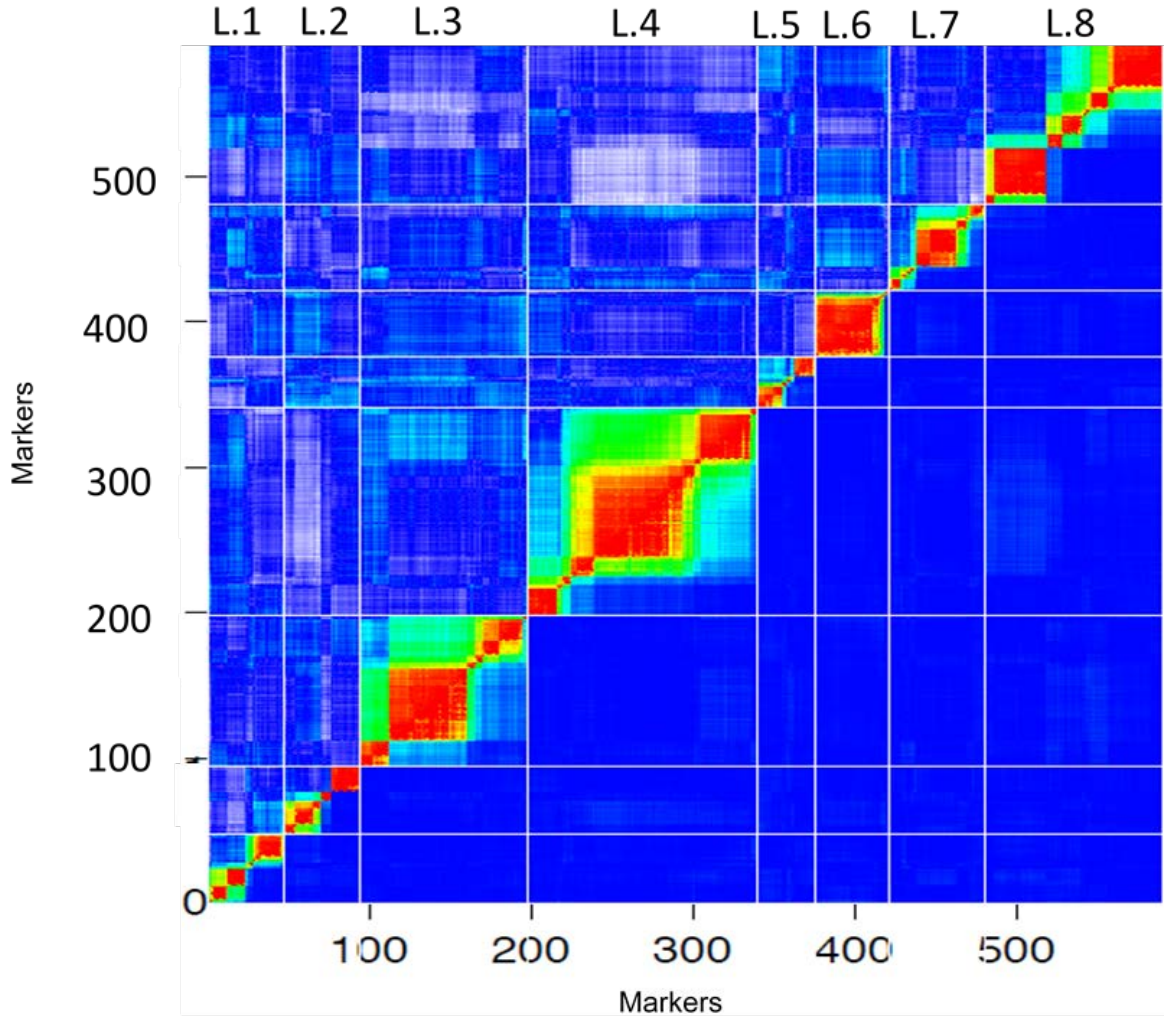

Figure S4: Heat-plot for Rupali/Genesis836 genetic map with 614 polymorphic markers (SNP and DArT). Upper left of the figure represent recombination fractions while lower right of the figure represent LOD scores for linkage for all pairs non-redundant polymorphic markers used in map construction. Markers are arranged in order of linkage groups (L.1- L.8). The colour series indicate the strength of linkage with red indicating high LOD score and lower recombination fraction while the opposite is true for blue color. Correct marker order is indicated by red signals aligning along the diagonal of the figure.

OST 32-56

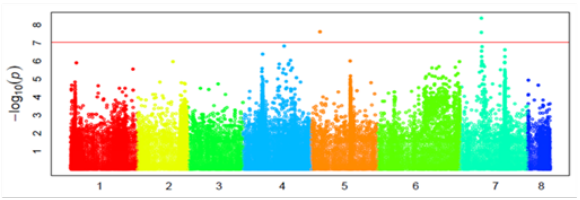

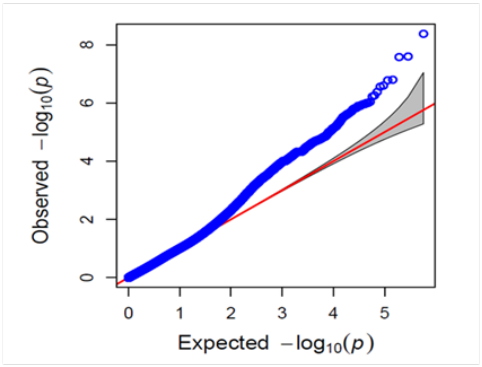

RGR 32-56

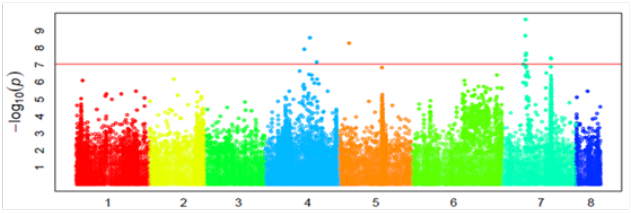

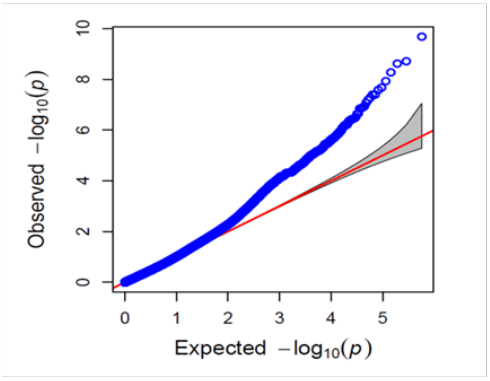

OST 41-50

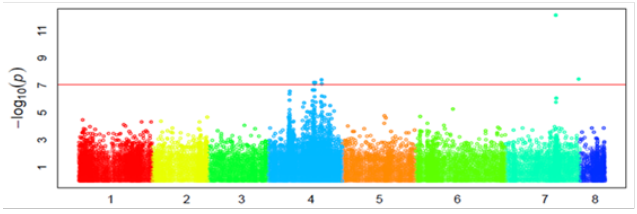

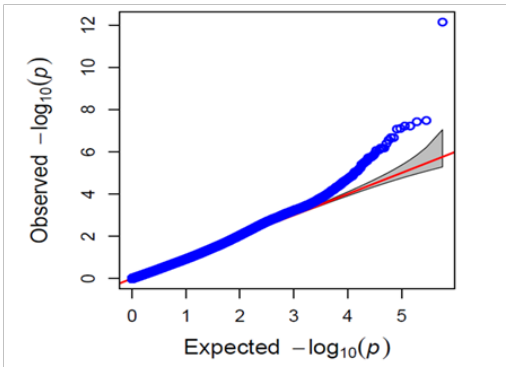

Projected shoot area ratio

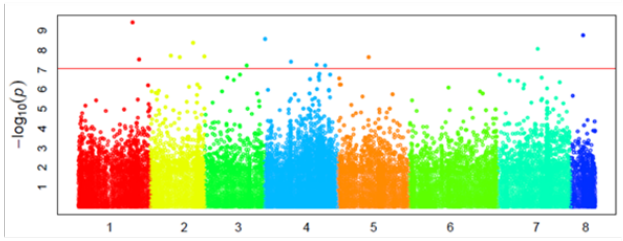

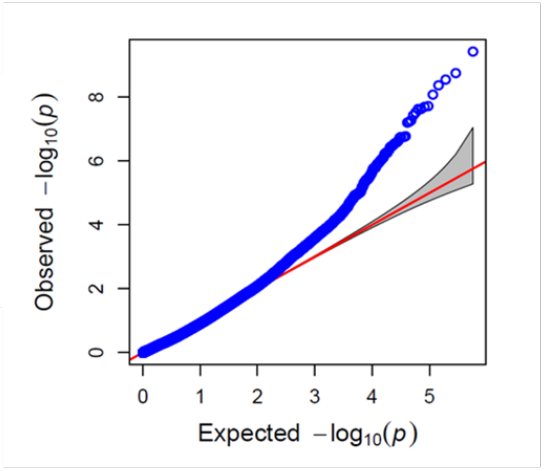

Harvest index

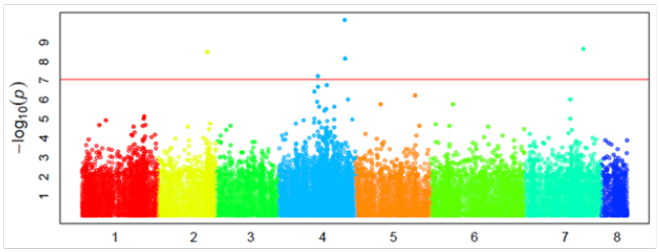

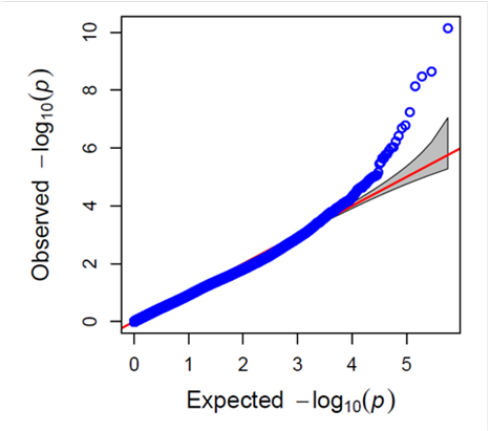

Harvest index ratio

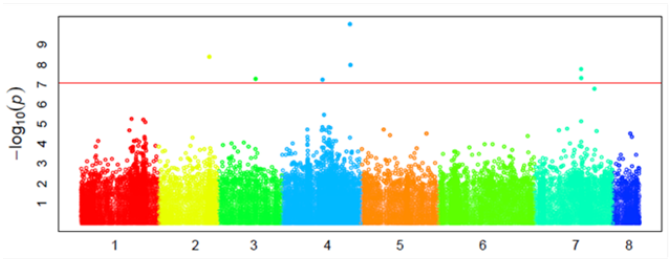

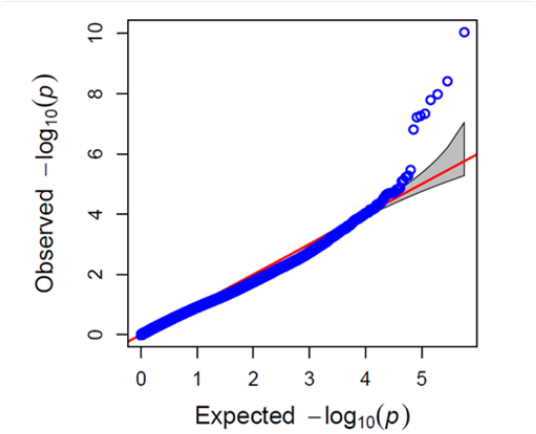

Sodium ions ratio

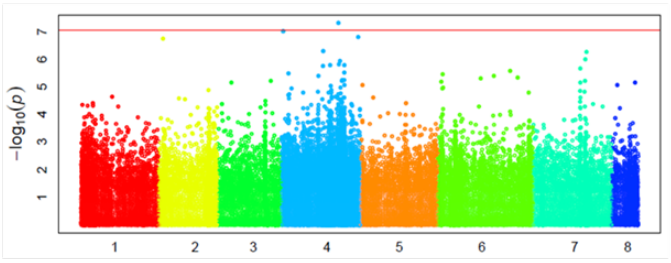

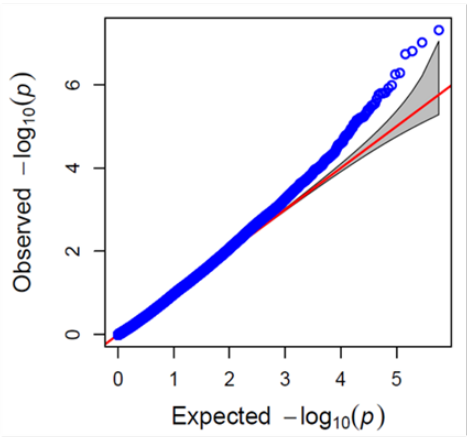

Potassium ions ratio

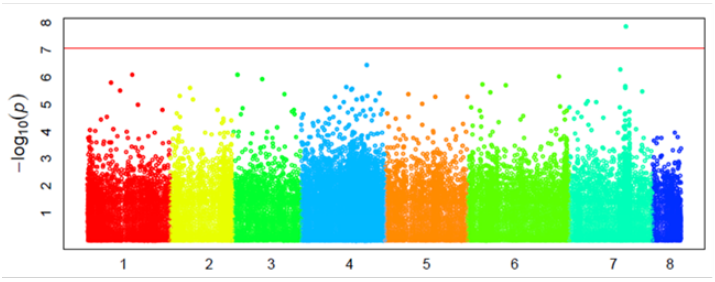

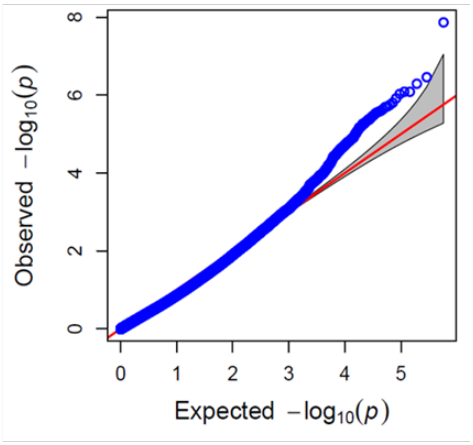

Na:K

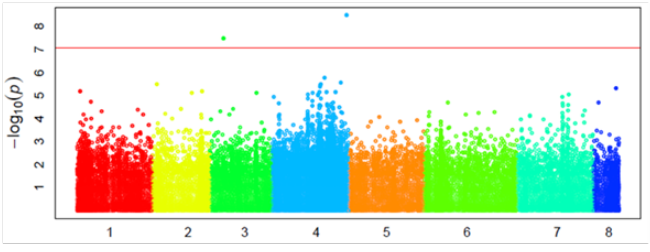

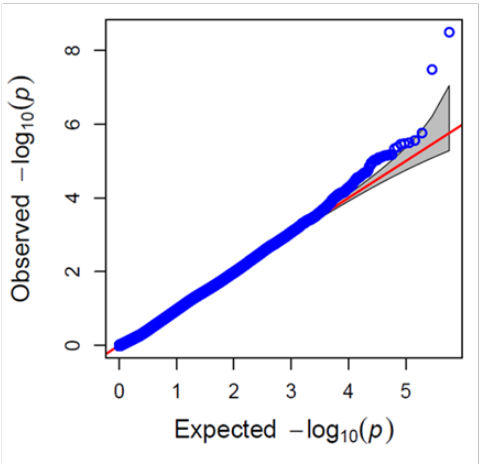

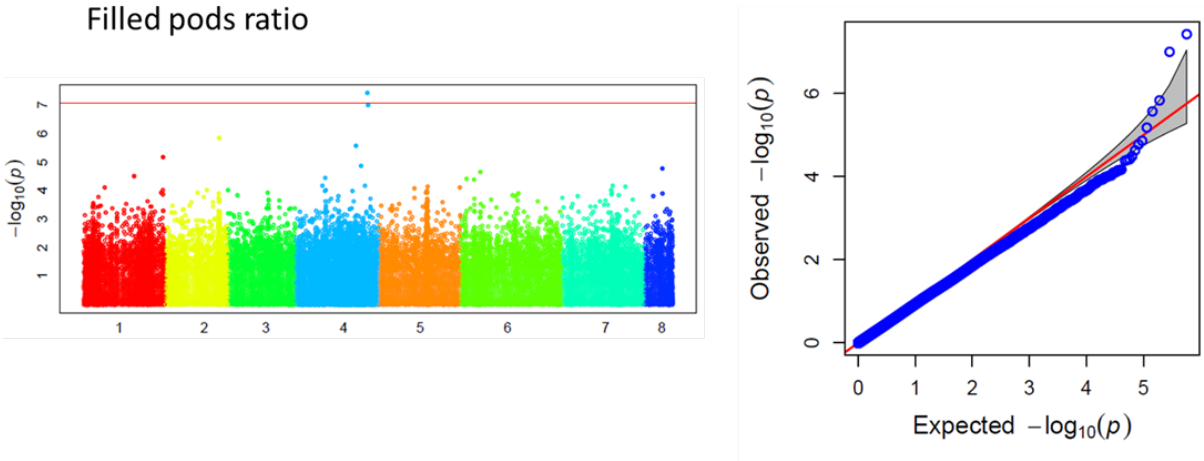

Figure S5: Manhattan plots showing significant marker-trait associations for salt tolerance related traits. Different colours indicate 8 chromosomes present in chickpea. SNPs above threshold set by 5% applied to Bonferroni correction (red line), Alpha threshold of 9.0×10^{-8}, are considered to be significantly associated with trait under analysis. Q-Q plot for the test statistic expected vs. observed show the suitability of MLM employing Q+K matrices to control false positives. True positives are enriched in tail.

Table S1: Information on association mapping panel used in the study.

Genotype	Origin	Biological classification	Market type
ICC 10018	India	Landrace	Desi
ICC 10341	Turkey	Landrace	Pea-shaped
ICC 10393	India	Landrace	Desi
ICC 10399	India	Landrace	Desi
ICC 1052	Pakistan	Landrace	Desi
ICC 10673	Turkey	Landrace	Desi
ICC 10685	Turkey	Landrace	Desi
ICC 10755	Turkey	Landrace	Kabuli
ICC 1083	Iran	Landrace	Desi
ICC 10885	Ethiopia	Landrace	Kabuli
ICC 10945	India	Landrace	Desi
ICC 1098	Iran	Landrace	Desi
ICC 11121	India	Landrace	Desi
ICC 11198	India	Landrace	Desi
ICC 11279	Pakistan	Landrace	Desi
ICC 11284	USSR	Landrace	Desi
ICC 11303	Chile	Landrace	Kabuli
ICC 11498	India	Breeding material	Desi
ICC 11584	India	Landrace	Desi
ICC 1161	Pakistan	Landrace	Desi
ICC 11627	India	Landrace	Desi
ICC 1164	Nigeria	Landrace	Desi
ICC 11664	India	Landrace	Desi
ICC 11764	Chile	Landrace	Kabuli
ICC 1180	India	Landrace	Desi
ICC 11879	Turkey	Landrace	Kabuli
ICC 11903	Germany	Landrace	Desi
ICC 1194	India	Landrace	Desi

ICC 11944	Nepal	Landrace	Desi
ICC 12028	Mexico	Landrace	Desi
ICC 12037	Mexico	Breeding material	Kabuli
ICC 1205	India	Landrace	Desi
ICC 12155	Bangladesh	Landrace	Desi
ICC 12299	Nepal	Landrace	Desi
ICC 1230	India	Landrace	Desi
ICC 12307	Myanmar	Landrace	Desi
ICC 12328	Cyprus	Landrace	Kabuli
ICC 12379	Iran	Landrace	Desi
ICC 12492	India	Landrace	Kabuli
ICC 12537	Ethiopia	Landrace	Desi
ICC 12654	Ethiopia	Landrace	Desi
ICC 12726	Ethiopia	Landrace	Desi
ICC 12824	Ethiopia	Landrace	Desi
ICC 12851	Ethiopia	Landrace	Desi
ICC 12866	Ethiopia	Landrace	Desi
ICC 12916	India	Landrace	Desi
ICC 12928	India	Landrace	Desi
ICC 12947	India	Landrace	Desi
ICC 13077	India	Landrace	Kabuli
ICC 13124	India	Landrace	Desi
ICC 13187	Iran	Breeding material	Kabuli
ICC 13219	Iran	Landrace	Desi
ICC 13283	Iran	Landrace	Kabuli
ICC 13357	Iran	Landrace	Kabuli
ICC 13441	Iran	Landrace	Kabuli
ICC 13461	Iran	Landrace	Kabuli
ICC 13523	Iran	Landrace	Kabuli
ICC 13524	Iran	Landrace	Desi
ICC 1356	India	Landrace	Desi
ICC 13599	Iran	Landrace	Desi
ICC 13628	Iran	Landrace	Kabuli
ICC 13764	Iran	Landrace	Kabuli
ICC 13816	USSR	Landrace	Kabuli
ICC 13863	Ethiopia	Landrace	Desi
ICC 1392	India	Landrace	Desi
ICC 1397	India	Landrace	Desi
ICC 1398	India	Landrace	Desi
ICC 14051	Ethiopia	Landrace	Desi
ICC 14077	Ethiopia	Landrace	Desi
ICC 14098	Ethiopia	Landrace	Desi
ICC 14199	Mexico	Breeding material	Kabuli
ICC 1431	India	Landrace	Desi
ICC 14402	India	Breeding material	Desi
ICC 14595	India	Landrace	Desi
ICC 14669	India	Landrace	Desi
ICC 14778	India	Landrace	Desi
ICC 14799	India	Landrace	Desi
ICC 14815	India	Landrace	Desi
ICC 14831	India	Landrace	Desi
ICC 1510	India	Landrace	Desi
ICC 15248	Iran	Landrace	Desi
ICC 15294	Iran	Landrace	Desi
ICC 15406	Morocco	Landrace	Kabuli
ICC 15435	Morocco	Landrace	Kabuli

ICC 15510	Morocco	Landrace	Desi
ICC 15518	Morocco	Landrace	Kabuli
ICC 15567	India	Breeding material	Desi
ICC 15606	India	Landrace	Desi
ICC 15610	India	Landrace	Desi
ICC 15612	Tanzania	Landrace	Desi
ICC 15614	Tanzania	Landrace	Desi
ICC 15618	India	Landrace	Desi
ICC 15697	Syria	Landrace	Kabuli
ICC 15762	Syria	Landrace	Desi
ICC 15785	Syria	Landrace	Desi
ICC 15802	Syria	Landrace	Kabuli
ICC 15868	India	Landrace	Desi
ICC 15888	India	Landrace	Pea-shaped
ICC 16207	Myanmar	Landrace	Desi
ICC 16261	Malawi	Landrace	Desi
ICC 16269	Malawi	Landrace	Desi
ICC 16374	Malawi	Breeding material	Desi
ICC 16524	Pakistan	Landrace	Desi
ICC 16654	China	Landrace	Kabuli
ICC 16796	Portugal	Landrace	Kabuli
ICC 16903	India	Landrace	Desi
ICC 16915	India	Landrace	Desi
ICC 1710	India	Landrace	Desi
ICC 1715	India	Landrace	Desi
ICC 1882	India	Landrace	Desi
ICC 1915	India	Landrace	Desi
ICC 1923	India	Landrace	Desi
ICC 2065	India	Landrace	Desi
ICC 2072	India	Landrace	Desi
ICC 2210	Algeria	Landrace	Desi
ICC 2242	India	Landrace	Desi
ICC 2263	Iran	Landrace	Desi
ICC 2277	Iran	Landrace	Kabuli
ICC 2482	Iran	Landrace	Kabuli
ICC 2507	Iran	Landrace	Desi
ICC 2580	Iran	Landrace	Desi
ICC 2593	Iran	Landrace	Kabuli
ICC 2629	Iran	Landrace	Desi
ICC 2720	Iran	Landrace	Desi
ICC 2737	Iran	Landrace	Desi
ICC 283	India	Landrace	Desi
ICC 2884	Iran	Landrace	Desi
ICC 2919	Iran	Landrace	Desi
ICC 2969	Iran	Landrace	Desi
ICC 2990	Iran	Landrace	Desi
ICC 3218	Iran	Landrace	Desi
ICC 3230	Iran	Landrace	Desi
ICC 3239	Iran	Landrace	Desi
ICC 3325	Cyprus	Landrace	Desi
ICC 3362	Iran	Landrace	Desi
ICC 3391	Iran	Landrace	Desi
ICC 3410	Iran	Landrace	Kabuli
ICC 3421	Israel	Landrace	Kabuli
ICC 3512	Iran	Landrace	Desi
ICC 3582	Iran	Landrace	Desi

ICC 3631	Iran	Landrace	Desi
ICC 3761	Iran	Landrace	Desi
ICC 3776	Iran	Landrace	Desi
ICC 3946	Iran	Landrace	Desi
ICC 4093	Iran	Landrace	Desi
ICC 4182	Iran	Landrace	Desi
ICC 4363	Iran	Landrace	Desi
ICC 440	India	Landrace	Desi
ICC 4418	Iran	Landrace	Desi
ICC 4463	Iran	Landrace	Desi
ICC 4495	Turkey	Landrace	Desi
ICC 4533	India	Landrace	Desi
ICC 456	India	Landrace	Desi
ICC 4567	India	Landrace	Desi
ICC 4593	India	Landrace	Desi
ICC 4639	India	Landrace	Desi
ICC 4657	India	Landrace	Desi
ICC 4814	Iran	Landrace	Desi
ICC 4841	Morocco	Landrace	Kabuli
ICC 4872	India	Landrace	Pea-shaped
ICC 4918	India	Advanced cultivar	Desi
ICC 4991	India	Advanced cultivar	Desi
ICC 506	India	Landrace	Desi
ICC 5135	India	Breeding material	Desi
ICC 5221	India	Breeding material	Desi
ICC 5337	India	Landrace	Kabuli
ICC 5383	India	Landrace	Desi
ICC 5434	India	Landrace	Desi
ICC 5504	Mexico	Landrace	Desi
ICC 5613	India	Landrace	Desi
ICC 5639	India	Landrace	Desi
ICC 5845	India	Landrace	Desi
ICC 5878	India	Landrace	Desi
ICC 6263	USSR	Landrace	Kabuli
ICC 6279	India	Landrace	Desi
ICC 6293	Italy	Landrace	Desi
ICC 6294	Iran	Advanced cultivar	Desi
ICC 6306	USSR	Advanced cultivar	Desi
ICC 637	India	Landrace	Desi
ICC 6537	Iran	Breeding material	Desi
ICC 6571	Iran	Landrace	Desi
ICC 6579	Iran	Landrace	Desi
ICC 67	India	Landrace	Desi
ICC 6802	Iran	Landrace	Desi
ICC 6811	Iran	Landrace	Desi
ICC 6816	Iran	Landrace	Desi
ICC 6874	Iran	Landrace	Desi
ICC 6875	Iran	Landrace	Desi
ICC 6877	Iran	Landrace	Desi
ICC 7052	Iran	Landrace	Desi
ICC 708	India	Landrace	Desi
ICC 7150	Turkey	Landrace	Desi
ICC 7184	Turkey	Landrace	Desi
ICC 7255	India	Landrace	Kabuli
ICC 7272	Algeria	Landrace	Kabuli
ICC 7305	Afghanistan	Landrace	Desi

ICC 7308	Peru	Landrace	Kabuli
ICC 7315	Iran	Landrace	Kabuli
ICC 7323	USSR	Landrace	Pea-shaped
ICC 7413	India	Landrace	Pea-shaped
ICC 7441	India	Landrace	Desi
ICC 7554	Iran	Landrace	Desi
ICC 7571	Israel	Landrace	Kabuli
ICC 762	India	Landrace	Desi
ICC 7668	USSR	Landrace	Kabuli
ICC 7819	Iran	Landrace	Desi
ICC 7867	Iran	Landrace	Desi
ICC 791	India	Landrace	Desi
ICC 8151	USA	Landrace	Kabuli
ICC 8195	Pakistan	Landrace	Desi
ICC 8200	Iran	Landrace	Desi
ICC 8261	Turkey	Landrace	Kabuli
ICC 8318	India	Landrace	Desi
ICC 8350	India	Landrace	Pea-shaped
ICC 8384	India	Landrace	Desi
ICC 8515	Greece	Landrace	Desi
ICC 8522	Italy	Landrace	Desi
ICC 8621	Ethiopia	Landrace	Desi
ICC 867	India	Landrace	Desi
ICC 8718	Afghanistan	Landrace	Desi
ICC 8740	Afghanistan	Landrace	Kabuli
ICC 8752	Afghanistan	Landrace	Kabuli
ICC 8855	Afghanistan	Landrace	Kabuli
ICC 8950	India	Landrace	Desi
ICC 9002	Iran	Landrace	Desi
ICC 9137	Iran	Landrace	Kabuli
ICC 9402	Iran	Landrace	Kabuli
ICC 9434	Iran	Landrace	Kabuli
ICC 95	India	Landrace	Desi
ICC 9586	India	Landrace	Desi
ICC 9590	Egypt	Landrace	Desi
ICC 9636	Afghanistan	Landrace	Desi
ICC 9643	Afghanistan	Landrace	Desi
ICC 9712	Afghanistan	Landrace	Desi
ICC 9755	Afghanistan	Landrace	Desi
ICC 9848	Afghanistan	Landrace	Pea-shaped
ICC 9862	Afghanistan	Landrace	Pea-shaped
ICC 9872	Afghanistan	Landrace	Kabuli
ICC 9895	Afghanistan	Landrace	Pea-shaped
ICC 9942	India	Landrace	Desi

Table S2: Quantitative trait loci from Genesis836/Rupali mapping population. a).QTLs under control condition, b). QTLs under salinity. c). trait abbreviations explained. Chr-chromosome, dist (cM)-genetic distance, %Var- genetic variation explained, LOD-logarithm of odds.

a)

Trait	Chr	Left Marker	dist(cM)	Right Marker	dist(cM)	Size	Pvalue	% Var	LOD
PH	L3	DArT850	29.55	DArT1046	40.32	2.457	0	6.9	3.6
NA	L7	DArT272(C)	68.63	DArT254(C)	88.75	-2.498	0.001	7.1	2.38
NA	L8	DArT52(C)	45.28	SNP9	47.32	2.427	0	6.7	4.398
WU	L4	SNP201	37.12	SNP1069(C)	63.87	-3.327	0	21.9	3.65
NA	L8	SNP27	50.65	SNP23	62.57	2.344	0.001	10.9	2.22
WUE	L4	SNP1069(C)	63.87	DArT1813	72.13	-353.758	0	7.5	3.648
NA	L8	DArT1786	18.49	DArT1798	20.52	367.059	0	8.1	4.589
PSA	L3	SNP343	17.13	DArT1762(C)	24.78	0.021	0.006	2.1	1.617
NA	L4	SNP201	37.12	SNP1069(C)	63.87	-0.047	0	10.6	4.743
NA	L4	DArT417	80.34	SNP180(C)	82.89	-0.027	0.001	3.6	2.275
NA	L4	DArT485	137.75	SNP188	139.26	0.031	0	4.6	3.865
NA	L8	DArT1786	18.49	DArT1798	20.52	0.043	0	8.9	8.136
X30AGR	L2	SNP225	61.85	SNP210	64.37	-2.253	0.001	6.4	2.259
NA	L3	SNP343	17.13	DArT1762(C)	24.78	1.783	0.002	4	2.043
NA	L4	SNP201	37.12	SNP1069(C)	63.87	-2.757	0	9.6	2.88
NA	L4	DArT417	80.34	SNP180(C)	82.89	-2.726	0	9.3	3.823
NA	L4	DArT485	137.75	SNP188	139.26	2.041	0	5.2	2.827
NA	L8	SNP27	50.65	SNP23	62.57	3.776	0	17.9	6.157
NA	L8	DArT1756	81.55	DArT10	82.85	-1.7	0.004	3.6	1.774
X34AGR	L4	SNP201	37.12	SNP1069(C)	63.87	-3.378	0	16	2.635
NA	L4	DArT417	80.34	SNP180(C)	82.89	-2.647	0	9.8	2.64
NA	L8	DArT1786	18.49	DArT1798	20.52	2.509	0	8.8	3.289
ADM	L1	SNP69	45.92	SNP423(C)	48.51	-0.582	0.001	5.7	2.541
NA	L3	DArT1750(C)	26.53	DArT850	29.55	0.743	0	9.2	4.042
NA	L7	DArT276	61.25	DArT272(C)	68.63	-0.716	0	8.5	2.978
NA	L8	SNP27	50.65	SNP23	62.57	0.696	0	8.1	2.826
TP	L3	SNP1056(C)	43.73	DArT1128(C)	45.09	-2.021	0.001	8.4	2.626
FP	L3	DArT1046	40.32	SNP1056(C)	43.73	-2.045	0	12.5	4.08
FPR	L8	DArT1251(C)	155.55	SNP11(C)	156.98	-0.012	0.005	25.7	1.706
SN	L2	DArT595	97.52	DArT553	111.41	-2.092	0.002	6.3	2.055
NA	L3	DArT1046	40.32	SNP1056(C)	43.73	-2.956	0	12.6	4.418
NA	L4	SNP1069(C)	63.87	DArT1813	72.13	2.101	0.001	6.4	2.341
SY	L5	SNP243	136.54	SNP613	138.36	0.37	0.001	7.2	2.491
SW	L2	SNP230	92.57	DArT595	97.52	0.941	0	4.2	3.226
NA	L3	DArT1762(C)	24.78	DArT1750(C)	26.53	0.738	0.002	2.6	2.015
NA	L3	SNP357	78.22	DArT1764(C)	81.16	0.735	0.006	2.6	1.659
NA	L4	SNP1069(C)	63.87	DArT1813	72.13	-1.979	0	18.7	13.586
NA	L5	SNP246	131	SNP259(C)	133.94	0.856	0	3.5	2.817
NA	L7	DArT253	102.73	SNP405	106.46	1.427	0.014	9.7	1.309
HI	L2	SNP210	64.37	SNP234	69.37	0.02	0.003	5.7	1.947

NA	L3	DArT850	29.55	DArT1046	40.32	-0.024	0	8.2	3.024
NA	L6	DArT1785	39.48	SNP397	43.37	0.017	0.003	4.3	1.909
NA	L7	DArT272(C)	68.63	DArT254(C)	88.75	0.037	0	19.4	4.576
Na	L3	SNP370	12.98	SNP343	17.13	-0.037	0.002	7.4	2.057
K	L3	DArT1750(C)	26.53	DArT850	29.55	-0.031	0	20.2	5.161
NA	L4	SNP1069(C)	63.87	DArT1813	72.13	0.025	0	13.3	3.129
NA	L6	SNP397	43.37	DArT148(C)	46.97	0.02	0.002	8.3	2.152
NA	L8	DArT1259(C)	31.28	DArT97(C)	32.27	-0.025	0	13.7	3.709
KNa	L4	SNP203(C)	77.52	DArT419(C)	78.8	0.039	0	11.4	3.386

b).

Trait	Chr	Left Marker	dist(cM)	Right Marker	dist(cM)	Size	Pvalue	% Var	LOD
PH	L3	DArT1750(C)	26.53	DArT850	29.55	2.149	0	5.7	3.183
WU	L4	SNP201	37.12	SNP1069(C)	63.87	-2.201	0	10.7	3.103
WUE	L4	SNP1069(C)	63.87	DArT1813	72.13	-580.139	0	18.5	3.973
NA	L8	DArT97(C)	32.27	SNP406	33.58	660.103	0	23.9	5.803
PSA	L1	SNP81	13.09	DArT210	28.77	0.023	0.007	2.5	1.558
NA	L4	SNP201	37.12	SNP1069(C)	63.87	-0.055	0	15.2	8.653
NA	L4	SNP188	139.26	SNP153(C)	143.33	0.023	0.001	2.6	2.397
NA	L8	DArT1786	18.49	DArT1798	20.52	0.035	0	5.9	3.916
NA	L8	SNP9	47.32	SNP27	50.65	0.019	0.026	1.8	1.074
X30AGR	L4	SNP201	37.12	SNP1069(C)	63.87	-2.534	0	9.9	4.956
NA	L8	SNP5	14.85	DArT1786	18.49	2.267	0	8	6.328
X34AGR	L4	SNP201	37.12	SNP1069(C)	63.87	-2.792	0	10.7	4.97
NA	L8	SNP5	14.85	DArT1786	18.49	2.541	0	8.9	6.341
X30AOST	L4	DArT419(C)	78.8	DArT417	80.34	0.045	0	37	3.654
X34AOST	L4	DArT419(C)	78.8	DArT417	80.34	0.048	0	42.6	3.587
TP	L4	SNP201	37.12	SNP1069(C)	63.87	1.939	0.001	7.6	2.562
FP	L2	DArT1165(C)	1.72	SNP208(C)	5.11	-1.544	0.001	5.7	2.594
NA	L2	SNP233	35.48	SNP277	44.22	2.76	0.001	18.2	2.376
NA	L3	SNP432(C)	57.96	DArT1139(C)	59.11	-1.135	0.004	3.1	1.835
NA	L4	SNP201	37.12	SNP1069(C)	63.87	1.338	0.006	4.3	1.669
FPR	L6	SNP377	14.69	SNP380	22.89	0.01	0.004	16.1	1.842
SN	L2	DArT1165(C)	1.72	SNP208(C)	5.11	-1.562	0.005	3.6	1.743
NA	L4	SNP1069(C)	63.87	DArT1813	72.13	2.346	0	8.2	3.881
NA	L6	DArT990	2.31	SNP377	14.69	1.886	0.001	5.3	2.446
SY	L4	SNP616(C)	147.03	DArT1758(C)	147.86	0.256	0.002	3.4	2.051
NA	L5	SNP246	131	SNP259(C)	133.94	0.317	0	5.3	2.908
SW	L3	SNP357	78.22	DArT1764(C)	81.16	0.984	0	4.7	3.672
NA	L4	SNP1069(C)	63.87	DArT1813	72.13	-1.711	0	14.1	13.106
NA	L5	SNP259(C)	133.94	SNP243	136.54	0.87	0	3.7	3.879
NA	L7	DArT253	102.73	SNP405	106.46	1.478	0.003	10.5	1.852
NA	L8	SNP27	50.65	SNP23	62.57	0.676	0.006	2.2	1.643

HI	L1	SNP58(C)	70.26	DArT167	79.15	0.018	0	4.8	2.762
NA	L5	SNP256(C)	106.46	SNP238(C)	113.68	0.013	0.002	2.5	2.101
NA	L6	DArT990	2.31	SNP377	14.69	0.02	0	5.7	4.34
NA	L7	DArT253	102.73	SNP405	106.46	0.032	0.001	14.9	2.217

c).

Traits	**Abbreviations**
Plant height	PH
Water use	WU
Water use efficiency	WUE
Projected shoot area	PSA
Relative growth rate from 30 DAS	X30 AGR
Relative growth rate from 34 DAS	X34 AGR
Relative growth rate ratio (salt/control) 30 DAS	X30 AOST
Relative growth rate ratio (salt/control)34 DAS	X34 AOST
Number of total pods	TP
Number of filled pods	FP
Number of filled pods as a ratio of total pods	FPR
Seed number	SN
Seed yield	SY
100-seed weight	SW
Harvest index	HI
Above ground dry matter (shoot biomass)	ADM
Sodium ions	Na
Potassium ions	K
potassium sodium ratio	KNa